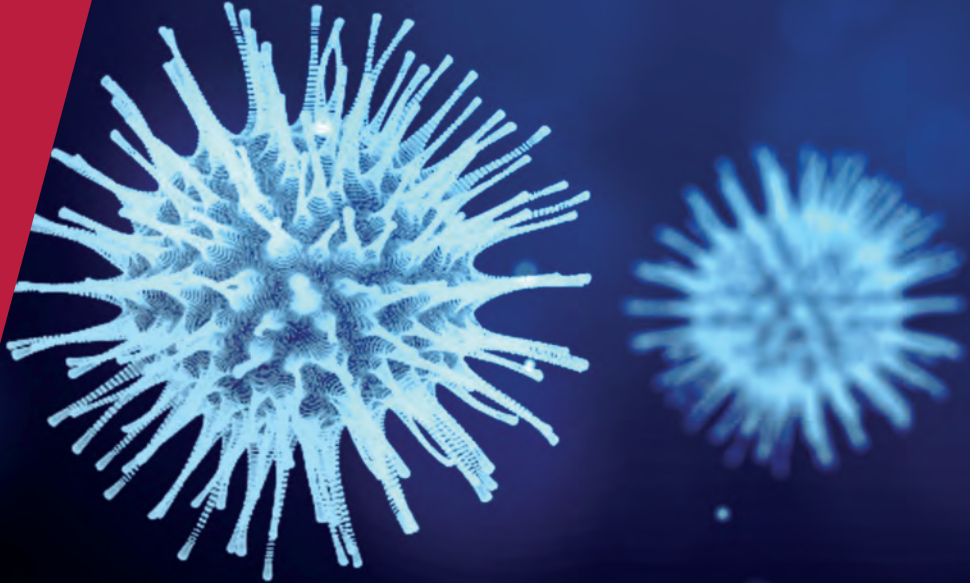


**CENTRE FOR  
ECONOMIC  
POLICY  
RESEARCH**

**CEPR PRESS**



**COVID ECONOMICS**  
VETTED AND REAL-TIME PAPERS

**ISSUE 56**  
9 NOVEMBER 2020

**WHEN VACCINES OR TREATMENTS  
ARE EXPECTED**

Miltiadis Makris and Flavio Toxvaerd

**WHICH RESTRICTIONS WORK?**

Matthew Spiegel and Heather Tookes

**CONSUMPTION UNDER LOCKDOWN  
AND LOCAL INFECTIONS**

Pascal Golec, George Kapetanios,  
Nora Neuteboom, Feiko Ritsema  
and Alexia Ventouri

**STATE VERSUS FEDERAL POLICIES**

Jean-Paul Renne, Guillaume Roussellet  
and Gustavo Schwenkler

**SUPPLY CHAIN NETWORKS  
ACROSS REGIONS AND LOCKDOWN  
EFFECTS**

Hiroyasu Inoue, Yohsuke Murase  
and Yasuyuki Todo

**FOOD SECURITY**

Tuan Anh Luong

---

# Covid Economics

## Vetted and Real-Time Papers

*Covid Economics, Vetted and Real-Time Papers*, from CEPR, brings together formal investigations on the economic issues emanating from the Covid outbreak, based on explicit theory and/or empirical evidence, to improve the knowledge base.

**Founder:** Beatrice Weder di Mauro, President of CEPR

**Editor:** Charles Wyplosz, Graduate Institute Geneva and CEPR

**Contact:** Submissions should be made at <https://portal.cepr.org/call-papers-covid-economics>. Other queries should be sent to [covidecon@cepr.org](mailto:covidecon@cepr.org).

Copyright for the papers appearing in this issue of *Covid Economics: Vetted and Real-Time Papers* is held by the individual authors.

### **The Centre for Economic Policy Research (CEPR)**

The Centre for Economic Policy Research (CEPR) is a network of over 1,500 research economists based mostly in European universities. The Centre's goal is twofold: to promote world-class research, and to get the policy-relevant results into the hands of key decision-makers. CEPR's guiding principle is 'Research excellence with policy relevance'. A registered charity since it was founded in 1983, CEPR is independent of all public and private interest groups. It takes no institutional stand on economic policy matters and its core funding comes from its Institutional Members and sales of publications. Because it draws on such a large network of researchers, its output reflects a broad spectrum of individual viewpoints as well as perspectives drawn from civil society. CEPR research may include views on policy, but the Trustees of the Centre do not give prior review to its publications. The opinions expressed in this report are those of the authors and not those of CEPR.

Chair of the Board

Sir Charlie Bean

Founder and Honorary President

Richard Portes

President

Beatrice Weder di Mauro

Vice Presidents

Maristella Botticini

Ugo Panizza

Philippe Martin

Hélène Rey

Chief Executive Officer

Tessa Ogden

---

# Editorial Board

**Beatrice Weder di Mauro**, CEPR

**Charles Wyplosz**, Graduate Institute Geneva and CEPR

**Viral V. Acharya**, Stern School of Business, NYU and CEPR

**Guido Alfani**, Bocconi University and CEPR

**Franklin Allen**, Imperial College Business School and CEPR

**Michele Belot**, European University Institute and CEPR

**David Bloom**, Harvard T.H. Chan School of Public Health

**Nick Bloom**, Stanford University and CEPR

**Tito Boeri**, Bocconi University and CEPR

**Alison Booth**, University of Essex and CEPR

**Markus K Brunnermeier**, Princeton University and CEPR

**Michael C Burda**, Humboldt Universitaet zu Berlin and CEPR

**Aline Bütikofer**, Norwegian School of Economics

**Luis Cabral**, New York University and CEPR

**Paola Conconi**, ECARES, Universite Libre de Bruxelles and CEPR

**Giancarlo Corsetti**, University of Cambridge and CEPR

**Fiorella De Fiore**, Bank for International Settlements and CEPR

**Mathias Dewatripont**, ECARES, Universite Libre de Bruxelles and CEPR

**Jonathan Dingel**, University of Chicago Booth School and CEPR

**Barry Eichengreen**, University of California, Berkeley and CEPR

**Simon J Evenett**, University of St Gallen and CEPR

**Maryam Farboodi**, MIT and CEPR

**Antonio Fatás**, INSEAD Singapore and CEPR

**Francesco Giavazzi**, Bocconi University and CEPR

**Christian Gollier**, Toulouse School of Economics and CEPR

**Timothy J. Hatton**, University of Essex and CEPR

**Ethan Ilzetzki**, London School of Economics and CEPR

**Beata Javorcik**, EBRD and CEPR

**Simon Johnson**, MIT and CEPR

**Sebnem Kalemli-Ozcan**, University of Maryland and CEPR Rik Frehen

**Tom Kompas**, University of Melbourne and CEBRA

**Miklós Koren**, Central European University and CEPR

**Anton Korinek**, University of Virginia and CEPR

**Michael Kuhn**, Vienna Institute of Demography

**Maarten Lindeboom**, Vrije Universiteit Amsterdam

**Philippe Martin**, Sciences Po and CEPR

**Warwick McKibbin**, ANU College of Asia and the Pacific

**Kevin Hjortshøj O'Rourke**, NYU Abu Dhabi and CEPR

**Evi Pappa**, European University Institute and CEPR

**Barbara Petrongolo**, Queen Mary University, London, LSE and CEPR

**Richard Portes**, London Business School and CEPR

**Carol Propper**, Imperial College London and CEPR

**Lucrezia Reichlin**, London Business School and CEPR

**Ricardo Reis**, London School of Economics and CEPR

**Hélène Rey**, London Business School and CEPR

**Dominic Rohner**, University of Lausanne and CEPR

**Paola Sapienza**, Northwestern University and CEPR

**Moritz Schularick**, University of Bonn and CEPR

**Flavio Toxvaerd**, University of Cambridge  
**Christoph Trebesch**, Christian-Albrechts-Universitaet zu Kiel and CEPR

**Karen-Helene Ulltveit-Moe**, University of Oslo and CEPR

**Jan C. van Ours**, Erasmus University Rotterdam and CEPR

**Thierry Verdier**, Paris School of Economics and CEPR

---

# Ethics

*Covid Economics* will feature high quality analyses of economic aspects of the health crisis. However, the pandemic also raises a number of complex ethical issues. Economists tend to think about trade-offs, in this case lives vs. costs, patient selection at a time of scarcity, and more. In the spirit of academic freedom, neither the Editors of *Covid Economics* nor CEPR take a stand on these issues and therefore do not bear any responsibility for views expressed in the articles.

## Submission to professional journals

The following journals have indicated that they will accept submissions of papers featured in *Covid Economics* because they are working papers. Most expect revised versions. This list will be updated regularly.

<i>American Economic Review</i>	<i>Journal of Economic Growth</i>
<i>American Economic Review, Applied Economics</i>	<i>Journal of Economic Theory</i>
<i>American Economic Review, Insights</i>	<i>Journal of the European Economic Association*</i>
<i>American Economic Review, Economic Policy</i>	<i>Journal of Finance</i>
<i>American Economic Review, Macroeconomics</i>	<i>Journal of Financial Economics</i>
<i>American Economic Review, Microeconomics</i>	<i>Journal of International Economics</i>
<i>American Journal of Health Economics</i>	<i>Journal of Labor Economics*</i>
<i>Canadian Journal of Economics</i>	<i>Journal of Monetary Economics</i>
<i>Econometrica*</i>	<i>Journal of Public Economics</i>
<i>Economic Journal</i>	<i>Journal of Public Finance and Public Choice</i>
<i>Economics of Disasters and Climate Change</i>	<i>Journal of Political Economy</i>
<i>International Economic Review</i>	<i>Journal of Population Economics</i>
<i>Journal of Development Economics</i>	<i>Quarterly Journal of Economics</i>
<i>Journal of Econometrics*</i>	<i>Review of Corporate Finance Studies*</i>
	<i>Review of Economics and Statistics</i>
	<i>Review of Economic Studies*</i>
	<i>Review of Financial Studies</i>

(\*) Must be a significantly revised and extended version of the paper featured in *Covid Economics*.

---

# Covid Economics

## Vetted and Real-Time Papers

Issue 56, 9 November 2020

## Contents

Great expectations: Social distancing in anticipation of pharmaceutical innovations <i>Miltiadis Makris and Flavio Toxvaerd</i>	1
Business restrictions and Covid-19 fatalities <i>Matthew Spiegel and Heather Tookes</i>	20
Disentangling the effect of government restrictions and consumers' reaction function to the Covid-19 pandemic: Evidence from geo-located transactions data for the Netherlands <i>Pascal Golec, George Kapetanios, Nora Neuteboom, Feiko Ritsema and Alexia Ventouri</i>	60
Preventing COVID-19 fatalities: State versus federal policies <i>Jean-Paul Renne, Guillaume Roussellet and Gustavo Schwenkler</i>	106
The impact of supply chain networks on interactions between the anti-COVID-19 lockdowns in different regions <i>Hiroyasu Inoue, Yohsuke Murase and Yasuyuki Todo</i>	157
Reopening the economy and food security <i>Tuan Anh Luong</i>	195

# Great expectations: Social distancing in anticipation of pharmaceutical innovations

Miltiadis Makris<sup>1</sup> and Flavio Toxvaerd<sup>2</sup>

Date submitted: 3 November 2020; Date accepted: 4 November 2020

*This paper analyzes equilibrium social distancing behavior when pharmaceutical innovations, such as effective vaccines and treatments, are anticipated to arrive. Once such innovations arrive, costly social distancing can be reduced. We characterize how the anticipation of such innovations influences pre-innovation social distancing. When vaccines are anticipated, equilibrium social distancing is ramped up as the arrival date approaches to increase the probability of reaching the post-innovation phase in the susceptible state. In contrast, under anticipated treatment, equilibrium social distancing is phased out by the time of arrival. We compare the equilibrium paths with the socially optimal counterparts and discuss policy implications.*

<sup>1</sup> School of Economics, University of Kent.

<sup>2</sup> Faculty of Economics, University of Cambridge.

Copyright: Miltiadis Makris and Flavio Toxvaerd

*“Our strategy is to suppress the virus, protecting the economy, education and the NHS, until a vaccine can make us safe”.*

*- Matt Hancock, UK Health Secretary, October 1, 2020.<sup>1</sup>*

*“Vaccines and therapeutic drugs might be available in a year or so’s time. But it is a foolish strategy to rely on them, and to keep us in lockdown – or other severe social-distancing measures – until such a time”.*

*- Ross Clark, The Spectator, April 2020.<sup>2</sup>*

In the absence of effective vaccines and antiviral treatments, individuals and public health authorities have been entirely reliant on non-pharmaceutical interventions such as social distancing and lockdowns. These interventions, while often justified, have proven extremely costly from both a social and an economic perspective and there is a general recognition that such restrictive measures as shelter-in-place orders are not sustainable in the long run. Equally, it is widely recognized that until effective pharmaceutical interventions become available, a return to normality is unlikely to be possible. In short, containing the epidemic will involve social distancing to some extent till vaccines and treatments become available. But an important question remains. Once the pharmaceutical innovations appear on the horizon, how will and should people behave leading up to that moment? In other words, how exactly is social distancing phased out? This is the question we consider in the present analysis.

In this paper, we study positive and normative questions of infection control via non-pharmaceutical interventions (NPIs), when pharmaceutical innovations are anticipated. In particular, we are interested in better understanding how the anticipation of effective vaccines and treatments changes ex-ante incentives to engage in social distancing and how such effects differ across innovations. To this end, we study a stylized susceptible-infected-recovered (SIR) model of infection control in which decision makers can reduce infection risk at a cost. At some known future time  $T$ , a perfectly functioning pharmaceutical innovation such as a vaccine or a treatment becomes available, obviating any further social distancing. A perfect treatment means that any infected individual who is treated immediately recovers, while a perfect vaccine means that anyone who is vaccinated obtains perfect and lasting immunity. In this setting, we characterize the equilibrium and socially optimal paths of social distancing. We show that these paths depend on whether the innovation is a treatment or a vaccine. The reason for this is that while treatment can be given to any infected individual regardless of when the individual was infected (in

<sup>1</sup><https://www.gov.uk/government/speeches/extended-measures-to-protect-more-areas-of-england-from-coronavirus>

<sup>2</sup>Britain Can’t Rely on a Vaccine to Ease Lockdown Restrictions, The Spectator, <https://www.spectator.co.uk/article/britain-can-t-rely-on-a-vaccine-to-ease-lockdown-restrictions>

particular, irrespective of whether the individual was infected before or after the arrival of the treatment), only susceptible individuals can benefit from the arrival of the vaccine. The effect of this is that for treatment, the value of social distancing decreases as the arrival date approaches. In fact, on the date of arrival, no social distancing takes place at all. In contrast, before the arrival of the vaccine, social distancing by individuals is ramped up just before arrival, to increase the chances that they can benefit from the vaccine.

To illustrate these points, we consider three scenarios. In the benchmark, no pharmaceutical innovation ever arrives and so the decision makers must resort to social distancing throughout the epidemic. In addition, we consider the case where the innovation arrives before peak prevalence is reached in the benchmark scenario and the case where it arrives after. These three cases allow us to not only determine how the arrival of the innovation influences pre-innovation social distancing efforts, but also how this dependence changes across the stages of the epidemic.

It should be noted that strictly speaking, the key date for the purpose of decision making is the date of availability, rather than the date of innovation. Thus our analysis equally applies to situations where the pharmaceutical innovations have already been made but where decision makers are awaiting delivery of the vaccine or treatment, as the case may be.

The paper contributes to the larger literature on economic epidemiology, in particular to the literatures on social distancing and on the interaction of several instruments of disease control. Rowthorn and Toxvaerd (2020) analyze the interaction of equilibrium and socially optimal social distancing and treatment in a model of recurrent infection (SIS) when both are present, while Toxvaerd and Rowthorn (2020) consider equilibrium and socially optimal use of treatment and vaccination in isolation in an SIR environment. Toxvaerd (2019) considers the welfare effects of policies such as pre-exposure prophylaxis in an SIS model of social distancing. Giannitsarou, Kissler and Toxvaerd (2020) study a model of socially optimal social distancing in an SEIRS model with vital dynamics. In their model, the social planner values lives beyond the active planning horizon, after which the disease is no longer a concern. They show that the social planner may have an incentive to increase the number of survivors at the end of the planning horizon, thus prompting an increase in social distancing as the end date approaches. Some of our results have a similar character, although they differ in the details and in their interpretation. Toxvaerd (2020) and Makris (2020) consider equilibrium social distancing in settings where no pharmaceutical interventions are forthcoming and are therefore comparable to our benchmark scenario.

In an important early paper, Auld (2003) considers the role of expectations of a



future vaccine arrival and incentives to self-protect. In particular, he distinguishes between anticipated and “surprise” innovations and the counterweighing effects of imperfect vaccines. In a macroeconomic model of disease propagation, Eichenbaum, Rebelo and Trabandt (2020) consider the possibility of a vaccine or a treatment that arrives with a constant probability in each period. As in our paper, they characterize how the possible arrival of these pharmaceutical innovations interact with other decisions, in their case over consumption and labour supply. In contrast to our results, they show that in the competitive equilibrium, the possibility of such innovations makes very little difference in their framework. A central difference between our setup and theirs is that the arrival process has a constant hazard rate (i.e. the arrival probability is constant over time), whereas in our model, individuals know that arrival is approaching as time passes. This introduces an additional source of non-stationarity to our model over and above that in the underlying epidemiological dynamics. Last, Bognanni et al. (2020) consider a spatial macroeconomic-epidemiological model of social distancing in which a vaccine may arrive. In contrast to our analysis, theirs do not feature forward-looking behavior and thus their results are not directly comparable to ours.

### 1. DECENTRALIZED DECISION MAKING

Consider a susceptible-infected-recovered compartmental model of an infectious disease. Time is continuous and at some instant  $t$ , an individual is either susceptible and belongs to the compartment  $\mathcal{S}(t)$ , infected and infectious and belongs to the compartment  $\mathcal{I}(t)$  or recovered and immune, thus belonging to the compartment  $\mathcal{R}(t)$ . We will denote the measures of these compartments by  $S(t)$ ,  $I(t)$  and  $R(t)$  respectively. In this model, infection spreads through meetings between susceptible and infected individuals at a rate that depends on underlying biology and social distancing behavior. In particular, we assume that behaviour reduces the infectiousness parameter  $\beta$  to some level  $\beta(1-d(t)) < \beta$ , where  $d(t) \in [0, 1]$  is a measure for social distancing. Once infected, individuals recover spontaneously at some exogenous rate  $\gamma > 0$ <sup>3</sup>. The dynamics are given by

$$\dot{S}(t) = -\beta(1-d(t))I(t)S(t) \quad (1)$$

$$\dot{I}(t) = I(t) [\beta(1-d(t))S(t) - \gamma] \quad (2)$$

$$\dot{R}(t) = \gamma I(t) \quad (3)$$

$$1 = S(t) + I(t) + R(t) \quad (4)$$

$$S(0) \approx 1, S(0) + I(0) = 1, S(0) > \gamma/\beta \quad (5)$$

<sup>3</sup>The model is readily extended to include the possibility of disease-induced mortality. One simple way to include this possibility is to replace  $\gamma$  with  $\gamma/(1-\sigma)$ , where  $\sigma \in [0, 1]$  is the probability that the individual will die of the disease before recovering. This formalisation of mortality is discussed further in Keeling and Rohani (2008).

Assume that the individuals earn some flow payoff  $\bar{\pi} > 0$  while susceptible but experience a decrease in flow payoffs to some level  $\underline{\pi} < \bar{\pi}$  while infected. Once they recover, they return to earning flow payoff  $\bar{\pi}$ . Individuals discount the future at rate  $\rho > 0$ .

Let  $p_i(t) \in [0, 1]$  denote the probability at instant  $t \geq 0$  of residence in health state  $i = \mathcal{S}, \mathcal{I}, \mathcal{R}$  for the individual. At time  $T > 0$ , a pharmaceutical intervention becomes available (either treatment or vaccine). For all times  $t < T$ , the individual can only mitigate infection risk by choosing social distancing  $d(t) \in [0, 1]$  at cost  $c(d(t))$  with  $c' > 0$  and  $c'' \geq 0$ . For simplicity, we can take  $c(d) = d^2/2$  where  $c'(d) = d$  and  $c''(d) = 1$ .

The problem to be solved by a susceptible individual is given by

$$\max_{d(t) \in [0,1]} \int_0^T e^{-\rho t} \{p_{\mathcal{S}}(t)[\bar{\pi} - c(d(t))] + p_{\mathcal{I}}(t)\underline{\pi} + p_{\mathcal{R}}(t)\bar{\pi}\} dt + e^{-\rho T} [p_{\mathcal{S}}(T)V_{\mathcal{S}} + p_{\mathcal{I}}(T)V_{\mathcal{I}} + p_{\mathcal{R}}(T)V_{\mathcal{R}}] \tag{6}$$

In this objective function,  $V_i$  is the expected net present value of entering the post-innovation phase inhabiting health state  $i = \mathcal{S}, \mathcal{I}, \mathcal{R}$ . These values depend on the nature of the pharmaceutical innovation and will be further characterized below.

The individual’s problem is solved subject to the following system of differential equations:

$$\dot{p}_{\mathcal{S}}(t) = -(1 - d(t))\beta I(t)p_{\mathcal{S}}(t), \quad p_{\mathcal{S}}(0) = 1 \tag{7}$$

$$\dot{p}_{\mathcal{I}}(t) = (1 - d(t))\beta I(t)p_{\mathcal{S}}(t) - \gamma p_{\mathcal{I}}(t) \tag{8}$$

$$\dot{p}_{\mathcal{R}}(t) = \gamma p_{\mathcal{I}}(t) \tag{9}$$

It is worth emphasizing that under decentralized decision making, each individual takes the aggregate dynamics as given and chooses a path of social distancing in order to maximize his or her individual expected discounted utility. The outcome is thus one of perfect foresight equilibrium, in which the aggregate dynamics that the individuals anticipate when choosing their social distancing policies actually materializes.

Let  $\lambda_i^D(t)$  denote the costate variables for the state variables  $p_i(t)$ ,  $i = \mathcal{S}, \mathcal{I}, \mathcal{R}$ . Then the individual’s current-value Hamiltonian is given by

$$H^D = p_{\mathcal{S}}(t)[\bar{\pi} - c(d(t))] + p_{\mathcal{I}}(t)\underline{\pi} + p_{\mathcal{R}}(t)\bar{\pi} \tag{10}$$

$$- \lambda_{\mathcal{S}}^D(t)(1 - d(t))\beta I(t)p_{\mathcal{S}}(t) \tag{11}$$

$$+ \lambda_{\mathcal{I}}^D(t)[(1 - d(t))\beta I(t)p_{\mathcal{S}}(t) - \gamma p_{\mathcal{I}}(t)] \tag{12}$$

$$+ \lambda_{\mathcal{R}}^D(t)\gamma p_{\mathcal{I}}(t) \tag{13}$$

A necessary condition for individual maximization is that

$$\frac{\partial H^D}{\partial d(t)} = -p_S(t)c'(d(t)) + \beta I(t)p_S(t)[\lambda_S^D(t) - \lambda_I^D(t)] = 0 \tag{14}$$

which can be re-written as

$$c'(d(t)) = \beta I(t)[\lambda_S^D(t) - \lambda_I^D(t)] \tag{15}$$

This equation just means that for the individual to be best responding, the marginal cost of social distancing must equal the marginal benefit, measured by the avoided expected utility cost from becoming infected. With quadratic costs, we get that

$$d(t) = \beta I(t)[\lambda_S^D(t) - \lambda_I^D(t)] \tag{16}$$

To complete the characterization of the equilibrium path of social distancing, we need to determine the evolution of the three costate variables and impose the appropriate transversality conditions. The laws of motion for the costate variables are:

$$\dot{\lambda}_S^D(t) = \rho \lambda_S^D(t) - \frac{\partial H^D}{\partial p_S(t)} \tag{17}$$

$$= \lambda_S^D(t) [\rho + (1 - d(t))\beta I(t)] - \lambda_I^D(t)(1 - d(t))\beta I(t) - [\bar{\pi} - c(d(t))]$$

$$\dot{\lambda}_I^D(t) = \rho \lambda_I^D(t) - \frac{\partial H^D}{\partial p_I(t)} \tag{18}$$

$$= \lambda_I^D(t) [\rho + \gamma] - \lambda_{\mathcal{R}}^D(t)\gamma - \underline{\pi}$$

$$\dot{\lambda}_{\mathcal{R}}^D(t) = \rho \lambda_{\mathcal{R}}^D(t) - \frac{\partial H^D}{\partial p_{\mathcal{R}}(t)} = \rho \lambda_{\mathcal{R}}^D(t) - \bar{\pi} \tag{19}$$

Last, the transversality conditions are

$$\lambda_S^D(T)e^{-\rho T} = V_S \tag{20}$$

$$\lambda_I^D(T)e^{-\rho T} = V_I \tag{21}$$

$$\lambda_{\mathcal{R}}^D(T)e^{-\rho T} = V_{\mathcal{R}} \tag{22}$$

The transversality conditions will play a prominent role in this analysis and so it is useful to recall their interpretation.<sup>4</sup> In general, the costate variable  $\lambda_i^D(t)$  captures the value of being in state  $i = \mathcal{S}, \mathcal{I}, \mathcal{R}$ . The transversality conditions simply express the present value of residence in the different health states on the date of innovation as being equal to the post-innovation continuation value, which depends on the health state in which the

<sup>4</sup>This is a fixed-end-time problem with a salvage value. The transversality conditions for this case are given in Caputo (2005, Theorem 10.3, p. 277).

individual enters this phase (and is further analyzed in what follows) and on the nature of the pharmaceutical intervention.

The salvage values on the right-hand sides of the transversality conditions (20), (21) and (22), are value functions that depend on the post-innovation regime, and on whether the innovation is a treatment or a vaccine. With costly or imperfect innovations, e.g. with a partially protective vaccine or a treatment that only induces recovery with a delay, there will generally be a role for social distancing even after the arrival of the pharmaceutical innovation. While this is conceptually a straightforward extension of our analysis, we focus on the simpler case in which the innovations are costless and perfect. This means that post-innovation, there is no role for social distancing. This simplification allows us to focus on the characterization of social distancing and how it is affected by the anticipation of the innovation. In a later section, we outline how our main conclusions are modified when imperfections in vaccines and treatment are taken into account.

After substituting the explicit policy (16) into (1)-(3) and (17)-(19), we have reduced the problem to analyzing the behavior of the system of differential equations for  $(S(t), I(t), R(t), \lambda_S^D(t), \lambda_I^D(t), \lambda_R^D(t))$  with appropriate terminal conditions for the costate variables and appropriate initial conditions for the epidemic variables.

Before embarking on the detailed analysis of equilibrium social distancing when pharmaceutical innovations are anticipated, we will briefly discuss the benchmark in which individuals only rely on non-pharmaceutical interventions throughout. In this setting, each individual's behavior is dictated by two considerations, namely current prevalence and the future path of the epidemic. First, because an individual's present probability of becoming infected is proportional to disease prevalence, as this changes so does the incentive to self-protect, all else equal. Second, the value of remaining healthy, which justifies engaging in costly social distancing, changes across the stages of the epidemic. From the perspective of an individual, who treats the path of the epidemic as exogenously given, infection risk is hump-shaped. This means that there will typically be two dates at which a given prevalence level is reached; at the first, prevalence is increasing while at the second, it is decreasing. But the individuals will value protection more on the second date than on the first. This is because on the first date, future infection hazards are much greater than on the second date and thus the value of getting safely through the next small time interval is higher later in the epidemic.

The upshot of this is that while the incentive of individuals to self-protect qualitatively follows disease prevalence, they also intensify over time, *ceteris paribus*.

For all simulations presented in this paper, we have used MATLAB R2017a on MacBook Pro, 2018, running macOS High Sierra version 10.13.6. We used the epidemiological parameters  $\gamma = 1/4.5$  and  $\beta = 0.5$ , drawing on Lourenco et al. (2020). For the economic

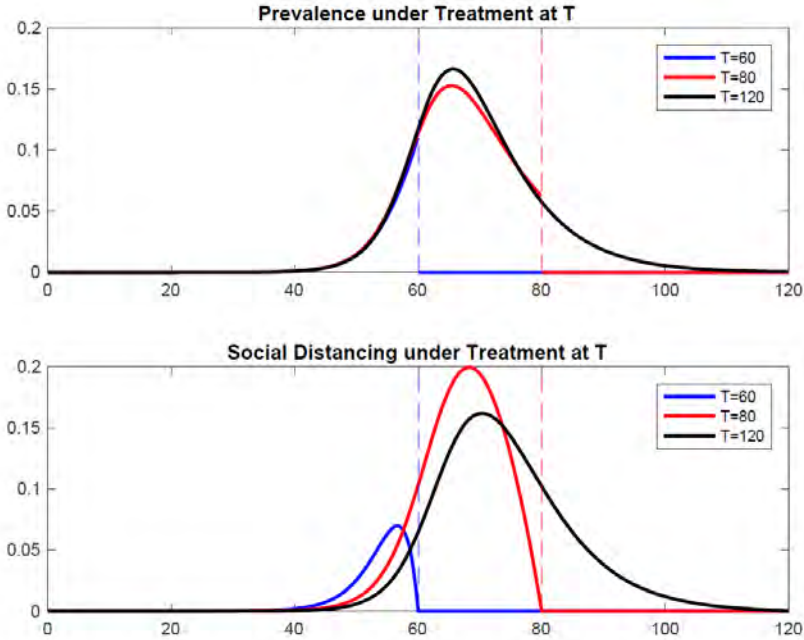


Figure 1: Equilibrium Prevalence and Social Distancing When Anticipating Treatment.

parameters, we use  $\bar{\pi} = 0$ ,  $\pi = -1$  and  $\rho = 0.05/365$ . We arrived at the numerical solution using the “shooting method”. Namely, we numerically solved for the initial values of the costate variables that ensure that the dynamic system satisfies the transversality conditions. For the derivation of the dynamic paths, we used the ODE solver `ode45.m`. For the numerical solution of the initial values of the costate variables, we used the gradient-free minimisation solver `fminsearch.m` to minimise the squared sum residuals between the simulated and the values required from the transversality conditions of the costate variables at  $T$ .

**1.1. The Case of a Perfect Treatment.** Assume that the treatment is costless and works instantaneously. This means that once the treatment becomes available, there is no need for costly social distancing. This is because any individual that becomes infected can immediately recover at no cost and thereby essentially neglect the risk of infection. Consequently, the value functions in the post-treatment phase are

$$V_S = V_I = V_R = \frac{\bar{\pi}}{\rho} \tag{23}$$

In other words, the health state of an individual going into the post-treatment phase is completely immaterial for the individual's wellbeing. A susceptible or recovered individual will earn flow payoff  $\bar{\pi}$  (recalling that the former will expend no effort on social distancing), while an infected individual can ensure this same flow payoff instantaneously through treatment at no cost.

The equilibrium dynamics in this scenario are illustrated in Figure 1, where the upper panel shows disease prevalence while the lower panel shows social distancing. We consider three cases, namely arrival of a treatment in period 60, 80 and 120, respectively. The black line shows the benchmark case in which the innovation arrives when the disease has practically died out, namely  $T = 120$ . In this case, treatment plays essentially no role for aggregate dynamics. In contrast, the blue line shows a case in which the treatment arrives before peak prevalence is reached in the benchmark. Several features of this case are worth noting. First, at early stages of the epidemic, social distancing is significantly higher than in the benchmark. This has the effect of suppressing disease prevalence. Second, we see that social distancing is gradually phased out entirely, reaching zero on the date that treatment arrives. The reason for this is that as the arrival of treatment approaches, the welfare loss from falling ill becomes lower, because there is a higher chance of making use of the treatment. An individual who becomes infected at time  $T - \varepsilon$  is not much worse off than someone who gets infected at time  $T$ , because he or she will only be in the infected state momentarily till the treatment arrives. Third, we note that there is a discontinuity in disease prevalence when the treatment arrives. The reason is that under our assumptions of costless and perfect treatment, once the innovation arrives at date  $T$ , infected individuals all get treated immediately, causing both disease prevalence and incidence (i.e. cases of new infections) to drop to zero. With imperfect treatment, these curves would have kinks at date  $T$  but not necessarily discontinuities.

Last, the red line shows a case in which the treatment only arrives after peak prevalence is reached in the benchmark. In this case, social distancing is also higher than the benchmark at the early stages (which in turn suppresses disease prevalence), and is eventually phased out entirely to reach zero on the date of arrival. It should be noted that the effects of anticipated innovations in treatment depend on the rate of recovery from infection. The faster people recover from infection, the lower is pre-innovation social distancing.

Overall, the paths of equilibrium social distancing start at a negligible level. Social distancing starts intensifying as prevalence picks up. It then peaks, before being phased out completely by the arrival date of the treatment. It is notable that the earlier the treatment arrives, the earlier is social distancing exerted and the faster does it peak. As a natural consequence of this path of social distancing, equilibrium disease prevalence is

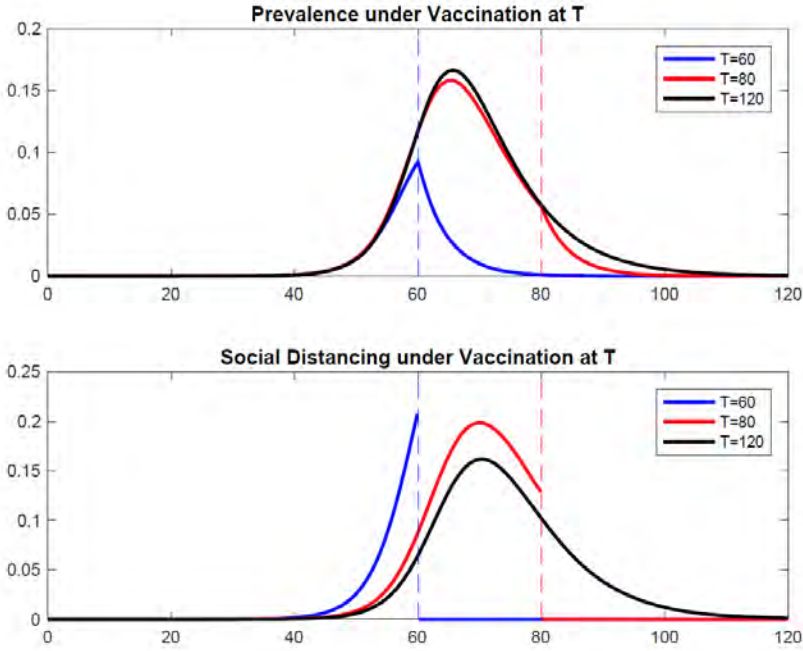


Figure 2: Equilibrium Prevalence and Social Distancing When Anticipating Vaccination.

on the whole lower than in the no-innovation benchmark.

**1.2. The Case of a Perfect Vaccine.** Assume that the vaccine is costless, has no side effects and provides instantaneous and perfect protection against infection in perpetuity. In this case, a susceptible individual will immediately vaccinate as soon as the vaccine becomes available and therefore earn flow payoff  $\bar{\pi}$  from then onward. This means that the value functions for susceptible and recovered individuals in the post-vaccine phase are

$$V_S = V_R = \frac{\bar{\pi}}{\rho} \tag{24}$$

In contrast, infected individuals cannot benefit from the vaccine and earn  $\pi$  while infected. Once recovered, their flow payoff increases to  $\bar{\pi}$ . Thus the value function for an infected individual is

$$V_I = \frac{1}{\rho} \left[ \frac{\rho\pi}{\rho + \gamma} + \frac{\gamma\bar{\pi}}{\rho + \gamma} \right] \tag{25}$$

This is simply the expected net present value for an individual who is infected and who will recover at rate  $\gamma > 0$ .

Direct inspection shows that for the case of a vaccine,  $V_I < V_S = V_R$ . This is the

reason that decision-makers, whether individuals or the social planner (discussed shortly), attach an added value to entering the post-vaccine regime while still susceptible.

The equilibrium dynamics for this scenario are illustrated in Figure 2. Again, the black line shows the benchmark case where vaccine only arrives when the disease has practically died out, at  $T = 120$ . The blue line shows the case where the vaccine arrives before peak prevalence has been reached in the benchmark. We see that in this case, social distancing is uniformly higher than in the benchmark case till the innovation arrives. In turn, this causes a suppression of disease prevalence. The same pattern is evident from the red line, showing a case where the vaccine arrives after the peak. In both cases, we note that disease prevalence is continuous. Once the vaccine arrives, all remaining susceptible individuals get costlessly immunized such that there are no new infections. Any individuals who entered the post-innovation phase as infected slowly recover, causing disease incidence to become negative. This accounts for the tapering off of prevalence after the innovation date.

In contrast to the case of treatment, when the vaccine arrives there is a discontinuity in social distancing. The reason is that as soon as the vaccine arrives, all remaining susceptible individuals immediately become immunized. As the vaccine and social distancing are perfect substitutes in avoiding infection but the vaccine is costless, it is optimal to cease social distancing and instead get immunized. In contrast, an individual who is still susceptible at time  $T - \varepsilon$  has a very strong incentive to engage in costly social distancing, because remaining susceptible for just a moment longer ensures that the individual can benefit from perfect and costless protection in the post-vaccine regime.

Last, we note that the earlier the vaccine arrives, the higher is the equilibrium path of social distancing. This in turn causes a lower path of disease prevalence.

## 2. CENTRALIZED DECISION MAKING

We next consider the first-best path of pre-innovation social distancing. The problem to be solved by the social planner is given by

$$\max_{d(t) \in [0,1]} \int_0^T e^{-\rho t} \{S(t)[\bar{\pi} - c(d(t))] + I(t)\underline{\pi} + R(t)\bar{\pi}\} dt + e^{-\rho T} [S(T)V_S + I(T)V_I + R(T)V_R] \tag{26}$$



subject to

$$\dot{S}(t) = -\beta(1 - d(t))I(t)S(t) \tag{27}$$

$$\dot{I}(t) = I(t) [\beta(1 - d(t))S(t) - \gamma] \tag{28}$$

$$\dot{R}(t) = \gamma I(t) \tag{29}$$

$$1 = S(t) + I(t) + R(t) \tag{30}$$

$$I(0) \approx 0, I(0) + S(0) = 1, S(0) > \gamma/\beta \tag{31}$$

Note that in contrast to the problem solved by the individuals under decentralized decision making, the social planner explicitly takes into account that its choice of aggregate social distancing influences the aggregate dynamics of the disease.

Letting  $\lambda_i^C(t)$  denote the costate variables for the state variables  $i = S(t), I(t), R(t)$ , the planner's current-value Hamiltonian is given by

$$H^C = S(t)[\bar{\pi} - c(d(t))] + I(t)\underline{\pi} + R(t)\bar{\pi} \tag{32}$$

$$-\lambda_S^C(t)(1 - d(t))\beta I(t)S(t) \tag{33}$$

$$+\lambda_I^C(t)[(1 - d(t))\beta I(t)S(t) - \gamma I(t)] \tag{34}$$

$$+\lambda_R^C(t)\gamma I(t) \tag{35}$$

A necessary condition for the optimal policy is that

$$\frac{\partial H^C}{\partial d(t)} = S(t) [-c'(d(t)) + \beta I(t) (\lambda_S^C(t) - \lambda_I^C(t))] = 0 \tag{36}$$

For quadratic costs, the socially optimal policy is given by

$$d^*(t) = \beta I(t) [\lambda_S^C(t) - \lambda_I^C(t)] \tag{37}$$

The laws of motion for the costate variables are then

$$\dot{\lambda}_S^C(t) = \rho\lambda_S^C(t) - \frac{\partial H^C}{\partial S(t)} \tag{38}$$

$$= \lambda_S^C(t) [\rho + (1 - d(t))\beta I(t)] - \lambda_I^C(t)(1 - d(t))\beta I(t) - [\bar{\pi} - c(d(t))] \tag{39}$$

$$\dot{\lambda}_I^C(t) = \rho\lambda_I^C(t) - \frac{\partial H^C}{\partial I(t)} \tag{40}$$

$$= \lambda_I^C(t) [\rho + \gamma - (1 - d(t))\beta S(t)] + \lambda_S^C(t)(1 - d(t))\beta S(t) - \lambda_R^C(t)\gamma - \underline{\pi} \tag{41}$$

$$\dot{\lambda}_R^C(t) = \rho\lambda_R^C(t) - \frac{\partial H^C}{\partial R(t)} = \rho\lambda_R^C(t) - \bar{\pi} \tag{42}$$

The transversality conditions are given by the counterparts of (20)-(22) under decentral-

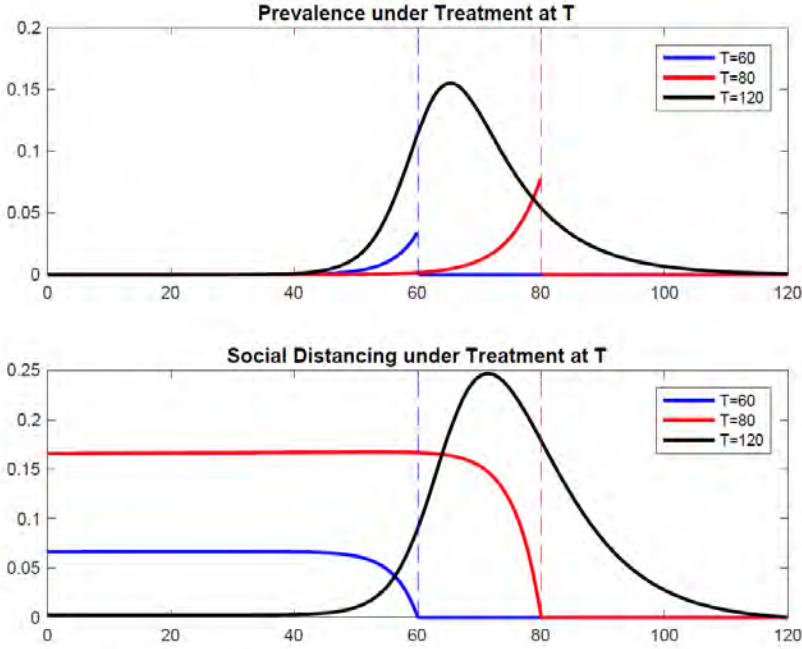


Figure 3: Optimal Prevalence and Social Distancing When Anticipating Treatment.

ized decision making, namely

$$\lambda_S^C(T)e^{-\rho T} = V_S \tag{43}$$

$$\lambda_I^C(T)e^{-\rho T} = V_I \tag{44}$$

$$\lambda_R^C(T)e^{-\rho T} = V_R \tag{45}$$

Before considering the effects of anticipated pharmaceutical interventions, we again consider the no-innovation benchmark. In contrast to individuals' equilibrium behaviour, the social planner cares about the welfare of the entire population, rather than that of a single individual. In practice, this means that the planner will want to keep track of both the evolution of susceptible and infected individuals. Under social planning, it is also the case that disease prevalence is hump-shaped, as was the case under equilibrium social distancing. But in addition, the planner is now sensitive to the wellbeing of the susceptibles, who decrease in measure over time. As in all SIR type models, herd immunity builds up over time, as infected individuals gradually recover and become immune to further infection.

**2.1. The Case of a Perfect Treatment.** Figure 3 shows the dynamics of prevalence and social distancing chosen by the central planner in anticipation of a treatment. Relative to the paths under equilibrium behavior, we note a number of differences, some qualitative and some quantitative. First, under first-best policies, social distancing is overall more extensive than in equilibrium except at the last stage before the innovation. This stems from the fact that the social planner factors in the positive externalities of disease prevention in choosing its optimal policy. This causes disease prevalence to be lower under the social optimum. Second, while the social planner also phases out social distancing completely by the innovation date, it implements a significant and relatively constant level from the outset until the late stages before the treatment arrives. This causes disease prevalence to be monotone increasing throughout the pre-innovation phase. On the innovation date, there is a discontinuous jump down to zero. In contrast, in equilibrium, prevalence can be non-monotone if the innovation date is after the date at which peak prevalence is reached in the no-innovation benchmark.

**2.2. The Case of a Perfect Vaccine.** Figure 4 shows disease prevalence and social distancing chosen by the central planner when anticipating a vaccine. Relative to the equilibrium paths of social distancing, the socially optimal ones have a few notable differences, qualitatively as well and quantitatively. First, optimal social distancing is generally more intensive than the equilibrium level (save for the final stretch before the innovation date). This is because the planner takes into account all external effects that flow from the imposed social distancing. In turn, this causes the socially optimal path of disease prevalence to be significantly lower than its equilibrium counterpart.

Second, while equilibrium social distancing roughly follows the path of disease prevalence, with very low initial levels and a subsequent gradual increase, the socially optimal path features significant social distancing from the outset until the late stages before the arrival of the vaccine. Note that when a vaccine is anticipated, neither optimal nor equilibrium social distancing is phased out before the innovation date, as is the case when a treatment is anticipated. Although the final pre-innovation equilibrium level of social distancing is higher than that chosen by the social planner at the same date, we cannot conclude that individuals engage in too much social distancing. The reason is that because individuals have engaged in less social distancing till that point, disease prevalence is much higher in equilibrium than it would have been under social planning and therefore the two levels of social distancing are not directly comparable.

Recall that when anticipating a treatment, both individuals and the planner decrease social distancing at the end of the pre-innovation phase. In contrast, under the anticipation of a vaccine, the individuals ramp up social distancing while the planner decreases it. This can be explained as follows. Individuals attach a high value to reaching the

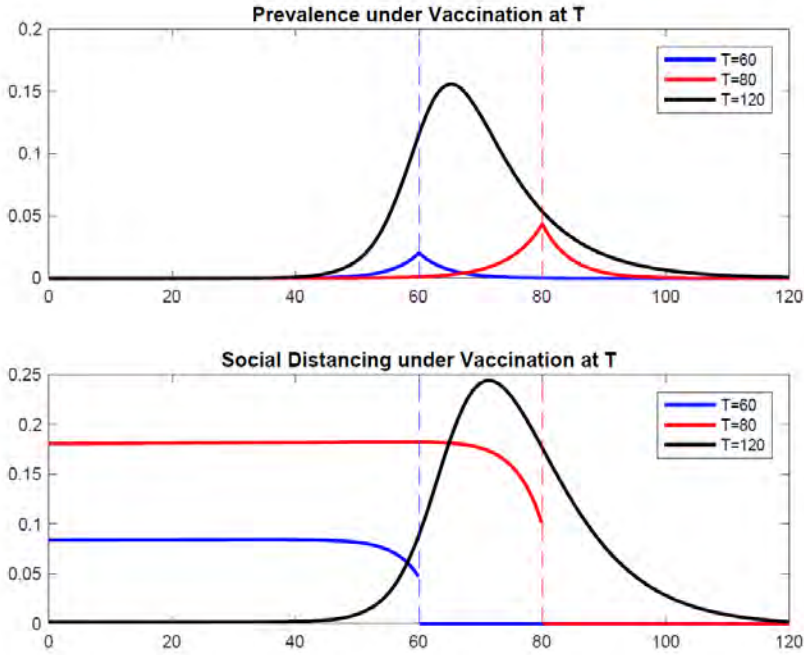


Figure 4: Optimal Prevalence and Social Distancing When Anticipating Vaccination.

post-vaccine phase as susceptibles and therefore ramp up protection till the very last moment. The planner also attaches a high value to this happening, but has managed aggregate prevalence throughout the pre-innovation phase. This means that just before the vaccine arrives, prevalence is relatively modest, allowing it to somewhat decrease social distancing. The optimal paths of social distancing are not phased out, but end at a strictly positive level. This is a testament to the value attached by the planner to increasing the measure of susceptibles that can benefit from the vaccine.

**2.3. Aligning Private and Social Incentives.** As is often the case in economic models of infection control, there is a wedge between private and social costs and benefits of social distancing. The reason is that individuals do not internalize the positive external effects that flow from their efforts to avoid infection. As shown in Rowthorn and Toxvaerd (2020), there are incentive schemes that correct for such external effects and implement the socially optimal outcomes. These can be subsidy/penalty schemes that are attached either to the protective behavior itself (like furlough schemes, which encourage people to stay at home rather than to go to work) or to the health status of individuals (like a reward for remaining uninfected). Often, such schemes are very complicated and must

be modified as the epidemic progresses, which severely limits their practical use. In contrast, in the present setup there is a scheme that is very simple to implement and which may provide individuals some incentives to self-protect. Under this scheme, once the vaccine becomes available, individuals who get vaccinated also receive a reward. As the health state of an individual is known in our model, only those who have never been infected by date  $T$  will get vaccinated. This means that only at-risk individuals are eligible. This scheme achieves two separate goals. First, it incentivizes vaccine uptake, itself an activity that has strong positive externalities (see Chen and Toxvaerd, 2014). Second, it incentivizes social distancing in the pre-vaccination phase by rewarding those who make it through to the vaccination phase having never been infected. This scheme is both easy to communicate and to implement. It should be noted that this is a decidedly second-best policy and that it is unlikely to be possible to implement the first best through this scheme. The incentive scheme that implements the first-best outcome modifies the entire path of the costate variables. In contrast, the proposed second-best scheme only fixes the value of the costate variables at date  $T$ .

### 3. DISCUSSION

In this paper, we have considered a stylized model of social distancing to analyze the effects of forthcoming pharmaceutical innovations on pre-innovation social distancing. We show that decision makers react differently to anticipated treatments and vaccines. When anticipating a vaccine, it is important for the decision maker to reach the post-innovation phase while still susceptible, for otherwise the vaccine has no value. This means that as the arrival date of the vaccine approaches, the risk-reducing efforts are increased over time till the individual is effectively immunized. In contrast, when anticipating a treatment, reaching the post-innovation phase while susceptible is less critical. This is because someone who is (still) infected by the time that treatment becomes available can still benefit from treatment, therefore reducing the value of social distancing just before it becomes available. Thus social distancing is in this case entirely phased out, ceasing completely by the time the treatment arrives.

Although antiviral treatment will have an important role to play in managing the epidemic, effective mass vaccination is likely to make the most difference on aggregate. Our analysis makes an important point and offers a clear policy recommendation. The anticipated arrival of an effective vaccine should not be taken as a license to loosen restrictions and reduce social distancing. In contrast, individuals and public health authorities should redouble their efforts to reduce the number of new cases to ensure that people may actually benefit from the protection afforded by an effective vaccine once it arrives.

In the main analysis, we have for simplicity assumed that treatments and vaccinations were both costless and perfect. This allowed us to express the post-innovation value

functions and thus the transversality conditions entirely in terms of model parameters. We will briefly discuss how our main insights change when the treatment or vaccine is imperfect.

In the case of imperfect treatment, there are several effects to consider. Assume that treatment, rather than inducing instant recovery, only does so with a delay. This is the formalization used in Toxvaerd and Rowthorn (2020). Since the treatment is costless, it will be taken up by any infected individual as soon as it becomes available. Thus the post-innovation value function will be a composite expression that takes into account both the flow payoff  $\underline{\pi}$  earned while infected and the flow payoff  $\bar{\pi}$  earned when recovered, suitably weighed by the rate at which the individual recovers under treatment. Thus relative to the case of a perfect treatment, the value function  $V_I$  is unambiguously lower. Turning to individuals who reach the post-innovation phase as susceptibles, it's clear that becoming infected now involves switching to a health state where the individual earns flow payoff  $\rho V_I$  rather than  $\bar{\pi}$ , as is the case when treatment induces instant recovery. For that reason, we have that  $\rho V_S < \bar{\pi}$ . In other words, the value of reaching  $T$  as susceptible has now decreased. This means that even though an imperfect treatment now becomes available, the individual must still engage in costly social distancing. The value  $V_R$  remains unchanged. Since two of the transversality conditions change in response to the imperfections in treatment, it is not possible in general to say what the net effect on pre-innovation social distancing is, without adding more structure.

In the case of an imperfect vaccine, the effects are simpler to describe. Assume that once a vaccine is taken, it reduces the infectivity parameter  $\beta$  to  $\sigma\beta$  where  $\sigma \in [0, 1]$  is the failure probability of the vaccine. This formalization nests two extreme cases. When  $\sigma = 0$ , we are back in the perfect vaccine case at which no further social distancing is chosen after date  $T$ . When  $\sigma = 1$ , then the vaccine is completely useless and the innovation date  $T$  has no impact on social distancing; the paths of social distancing and prevalence mirror those of the  $T \rightarrow \infty$  benchmark. For any intermediate value of the failure probability  $\sigma$ , the nature of the individual's problem is the same before and after the innovation date, but the post-innovation infectivity rate is now reduced because of the partial protection afforded by the vaccine. But relative to the perfect vaccine case, the post-innovation value function  $V_S$  is unambiguously lower as the individual will have to still engage in costly social distancing after vaccination, while the value functions  $V_I$  and  $V_R$  remain unchanged. This means that the transversality conditions are altered to make it less valuable to enter the post-innovation phase as a susceptible. This is reflected in a lower incentive to engage in social distancing ex-ante-innovation.

Last, it now seems increasingly likely that immunity gained by recovered individuals wanes over time, although the extent of this waning is not yet fully understood. While we

have conducted our analysis within the framework of the SIR model, in which recovered individuals obtain permanent immunity to re-infection, our main insights are robust to the possibility of waning immunity. While waning immunity changes the underlying dynamics of the disease, the non-stationarity introduced by the anticipation of pharmaceutical innovations remains, as does the incentives to prevent infection in the pre-innovation phase.

## REFERENCES

- [1] Auld, M. C. (2003). Choices, Beliefs, and Infectious Disease Dynamics, *Journal of Health Economics*, 22(3), 361-377.
- [2] Caputo, M. R. (2005). Foundations of Dynamic Economic Analysis: Optimal Control Theory and Applications, *Cambridge University Press*.
- [3] Chen, F. and F. Toxvaerd (2014). The Economics of Vaccination, *Journal of Theoretical Biology*, 363, 105-117.
- [4] Eichenbaum, M. S., S. Rebelo and M. Trabandt (2020). The Macroeconomics of Epidemics, *mimeo*.
- [5] Giannitsarou, C., S. Kissler and F. Toxvaerd (2020). Waning Immunity and the Second Wave: Some Projections for SARS-CoV-2, *CEPR Discussion Paper DP14852*.
- [6] Keeling, M. J. and P. Rohani (2008). Modeling Infectious Diseases in Humans and Animals, *Princeton University Press*.
- [7] Lourenco, J., R. Paton, M. Ghafari, M. Kraemer, C. Thompson, P. Simmonds, P. Klenerman and S. Gupta (2020). Fundamental Principles of Epidemic Spread Highlight the Immediate Need for Large-Scale Serological Surveys to Assess the Stage of the SARS-CoV-2 Epidemic, *medRxiv*.
- [8] Makris, M. (2020). Covid and Social Distancing with a Heterogenous Population, *University of Kent Department of Economics Working Paper Series No: 2002*.
- [9] McAdams, D. (2020). Nash SIR: An Economic-Epidemiological Model of Strategic Behavior During a Viral Epidemic, *Covid Economics*, 16, <https://cepr.org/sites/default/files/CovidEconomics16.pdf#Paper6>.
- [10] Bognanni, M., D. Hanley, D. Kolliner and K. Mitman (2020). Economics and Epidemics: Evidence from an Estimated Spatial Econ-SIR Model, *IZA DP No. 13797*.
- [11] Rowthorn, R. and F. Toxvaerd (2020). The Optimal Control of Infectious Diseases via Prevention and Treatment, *Cambridge-INET Working Paper Series No: 2020/13*.

- [12] Toxvaerd, F. (2019). Rational Disinhibition and Externalities in Prevention, 2019; *International Economic Review*, 60(4), 1737-1755.
- [13] Toxvaerd, F. (2020). Equilibrium Social Distancing, *Covid Economics*, 15, <https://cepr.org/sites/default/files/CovidEconomics15.pdf#Paper5>.
- [14] Toxvaerd and Rowthorn (2020). On the Management of Population Immunity, *Bennett Institute Working Paper*.



# Business restrictions and Covid-19 fatalities<sup>1</sup>

Matthew Spiegel<sup>2</sup> and Heather Tookes<sup>3</sup>

Date submitted: 5 November 2020; Date accepted: 5 November 2020

*We hand-collect a time-series database of business closures and related restrictions for every county in the United States since March 2020. We then relate these policies to future growth in deaths due to Covid-19. To our knowledge, ours is the most comprehensive database of U.S. Covid-19 business policies that has been assembled to date. Across specifications, stay-at-home orders, mandatory mask requirements, beach and park closures, restaurant closures, and high risk (Level 2) business closures are the policies that most consistently predict lower 4- to 6- week-ahead fatality growth. For example, baseline estimates imply that a county with a mandatory mask policy in place today will experience 4- week and 6- week ahead fatality growth rates that are each 1% lower (respectively) than a county without such an order in place. This relationship is significant, both statistically and in magnitude. It represents 12% of the sample mean of weekly fatality growth. The baseline estimates for stay-at-home, restaurant and high-risk business closures are similar in magnitude to what we find for mandatory mask policies. We fail to find consistent evidence in support of the hypothesis that some of the other business restrictions (such as spa closures, school closures, and the closing of the low- to medium- risk businesses that are typically allowed in Phase I reopenings) predict reduced fatality growth at four-to-six- week horizons. Some policies, such as low- to medium- business risk closures may even be counterproductive. To address potential endogeneity concerns, we conduct two tests. First, we exploit the fact that many county regulations are imposed at the state-level through Governors' executive orders. Following the intuition that smaller counties often inherit state-level regulations that are intended to*

1 We would like to thank Timothy Akintayo, William Babalola, William Cook, Nora Draper, Golden Gao, Patrick Hayes, Kevin Hong, Aykhan Huseynov, Ryan Jennings, Christine Liaw, Gen Li, Emily Lin, Natalie Lord, Paul Nash, Daniel Nguyen, Joojo Ocran, Preston Smith, Mingjun Sun and Crystal Wang for excellent research assistance.

2 Professor of Finance, Yale School of Management.

3 Professor of Finance, Yale School of Management.

Copyright: Matthew Spiegel and Heather Tookes

*reduce transmission and deaths in more populous regions, we remove the 5 most populous counties in each state from the sample. In the second test, we match counties that lie near (but not on) state borders to counties in different states that are also near (but not on) state borders and are within 100 miles of that county. Absent policy differences, these nearby counties should see similar trends in virus transmission; making them good controls. We continue to find that stay-at-home, mandatory masks, beach and park closures, restaurant closures, and high risk business closures all predict declines in future fatality growth.*

Worldwide, the Covid-19 pandemic has taken more than one million lives to date. In an attempt to slow this loss of life, policy-makers around the globe have introduced a wide range of interventions. But there is still widespread disagreement about which policies are effective. Given concerns about the economic costs of widespread business and social restrictions, it is crucial that policy-makers make informed trade-offs. This paper aims to shed empirical light on this issue. We construct a time-series database of business closures and related restrictions for every county in the United States since March 2020 and we relate these policies to future growth in deaths due to Covid-19. County-level restrictions are the unit of interest because a county is the finest level of detail for which daily death counts are available. To our knowledge, ours is the most comprehensive database of U.S. Covid-19 business restrictions that has been assembled to date.

State and county governments in the US have introduced a variety of policies to reduce virus transmission and deaths. These include: stay-at-home orders; general business closures; specific closures targeting bars, restaurants, gyms and spas; no visitation policies at nursing homes; mandatory mask orders; park and beach closures; and limits on the size of gatherings. We collect start and end dates (and policy restarts, where applicable) for each of these and we use them to relate current policy interventions to future growth in fatalities. The variety of tools available to regulators, heterogeneous adoption and staggered timing that we observe in the data can help us understand the role of policy. Recent papers report somewhat conflicting results on how effective various policies have been. For example, Courtemanche et al. (2020) find evidence that some government-imposed restrictions have aided in Covid-19's control, while Atkeson et al. (2020) suggest that they may not. Another strand of literature seeks indirect evidence of the impact of policies on health by looking at changes in mobility (e.g., Dave et al., 2020a; Nguyen et al. 2020 both report evidence that restrictions do decrease mobility). Many of these recent papers focus on policies introduced at the state level (e.g., Abouck and Heydari, 2020; Friedson et al., 2020; Dave et al., 2020) or they rely on cross-country evidence (e.g. Askatas, Tatsiramos and Verheyden, 2020), where social norms, healthcare infrastructure, and demographics are likely to vary widely. We analyze counties rather than states (or countries) so that we can exploit the granularity of the available fatality data as well as county location and relative size within a state (to improve the overall interpretation of our findings). We focus on fatalities rather than cases because of substantial variation in testing capacity over time and region. We examine a number of specifications that are designed to deal with the twin issues of potential false positives and false negatives. Given the progression of the virus (i.e., days from

exposure to infection to hospitalization and death), we focus most of the discussion on the 4- to 6- week ahead horizons because these are more likely to capture the true effects of current policies.

Overall, we find that stay-at-home orders, mandatory mask requirements, beach and park closures, restaurant closures, and high risk (Level 2) business closures are the policies that most consistently predict lower 4- to 6- week-ahead fatality growth. These relationships are significant, both statistically and in magnitude. For example, baseline estimates imply that a county with a mandatory mask policy in place today will experience 4- week and 6- week ahead fatality growth rates that are each 1% lower than a county without one. These reductions represent 12% of the sample mean of weekly fatality growth. Stay-at-home policies, restaurant closures, beach and park closures, and high risk business closures are all associated with reductions in fatalities that are similar in magnitude. While we do find some evidence that closing gyms and limiting gatherings to 10 people also predict lower fatality growth, we fail to find consistent evidence in support of the hypothesis that closing spas, schools, and general low to medium-risk businesses reduce fatality growth.<sup>1</sup> In fact, closing retail establishments and relatively low risk businesses (those allowed to reopen in a typical Phase 1 reopening) appears to have been counterproductive. This may indicate substitution by the public into other types of activities that increase transmission.

Any study that tries to link policy interventions and outcomes has to somehow distinguish between correlation and causation. Policies that are put in place near the natural peak of the outbreak will be followed by mechanical declines in death rates and can lead to false positives. Policies that only partially mitigate death rates may yield false negatives. We try to deal with the false positive and negative issue through a variety of methods. First, all of our regressions control for the current level of deaths per capita, lagged fatality growth rates, and a number of demographic and weather-related variables. Thus, our regressions predict differences in the future growth in fatalities in two counties that today have the same current level of deaths per capita, the same recent trajectory in deaths and similar demographics and climate. They differ in that their governments have introduced different policy interventions.

<sup>1</sup>These are businesses that are allowed to open in what many states call Phase 1. Businesses in this category vary according to the counties' definitions of risk, but the often include retail outlets, offices, outdoor dining at restaurants, childcare services, and manufacturing facilities. Phase 2 typically expands the list to barbers, spas, gyms and other personal care services.

Second, we use the fact that many of the county regulations that we observe are imposed at the state-level through Governors' executive orders. Even if we assume optimal policy-setting by the states, it is likely that what is optimal for some counties within a given state is not optimal for others. Moreover, a state's most populous areas are likely to be an important focus of state regulators. Following this intuition, we remove the top 5 most populous counties in each state from the sample and we repeat the analysis. The idea is that smaller counties often inherit state-level regulations that are intended to reduce transmission and deaths in more populous regions of each state. To date, we have seen legal challenges to state regulations brought by rural counties in Pennsylvania, reports of defiance of state mandates in some California and Texas counties, and requests by some North Carolina and Maryland counties for looser state restrictions. All of this suggests less populous areas are not driving policy. This lets us examine potentially "out of equilibrium" policies in the more rural areas to help with identification.<sup>2</sup> When we do so, we continue to find that masks mandates, masks for employees, beach and park closures, and gym closures are all significantly negatively related to fatality growth, both 4- and 6- weeks ahead. In addition, stay-at-home orders, restaurant closures, bar closures and the closure of higher risk businesses (those typically associated with Phase 2 reopenings) predict lower fatalities 6 weeks out. Other policies, such as closing schools and some higher risk businesses closures (those businesses typically associated with Phase 3 reopenings) fail to yield consistently negative and statistically significant parameters. Limiting gatherings to between 11 and 100 people and closing low risk businesses appear to be counterproductive. The evidence on gatherings is somewhat surprising. It may be that limits at 100 simply encourage smaller close contact gatherings.

Finally, we conduct matched-sample tests in which we focus on policy variation near state borders. However, unlike typical designs that exploit discontinuities by focusing on differences between counties that lie on state boundaries, we focus on the subset of counties that lie near, but not on, a state border. For expositional purposes, we refer to these counties as "near-border" counties. We examine these near-border counties (as opposed to on-the-border counties) to reduce spillover effects. These spillovers come in two forms. First, if a neighbor's policy reduces disease

<sup>2</sup> See e.g., County of Butler, et al. v. Thomas W. Wolf, et al. (Civil Action No. 2:20-cv-677); "Newsom threatens California counties that defy coronavirus rules as cases spike" San Francisco Chronicle 6/24/2020; "North Texas counties are declaring themselves 100% open for business despite COVID limits," Fort-Worth Star Telegram 6/19/2020; "Governor to Henderson County: Decision to reopen economy will be based on experts, officials", Times-News, 5/4/2020; and "Commissioners to Hogan: Let us reopen" Herald Mail Media, 5/22/2020.

transmission in its jurisdiction, it will also lower the transmission level across the border and thereby reduce fatalities in the county of interest. Second, a restrictive policy in one county (such as bar closures) and a less restrictive one in a neighboring county may induce residents of the county with the tighter restriction to travel to and engage in otherwise prohibited activities in the less restrictive one. These spillovers can cause direct comparisons between the counties that share a border to generate false negatives and false positives. We try to mitigate this problem by putting at least a one-county buffer between any near-border county in our sample and its neighboring state.

In the near-border county analysis, potential matches must be in another state and have a population centroid within 100 miles of the target county's population centroid. Among this group, the county that is closest to the county of interest across several population and weather characteristics (based on a Euclidean measure) is then selected. Once a match is selected, the near-border neighboring county's policies are added as control variables in the predictive regressions. The underlying assumption is that differences in policies across state borders are likely due to differences in opinion (which introduces exogenous error). Under these assumptions, we find that stay-at-home orders, mandatory masks, park and beach closures, and some gathering limits predict lower future fatality growth at both the 4- and 6- week horizons. Policies restricting nursing home visits, restaurant closures, some of the tighter gathering limits, and closures of higher risk businesses predict lower future fatality at either the 4- or 6-week horizons. Gym closures, spa closures, school closures, as well as general low-risk business closures do not appear to curb fatality growth rates. Low risk business closures again seem counterproductive.

In addition to current deaths per capita and lagged growth rates, we include a number of additional controls variables to sharpen the overall interpretation. We control for population demographics, including age, race, and the fraction of the population residing in nursing homes. We also control for per capita income, housing and population density, extreme weather conditions (which might drive the population indoors), time since a county's first reported case, and time since March 1, 2020 to control for potential improvements over time in the management and treatment of Covid-19. Some of the control variables are of independent interest. For example, our evidence is consistent with findings in the literature on demographic disparities in Covid-19 (e.g., Millitt et al. 2020; Moore et al. 2020), with higher growth in deaths in counties with a greater proportion of

Black and Hispanic individuals in the population, in counties with lower per-capita income, and in those counties with high rates of some comorbidities such as diabetes. We also find that extreme weather has additional explanatory power.

We leave policy-makers with the unenviable task of balancing public health concerns with the costs and benefits associated with the various restrictions that have been considered. Our primary goal is to provide data that can inform the calculation. Still, we also emphasize that mask mandates appear to be effective in every specification and are accompanied by relatively low economic and social costs. The evidence that masks are beneficial is growing rapidly (Howard et. al (2020) provide a review of the literature<sup>3</sup>), but our paper is the first (to our knowledge) to compare its effectiveness to such a wide range of alternative interventions. Other policies come at higher cost. In those cases, we hope our results can help policy makers better assess the necessary tradeoffs.

The paper proceeds as follows. Section 2 provides a description of the data and county-level policy variables. Section 3 relates policies to future  $t$ -week ahead growth rates in fatalities. Section 4 concludes.

## 2. Data

The main goal of this paper is to relate weekly growth in fatalities to policies restricting businesses and related activities. The data come from a variety of sources, which we describe below.

### 2.1 Growth in New Deaths

The fatalities data are from USAFacts.org, which disseminates daily U.S. deaths and confirmed cases at the county level. For each week  $t$ , we examine the relationship between policies in place and the future growth in new deaths due to Covid-19. The dependent variable of interest is the  $t$ -week ahead growth in fatalities. Due to potential irregular reporting following weekends, we focus the analysis on Wednesday-to-Wednesday weekly growth rates, calculated as:

$$Growth(t) = \ln\left(\frac{Deaths_{i,t}}{Deaths_{i,t-1}}\right), \text{ where } Deaths_{i,t} \text{ is the total cumulative deaths in county } i \text{ at the end of}$$

week  $t$ .

We control for 6 weeks of lagged weekly growth rates in all regressions. Because the growth variable is undefined if a county has zero deaths, we begin the analysis 6 weeks after each county's

<sup>3</sup> See also Abuluck et al (2020) and Lyu and Wehby (2020).

first reported death.<sup>4</sup> The last forecast date is September 1, 2020, which means that we predict fatality growth through October 13, 2020. We end the forecast period on September 1, 2020 in part to avoid trying to estimate how school re-openings may impact overall transmission and ultimately fatalities. In many states, school re-openings have been occurring at the district level. In some cases, these openings were reversed following infections, and then reopened after a quarantine period. All of this introduces substantial within-county and between-county variation that we have not gathered data on and for which we cannot control in the regressions. Moreover, school reopenings vary widely in their implementation (e.g., some schools following various hybrid models, some fully in-person), adding further complications to the analysis.

## 2.2 Policies

We collect the county-level restrictions through internet searches for county and state orders (usually available on their websites) as well as news publications. When the state document that imposes an order is found but does not clarify the date on which a restriction becomes effective or ends, we conduct a search of news articles to determine the start or end date. Because news reports can provide inconsistent information, we try to find at least two articles to confirm the date.<sup>5</sup>

Table 1 shows the full list of policies that we track. In many cases, the date that a particular order goes into effect is collected from Governors' executive orders and impacts all counties within a given state. In some cases, county commissioners issue their own orders. In a few others, state courts overturned some or all of the regulations. When gathering the data, unless a state order applies to every county and negates all of the individual county orders, the date of the state's order is entered only into the counties to which it applies. A county is recorded as having an order in place on a particular date if either the county or the state imposes that order on or before the date in question and neither the county nor the state is recorded as having ended the order. A court order ending

<sup>4</sup> In the Appendix, we provide robustness analysis in which we replace weekly death growth rates with the change in deaths per capita from week  $t-1$  to week  $t$ . This allows us to preserve all data for counties with zero deaths to date. While the estimated magnitudes can differ with the alternative definition of fatality growth and the statistical significance increases with this larger sample size, many of our main findings are qualitatively similar.

<sup>5</sup> To further improve the data's accuracy, most of the entries have been verified two or three times by different individuals.



a restriction is entered into the counties to which it applies on the date that the court order goes into effect.

In addition to county and state government websites, emails were sent to all counties (usually public health divisions, where such contact information is listed on county websites) to confirm the restrictions and dates that in our data. In most cases, when we heard back, respondents provided confirmation that the information was either correct or that our start or end date was off by less than one week.<sup>6</sup> Whenever we receive corrections, we replace our data with the data from the email response.

### 2.3 Other Control Variables

We control for several demographic variables known to be associated with Covid-19 fatalities. These include: the fraction of the population that are Black, Hispanic, Asian, Native American and other races (*Black*, *Hispanic*, *Asian*, *Native American and Other*, respectively); fraction of the population that is over the age of 65 (*Age65plus*) and over the age of 85 (*Age85plus*); the fraction of the population living in nursing home facilities (*Nursing Home Pop.*); per capita income; the fraction of the population with diabetes, are obese or who smoke (*Diabetes*, *Obesity*, *Smokers*, respectively); density of the population, defined as total population divided by the land square miles of the county; and housing density. The demographic controls that come from the U.S. Census are based on the most recent year for which data are available. Per capita income is from the Bureau of Economic Analysis. Finally, county health data on diabetes, obesity and smoking comes from County Health Rankings & Roadmaps (see <https://www.countyhealthrankings.org/> for additional details).

We also control for weather conditions, given the evidence that indoor transmission is more likely than outdoor spread and that climate has the potential to play a role (e.g., Baker et al. (2020); Quian et al. (2020); Carlson et al. (2020)). We introduce five weather variables to capture the propensity of people to find outdoor air uncomfortable and to seek temperature-controlled indoor environments: *HotHumidWeekdays*, equals 1 if the average weekday temperature is above 80 degrees and the average weekday dew point is above 60; *HotHumidWeekends*, the percentage of weekend days

<sup>6</sup> At the time of this writing, we received replies from 240 counties. In 61.3% (147) of the responses, there were no suggested changes. When we received changes, they were: additions to the list of orders (18.3 percent of responses); date corrections within one week of the original week (4.2%); and date corrections exceeding 7 days of the original week (2.9%). The remainder (13.3 percent of the responses) contained other information, such as links (without further clarification) to orders we had already parsed.

in which the average weekend temperature is above 80 degrees and the average weekend dew point is above 60; *ColdWeekdays*, the percentage of weekdays (Monday through Friday) in which the average temperature is below 60 degrees; *ColdWeekends*, the percentage of weekend days in which the average temperature is below 60 degrees; and *AverageTemperature*, the absolute value of the difference between the average daily temperature for the week and 70 degrees. The weather data are at the station level and are obtained from the National Climatic Data Center. We take the daily average of each temperature and dew point variable from the 3 weather stations that are closest to the coordinates of the county's population centroid.

Finally, we consider the number of days since the county's first reported case of Covid-19 and the number of days since March 1, 2020. The latter is included to control for potential improvements in the treatment and management of the virus over time. Table 2 summarizes all of the fatality, policy, and control variables that we use in the analysis.

### 3. Empirical Analysis

#### 3.1 Forecasting $t$ -week-ahead fatality growth

We begin with a baseline specification, in which we forecast one-, two-, four- and six- week ahead fatality growth rates as a function of: current and lagged deaths per capita; a vector of lagged weekly death growth rates; the interaction between lagged growth rates and the current level of deaths per capita; time since the first positive Covid-19 case in the county; and the time since March 1, 2020. We also include the controls for current weather conditions and county demographics. The results are in Table 3.

From Column (1) of Table 3, we observe that weekly fatality growth rates are positively autocorrelated at up to approximately 4 lags, are increasing with the current level of fatalities, and decreasing in the lagged level of fatalities and with the interaction of current fatalities and past growth rates (i.e., when recent growth rates and current deaths per capita are high, future growth in deaths is predicted to be lower). We also find that the growth in deaths is generally higher in climates where temperatures are uncomfortable (i.e., they deviate more from 70 degrees) and on hot and humid weekdays. Colder temperatures on weekdays and weekends appear to dampen the relationship between uncomfortable weather and deaths. For whatever reason, people may interact less during colder weather. We find that counties with greater Black, Hispanic and Native American populations experience greater fatality growth than other counties. Counties with larger nursing

home populations<sup>7</sup>, higher population densities and more residents who are obese or smoke also see greater future growth in fatalities. Per capita income predicts lower future fatalities. We also find that housing density is associated with lower future fatalities. It may be that urban areas with more dense housing are also those with better medical care or better adherence to distancing practices.<sup>8</sup>

From this baseline specification, we add policy variables so that we can examine the main economic question of interest. The goal is to hold the constant the current level and recent trajectory of new deaths so that we can compare the future growth in fatalities in counties with and without various restrictions in place at time  $t$ .

### 3.2 Baseline Analysis: Policy interventions and t-week ahead weekly fatality growth

The main regression specification, in which we forecast the  $t$ -week ahead weekly growth in fatalities ( $Growth(t+x)$ ) is as follows.

$$\begin{aligned} \ln\left(\frac{Deaths_{i,t+X}}{Deaths_{i,t+X-1}}\right) &= \alpha + \beta_1 Policies_{i,t} + \sum_{\tau=0}^6 \beta_{2,t-\tau} DeathsPerCapita_{i,t} \\ &+ \sum_{\tau=1}^6 \beta_{3,t-\tau} \ln\left(\frac{Deaths_{i,t-\tau}}{Deaths_{i,t+\tau-1}}\right) + \sum_{\tau=1}^6 \beta_{4,t-\tau} \ln\left(\frac{Deaths_{i,t-\tau}}{Deaths_{i,t+\tau-1}}\right) * DeathsPerCapita_{i,t} \\ &+ \beta_5 * DaysFirst + \beta_6 * t + \beta_6 * Controls + \varepsilon_{i,t} \end{aligned} \quad (1)$$

In the calculated growth rate,  $X$  is set to 1, 2, 4 or 6 depending on the specification. *Policies* is the vector of policies in place in county  $i$  during week  $t$ , as defined in Table 1; *DaysFirst* is the number of days since the first case is reported in the county;  $t$  is the number of days since the beginning of the sample period (March 1, 2020), and *Controls* are a vector of population demographics and other county-level control variables, as shown in Table 2. All standard errors are clustered at the county level.

The specification in Equation (1) uses information available through week  $t$  to forecast the  $X$  week-ahead weekly growth rate in fatalities. We focus on the relationship between fatalities and policies in place as of week  $t$ , after controlling for the current level of deaths per capita, the recent trajectory of growth rates, and a number of demographic and other controls. According to the

<sup>7</sup> The fraction of the population residing in nursing home residents is more important than the fraction of the population that is elderly in predicting future fatalities.

<sup>8</sup> See e.g., Hamidi, Sabouri and Ewing (2020).

CDC, the median incubation period from exposure to symptom onset is 4-5 days. Among people with severe disease, the median time to ICU admission from the onset of illness or symptoms ranges from 10-12 days.<sup>9</sup> For patients admitted to the hospital and who do not survive, Lewnard et al. (2020) report a median duration of hospital stay of 12.7 days (ranging from 1.6 to 37.7). Given the progression of the virus, we focus the discussion on the 4- to 6- week ahead horizons because these are more likely to capture the true effects of current policies than the 1- and 2-week ones. Links between policies and short-term fatality growth could reflect autocorrelation in policies (i.e., we could observe a link between a given policy and week-ahead deaths because that policy remains in place in a county for some time). But they might also indicate existing trends or show when a policy is perhaps coincidental or even reactive. The longer-horizon forecasts are less likely to reflect trends or reactive policies.

Results from the above analysis are in Table 4. Columns (3) and (4), in which we predict 4- and 6- week ahead weekly fatality growth, are of greatest interest. Policies that have negative and significant coefficient estimates (i.e., predict lower future fatality growth) at both 4- and 6- weeks are: employee mask recommendations, mandatory mask use for the general population, restaurant closures, gym closures, and beach and park closures. Those with negative and significant coefficients at one of these horizons are: stay at home orders, no elective procedures, limiting gatherings to 10 and high-risk business closures (Risk Level 2).<sup>10</sup>

Among the policies with statistically significant and negative coefficients, it is possible that some of the coefficients reflect existing trends that are not captured in the lagged fatality controls. We compare the findings for short- and longer- horizon fatality growth to help with the overall interpretation. If the week 1 and week 2 coefficient values and significance levels are different from what we see in weeks 4 and 6, then it is less likely that the findings at the horizons of interest reflect a trend. In Table 4, the estimated coefficients on stay-at-home, employee masks, mandatory mask policies, beaches and park closures, elective procedures, restaurant closures, and Risk Level 2 closure policies are all more negative and/or more significant as we lengthen the horizon from 1- and 2- weeks to 4- and 6- weeks. This strengthens the conclusion that these policies are likely to reduce

<sup>9</sup> <https://www.cdc.gov/coronavirus/2019-ncov/hcp/clinical-guidance-management-patients.html>.

<sup>10</sup> Bar closures also show a negative and significant coefficient at the 6-week horizon, but that coefficient is positive and significant at 4 weeks. It may take time for policies that could impact transmission among the bar-going population to impact deaths in those more vulnerable to the virus. Also note that bars are closed whenever restaurants are closed, but they often stay closed longer.

fatality growth. The employee mask, no elective procedures, and high-risk business closure (Risk Level 2) coefficients even switch signs as we vary the horizon.

Table 4 shows that some policies are associated with higher future fatality growth. State of emergency declarations and spa closures show significant coefficient estimates for both 4- and 6-weeks. The state of emergency findings are consistent with what one might expect since these declarations indicate that a policy maker expects to need resources to manage a future crisis. The spa closure findings are more surprising, but could indicate a movement of these services into other less safe settings. Policies where the estimated coefficient is positive and significant at either the 4- or 6-week horizon are: gathering limits set at 100, closing low- to medium risk businesses (Risk Level 1) and re-openings reversed. In most of these cases, the coefficients become more positive and significant as the forecast horizon is lengthened. The Risk Level 1 and re-opening reversal policies are consistent with one another since lower risk businesses are often closed when reopenings are reversed. The findings may indicate that broad business closure policies are actually counterproductive. The gathering limit finding is somewhat surprising, especially in light of the negative relationship between the tighter gathering variable and future deaths. It may be that gathering limits set at 100 encourage larger-than-ideal small group events.

Nursing homes are a major source of coronavirus fatalities.<sup>11</sup> The finding in Table 4 that banning family nursing home visits did not lead to a strong reduction in future fatalities seems inconsistent with what we know about the number of nursing home deaths relative to the rest of the population. However, all of the regressions control for the number of nursing home residents relative to total population (coefficients on this variable are positively and significant at all horizons, as shown in Table 3). It may be that most of the nursing home cases resulted from unregulated factors rather than family visits. As documented in Chen, Chevalier and Long (2020) staff and service people frequently travel between nursing homes and they may have been the primary spreaders of infections.

Because the policy variables are dummies, the estimated magnitudes of the coefficients in Columns (3) and (4) of Table 4 are directly comparable. For example, the estimated coefficients of  $-0.010$  and  $-0.017$  on mandatory masks and employee masks, respectively, are significant both statistically and in magnitude (they imply reductions in fatality growth that are between 12 and 20%

<sup>11</sup> As of October 30, the New York Times reports that approximately 38% of U.S. Coronavirus deaths have been linked to nursing homes. <https://www.nytimes.com/interactive/2020/us/coronavirus-nursing-homes.html>

of the sample mean fatality growth of 0.085). These are in line with the magnitudes of the estimated coefficients on stay-at-home orders (-0.010), restaurant closures (-0.011), gym closures (-0.013), and Risk Level 2 business closures (-0.014). This type of comparison useful because the costs of these policies are likely to differ substantially.

Below, we summarize the main findings from Table 4. The table lists policies with significant estimated coefficients at the 4- and 6- week horizons. We consider a particular result “significant” if we observe a statistically significant coefficient at one or both of the horizons (i.e., 4-week and/or 6-week) and where we do not observe a statistically significant coefficient of the opposite sign over either horizon. The policies in bold indicate a change sign or change in significance when we vary the horizon from short (1- to 2- weeks) to longer.

**Summary of Findings in Table 4. Relationships between policy variables and future fatality growth.**

	<b>Significant at 4 or 6 Week Horizon</b>	<b>Significant at both 4 and 6 Week Horizons</b>
<b>Negative, Significant</b>	<b>Stay-At-Home, Risk Level 2 Closed, No Elective Procedures, Gatherings limited to 10</b>	<b>Employee Masks, Restaurants Closed, Mandatory Masks, Gyms Closed, Beaches or Parks Closed</b>
<b>Positive, Significant</b>	<b>No gatherings over 100, Risk Level 1 Closed, Reopenings Reversed</b>	State of Emergency, Spas Closed

**Bold** indicates a change sign or change in significance when we vary the horizon from short to longer.

**3.3 Removing counties likely to be the focus of regulators (the state’s most populous counties)**

While suggestive, the evidence in Table 4 does not establish a causal link between policies and future fatality growth rates. The overall interpretation is blurred by the fact that some policies may be put in place near the natural peak of the outbreak and therefore, mechanical declines in death rates can coincide with policy introductions. Controlling for current and past fatality and growth in fatalities, as well as varying the horizon over which we predict future weekly deaths helps with the

interpretation. An ideal experiment would take pairs of identical counties, impose regulation  $R$  in one county and not the other, and then measure differences in future fatalities across the “treated” counties versus those that are untreated. Because we do not have access to this type of experiment, we use the fact that many county regulations are imposed at the state level (through Governors’ orders) to help with the identification. If we assume that state regulators primarily focus on the state’s most populous counties, then smaller counties inherit state-level regulations that are intended to reduce transmission and deaths in the more populous regions of each state (allowing us to observe “out-of-equilibrium” policies). Following this intuition, we remove each state’s 5 most populous counties from the sample and repeat the analysis in Table 4.

The results using only the less populous counties are in Table 5. Here, stay-at-home orders, asking employees to wear masks, mask mandates, park closures, restricting elective procedures, restaurant closures, gym closures, and high risk business closures all show comparable or stronger negative relationships with future fatality growth than in the full sample. Assuming the initiation of these policies was driven by infection rates in the more populous counties, these results buttress the idea that all of these policies indeed reduce infection rates and thus ultimately deaths. Unlike in Table 4, we no longer see evidence that gathering limits to 10 are helpful. For this variable, the estimated coefficients for both 4- and 6-week ahead fatality growth are no longer significant, even the 10% level.

Like Table 4, the estimates in Table 5 suggest that some policies were counterproductive. Spa closures again produce positive and significant coefficient coefficients. We also, again, observe positive and significant coefficients on closing firms designated as Level 1 Risk and reversing some business re-openings. However, only one of the two coefficients is statistically significant and, in the case of Level 1 Risk businesses, the estimated values are not much different from those in the 1 and 2 week columns. Table 5 also shows that issuing a state of emergency and imposing gathering limits of between 11 and 100 people also generates positive coefficient estimates 4 and 6 weeks out. As in Table 4, school closings, mask recommendations (distinct from mandates for the general population or guidelines for employees), and nursing home visitation policies are all insignificant at the 4- and 6-week horizons. We summarize the Table 5 findings below.

**Summary of Findings in Table 5. Relationships between policy variables and future fatality growth, excluding the State’s most populous counties**

	<b>Significant at 4 or 6 Week Horizon</b>	<b>Significant at both 4 and 6 Week Horizon</b>
<b>Negative, Significant</b>	<b>Stay-At-Home, No Elective Procedures, Restaurants Closed, Risk Level 2 Closed, Risk Level 3 Closed</b>	<b>Employee Masks, Mandatory Masks, Beaches or Parks Closed, Gyms Closed</b>
<b>Positive, Significant</b>	State of Emergency, <b>No gatherings over 100</b> , Risk Level 1 Closed, Reopenings Reversed	Spas Closed

**Bold** indicates a change sign or change in significance when we vary the horizon from short to longer.

### 3.4 County pair analysis

In this section, we exploit variation in policies across matching counties to help sharpen the interpretation. Standard methodology would compare outcomes in two counties that share a border but are in different states – a nearest neighbor analysis. In this setting, there are significant concerns about spillover effects. That is, a policy that reduces infections and ultimately fatalities in one county is likely to be helpful to neighbors as well. These cross-border effects may then yield estimates that imply a policy has no value to the jurisdiction imposing it when, in reality it is not only effective, but so effective that its neighboring jurisdictions benefit as well.<sup>12</sup>

To help mitigate the policy spillover problem, this paper uses a variant of the nearest neighbor pairing system. We still focus on counties that are near state borders, but any county with a border on the state line is removed from the database. This leaves only counties interior to their state, putting at least one county between them and the impact of a neighboring state’s policies. From the list of interior counties, we calculate the distance between its population centroids it and the population centroids of all other counties. For a given target county, any interior county whose population centroid lies within 100 miles of the target and is located in a different state is then

<sup>12</sup> Spillover effects can also generate false positives. Suppose a county with a large number of infections relative to its neighbor closes a venue (such as bars) and its neighbor does not. Residents of the county with the higher infection rate and tighter restriction may travel across the border to circumvent the regulation. Transmissions will then increase in the neighboring county relative to the county that imposed the rule. It will then appear, on a relative basis, that the rule reduced the fatality rate in counties that imposed it. In reality, the rule just increased fatalities in neighboring county.



considered as a possible match. From the set of possible matches, counties are compared on per capita income, fraction of the population over 85, population density, housing density, weekly temperature and rain. These variables are all standardized so that a difference of 1 standard deviation is coded as 1. The distance between the counties in characteristic space is then the equally weighted Euclidean distance based on a list of demographic and weather variables.

$$d_{i,j} = \sqrt{\sum_{k=1}^n (x_{k,i} - x_{k,j})^2} \quad (2)$$

Where  $d_{ij}$  is the hedonic distance between county  $i$  and  $j$ . The  $x_{k,i}$  and  $x_{k,j}$  represent the standardized value of characteristic  $k$  for county  $i$  and  $j$  respectively. A county  $i$  is then paired with the county that generates the lowest value of  $d_{ij}$  among the eligible set. By matching on both demographic and weather-related properties, the two counties should have similar propensities with regard to infection rates and ultimately fatalities while minimizing spillover effects.

The results of the matched county analysis are in Table 6. We find that stay at home orders, mask mandates for the general population, closing parks, and limiting gathering sizes all bring statistically significant lower death rates at both the 4- and 6- week horizons. The magnitudes of the estimated coefficients on these variables in Table 6 are all larger than those in the earlier tables; however, we also find the estimated coefficients on mask mandates and beach and park closures to be more similar as we vary the horizon from 1- to 6- weeks than in the earlier tables. This could be due to autocorrelation in policies, where these policies remain in effect for much of the sample period for the nearby border county subsample. We also find that restaurant closures, nursing home visitation policies, rules that require acceptance of Covid-positive patients, and Risk Level 2 business closures are related to lower death rates at the 6-week horizon. And all three gathering limits predict lower 4-week ahead fatality growth.

As in Tables 4 and 5, the evidence in Table 6 again suggests that low-risk business closures and reopening reversals may be counterproductive.. The estimated coefficients on these policies are statistically insignificant in the regressions forecasting fatality growth 1- and 2- weeks out and they become significant at the 4- and 6-week horizons, which supports the interpretation that the reversals may have been counterproductive. We also find that bar closures and school closures are associated with greater fatality growth at the 4-week horizon. This relationship becomes negative but insignificant at the 6-week horizon.

Table 6 shows no relationship between several of the policies and future growth in fatalities. Unlike in the earlier tables, we do not find a significant relationship between gym and spa closures and future fatalities at the 4- and 6- week horizons in the near-border analysis. Because the matched county analysis is least likely to suffer from endogeneity problems, we interpret the earlier evidence on the effectiveness of these specific policies with some caution. Below, we summarize the findings in Table 6.

**Summary of Findings in Table 6. Relationships between policy variables and future fatality growth near state borders**

	<b>Significant at 4 or 6 Week Horizon</b>	<b>Significant at both 4 and 6 Week Horizon</b>
<b>Negative, Significant</b>	<b>Nursing Homes Accept Pos., No Nursing Home Visits, Restaurants Closed, Gatherings limited to 10, No gatherings over 100, Risk Level 2 Closed</b>	Stay-At-Home, Mandatory Masks, Beaches or Parks Closed, Gatherings limited to >100
<b>Positive, Significant</b>	<b>No Elective Procedures, Risk Level 1 Closed, Schools Closed</b>	<b>Reopenings Reversed, State of Emergency</b>

**Bold** indicates a change sign or change in significance when we vary the horizon from short to longer.

A condensed summary of all of the estimates in the paper (across Tables 4, 5, and 6) can be found in Appendix Table A.1. For those focusing on the restrictions with the most robust results, in terms of reducing fatality growth, they are: Stay-at-home orders, mandatory mask requirements, beach and park closures, restaurant closures, and high risk (Level 2) business closures. These policies predict lower 4- to 6- week-ahead fatality growth in all 3 empirical approaches.

**3.5 Robustness to the inclusion of counties with zero deaths to date**

We focus the analysis on counties that have already experienced fatalities due to Covid-19. One benefit of doing so is that we can examine the relationship between policies and future fatalities in settings where we are sure that the virus is in the community. To check the robustness of the results to the inclusion of counties with zero deaths to date, we repeat the analysis using the weekly change

Covid Economics 56, 9 November 2020: 20-59

in fatalities per 10,000 population instead of  $\ln\left(\frac{Deaths_{i,t}}{Deaths_{i,t-1}}\right)$ . This alternative definition of fatality growth allows us to preserve data for the counties without any fatalities to date.

The results can be found in the Appendix Tables A.2 through A.5 and many of them are consistent with what we report in the main text. Under this alternative metric, employee mask policies, mask mandates for the general population, and high risk business closures are associated with lower future growth in fatalities in all three empirical approaches. These are consistent with the main findings, although it is Risk Level 3 rather than Risk Level 2 businesses that appear to be most helpful under the alternative definition. Restaurant closures and gym closures appear to be helpful in two of three specifications, as does limiting gatherings to 10 people. Also consistent with what we find in the main tables, some policies, like keeping Risk Level 1 businesses shut, reversing a prior reopening, and limiting gatherings to 100 seem counterproductive in two of three specifications (all except the near-border analysis in Table A.5).

While most findings are qualitatively similar, there are a few differences. The main qualitative difference between the findings in the Appendix Tables and those in the main text is that, once we consider counties with zero current deaths and define fatality growth as the change in deaths per capita, the estimated sign on the stay-at-home coefficients become positive and significant. It may be that people in areas with very low current deaths due to the virus feel comfortable substituting into riskier activities when faced with stay-at-home orders. The nursing home visitation policy coefficients are also positive, while they are mixed in the main tables. Closing spas appears to be helpful at the 4- to 6- week horizon (it appears to be counterproductive in Tables 4 and 5), and closing parks and beaches does not appear to impact future increases in deaths per capita. These differences suggest that the effectiveness of some policy tools can depend on the prevalence of Covid-19 in the county. The consistency of the findings for masks and high risk business closures suggest that these policy tools can mitigate future deaths, regardless of the current prevalence of the virus.

#### 4. Conclusion

U.S. policy-makers have the unenviable job of trading off costs and benefits in a situation where human lives are at stake. This paper aims to aid in this decision-making by providing evidence that relates a variety of policies to future growth in fatalities due to Covid-19. We find that stay-at-home orders, mandatory mask requirements, beach and park closures, restaurant closures,

and high risk (Level 2) business closures are the policies that most consistently predict lower 4- to 6- week-ahead fatality growth. These relationships are significant, both statistically and in magnitude. We also find some evidence that employee mask policies, closing gyms, and limiting gatherings to 10 people are associated with lower fatality growth.

At the same time, some policies may have been counterproductive: closing spas, closing risk level 1 businesses, reversing openings, and rules that limit gatherings to a maximum of up to 100 are all associated with higher future fatality growth in at least two of three specifications. State of Emergency orders also fall into this category. However, unlike the other policies examined in this paper, emergency declarations do not in and of themselves impose any restrictions on the population. In this case we may be seeing evidence that policy makers are foreseeing the troubles that lie ahead.

The regressions produce estimates of the magnitude of policy effectiveness, which can be weighed against each policy's cost. Lawmakers place their own weights in their policy objective functions when balancing various tradeoffs. However, lower-cost regulations such as mask mandates appear to be obvious choices as the world waits for advances in science. This is consistent with recommendations in Abaluck et. al (2020); Lyu and Wehby (2020).

There are some limits to the overall interpretation of this paper's findings. For example: there is likely to be unobserved variation in enforcement and adherence to policies, some populations may voluntarily limit their activities, and we lack a clean experimental setting that would allow us to make unambiguous causal statements. Still, the results in this paper strongly suggest that a small number of targeted interventions are likely to curb the loss of life, while other potentially costly measures are less effective.

This paper does not address other outcomes that are of considerable interest, such as hospitalizations (relevant to younger segments of the population than fatalities) and positivity rates.<sup>13</sup> At the time of this writing, county-level data on these variables is still very limited; thus, we leave these analyses to future research.

<sup>13</sup> Huber and Langen report that earlier lockdown restrictions led to lower hospitalizations and death rates in Germany.

## References

Abouk, Rahi and Babak Heydari, 2020. The immediate effect of Covid-19 policies on social distancing behavior in the United States.

Abaluck, Jason, Judith Chevalier, Nicholas Christakis, Howard Forma, Edward H. Kaplan, Albert Ko, and Sten H. Vermund, 2020. The case for universal cloth mask adoption and policies to increase the supply of medical masks for health workers, *Covid Economics* 5, 147-159.

Askitas, Nikos Konstantinos Tatsiramos, and Bertrand Verheyden, 2020. Lockdown strategies, mobility patterns and Covid-19, *Covid Economics* 23, 263-302.

Atkeson, Andrew, Karen Kopesky and Tao Zha, 2020. Four stylized facts about Covid-19, NBER working paper <http://www.nber.org/papers/w27719>.

Baker Rachel E., Wenchang Yang, Gabriel A. Vecchi, C Jessica E. Metcalf, and Bryan T. Grenfell, 2020. Susceptible supply limits the role of climate in the early SARS-CoV-2 pandemic, *Science*. 2020 Jul 17;369(6501):315-319.

Carlson, Colin J., Anna C. R Gomez, Shweta Bansal and Satie J. Ryan, 2020. Misconceptions about weather and seasonality must not misguide Covid-19 response, *Nature Communications* 11, 4312.

Chen, M. Keith, Judith A. Chevalier and Elisa L. Long, 2020. Nursing home staff networks and Covid-19, NBER Working Paper 27608.

Courtemanche, Charles, Joseph Garuccio, Anh Le, Joshua Pinkston, and Aaron Yelowitz, 2020. Strong social distancing measures in the United States reduced the COVID-19 growth rate, *Health Affairs* 39(7), 1237-1246.

Dave, Dhaval., Andrew I. Friedson, Kyutaro Matsuzawa, and Joseph H. Sabia, 2020. When do shelter-in-place orders fight Covid-19 best? Policy heterogeneity across states and adoption time.

Dave, Dhaval., Andrew I. Friedson, Kyutaro Matsuzawa, Joseph H. Sabia and Safford, Samuel, 2020. Were urban cowboys enough to control Covid-19? Local shelter-in-place orders and coronavirus case growth. NBER Working Paper 27229.

Hamidi, Shima, Sabouri, Sadegh, and Reid Ewing, 2020, Does density aggravate the covid-19 pandemic? *Journal of the American Planning Association* 86(4), 495-509.

Friedson, Andrew I., Drew McNichols, Joseph J. Sabia, and Dhaval Dave, 2020. Did California's Shelter-in-Place Order Work? Early Coronavirus-Related Public Health Effects, NBER Working Paper No 26920.

Gupta, Sumedha Thuy D. Nguyen, Felipe Lozano Rojas, Shyam Raman, Byungkyu Lee, Ana Bento, Kosali I. Simon, Coady Wing, 2020. Tracking public and private responses to the Covid-19 epidemic: Evidence from state and local government actions, NBER Working Paper 27027.

Howard, Jeremy, Austin Huang, Zhiyuan Li, Zeynep Tufekci, Zdimir Vladimir, Helene-Mari van der Westhuizen, Arne von Delfto, Amy Pricen, Lex Fridmand, Lei-Han Tangi, Viola Tang, Gregory L. Watson, Christina E. Baxs, Reshama Shaikhq, Frederik Questier, Danny Hernandez, Larry F. Chun, Christina M. Ramirez, and Anne W. Rimoint, April 12, 2020. Face masks against Covid-19: An evidence review, PNAS Preprint.

Huber, Martin and Henrika Langen, 2020. The impact of response measures on Covid-19-related hospitalization and death rates in Germany and Switzerland.

The Initiative on Global Markets, March 27, 2020. Policy for the Covid-19 Crisis (Survey).

Lewnard, Joseph A., Lewnard, Vincent X. Liu, Michael L. Jackson, Mark A. Schmidt, Britta L. Jewell, Jean P. Flores, Chris Jentz, Graham R. Northrup, Ayesha Mahmud, Arthur L. Reingold, Maya Petersen, Nicholas P. Jewell, Scott Young, and Jim Bellows, 2020. Incidence, clinical outcomes, and transmission dynamics of severe coronavirus disease 2019 in California and Washington: prospective cohort study, *BMJ*; 369:m1923.

Lyu, Wei, and George L. Wehby, Evidence from a natural experiment of state mandates in the U.S., *Health Affairs* 39(8), 1419-1425.

Millett, Gregorio A., Austin T. Jones, David Benkeser, Stefan Baral, Laina Mercer, Chris Beyrer, Brian Honermann, Elise Lankiewicz, Leandro Mena, Jeffrey S. Crowley, Jennifer Sherwood, Patrick S. Sullivan, 2020. Assessing differential impacts of Covid-19 on black communities, *Annals of Epidemiology* 47, 37-44.

Moore, Jazmyn T. , Jessica N. Ricaldi, Charles E. Rose, Jennifer Fuld, Monica Parise, Gloria J. Kang, Anne K. Driscoll, Tina Norris, Nana Wilson, Gabriel Rainisch, Eduardo Valverde, Vladislav Beresovsky, Christine Agnew Brune, Nadia L. Oussayef, Dale A. Rose, Laura E. Adams, Sindoos Awel; Julie Villanueva, Dana Meaney-Delman, Margaret A. Honein, 2020. CDC Morbidity and Mortality Weekly Report, August 21, 2020. Disparities in incidence of Covid-19 among underrepresented racial/ethnic groups in counties identified as hotspots.

Nguyen, Thuy D., Sumedha Gupta, Martin Andersen, Ana Bento, Kosali Simon and Cody Wing, 2020, Impacts of state reopening policy on human mobility, NBER Working Paper 27235.

Qian, Hua, Te Mao, Li LIU, Xiohong Zheng, Danting Luo, and Yuguo Li, 2020. Indoor transmission of SARS-CoV-2.

**Table 1: County-Level Business Restrictions due to Covid-19**

This table provides descriptions of each of the policy interventions. Policy variables are dummies equal to one if a given policy is effective during week  $t$  and zero otherwise.

Policy Intervention	Description
Stay at Home	"Stay-at-home order" issued by state or county government.
State of Emergency	"State of Emergency" issued by state or county government.
Nursing Home Must Accept Positive	Nursing homes required to accept Covid-19 positive residents.
No Nursing Home Visitation	Nursing home visitors prohibited.
Schools Closed <sup>14</sup>	Schools closed.
Employee masks	Mandatory or recommended face coverings for employees.
Masks recommended in public	Recommended face coverings in public.
Mandatory masks in public	Mandatory face coverings anywhere. This includes policies that mandate face coverings in all public places, as well as those that require masks in a subset of public places.
Beaches and parks closed	Beaches or parks completely closed to the public. Closures must be total; no pedestrian traffic.
No elective procedures	Any elective medical procedures (medical procedures including dental and eye) prohibited.
Restaurants closed	Restaurants closed with the possible exception of take-out services.
Bars closed	Bars and nightclubs closed with the possible exception of take-out services.
Gyms closed	Fitness facilities and gyms closed to all indoor activities.
Spas closed	Personal care services spas closed to all indoor activities.

<sup>14</sup> The sample ends on September 1, 2020, just as schools began to reopen. Most schools in the U.S. were closed from sometime in March through the end of August. Thus, the *Schools Closed* variable captures variation in school closures at the onset of the crisis.

Table 1 (cont'd)

<b>Policy Intervention</b>	<b>Description</b>
Gatherings limited to 10	Gathering ban, where gatherings are limited to 10 people.
No gatherings over 100	Gathering ban, where the limit is less than or equal to 100 people, and greater than 10.
No gatherings, limit>100	Gathering ban, where the limit exceeds 100 people.
Risk Level 1 Closed	General business closure policy in effect. Business risk levels are defined in accordance with the reopening phases set by counties. When a county adopts more than 4 phases, we group additional phases according to their proximity to one another in time. If all businesses are open, Risk Level 1, Risk Level 2, Risk Level 3, Risk Level 4 dummies all equal zero. When a general business closure policy is in effect, Risk Level 1, Risk Level 2, Risk Level 3, Risk Level 4 dummies all equal one.
Risk Level 2 Closed	Phase 1 reopening policy in effect, where all but low and medium-risk businesses remained closed. When a county is in Phase 1, the Risk Level 1 dummy equals zero and the dummies for Risk Levels 2, 3, and 4 all equal one.
Risk Level 3 Closed	Phase 2 reopening policy in effect, where higher and highest risk businesses remained closed. When a county is in Phase 2, the Risk Level 1 and 2 dummies equals zero and the dummies for Risk Levels 3 and 4 equal one.
Risk Level 4 Closed	Phase 3 reopening policy in effect, all but the highest risk businesses remain closed. When a county is in Phase 3, the Risk Level 1, 2, and 3 dummies equals zero and the dummy for Risk Levels 4 equals one.
Business re-openings reversed	Phased business reopening reversed



Table 2

This table summarizes the fatality, policy, demographic and weather variables. Each observation is a county-week between March 1, 2020 and September 1, 2020. Fatality variables are in Panel A. *Deaths Per Capita* is defined as total deaths per 10,000 population as of week  $t$ . Weekly fatality growth (*Growth<sub>t</sub>*) is the natural log of: total deaths as of week  $t$ , divided by the total deaths as of week  $t-1$ . Only counties with at least one death as of week  $t-6$  are included in the sample. Weekly change in deaths per capita is the first-difference of *Deaths Per Capita* from week  $t-1$  to week  $t$ . Panel B shows the policy variables. All policy variables are dummies equal to one if a given policy is effective during week  $t$ . Policies are defined in Table 1. Demographics and other controls are in Panel C. *Black*, *Hispanic*, *Asian*, *Native American* and *Other*, are the fraction of the county's population that are White, Black, Hispanic, Asian, Native American and other races/ethnicities (respectively). *Age65plus* and *Age85plus* are the fractions of the population that are over the age of 65 and over age 85. *Nursing Home Population* is the fraction of the population living in in skilled nursing facilities. *Per Capita Income* is the average per capita income in the county. *Diabetes*, *Obesity* and *Smokers* are the fractions of the population with diabetes, are obese or who smoke, respectively. *Population density* is defined as total population divided by the land square miles of the county. *Housing Density* is defined as the total number of homes in the county divided by residential land area. *HotHumidWeekdays* and *HotHumidWeekends* are the percentage of weekdays and weekend days (respectively) in which the average temperature is above 80 degrees and the dew point is above 60. *ColdWeekdays* and *ColdWeekends* are percentage of weekdays and weekend days in which the average high temperature is below 60 degrees. *AverageTemperature*, the average daily temperature for the week. *Time Since First Case* is the natural log of the number of days since the first reported case of Covid-19 in a county and  $t$  is the natural log of the number of days since March 1, 2020.

Panel A. Fatalities						
Variable	N	Mean	Median	25th Pctl	75th Pctl	Std Dev
Deaths per capita	25,459	3.354	1.776	0.725	4.204	4.338
Growth <sub>t</sub>	25,459	0.085	0.000	0.000	0.105	0.166
Weekly change in deaths per 10,000	25,459	0.212	0.000	0.000	0.241	0.464

Panel B. Policies						
Variable	N	Mean	25 <sup>th</sup> Pctl	Median	75 <sup>th</sup> Pctl	Std Dev
Stay at Home	25,459	0.076	0.000	0.000	0.000	0.265
State of Emergency	25,459	0.991	1.000	1.000	1.000	0.097
Nursing Home Accept Pos.	25,459	0.204	0.000	0.000	0.000	0.403
No Nursing Home Visit	25,459	0.690	0.000	1.000	1.000	0.462
Schools Closed	25,459	0.992	1.000	1.000	1.000	0.088
Employee Masks	25,459	0.816	1.000	1.000	1.000	0.388
Masks Recommended	25,459	0.930	1.000	1.000	1.000	0.255
Mandatory Masks	25,459	0.489	0.000	0.000	1.000	0.500
Parks Closed	25,459	0.032	0.000	0.000	0.000	0.175
No Elective Procedures	25,459	0.053	0.000	0.000	0.000	0.225
Restaurants Closed	25,459	0.113	0.000	0.000	0.000	0.317
Bars Closed	25,459	0.354	0.000	0.000	1.000	0.478
Gyms Closed	25,459	0.192	0.000	0.000	0.000	0.394
Spas Closed	25,459	0.147	0.000	0.000	0.000	0.354
Gatherings Limited to 10	25,459	0.462	0.000	0.000	1.000	0.499
No gatherings over 100	25,459	0.419	0.000	0.000	1.000	0.493
Gathering limit over 100	25,459	0.082	0.000	0.000	0.000	0.275
Risk Level 1 Closed	25,459	0.024	0.000	0.000	0.000	0.154
Risk Level 2 Closed	25,459	0.139	0.000	0.000	0.000	0.346
Risk Level 3 Closed	25,459	0.399	0.000	0.000	1.000	0.490
Risk Level 4 Closed	25,459	0.630	0.000	1.000	1.000	0.483
Bus. Openings Reversed	25,459	0.057	0.000	0.000	0.000	0.233

Panel C: Demographic and Other Controls						
Black	25,459	12.900	1.500	5.500	18.300	16.418
Hispanic	25,459	9.781	2.500	5.000	10.900	12.948
Asian	25,459	1.998	0.500	0.900	2.100	3.404
Native American	25,459	1.232	0.200	0.300	0.600	4.930
Other	25,459	17.065	14.500	16.800	19.100	4.111
Age65plus	25,459	2.038	1.600	1.900	2.400	0.710
Age85plus	25,459	2.338	0.500	1.200	2.600	3.577
Nursing Home Population	25,459	0.608	0.352	0.551	0.784	0.378
Per Capita Income	24,952	45,438	37,363	42,483	49,863	14,365
Diabetes	25,459	12.172	9.400	11.600	14.400	3.952
Obesity	25,459	32.801	29.300	33.300	36.600	5.619
Smokers	25,459	17.401	15.059	17.335	19.591	3.341
Population Density	25,459	488.564	39.756	93.488	289.373	2,558.500
Housing Density	25,459	209.157	19.160	42.514	123.633	1,214.750
Average Temperature	25,459	7.275	3.666	7.034	10.129	4.639
Hot Humid Weekdays	25,459	0.180	0.000	0.000	0.000	0.385
Hot Humid Weekends	25,459	0.241	0.000	0.000	0.000	0.427
Cold Weekday	25,459	0.057	0.000	0.000	0.000	0.190
Cold Weekend	25,459	0.059	0.000	0.000	0.000	0.221
Time Since First Case	25,459	4.678	4.477	4.727	4.927	0.297
t	25,459	4.856	4.682	4.913	5.056	0.253

**Table 3**

This table shows results of regressions in which we regress one-week-ahead death growth rates on: current and lagged cumulative deaths per 10,000 population in the county (*Deaths Per Capita*); lagged one-week fatality growth rates; the interaction between current per capita deaths and the lagged one-week growth rates; and time controls.  $Growth(t-x)$  denotes the x-week lagged growth rate in deaths.  $Deaths\ Per\ Capita(t-x)$  denotes the x-week lagged cumulative deaths per 10,000 population in the county.  $Int(t-x)$  denotes  $Deaths\ Per\ Capita * Growth(t-x)$ . *Time Since First Covid Case* is the number of days since the first reported case of Covid-19 in a county and  $t$  is the number of days since March 1, 2020. The demographic variables are defined in Table 2. Each observation is a county-week. All standard errors (in parentheses) are clustered at the county level. \*\*\* denotes significance at the 1% level; \*\* denotes significance at the 5% level; \* denotes significance at the 10% level.

VARIABLES	(1)		(2)		(3)		(4)	
	Growth <sub>t+1</sub>	S.E.	Growth <sub>t+2</sub>	S.E.	Growth <sub>t+4</sub>	S.E.	Growth <sub>t+6</sub>	S.E.
Deaths Per Capita	0.0293***	0.0088	0.0181*	0.0108	-0.0010	0.0057	0.0002	0.0046
Growth <sub>t-1</sub>	0.1586***	0.0121	0.1368***	0.0121	0.0571***	0.0086	0.0142*	0.0080
Growth <sub>t-2</sub>	0.1110***	0.0115	0.0538***	0.0094	0.0164**	0.0076	-0.0073	0.0068
Growth <sub>t-3</sub>	0.0391***	0.0088	0.0277***	0.0077	0.0010	0.0078	-0.0062	0.0065
Growth <sub>t-4</sub>	0.0234***	0.0071	-0.0032	0.0062	-0.0140**	0.0060	-0.0164***	0.0057
Growth <sub>t-5</sub>	-0.0033	0.0055	-0.0023	0.0058	-0.0134***	0.0047	-0.0182***	0.0054
Growth <sub>t-6</sub>	0.0006	0.0045	-0.0117***	0.0042	-0.0204***	0.0039	-0.0169***	0.0038
Deaths Per Cap <sub>t-1</sub>	-0.0300**	0.0124	-0.0206*	0.0116	-0.0062	0.0067	-0.0198***	0.0057
Deaths Per Cap <sub>t-2</sub>	-0.0006	0.0094	-0.0124*	0.0065	-0.0016	0.0051	0.0085	0.0053
Deaths Per Cap <sub>t-3</sub>	-0.0158***	0.0052	0.0054	0.0043	-0.0064*	0.0035	0.0008	0.0036
Deaths Per Cap <sub>t-4</sub>	0.0080**	0.0040	-0.0002	0.0030	0.0051*	0.0029	-0.0026	0.0031
Deaths Per Cap <sub>t-5</sub>	0.0057**	0.0028	0.0040	0.0028	0.0029	0.0024	0.0047**	0.0023
Deaths Per Cap <sub>t-6</sub>	-0.0029*	0.0016	-0.0012	0.0017	-0.0002	0.0016	0.0008	0.0016
Int <sub>t-1</sub>	-0.0343***	0.0074	-0.0287***	0.0090	-0.0158***	0.0046	-0.0131***	0.0036
Int <sub>t-2</sub>	-0.0094*	0.0054	-0.0085**	0.0040	-0.0038	0.0032	0.0049	0.0038
Int <sub>t-3</sub>	-0.0052**	0.0024	0.0002	0.0022	-0.0011	0.0019	0.0008	0.0016
Int <sub>t-4</sub>	0.0019	0.0017	0.0018	0.0012	0.0034***	0.0012	0.0015	0.0011
Int <sub>t-5</sub>	0.0033***	0.0010	0.0015	0.0010	0.0030***	0.0008	0.0035***	0.0008
Int <sub>t-6</sub>	0.0006	0.0007	0.0022***	0.0007	0.0022***	0.0008	0.0016**	0.0007
Days Since First Case	0.0294**	0.0128	0.0429***	0.0140	0.0377***	0.0136	0.0162	0.0157
Days Since Mar. 1	-0.0048	0.0156	-0.0381**	0.0168	-0.0586***	0.0166	-0.0605***	0.0195
Avg Temperature	0.0019***	0.0003	0.0027***	0.0004	0.0026***	0.0003	0.0026***	0.0003
Hot Humid Weekday	0.0189***	0.0040	0.0192***	0.0038	0.0157***	0.0037	0.0056	0.0035
Hot Humid Weekend	0.0007	0.0034	-0.0010	0.0034	0.0019	0.0031	-0.0065**	0.0031
Cold Weekdays	0.0102	0.0081	0.0058	0.0092	-0.0109	0.0081	-0.0335***	0.0073
Cold Weekend	-0.0183***	0.0055	-0.0272***	0.0059	-0.0336***	0.0059	-0.0358***	0.0050
Age 65+	0.0002	0.0004	0.0003	0.0004	0.0001	0.0005	0.0001	0.0005
Age 85+	-0.0008	0.0025	-0.0015	0.0028	-0.0014	0.0029	-0.0003	0.0030
Asian	0.0002	0.0003	0.0002	0.0003	0.0002	0.0004	0.0002	0.0004
Black	0.0007***	0.0001	0.0007***	0.0001	0.0007***	0.0001	0.0006***	0.0001
Hispanic	0.0007***	0.0002	0.0007***	0.0002	0.0009***	0.0002	0.0009***	0.0002
Native Americans	0.0007***	0.0003	0.0007**	0.0003	0.0003	0.0003	0.0003	0.0003
Other	0.0007	0.0005	0.0005	0.0006	0.0004	0.0006	-0.0002	0.0005
Per Capita Income	-0.0000***	0.0000	-0.0000***	0.0000	-0.0000***	0.0000	-0.0000***	0.0000
Population Density	0.0000***	0.0000	0.0000***	0.0000	0.0000***	0.0000	0.0000***	0.0000
Diabetes	0.0015***	0.0004	0.0018***	0.0004	0.0021***	0.0004	0.0019***	0.0004
Obesity	-0.0004	0.0003	-0.0005*	0.0003	-0.0007**	0.0003	-0.0005	0.0003
Smokers	0.0005	0.0004	0.0006	0.0005	0.0010*	0.0005	0.0010*	0.0005
Housing Density	-0.0000**	0.0000	-0.0000**	0.0000	-0.0000**	0.0000	-0.0000***	0.0000
Nursing Home Pop.	0.0123***	0.0039	0.0155***	0.0044	0.0134***	0.0048	0.0157***	0.0048
Constant	-0.0863***	0.0304	0.0189	0.0316	0.1589***	0.0329	0.2683***	0.0355
Observations	24,952		24,952		24,950		24,950	
Adjusted R-squared	0.1021		0.0863		0.0749		0.0684	

**Table 4. Policy interventions and  $t$ -week-ahead weekly fatality growth**

This table shows results of regressions in which we regress  $x$ -week-ahead weekly death growth rates  $Growth(t+x)$  on policy dummies and county demographic variables. All of the variables are defined in Tables 1 and 2. As in Table 3, we also control for current and lagged cumulative deaths per 10,000 population in the county; lagged one-week fatality growth rates; the interaction between current per capita deaths and the lagged one-week growth rates; time controls; and demographics controls. These controls are estimated but not reported in the table. Each observation is a county-week. All standard errors (in parentheses) are clustered at the county level. \*\*\* denotes significance at the 1% level; \*\* denotes significance at the 5% level; \* denotes significance at the 10% level.

VARIABLES	(1) Growth <sub>t+1</sub>	S.E.	(2) Growth <sub>t+2</sub>	S.E.	(3) Growth <sub>t+4</sub>	S.E.	(4) Growth <sub>t+6</sub>	S.E.
Stay at Home	0.000	0.004	0.003	0.005	0.004	0.005	-0.010**	0.004
State of Emergency	0.022***	0.008	0.025***	0.010	0.024**	0.010	0.027***	0.011
Nursing Accept Pos.	-0.000	0.003	0.001	0.003	0.002	0.003	-0.001	0.003
No Nursing Visits	0.015***	0.002	0.012***	0.003	0.003	0.003	0.003	0.003
Schools Closed	-0.015	0.012	-0.019	0.014	-0.019	0.016	-0.008	0.017
Employees Masks	0.007**	0.003	0.006*	0.004	-0.015***	0.004	-0.017***	0.004
Masks Recommended	0.002	0.005	-0.000	0.005	-0.005	0.005	0.000	0.005
Mandatory Masks	-0.005*	0.002	-0.007***	0.003	-0.010***	0.003	-0.010***	0.003
Beaches or Parks Closed	-0.004	0.005	-0.012***	0.005	-0.013***	0.004	-0.010**	0.005
No Elective Procedures	0.022***	0.008	0.010	0.008	-0.012*	0.007	0.006	0.006
Restaurants Closed	0.000	0.004	-0.002	0.005	-0.010**	0.005	-0.011**	0.004
Bars Closed	0.013***	0.003	0.010***	0.003	0.007**	0.003	-0.007**	0.003
Gyms Closed	-0.007**	0.003	-0.013***	0.003	-0.016***	0.003	-0.013***	0.004
Spas Closed	0.008**	0.003	0.011***	0.004	0.016***	0.004	0.019***	0.004
Gatherings Limited to 10	-0.015***	0.006	-0.021***	0.007	-0.014**	0.007	-0.000	0.006
No Gatherings Over 100	-0.013**	0.006	-0.015**	0.007	0.005	0.007	0.011*	0.006
No Gatherings Limit>100	-0.018***	0.007	-0.025***	0.007	-0.008	0.007	-0.003	0.007
Risk Level 1 Closed	0.008	0.006	0.004	0.007	0.006	0.005	0.011**	0.005
Risk Level 2 Closed	0.007**	0.003	0.006*	0.003	0.005	0.004	-0.014***	0.003
Risk Level 3 Closed	0.001	0.003	0.005	0.003	-0.003	0.003	-0.002	0.003
Risk Level 4 Closed	-0.010***	0.003	-0.009***	0.003	-0.003	0.003	0.000	0.003
Re-openings Reversed	0.028***	0.007	0.035***	0.008	0.041***	0.010	-0.004	0.007
Constant	-0.141***	0.042	-0.012	0.044	0.176***	0.047	0.250***	0.047
Observations	24,952		24,952		24,950		24,950	
Adjusted R-squared	0.108		0.093		0.084		0.080	
Controls	YES		YES		YES		YES	

**Table 5. Policy interventions and t-week-ahead weekly fatality growth in less populous counties.**

This table shows results of regressions in which we regress x-week-ahead weekly death growth rates  $Growth(t+x)$  on policy dummies. As in Table 3, we also control for current and lagged cumulative deaths per 10,000 population in the county; lagged one-week fatality growth rates; the interaction between current per capita deaths and the lagged one-week growth rates; time controls; and demographics controls. These controls are estimated but not reported in the table. The specification is identical to that in Table 3 except we remove the 5 most populous counties in each state. All standard errors (in parentheses) are clustered at the county level. \*\*\* denotes significance at the 1% level; \*\* denotes significance at the 5% level; \* denotes significance at the 10% level.

VARIABLES	(1)		(2)		(3)		(4)	
	Growth <sub>t+1</sub>	S.E.	Growth <sub>t+2</sub>	S.E.	Growth <sub>t+4</sub>	S.E.	Growth <sub>t+6</sub>	S.E.
Stay at Home	-0.004	0.005	0.001	0.006	0.001	0.006	-0.012**	0.005
State of Emergency	0.019*	0.010	0.022*	0.012	0.020	0.013	0.023*	0.013
Nursing Accept Pos.	-0.001	0.003	0.000	0.003	0.003	0.004	0.001	0.003
No Nursing Visits	0.017***	0.003	0.013***	0.003	0.003	0.003	0.003	0.003
Schools Closed	-0.018	0.017	-0.017	0.019	-0.003	0.017	0.016	0.016
Employees Masks	0.009**	0.004	0.009**	0.004	-0.015***	0.004	-0.017***	0.004
Masks Recommended	0.002	0.006	-0.001	0.006	-0.009	0.007	-0.003	0.006
Mandatory Masks	-0.006**	0.003	-0.010***	0.003	-0.013***	0.003	-0.012***	0.003
Beaches or Parks Closed	-0.009	0.006	-0.016***	0.006	-0.014**	0.006	-0.011*	0.006
No Elective Procedures	0.031***	0.010	0.015	0.009	-0.013*	0.008	0.005	0.007
Restaurants Closed	0.004	0.005	0.001	0.005	-0.009	0.006	-0.011**	0.005
Bars Closed	0.015***	0.003	0.010***	0.003	0.008**	0.004	-0.008**	0.004
Gyms Closed	-0.006*	0.004	-0.012***	0.004	-0.013***	0.004	-0.010**	0.004
Spas Closed	0.009**	0.004	0.013***	0.004	0.019***	0.004	0.022***	0.005
Gatherings Limited to 10	-0.014**	0.007	-0.017**	0.007	-0.009	0.007	0.006	0.007
No Gatherings Over 100	-0.013*	0.007	-0.012	0.007	0.011	0.008	0.017**	0.007
No Gatherings Limit>100	-0.018**	0.007	-0.023***	0.008	-0.003	0.008	0.002	0.008
Risk Level 1 Closed	0.014*	0.008	0.010	0.009	0.009	0.006	0.011*	0.006
Risk Level 2 Closed	0.008**	0.004	0.006	0.004	0.005	0.004	-0.016***	0.004
Risk Level 3 Closed	-0.002	0.003	0.002	0.003	-0.006*	0.004	-0.005	0.004
Risk Level 4 Closed	-0.009***	0.003	-0.009**	0.003	-0.001	0.004	0.002	0.004
Re-openings Reversed	0.027***	0.008	0.035***	0.008	0.043***	0.011	-0.006	0.007
Constant	-0.183***	0.049	-0.043	0.050	0.133***	0.050	0.206***	0.051
Observations	21,347		21,347		21,347		21,347	
Adjusted R-squared	0.100		0.087		0.082		0.077	
Control	YES		YES		YES		YES	

**Table 6. Policy variation across the state border: Interventions and t-week-ahead weekly fatality growth (100 Miles)**

This table shows results of regressions in which we regress  $x$ -week-ahead weekly death growth rates  $Growth(t+x)$  on policy dummies and county demographic variables. The specification is identical to that in Tables 4 and 5 we include in the sample only those counties that are within 100 miles of another county in a different state and with which they do not share a border (“nearby county”) and we add the nearby county policies to the specification. Nearby county policies are estimated but not reported in the table. All standard errors (in parentheses) are clustered at the county level. \*\*\* denotes significance at the 1% level; \*\* denotes significance at the 5% level; \* denotes significance at the 10% level.



VARIABLES	(1)		(2)		(3)		(4)	
	Growth <sub>t+1</sub>	S.E.	Growth <sub>t+2</sub>	S.E.	Growth <sub>t+4</sub>	S.E.	Growth <sub>t+6</sub>	S.E.
Stay at Home	-0.017*	0.009	-0.014	0.009	-0.023***	0.009	-0.029***	0.008
State of Emergency	0.017*	0.010	0.022**	0.011	0.028**	0.011	0.032***	0.012
Nursing Accept Pos.	-0.006	0.005	-0.006	0.005	-0.006	0.005	-0.009*	0.005
No Nursing Visits	0.012**	0.005	0.005	0.005	-0.008	0.005	-0.013**	0.005
Schools Closed	-0.011	0.026	0.026	0.016	0.030**	0.012	0.015	0.010
Employees Masks	0.011*	0.006	0.014**	0.007	0.003	0.008	-0.005	0.008
Masks Recommended	-0.016*	0.010	-0.016	0.010	-0.001	0.009	-0.008	0.010
Mandatory Masks	-0.010**	0.005	-0.014***	0.005	-0.013**	0.005	-0.014***	0.005
Beaches or Parks Closed	-0.019***	0.007	-0.025***	0.007	-0.020***	0.007	-0.019***	0.007
No Elective Procedures	0.027	0.021	0.033	0.025	0.011	0.011	0.019*	0.011
Restaurants Closed	0.007	0.008	0.007	0.009	-0.005	0.007	-0.014**	0.007
Bars Closed	0.015***	0.006	0.012**	0.006	0.010*	0.006	-0.007	0.006
Gyms Closed	-0.003	0.005	-0.009	0.006	-0.006	0.006	-0.001	0.006
Spas Closed	0.005	0.006	0.005	0.007	0.010	0.007	0.010	0.007
Gatherings Limited to 10	-0.027**	0.012	-0.030**	0.013	-0.027**	0.012	-0.012	0.012
No Gatherings Over 100	-0.032***	0.012	-0.035***	0.013	-0.021*	0.012	0.001	0.012
No Gatherings Limit>100	-0.038***	0.013	-0.045***	0.015	-0.032**	0.013	-0.024*	0.013
Risk Level 1 Closed	-0.003	0.012	-0.007	0.015	0.001	0.012	0.016*	0.009
Risk Level 2 Closed	0.016**	0.006	0.014**	0.007	0.009	0.007	-0.012*	0.006
Risk Level 3 Closed	-0.009*	0.005	-0.002	0.005	-0.006	0.006	0.001	0.006
Risk Level 4 Closed	-0.003	0.005	-0.004	0.006	-0.001	0.006	0.006	0.006
Re-openings Reversed	0.015	0.012	0.022	0.014	0.058***	0.020	0.055***	0.015
Constant	-0.094	0.096	-0.251**	0.102	-0.141	0.107	-0.083	0.119
Observations	9,220		9,220		9,220		9,220	
Adjusted R-squared	0.087		0.075		0.073		0.078	
Control	YES		YES		YES		YES	
Border County Policies	YES		YES		YES		YES	

**APPENDIX TABLES**

Appendix Table A.5 summarizes the findings in Tables 4 through 6 of the main text. Appendix Tables A.2 through A.5 are identical to Tables 3 through 6 of the main text except we replace the weekly growth rate variable with the first difference in deaths per capita. We also remove the weekly lagged levels of deaths per capita and the interactions of growth with deaths per capita as controls variables.

**Table A.1 Summary of Coefficients from Tables 4, 5 and 6 (4- and 6- Week Horizons)**

The “-” and “+” indicate negative and positive estimated coefficients for the 4- and 6- week horizons (respectively) where at least one of the coefficients is statistically significant. \* indicates a change in significance or sign as the horizon goes from shorter (1- to 2- weeks) to longer. The “Overall” column includes an icon if at least two tables have the same icon and the third table does not have a countervailing icon. For example, Employee Masks have a -\* in the “Overall” columns since two tables have a -\* and the third does not have +. The Overall column is blank for No Nursing Visits since only one table has a -\*.

	Table 4	Table 5	Table 6	Overall
Stay at Home	-*	-*	-	-*
State of Emergency	+	+	+	+
Nursing Accept Pos.			-*	
No Nursing Visits			-*	
Schools Closed			+*	
Employees Masks	-*	-*		-*
Masks Recommended		-*		
Mandatory Masks	-	-	-	-
Beaches or Parks Closed	-	-	-	-
No Elective Procedures	-*	-*	+*	
Restaurants Closed	-*	-*	-*	-*
Bars Closed			+	
Gyms Closed	-	-		-
Spas Closed	+	+		+
Gatherings Limited to 10	-		-	-
No Gatherings Over 100	+*	+*	-	
No Gatherings Limit>100			-	
Risk Level 1 Closed	+*	+	+*	+*
Risk Level 2 Closed	-*	-*	-*	-*
Risk Level 3 Closed		-*		
Risk Level 4 Closed				
Re-openings Reversed	+	+	+*	+

**Table A.2**

This table shows results of regressions in which we regress one-week-ahead change in deaths per capita rates on: current cumulative deaths per 10,000 population in the county (*Deaths Per Capita*); lagged changes in deaths per capita, and time controls. *Growth(t-x)* denotes the x-week lagged weekly change in deaths per 10,000 population in deaths. *Time Since First Covid Case* is the number of days since the first reported case of Covid-19 in a county and *t* is the number of days since March 1, 2020. The demographic variables are defined in Table 2. Each observation is a county-week. All standard errors (in parentheses) are clustered at the county level. \*\*\* denotes significance at the 1% level; \*\* denotes significance at the 5% level; \* denotes significance at the 10% level.

VARIABLES	(1)		(2)		(3)		(4)	
	Growth <sub>t+1</sub>	S.E.	Growth <sub>t+2</sub>	S.E.	Growth <sub>t+4</sub>	S.E.	Growth <sub>t+6</sub>	S.E.
Deaths Per Capita	-0.0045***	0.0014	-0.0067***	0.0016	-0.0081***	0.0018	-0.0080***	0.0017
Growth <sub>t-1</sub>	0.3015***	0.0204	0.2710***	0.0152	0.1456***	0.0132	0.0707***	0.0128
Growth <sub>t-2</sub>	0.1972***	0.0155	0.1129***	0.0138	0.0522***	0.0102	0.0215*	0.0111
Growth <sub>t-3</sub>	0.0586***	0.0141	0.0417**	0.0183	0.0222	0.0141	0.0568*	0.0344
Growth <sub>t-4</sub>	0.0072	0.0105	-0.0014	0.0096	-0.0129	0.0130	-0.0061	0.0129
Growth <sub>t-5</sub>	-0.0049	0.0095	-0.0037	0.0121	0.0590	0.0437	-0.0146	0.0091
Growth <sub>t-6</sub>	-0.0041	0.0128	0.0011	0.0093	-0.0127	0.0172	0.0141	0.0097
Days Since First Case	0.0212***	0.0039	0.0220***	0.0059	0.0263***	0.0057	0.0161**	0.0074
Days Since March 1	-0.0036	0.0095	-0.0221*	0.0125	-0.0224*	0.0130	0.0106	0.0146
Avg Temperature	0.0027***	0.0004	0.0044***	0.0005	0.0060***	0.0005	0.0069***	0.0005
HotHumid Weekday	0.0541***	0.0100	0.0802***	0.0118	0.0952***	0.0126	0.0773***	0.0137
HotHumid Weekend	-0.0054	0.0080	0.0067	0.0086	0.0166*	0.0094	0.0151	0.0105
Cold Weekdays	0.0170*	0.0094	-0.0007	0.0106	-0.0278**	0.0117	-0.0654***	0.0114
Cold Weekend	-0.0107*	0.0064	-0.0301***	0.0062	-0.0420***	0.0072	-0.0476***	0.0070
Age 65+	0.0010*	0.0005	0.0010	0.0007	0.0020**	0.0009	0.0022**	0.0010
Age 85+	-0.0030	0.0039	-0.0030	0.0051	-0.0089	0.0061	-0.0093	0.0067
Asian	-0.0007	0.0008	-0.0008	0.0011	-0.0004	0.0011	-0.0005	0.0010
Black	0.0036***	0.0003	0.0044***	0.0003	0.0056***	0.0004	0.0058***	0.0004
Hispanic	0.0018***	0.0003	0.0023***	0.0004	0.0031***	0.0005	0.0038***	0.0006
Native Americans	0.0011*	0.0006	0.0015**	0.0008	0.0022**	0.0010	0.0026**	0.0011
Other	0.0012	0.0012	0.0013	0.0014	0.0011	0.0018	-0.0001	0.0020
Per Capita Income	0.0000	0.0000	0.0000	0.0000	0.0000	0.0000	-0.0000	0.0000
Population Density	0.0001***	0.0000	0.0001***	0.0000	0.0000***	0.0000	0.0000	0.0000
Diabetes	0.0020***	0.0006	0.0024***	0.0007	0.0032***	0.0009	0.0038***	0.0011
Obesity	-0.0000	0.0004	-0.0001	0.0006	-0.0001	0.0007	-0.0004	0.0008
Smokers	0.0016**	0.0008	0.0021**	0.0010	0.0029**	0.0013	0.0036***	0.0013
Housing Density	-0.0001***	0.0000	-0.0001***	0.0000	-0.0001***	0.0000	-0.0000	0.0000
Nursing Home Pop.	0.0257***	0.0052	0.0344***	0.0068	0.0522***	0.0092	0.0664***	0.0105
Constant	-0.1629***	0.0437	-0.1032*	0.0554	-0.1405**	0.0653	-0.2423***	0.0688
Observations	64,348		64,348		64,348		64,348	
Adjusted R-squared	0.2391		0.1713		0.1015		0.0743	

**Table A.3. Policy interventions and  $t$ -week-ahead weekly fatality growth**

This table shows results of regressions in which we regress one-week-ahead change in deaths 10,000 population on policy variables defined in Table 1. As in Table A.2, we also include controls for: current cumulative deaths per 10,000 population in the county (*Deaths Per Capita*); lagged changes in deaths per capita, time controls, and demographics controls. These controls are estimated but not reported in the table. Each observation is a county-week. All standard errors (in parentheses) are clustered at the county level. \*\*\* denotes significance at the 1% level; \*\* denotes significance at the 5% level; \* denotes significance at the 10% level.

VARIABLES	(1)		(2)		(3)		(4)	
	Growth <sub>t+1</sub>	S.E.	Growth <sub>t+2</sub>	S.E.	Growth <sub>t+4</sub>	S.E.	Growth <sub>t+6</sub>	S.E.
Stay at Home	0.031***	0.006	0.043***	0.007	0.050***	0.009	0.031***	0.008
State of Emergency	0.019*	0.011	0.016	0.014	0.031*	0.016	0.062***	0.018
Nursing Accept Pos.	0.032***	0.007	0.033***	0.008	0.037***	0.009	0.036***	0.009
No Nursing Visits	0.012***	0.004	0.005	0.006	-0.001	0.008	0.015**	0.007
Schools Closed	-0.017*	0.009	-0.022*	0.012	-0.044*	0.025	-0.035	0.025
Employees Masks	0.003	0.005	0.006	0.006	-0.015**	0.007	-0.013*	0.008
Masks Recommended	-0.011*	0.006	-0.013*	0.007	-0.014	0.008	-0.009	0.008
Mandatory Masks	-0.001	0.005	-0.005	0.006	-0.021***	0.007	-0.030***	0.007
Beaches or Parks Closed	-0.023***	0.006	-0.025***	0.008	-0.012	0.009	-0.001	0.009
No Elective Procedures	0.030***	0.007	0.043***	0.009	0.032***	0.010	0.032***	0.009
Restaurants Closed	-0.021***	0.008	-0.024**	0.010	-0.017*	0.009	-0.014	0.009
Bars Closed	0.015***	0.005	0.012**	0.006	0.006	0.008	-0.024***	0.009
Gyms Closed	-0.006	0.006	-0.019***	0.007	-0.033***	0.008	-0.033***	0.008
Spas Closed	-0.012**	0.005	-0.010	0.006	-0.023***	0.008	-0.009	0.008
Gatherings Limited to 10	-0.003	0.007	-0.001	0.009	-0.017	0.012	-0.028*	0.015
No Gatherings Over 100	0.009	0.007	0.028***	0.010	0.059***	0.013	0.046***	0.016
No Gatherings Limit>100	0.012	0.010	0.015	0.014	0.017	0.016	-0.006	0.020
Risk Level 1 Closed	0.045***	0.007	0.039***	0.009	0.044***	0.009	0.047***	0.008
Risk Level 2 Closed	0.018***	0.006	0.015**	0.007	0.011	0.007	-0.012	0.008
Risk Level 3 Closed	0.001	0.005	0.006	0.006	-0.008	0.007	-0.018**	0.009
Risk Level 4 Closed	-0.033***	0.005	-0.032***	0.006	-0.032***	0.008	-0.032***	0.009
Re-openings Reversed	0.070***	0.014	0.098***	0.018	0.156***	0.022	0.064***	0.022
Constant	-0.270***	0.055	-0.154**	0.069	-0.086	0.081	-0.163**	0.081
Observations	64,348		64,348		64,348		64,348	
Adjusted R-squared	0.243		0.177		0.111		0.083	
Control	YES		YES		YES		YES	

**Table A.4. Policy interventions and t-week-ahead weekly fatality growth in less populous counties.**

This table shows results of regressions in which we regress one-week-ahead change in deaths 10,000 population on policy variables defined in Table 1. The specification is identical to that in Table A.3 except we remove the 5 most populous counties in each state. All standard errors (in parentheses) are clustered at the county level. \*\*\* denotes significance at the 1% level; \*\* denotes significance at the 5% level, \* denotes significance at the 10% level.

VARIABLES	(1) Growth <sub>t+1</sub>	S.E.	(2) Growth <sub>t+2</sub>	S.E.	(3) Growth <sub>t+4</sub>	S.E.	(4) Growth <sub>t+6</sub>	S.E.
Stay at Home	0.025***	0.006	0.035***	0.008	0.040***	0.009	0.025***	0.009
State of Emergency	0.020	0.012	0.016	0.017	0.030	0.019	0.064***	0.021
Nursing Accept Pos.	0.020***	0.007	0.019**	0.008	0.029***	0.010	0.033***	0.010
No Nursing Visits	0.013***	0.005	0.005	0.007	-0.001	0.008	0.017**	0.008
Schools Closed	-0.019*	0.011	-0.024*	0.014	-0.050*	0.029	-0.040	0.029
Employees Masks	0.004	0.005	0.009	0.006	-0.014*	0.008	-0.014*	0.008
Masks Recommended	-0.016***	0.006	-0.013*	0.008	-0.011	0.009	-0.006	0.009
Mandatory Masks	0.001	0.005	-0.003	0.006	-0.020***	0.008	-0.030***	0.008
Beaches or Parks Closed	-0.027***	0.007	-0.026***	0.009	-0.013	0.010	-0.002	0.009
No Elective Procedures	0.034***	0.008	0.051***	0.010	0.041***	0.010	0.040***	0.009
Restaurants Closed	-0.009	0.008	-0.006	0.010	-0.003	0.010	-0.003	0.010
Bars Closed	0.016***	0.005	0.013*	0.007	0.008	0.009	-0.024**	0.010
Gyms Closed	-0.005	0.006	-0.015**	0.007	-0.028***	0.009	-0.029***	0.009
Spas Closed	-0.013**	0.006	-0.012*	0.007	-0.023***	0.008	-0.010	0.009
Gatherings Limited to 10	-0.005	0.008	-0.003	0.010	-0.018	0.013	-0.030*	0.016
No Gatherings Over 100	0.008	0.008	0.027***	0.010	0.060***	0.014	0.048***	0.017
No Gatherings Limit>100	0.011	0.011	0.017	0.015	0.020	0.017	-0.005	0.021
Risk Level 1 Closed	0.040***	0.008	0.033***	0.009	0.042***	0.010	0.045***	0.009
Risk Level 2 Closed	0.022***	0.007	0.020***	0.008	0.014*	0.008	-0.009	0.009
Risk Level 3 Closed	-0.001	0.005	0.004	0.006	-0.012	0.008	-0.020**	0.009
Risk Level 4 Closed	-0.033***	0.005	-0.034***	0.007	-0.033***	0.008	-0.032***	0.010
Re-openings Reversed	0.071***	0.015	0.096***	0.019	0.154***	0.024	0.061***	0.023
Constant	-0.303***	0.060	-0.206***	0.075	-0.150*	0.089	-0.222**	0.090
Observations	58,749		58,749		58,749		58,749	
Adjusted R-squared	0.219		0.161		0.108		0.083	
Control	YES		YES		YES		YES	

**Table A.5. Policy variation across the state border: Interventions and t-week-ahead weekly fatality growth (100 miles)**

This table shows results of regressions in which we regress one-week-ahead change in deaths 10,000 population on policy variables defined in Table 1. The specification is identical to that in Tables A.3 and A.4 except we include in the sample only those counties that are within 100 miles of another county in a different state and with which they do not share a border (“nearby county”) and we add the nearby county policies to the specification. Nearby county policies are estimated but not reported in the table. All standard errors (in parentheses) are clustered at the county level. \*\*\* denotes significance at the 1% level; \*\* denotes significance at the 5% level; \* denotes significance at the 10% level.

VARIABLES	(1)		(2)		(3)		(4)	
	Growth <sub>t+1</sub>	S.E.	Growth <sub>t+2</sub>	S.E.	Growth <sub>t+4</sub>	S.E.	Growth <sub>t+6</sub>	S.E.
Stay at Home	0.026***	0.010	0.037***	0.012	0.031**	0.012	0.012	0.012
State of Emergency	0.008	0.014	0.001	0.020	0.015	0.023	0.050*	0.026
Nursing Accept Pos.	0.029***	0.010	0.028**	0.013	0.031*	0.017	0.020	0.017
No Nursing Visits	0.023***	0.009	0.021	0.013	0.018	0.014	0.025*	0.014
Schools Closed	-0.078	0.048	-0.017	0.049	0.006	0.053	-0.001	0.050
Employees Masks	-0.011	0.008	-0.009	0.010	-0.029**	0.013	-0.025*	0.014
Masks Recommended	-0.031***	0.010	-0.037***	0.013	-0.046***	0.017	-0.026	0.016
Mandatory Masks	-0.011	0.009	-0.016	0.011	-0.025**	0.013	-0.035**	0.014
Beaches or Parks Closed	-0.048***	0.012	-0.053***	0.015	-0.028	0.017	-0.015	0.017
No Elective Procedures	0.011	0.013	0.030*	0.016	0.030**	0.015	0.024	0.017
Restaurants Closed	-0.013	0.014	-0.000	0.018	-0.006	0.015	-0.017	0.015
Bars Closed	0.023**	0.011	0.015	0.014	0.016	0.017	-0.007	0.018
Gyms Closed	-0.011	0.010	-0.019*	0.011	-0.015	0.014	-0.013	0.014
Spas Closed	-0.019*	0.010	-0.011	0.012	-0.016	0.014	0.007	0.016
Gatherings Limited to 10	-0.010	0.012	-0.008	0.017	-0.015	0.023	-0.030	0.027
No Gatherings Over 100	0.005	0.013	0.022	0.017	0.043*	0.024	0.044	0.029
No Gatherings Limit>100	-0.004	0.016	-0.008	0.023	0.002	0.031	-0.017	0.035
Risk Level 1 Closed	0.015	0.015	0.002	0.018	-0.008	0.017	0.017	0.015
Risk Level 2 Closed	0.035***	0.013	0.035**	0.015	0.041**	0.016	0.013	0.017
Risk Level 3 Closed	-0.018**	0.008	-0.017*	0.010	-0.031**	0.013	-0.033**	0.015
Risk Level 4 Closed	-0.014*	0.008	-0.004	0.011	-0.004	0.013	-0.001	0.015
Re-openings Reversed	0.008	0.027	0.004	0.035	0.038	0.046	0.052	0.046
Constant	-0.297***	0.083	-0.386***	0.102	-0.467***	0.126	-0.330**	0.144
Observations	22,736		22,736		22,736		22,736	
Adj. R-Squared	0.266		0.184		0.103		0.082	
Controls	YES		YES		YES		YES	
Border County Policies	YES		YES		YES		YES	



# Disentangling the effect of government restrictions and consumers' reaction function to the Covid-19 pandemic: Evidence from geo-located transactions data for the Netherlands<sup>1</sup>

Pascal Golec,<sup>2</sup> George Kapetanios,<sup>3</sup> Nora Neuteboom,<sup>4</sup>  
Feiko Ritsema<sup>5</sup> and Alexia Ventouri<sup>6</sup>

Date submitted: 2 November 2020; Date accepted: 4 November 2020

*Using transaction data from 2 million customers of ABN AMRO bank, this paper distinguishes the economic effects of voluntary responses to Covid-19 from those attributable to government lockdown measures. We compare municipalities that experienced large Covid-19 outbreaks with municipalities that had few or no cases, and find that the scale of the outbreak in a municipality has a strong negative effect on physical transactions by consumers, including for sectors that were allowed to stay open during the lockdown. We show that these responses are correlated with the intensity of the local outbreak rather than provoked by general perceptions of the outbreak. Our findings imply that the reaction function of the consumer stimulates self-isolation, which has a negative economic impact at the local level. Therefore, one potential path for long-term economic recovery is to diminish the effect of fear and restore consumer confidence by addressing the spread of the virus itself.*

- 1 We are grateful to ABN AMRO bank for providing us with their data. All individual data used in this analysis has been anonymized. Special thanks to Chief Economist Sandra Phlippen, Sinem Hocioglu and Rolf van der Velden for their support and comments.
- 2 Data Scientist, ABN AMRO Bank.
- 3 Professor of Finance and Econometrics, Kings College London.
- 4 PhD at Data Analytics for Finance and Macro (DAFM) Research Centre, Kings College London
- 5 Data Scientist, ABN AMRO Bank.
- 6 Senior Lecturer in Banking and Finance, Kings Business School.

Copyright: Pascal Golec, George Kapetanios, Nora Neuteboom, Feiko Ritsema and  
Alexia Ventouri

## 1 Introduction

The outbreak of Covid-19 has disrupted the Dutch economy. Countries around the globe, including the Netherlands, implemented strict public health measures to respond to the outbreak. These measures range from social distancing to complete lockdown, invariably constraining economic activities with serious ramifications. However, it is not clear to what extent the drop in economic activity during the lockdown was attributable to these restrictive policies or to the response function of consumers. When people are either infected or afraid of getting infected by the virus, they may choose to voluntarily stay at home. Understanding the different effect that the two factors have on economic activity is key for policy making. Quantifying the extent to which the economic fallout was driven by fear or by lockdown measures should help policy makers to make better decisions in terms of dealing with a second Covid-19 wave. Using transaction data with geolocation tags for 299 municipalities in the Netherlands, this paper examines the impact of the response function of consumers on economic activity. Our empirical strategy separates the effects of voluntary distancing from those of lockdown measures by comparing municipalities that have seen large Covid-19 outbreaks with municipalities that had few to no Covid-19 cases.

On 12 March, the Dutch government announced an “intelligent lockdown”. Effectively, the next day, all events (concerts, sports) and all meetings with more than 100 people were forbidden. Bars, restaurants and other public places or venues where people gather had to close. The timing and severity of the measures were generally comparable to most of northern Europe (such as Germany, the Netherlands and Norway), but less restrictive than in southern Europe, where the virus spread more rapidly (such as Italy, France and Spain). Figure 3 shows the overall government response index for the Netherlands, measured by stringency, over time.<sup>1</sup> It also shows the change in consumption year on year and the amount of new hospitalized Covid-19 cases. Part of the lockdown measures were relaxed on 11 May. The measures were eased further on 1 June, as the economy “reopened” (see the list of measures in Figure 1).

<sup>1</sup>This government response index proxies the strictness of the lockdown policy over time by country. See: <https://www.bsg.ox.ac.uk/research/research-projects/coronavirus-government-response-tracker>

Table 1: Phased relief of the lockdown restrictions in the Netherlands

11 May 2020
<b>Partial relaxation of restrictions</b>
Outdoor sports for people aged 19 or older allowed
Most close-contact roles, such as hairdressers and physiotherapists, were allowed to reopen
Primary schools reopened
01 June 2020
<b>Reopening of economy</b>
Secondary education started up
Hospitality venues, cinemas and theaters open with 1.5 metre social distancing and no more than 100 people
People were allowed to meet again
Public transport returns to normal timetable (only essential travel)
01 July 2020
<b>Smart restart</b>
All indoor and outdoor sports permitted
No limit for number of visitors to events; reservations and pre-entry health checks are mandatory
Non-essential use of public transport allowed
All close-contact roles back to work

The Dutch government’s strategy of a nationwide lockdown presented an advantage for our empirical estimation strategy: While the lockdown policy was implemented nationwide on 12 March, both the incidence of the illness and its timing have varied substantially across the provinces. Therefore, while the lockdown measures induced homogeneous expenditure dynamics across the Netherlands, spatial heterogeneity remains because the Covid-19 virus may have had different effects in different municipalities across the country. In this study we single-out the effect of the local magnitude of the Covid-19 pandemic on private consumption. We find that the amount of new hospitalized Covid-19 cases in a municipality has a strong negative and statistically significant effect on volume of physical transactions by consumers. In other words, municipalities in the Netherlands that have seen a large Covid-19 outbreak have struggled more in economic terms than municipalities that seen few or no Covid-19 cases. This effect cannot be explained by lockdown measures, because in the Netherlands the lockdown was imposed for all municipalities on the same date and with the same stringency. Our findings imply that people adapt their physical spending behavior, on top of the imposed lockdown measures. What are the underlying reasons for people to spend less physically during an virus outbreak? It could be fear of getting the virus, or it could be due to the fact that a considerable part of the population gets sick, or is afraid of having the virus (while showing little or no symptoms) and don’t want to go outside to prevent spreading. Another possible reasons is that the local virus outbreak adds to the negative sentiment, or reminds people that tough economic

times are about to come and therefore they increase their precautionary savings at the costs of spending. Another theory is that people already anticipate lockdown measures.

We find that Covid-19 is strongly negatively related to the frequency of supermarket visits by municipality, indicating that people are more afraid to go outside when there is larger virus outbreak in their local area. Groceries are necessity goods and we don't see a decline in total spending on groceries, only a decline in the amount of visits – which implies that people spend more every time they visit a supermarket. Also, consumers living in badly affected areas order more groceries online, most likely to prevent having to go outside the house to buy groceries in person. Digging further into this notion of fear, we investigate whether it is “rational” fear that people feel because of the intensity of the local outbreak, or whether it is “irrational” fear more related to the “perception” of how big the outbreak is, rather than the real local numbers. We look at how consumers respond to outbreaks in their province, compared to their local outbreaks, and test the relationship with supermarket visits. By performing panel regressions, we find that supermarket visits are not correlated to the virus outbreak on a province level, but only on a local level, from which we draw the conclusion that it is mainly rational fear driving consumer behavior.

The remainder of this paper is organized as follows. In section 2, we discuss relevant theory and earlier empirical evidence from other countries. Section 3 describes our transaction data for the Dutch municipalities and section 4 deals with the model and methods that we use in this paper. In section 5 we discuss the results. Section 6 concludes the study.

## 2 Literature review

Our work builds on and contributes to a rapidly evolving literature on measuring the economic impacts of Covid-19 (see e.g. Brodeur et al. (2020) [9]). Our paper combines two strands of research: (i) literature that uses high-frequency transaction data to measure the economic impact of the Covid-19 outbreak, and (ii) literature that focuses directly on the impact of lockdown policies.

Recent papers use high-frequency transaction data, analogous to the data we assemble here, to analyze aggregate consumer spending (e.g., Sobolevsky et al. 2017 [26], Carvalho et al. 2020 [11], Baker et al. 2020 [7], Baker et al. 2020 [? ], Chen, Qian, and Wen 2020 [13], Andersen et al. 2020 [4], Hacıoglu, Känzig and Surico, 2020 [20]). These papers identify a number of important findings, such as: i) there are concentrated impacts on spending in certain industries (e.g. food and accommodation); ii) some social distancing is a result of voluntary choices rather than legislation and iii) there has been a severe drop in consumption caused the pandemic.

Carvalho et al. (2020) [12] find that by the end of March 2020, the effects of the lockdown on expenditure growth was very similar across regions, irrespective of the number of confirmed cases. Using panel data, they confirm that neither GDP per capita nor the daily evolution of the regional incidence of the illness correlate robustly with the daily regional expenditure growth rate. They do, however, find a heterogeneity at a more granular level of disaggregation. When looking at the Madrid region in detail, Carvalho et al. (2020) [12] find that the fall of expenditure induced by the lockdown is larger in local areas within the region where the pandemic has caused more distress. Chetty et al. (2020) [14] examine the effect of executive lockdown orders on changing consumer spending in the US. Many states enacted stay-at-home orders and shutdowns of businesses in an effort to limit the spread of Covid-19 infections and later reopened their economies by removing these restrictions. They find that spending fell sharply in most states before formal state closures. Moreover, states' reopenings had little immediate impact on economic activity. They conclude that health concerns are the core driver of reductions in spending, rather than government-imposed restrictions. Chetty et al. (2020) [14] use US state-level data, which contain large heterogeneity across and within states in the precise form that the lockdown and the reopening took. They

therefore argue that their estimates should be viewed as a broad assessment of the average impact of typical reopening efforts on aggregate economic activity and the authors defer from a more detailed analysis of how different types of reopenings affect different sectors.

Goolsbee and Syverson (2020) [18] examine to what extent the reduction in economic activity was due to government restrictions or to people's voluntary decision to stay at home. They perform a detailed analysis of customer visits on a county level with the use of cellular phone record data. By comparing consumer behavior within the same commuting zones but across counties with different government restrictions, they find that lockdown orders account for only a modest share of the decline in economic activity. They argue that although overall consumer traffic fell by 60%, legal restrictions explain a decline of only 7%. Our study differs from that of Goolsbee and Syverson (2020) [18] in that we use actual spending data instead of personal mobility data. What is more, Goolsbee and Syverson (2020) [18] implicitly assume that the number of visits corresponds to the amount of economic activity. Our data show that although people may visit stores less often during the Covid-19 crisis, they spend more time during every visit (see Figure 1). This implies that travel to stores may decline rapidly, but spending does not decline at the same rate. Similar to Goolsbee and Syverson (2020) [18], Gupta et al. (2020) [19] study smart-device data that proxy mobility patterns. They find large declines in mobility in all states since the start of the pandemic, even those without major mitigation mandates. This indicates a substantial share of the fall in mobility was not induced by strong lockdown mandates such as stay-at-home orders. Their findings show that state level emergency declarations account for about 55% of the decline between the first week of March and the second week in April, with the remaining 45% of the decline attributable to secular trends that they interpret as the private (residual to policy) response to the pandemic.

Chen, Qian and Wen 2020 [13] find a similar result to that of Goolsbee and Syverson (2020) [18] for China. They study the drop in card and QR scanner transactions through UnionPay. They also find that the effect on consumption is stronger in cities that have had more Covid-19 cases. More specifically, they argue that in the 20 cities that received the highest inflow of Wuhan residents (the epicentre of the Covid-19 outbreak), consumption decreased by 12% more than in other cities in their sample. For cities reporting zero cases (as of late March), the decrease in

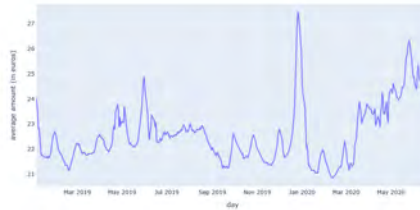


Figure 1: Average amount per transaction in euros spent with debit cards in the Netherlands, 7-days rolling average

offline consumption was 13% less than for cities with positive Covid-19 cases in the same time period. They find that a doubling of the number of infected cases at the city-level was associated with a 2.8% greater decrease in offline consumption. In addition, they find that fears regarding local hospital capacity and the first local Covid-19 related death drive consumption down further. Chen, Qian and Wen 2020 [13] conclude that management of the public health crisis is crucial for reinvigorating the economy. As fear of the virus spreads, (physical) consumption decreases. This hypothesis is supported by a recent study by Altig et al. [2], who constructed a newspaper- and Twitter-based sentiment measure that is closely aligned with the perceptions of households. The sentiment measure peaked during the Covid-19 outbreak as news and social media were becoming more negative in tone.

Other papers study the effects of Covid-19 and the imposition of lockdown on different aspects of the economy. Aum, Lee and Shin [5] perform a regional analysis of the effect of the Covid-19 outbreak on unemployment in Korea. Korea did not implement a lockdown, like many Western countries, but instead relied on testing and contact tracing. They find that a one per thousand increase in infections caused a 2 to 3% drop in local employment. Non-causal estimates of this coefficient from the US and UK, which implemented large-scale lockdowns, range from 5 to 6% , suggesting that at most half of the job losses in the US and UK can be attributed to lockdowns. The authors conclude that the primary culprit in the Covid-19 recession is Covid-19 itself, rather than lockdowns, and so the lifting of lockdowns around the world may lead to only modest recoveries unless infection rates also fall. Hiroyasu and Todo (2020) [21] quantifies the economic effect of a possible lockdown in Tokyo, Japan. Applying an agent-based model they find that when Tokyo is

locked down for a month, the indirect effect on other regions would be twice as large as the direct effect on Tokyo, leading to a total production loss of 5.3% of Japan's annual GDP.

Our research is most related to the study by Chen, Qian and Wen (2020) [13]. We do, however, examine different geographical levels, as Chen, Qian and Wen 2020 [13] focus specifically on cities, whereas we consider municipalities. Also, China has had a more heterogeneous lockdown policy across different cities, because some were forced into full quarantine (such as Wuhan) whereas other cities faced milder lockdowns. Also the imposition dates of the lockdowns differ between cities in China. The lockdown policy in the Netherlands, which was consistent among regions in terms of stringency and imposition date, offers an empirical advantage for distinguishing the effect of Covid-19 from that of the lockdown policy.



### 3 Data

We use unique transaction data from ABN AMRO cardholders, the Stringency Index (which measures the strictness of lockdown measures) provided by the Blavatnik School of Government and the amount of hospitalized Covid-19 cases provided by the Dutch National Institute for Public Health and the Environment (RIVM). In the following section we describe each dataset in more detail. We show how we transform the raw transaction data and explain how we acquire geolocation data on a municipality level.

#### Transaction data

We use transaction data from ABN AMRO cardholders. ABN AMRO is the third biggest bank in the Netherlands and has approximately 18% of the total market share in the country [29]). As a consumer bank, ABN AMRO has around 3.1 million unique account holders. This covers around 22% of the total adult (18 +) population. ABN AMRO is a broad retail bank present in all parts of the country and catering to all types of customers. Our data are therefore largely representative of the adult population of The Netherlands in terms of gender, age, geographical representation and income (see Figure 2). Collectively, ABN AMRO account holders spend over 65 million euros on a daily basis, with an average transaction size of 23 euro. On average, over the sample period, our dataset comprises 2,745,651 physical pin transactions a day and around 344,753 online transactions a day.

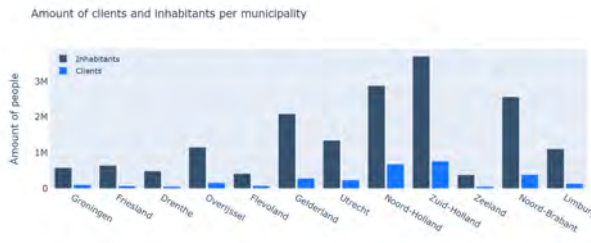


Figure 2: Amount of ABN AMRO clients in different provinces of the Netherlands

We acquire Point of Sale (PoS) data from pin terminals documenting every transaction. The data for each transaction include a timestamp, the amount in euros, the corresponding account number, the counter party description and the counterparty account number. We have used a labeling function based on keywords in the transaction description to identify the category the transaction belongs to.<sup>2</sup>

Our transaction data only incorporate accounts held by individuals and households. We exclude corporate accounts (SMEs) by excluding transactions backed by a debit card issued to a corporation as a “company card”. The purpose of this is to ensure that we make a correct analysis of domestic consumption that is not biased by corporate expenditure.<sup>3</sup> We include spending by credit cards in the total spending, but were not able to identify credit card expenditures by category due to privacy issues.<sup>4</sup>

### Stringency index

We make use of the stringency index for the Netherlands based on the Oxford Covid-19 government response tracker. This tracker collects information on several different common policy responses that governments have taken to respond to the pandemic, using 17 indicators such as school closures and travel restrictions. The data from the 17 indicators are aggregated into a set of four common indices, reporting a number between 1 and 100 to reflect the level of government action. Figure 3 depicts the stringency index for the Netherlands<sup>5</sup>.

### Covid-19 Data

We report the number of new hospitalized Covid-19 cases each day, for each municipality, using publicly available data from the National Institute for Public Health and the Environment,<sup>6</sup> National

<sup>2</sup>Note that our dataset does not include transactions made by foreign (non-Dutch) tourist in the Netherlands. The total economic contribution from foreign tourists in the Netherlands is relatively small; 1,7% of GDP

<sup>3</sup>Note that this is a drawback of the Carvalho et al. (2020) [12] data. The study cannot distinguish the identity of the buyer in each transaction and therefore the data represent a mixture of final consumption expenditure by households and corporate firms’ intermediate input purchases.

<sup>4</sup>In the Netherlands credit cards are not widely used as a payment option. This is confirmed by Jonker et al. (2017) [23], who argue that debit cards are the dominant payment method in the Netherlands. Moreover, the number of local Covid-19 cases should not meaningfully affect the ratio between debit and credit card usage compared to other parts of the country, and therefore the omission of credit card data should not bias our analysis.

<sup>5</sup><https://www.bsg.ox.ac.uk/research/research-projects/coronavirus-government-response-tracker>

<sup>6</sup><https://www.rivm.nl/>

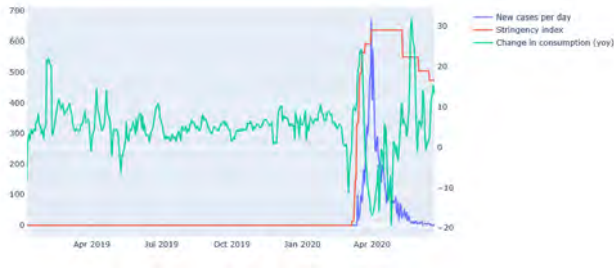


Figure 3: Year on year transactions, new Covid-19 hospitalized cases and the proxy of the lockdown measured by the stringency index in the Netherlands (stringency scaled \* 8)

Institute for Public Health and the Environment provides the cumulative number of hospitalized Covid-19 cases on a daily basis by municipality. For the amount of hospitalized cases we report two daily series by municipality: a seven-day moving average of new daily totals and a seven-day moving average of the cumulative total to the given date. Figure 4 shows the aggregate cumulative and new amounts of Covid-19 hospitalized cases in the Netherlands. Figure 3 shows the year on year change in transactions, the stringency index and the new Covid-19 hospitalized cases. From the plot it is seen that the initial spike in new Covid-19 cases corresponds with a severe drop in transactions. Moreover, as new Covid-19 cases fall, the average spending increases again.

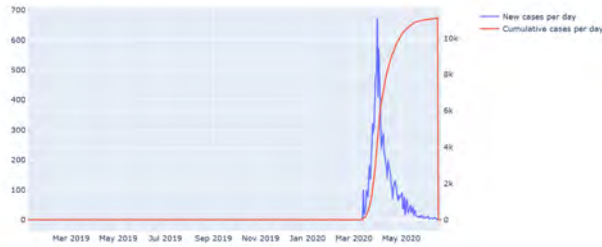


Figure 4: Cumulative and new amounts of hospitalized Covid-19 cases in the Netherlands

### 3.1 Data transformations

We analyze year on year growth rates of the aggregate amount of spending by municipality on a particular date. In order to control for seasonality trends in expenditure we proceed as follows: We pair every day following 2 January, 2020 with its equivalent day in the equivalent week of the previous year:

$$\Delta Expenditure_i = \frac{Expenditure_{it} - Expenditure_{it-365}}{Expenditure_{it-365}} \quad (1)$$

where  $Expenditure_{it}$  is *total transactions*  $\times$  *average amount in euros* on day  $t$  for municipality  $i$ . In addition to adjusting for seasonal patterns, we also manually adjust for calendar effects. These are events and holidays related to the calendar that usually have an irregularly recurring pattern. We compared specific holidays with the same holiday in the previous year, despite the fact that it may have fallen on a different week- or weekend day. Moreover, we deleted data for 29 February 2020 because this date only occurs in a leap year, as a additional day. The data depict large periodic fluctuations across days. We address such fluctuations through aggregation, e.g. reporting 7-day moving averages to smooth daily fluctuations.

### 3.2 Geolocation

We use transaction-weighted density-based clustering to predict POS geolocations (see Appendix A).

For every account-holder we have the zipcode of their registered home address. These zipcodes are merged with an external dataset featuring all Dutch zipcodes and their latitudes and longitudes<sup>7</sup> in order to obtain geolocations (expressed as latitude and longitude). Customers' home locations often have a clear relationship to payment point locations, with most payment points being situated in a dense cluster around consumer home location points. The purpose is thus to identify one cluster in these points and to classify other transactions as outliers. Then using only the main cluster points, we proceed by determining the payment point location. The final implementation

<sup>7</sup><http://geonames.org>

consists of several steps, of which clustering is the first, followed by determining the location and confidence using weighted transactions and finally correcting low-confidence predictions. The full methodology is described in Appendix A. This methodology offers the advantage of predicting the correct province with 95% accuracy, the correct municipality with 86% accuracy and the correct city with 67% accuracy.

For every municipality we calculate the average expenditure by

$$\frac{\sum_i^T \text{expenditure}}{T}$$

where  $T$  is the amount of days in our dataset. In order to ensure that we have adequate coverage of transactions within every municipality ( $i$ ), we delete the lowest 5 percentiles of municipalities based on the ABN AMRO clients to total inhabitants ratio. We also delete municipalities for which we have incomplete data, which leaves us with a dataset of 299 municipalities out of 355. For the online iDEAL (sepa) transactions, we locate transactions at the home address of the ABN AMRO client, which is part of the meta data that is provided for every ABN AMRO account-holder.

### 3.3 Descriptive analysis

Figure 5 shows a comparative bubble chart. The vertical axis shows the average year on year drop in transactions between March 14 and April 16 and the horizontal axis shows the logarithm of cumulative hospitalized Covid-19 cases up to April 16. The size of the bubble indicates the population size of the municipality. The trend-line shows a negative correlation between cumulative Covid-19 cases and growth in transactions. It also shows that in general larger municipalities (in terms of population size) have faced larger Covid-19 outbreaks and experienced a larger drop in transactions.

Figure 7 shows the average year on year change in total expenditure. Figure 7 and figure 8 show average spending on offline and online groceries, respectively. From the graphs it is seen that both categories show increased spending from the middle of March onwards. In particular, online grocery shopping saw a large jump, at the end of April, at the peak, people spend around four

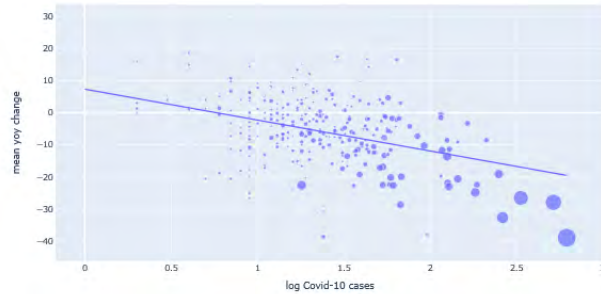


Figure 5: Comparative bubble chart. On the vertical axis, the average year on year drop in transactions between March 14 and April 16 and on the horizontal axis, the logarithm of cumulative Covid-19 cases up to April 16. The size of the bubble indicates the population size of the municipality.

times as much on online groceries as a year before. However, as figure 8 shows, as the Covid-19 crisis starts the wane during May and June, the total increase in online grocery shopping also starts to fall. Figure 9 shows the year on year changes in total consumption, offline supermarket consumption and online supermarket consumption in one plot. This figure clearly shows that whereas overall consumption dropped significantly after mid-March, supermarket and online supermarket expenditure show an inverse trend and performed remarkably well.



Figure 6: Average year on year change in total expenditure, 7-days rolling average

Figure 10 shows the sharp drop in expenditure in sectors that were forced to close during the nationwide lockdown (see Table 2 for a list of spending categories in “closed” sectors). Figure 10 also shows the stringency index for the Netherlands. It is striking to see that with every step the government took to lift the lockdown measures (proxied by the change in the stringency index)

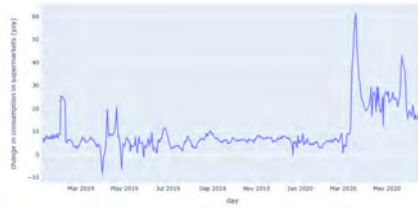


Figure 7: Average year on year change in supermarket expenditure, 7-days rolling average

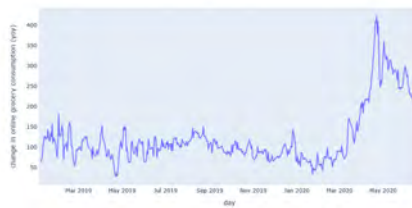


Figure 8: Average year on year change in online grocery expenditure, 7-days rolling average

the total transactions in closed sectors increases. Figure 10 shows that the total consumption is very closely correlated with consumption in the sectors that were still open during the lockdown measures (correlation of 98%). Indeed, as the lockdown in the Netherlands was relatively mild, the sum of the sectors that had to close represented only a small proportion of total consumer expenditure. This strengthens our view that solely looking at the economic impact of the lockdown measures is not sufficient in order to assess the economic impact of the epidemic.

Figure 11 shows the year on year change in transactions between March 13 and June 1 (the end of the nationwide lockdown) by region. Blue indicates an increase in transactions and red indicates a decrease in transactions. Figure 12 shows a geographical map of the cumulative amount of hospitalized Covid-19 cases on June 1. Dark red indicates a large number of Covid-19 cases and light red indicates few Covid-19 cases. Municipalities that are coloured white have seen zero Covid-19 cases. Comparing the two maps 11 and 12 reveals that municipalities that have seen larger Covid-19 outbreaks, mostly located in the centre and south of the Netherlands, also show a larger drop in physical pin transactions (PoS). Figure 13 and figure 14 plot the year on year

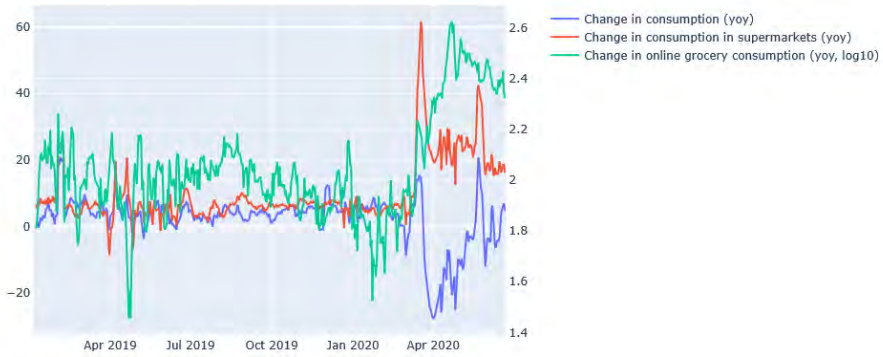


Figure 9: Year on year change in different expenditure types, 7-days rolling average



Figure 10: Year on year change in transactions for total consumption, consumption in sectors that were forced to close during the lockdown and sectors that could remain open. Stringency (inverse) is a proxy of the lockdown.

physical pin transactions, the inverse of new Covid-19 hospitalized cases and the stringency index, for two municipalities with a relatively small population size; Veendam and Bernheze. Veendam had almost no Covid-19 cases, and although the pin transaction data show an initial spike just before the imposition of the lockdown and a small drop afterwards, it recovers almost immediately to normal levels of expenditure. This is contrary to the municipality of Bernheze, where the drop in pin transactions is very pronounced (50% at its lowest level), and moves alongside the number of new confirmed Covid-19 cases. This same conclusion holds if we compare two big cities; Amsterdam and Groningen (see Figure 15 and Figure 16). The total physical pin transactions dropped by 50%



Table 2: Categories of consumer spending that were forced to close during the nationwide lockdown in the Netherlands

Closed sectors during the Covid-19 crisis
Restaurants
Wellness
Casinos
Cinemas
Concert halls
Museums
Theme parks
Bars
Dining
Fastfood
Hairdressers
Solariums
Spas
Other entertainment

in Amsterdam, whereas in Groningen transactions bottomed out at around 35% below prior year's level. Notice that for Amsterdam the pin transactions had not returned to positive levels at the end of the lockdown.

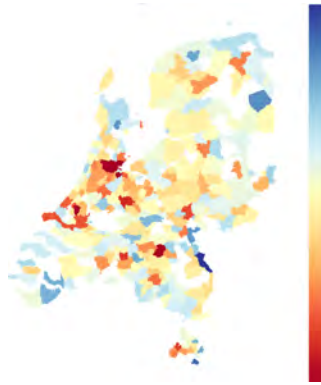


Figure 11: Map of the Netherlands showing the change in transactions (year on year) per municipality between March 13 and June 1 (the end of the nationwide lockdown). Blue indicates an increase in transactions and red indicates a decrease in transactions



Figure 12: Map of the Netherlands showing the cumulative Covid-19 cases per municipality at June 1. Dark red indicates a large number of Covid-19 cases and light red indicates few Covid-19 cases. Municipalities that are coloured white have seen zero Covid-19 cases.

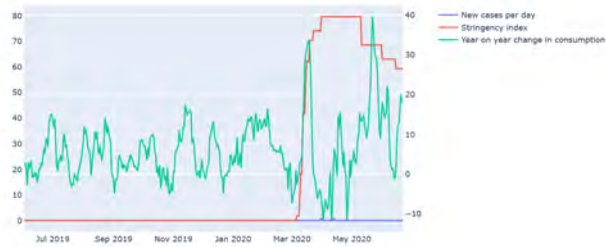


Figure 13: Year on year transactions, new hospitalized Covid-19 cases and the proxy of the lockdown measured by the stringency index for Veendam



Figure 14: Year on year change in transactions, new hospitalized Covid-19 cases and the proxy of the lockdown measured by the stringency index for Bernheze

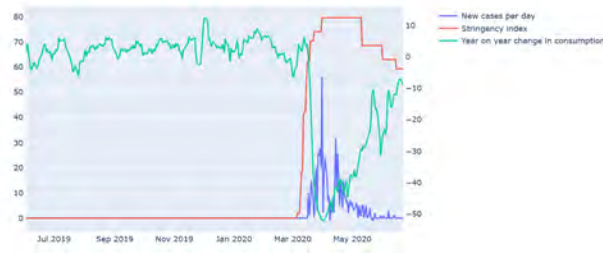


Figure 15: Year on year transactions, new hospitalized Covid-19 cases and the proxy of the lockdown measured by the stringency index for Amsterdam



Figure 16: Year on year transactions, new hospitalized Covid-19 cases and the proxy of the lockdown measured by the stringency index for Groningen

## 4 Model and research design

Throughout this paper, we use the following terms:

- *The dependent variable* is denoted  $Y_{it}$  for municipality  $i$  at time  $t$ .
- *The target variable of interest* is denoted  $X_{it}$  for municipality  $i$  at time  $t$ .
- *Control variables* are denoted  $X_i$  and  $X_t$  for the sets of control variables  $(X_{i1}, x_{i2}, \dots, X_{in})$  and  $(X_{t1}, X_{t2}, \dots, x_{tm})$ , which are time-invariant and entity-invariant, respectively <sup>8</sup>.

To measure whether the severity of the Covid-19 outbreak at the local (municipality) level has a significant impact on transactions, we use a fixed effects (FE) panel regression. FE estimation is performed by *time demeaning* the data. Demeaning deals with unobservable factors because it takes out any component that is constant over time and entity. By assumption, this would be the entire effect of the unobservable variables (see Appendix B for an investigation into what sort of entity fixed effects we are capturing in the regression). We use the following equation:

$$Y_{it} = \alpha_i + \gamma_t + \beta_1 X_{it} + \varepsilon_{it}, \quad (2)$$

where  $Y_{it}$  is the observation for the  $i$ th cross-section unit at time  $t$  for  $i = (1, 2, \dots, N)$  and  $t = (1, 2, \dots, T)$ .  $\alpha_i$  denotes unobserved characteristics for each cross-sectional unit that don't vary over time; a  $m \times 1$  vector of unobserved common effects.  $\gamma_t$  are unobserved characteristics for each time unit  $t$  that don't vary over entity; hence a  $k \times 1$  vector of unobserved common effects.  $X_{it}$  is a  $1 \times n$  (include constants) of observed independent variables, including our variable of interest, new hospitalized Covid-19 cases.  $\varepsilon_{it}$  are the individual-specific (idiosyncratic) errors assumed to be distributed independently of  $X_{it}$  and  $\alpha_i$ . By including fixed effects  $\alpha_i$  and  $\gamma_t$ , we are controlling

<sup>8</sup>These variables control for factors that could potentially impact  $Y_{it}$  and/or  $X_{it}$ .

for the average differences across municipalities in any unobservable predictors, which allows us to eliminate the omitted variable bias.<sup>9</sup>

In general, however, the unobserved factors  $\alpha_i$  could be correlated with  $X_{it}$ . Pesaran (2006) [25] shows that by including the cross-sectional averages in the regression the differential effects of unobserved common factors are eliminated. This approach is favoured above the principal components approach brought forward by Coakley, Fuertes and Smith (2002) [15] because we want to avoid inconsistent results in the situation that the unobserved factors and the included regressors are correlated. Moreover, the approach by Pesaran [25] allows us to use ordinary least squares (OLS) when we specify an auxiliary regression where the observed regressors are augmented by cross-sectional (weighted) averages of the dependent variable ( $Y_{it}$ ) and observable variables  $X_{it}$  and possibly other control variables  $X_i$  and  $X_t$  (see also Kapetanios and Pesaran, 2005 [24]). We therefore run the regression in two stages:

First stage regressions:

$$Y_{it} = \beta_1 \mu_t^Y + \beta_2 \mu_t^X + e_{it}^y X_{it} = \beta_1 \mu_t^Y + \beta_2 \mu_t^X + e_{it}^x \tag{3}$$

where  $\mu_t^Y$  and  $\mu_t^X$  are the cross-sectional averages of  $Y_{it}$  and  $X_{it}$  respectively over time  $t$ .  $e_{it}^y$  and  $e_{it}^x$  capture the residuals of equation 3.

Second stage regression:

$$e_{it}^y = e_{it}^x + w_{it}, \tag{4}$$

---

<sup>9</sup>The random effects (RE) model is more appropriate when the entities in the sample can be thought of as having been randomly selected from the population. A RE model allows all unobserved effects to be relegated to the error term by specifying the model as

$$Y_{it} = \beta_1 X_{it} + v_{it}$$

where  $v_{it} = \omega_i + \varepsilon_{it}$ . A critical assumption of the RE model is that the unobserved individual effect ( $\omega_i$ ) isn't correlated with the independent variable(s). For the research question at hand, we cannot eliminate the possibility that there are unobserved factors that are correlated with  $X_{it}$ . Moreover, although  $\varepsilon_{it}$  satisfies the classical linear regression model (CLRM) assumptions, the inclusion of  $\omega_i$  in the composite error  $v_{it} = \omega_i + \varepsilon_{it}$  results in a CLRM assumption violation. If you relegate the individual effects ( $\omega_i$ ) to the error term, you create a positive serial correlation in the composite error. As a result, a RE estimation requires feasible generalized least squares rather than ordinary least squares (OLS) to appropriately eliminate serial correlation in the error term and to produce the correct standard errors. Therefore, we prefer the FE specification.

Under the assumptions explained in Pesaran, 2006 [25], for any fixed  $m$  in  $\alpha_i$  these residuals provide consistent estimates of  $\varepsilon_{it}$  in the multifactor model (2) and could be used as “observed data” to obtain estimates of the factors  $\alpha_i$ . The factor estimates can then be used directly as (generated) regressors in regression equation 4. Effectively, in the second stage we try to explain the variance of  $Y_{it}$  with the variance of  $X_{it}$ , thereby eliminating all the other fixed effects.

To further investigate the effects of our selection of control variables, we also run a Panel OLS model including only time fixed effects and control variables that vary among municipalities (but not over time):

$$Y_{it} = \gamma_t + \beta_1 X_{it} + \varepsilon_t, \quad (5)$$

where  $X_{it} = X_{it} + X_i$  and  $X_i$  is a set of control variables  $(x_1, x_2, \dots, x_n)$ , e.g.  $n \times 1$  vector of observed common effects. Notice that this is a less strict specification compared to equation (2) because we cannot account for entity fixed effects.

Moreover, to test the importance of the lockdown measures on physical spending, we run a FE model that includes entity fixed effects and control variables that vary over time (but not over municipality):

$$Y_{it} = \alpha_i + \beta_1 X_{it} + \varepsilon_t, \quad (6)$$

where  $X_{it} = X_{it} + X_t$  and  $X_t$  is a set of control variables  $(x_1, x_2, \dots, x_v)$ , e.g.  $v \times 1$  vector of observed common effects. As this specification does not include time fixed effects, this is also a less strict specification than equation (2).

## 5 Results

Table 3 column (1) shows the regression results for the fixed effects panel regression of equation (2). The dependent variable ( $Y_{it}$ ) is the year on year change in total volume of transactions by municipality  $i$  for time  $t$ . The key explanatory variable is the new amount of hospitalized Covid-19 cases ( $X_{it}$ ) in municipality  $i$  for time  $t$ . The regression also includes both municipality and time fixed effects. We cluster standard errors at the municipality level (see Appendix B for an investigation of what the entity fixed effects in this regression are potentially capturing). We find a strong statistically significant negative coefficient on the explanatory variable ( $X_{it}$ ). The results show that on average, each additional hospitalized Covid-19 case reduces year on year transactions by -2.79%. Given that in the Netherlands the stringency and timing of the lockdown were identical for all municipalities, the lockdown effect in the regression is captured by time fixed effects.<sup>10</sup>

Table 3: Dependent Variable: Percentage change in transactions year on year

Regressor	Column 1	Column 2	Column 3
Covid-19 cases	-1.2094*** (0.0413)	-2.796*** (0.0470)	-2.8521*** (0.0470)
Stringency		-0.0473*** (0.0010)	-0.0217*** (0.0019)
AEX			-0.0011 (0.0011)
EURIBOR			-20.402*** (0.7977)
<i>N</i>	299	299	299
<i>T</i>	386	386	386
<i>FE</i>	Entity and Time	Entity	Entity
<i>R</i> <sup>2</sup>	0.0074	0.0598	0.0654

(Standard errors in parentheses)  
 \*\*\*  $p < 0.01$ ; \*\*  $p < 0.05$ ; \*  $p < 0.1$

Table 3 column (2) shows the results including the stringency index as a control variable ( $X_{1t}$ ), which is a proxy of the strictness of the lockdown measure over time (see equation 6). This index is constant over municipality because the Netherlands faced a nationwide lockdown. The panel regression also includes municipality fixed effects, but no time fixed effects because the stringency

<sup>10</sup>For all our regression, the value of  $R^2$  is relatively low. This is contrary to findings of Chen, Qian and Wen (2020) [13] and Goolsbee and Syverson (2020) [18], who report a relative large  $R^2$ . This is mainly because of differences in specifications. Both of those studies use dummy variables to single out specific subgroups of panel data, and therefore they measure the effects between two different groups over time. In contrast, we look at the fit of all municipalities (299) over time. Moreover, they transform the data into logged values, whereas we prefer to use a linear model and to keep the amount of transformations to the data as minimal as possible.

variable is constant over municipality but differs over time. Both variables are significant; however, the coefficient on the number of new Covid-19 cases is substantially larger than the coefficient on the stringency index. This suggests that if the lockdown policy becomes one unit more strict on a scale of 0–100, transactions will drop by 0.05%. The beta coefficient of  $X_{it}$  suggests that one additional Covid-19 case will cause transactions to drop by 2.79%. These regression results show that economic activity is reduced by both Covid-19 itself as well as the government lockdown restrictions.

Table 3 column (3) shows the results including the stringency index and two other high-frequency macro variables that are constant over municipality but differ over time ( $X_t$  in equation 6). The AEX Index is the Dutch stock market index, which proxies investors sentiment. EURIBOR stands for the Euro Interbank Offered Rate, the average rate that European banks issue loans to other banks. These variables proxy the growth of the economy and the level of inflation. The inclusion of both high-frequency macro variables into the fixed effects panel regression has little effect on the results. Table 3, column (3) shows that the coefficients on target variable, the number of new hospitalized Covid-19 cases ( $X_{it}$ ), the stringency index and the EURIBOR are statistically significant. Moreover, the inclusion of the two macro variables reduces some of the explanatory power of the stringency index, which reduces by more than half from -0.05 to -0.021. The coefficient on the AEX Index is not statistically significant. This is not surprising given that financial markets have performed remarkable well during the Covid-19 crisis. After a short dip in the beginning of March, the stock index recovered rapidly.

Table 4 shows the results of the two-stage regression (see equation (4)). This specification allows us to eliminate the differential effects of unobserved common factors (see section 4). The result is significant at the 1% level. The interpretation of the beta coefficient is not straightforward because it is the beta coefficient of the residual of the original regression. The sign of the coefficient is as anticipated; the number of hospitalized Covid-19 ( $X_{it}$ ) cases has a negative effect on year on year average transactions. If we include time-variant control variables ( $X_t$ ) in the first stage regression (equation 3) and estimate ( $X_{it}$ ) in the second stage, the variable is still statistically significant and the beta coefficient does not change. This suggests that the set of control variables  $X_t$  has no



correlation with the variable of interest ( $X_{it}$ ). Moreover, if we add these control variables to the final regression (equation (4)) we find that all control variables are not statistically significant, whereas  $X_{it}$  remains highly significant, which implies that their variance does not have any explanatory power for the variance of  $Y_{it}$ .

Table 4: Dependent Variable: Residuals for percentage change in transactions year on year

Regressor	Column 1
Residual Covid-19 cases	-1.6004*** (0.0499)
$N$	299
$T$	386
$FE$	NO
$R^2$	0.0089

(Standard errors in parentheses)

\*\*\*  $p < 0.01$ ; \*\*  $p < 0.05$ ; \*  $p < 0.1$

## 5.1 Time lags

As we make use of high-frequency daily data, we also investigate the sensitivity of time lags (inter-temporal shifting). Figure 17 shows the beta coefficient on the explanatory variable ( $X_{it}$ ), the new amount of hospitalized Covid-19 cases, shifted over time. We use the second-stage regression (the regression of the residuals) to show the evolution of the beta coefficient. The horizontal axis  $t$  indicates the time in days, the vertical axis shows the beta coefficient on ( $X_{it}$ ). The figure shows that the beta coefficient has the highest negative explanatory power when  $t = 0$ . The beta coefficient becomes smaller as  $t$  shifts over time, and this is unequally distributed between  $t_+$  and  $t_-$ . This makes intuitive sense, as for instance the use of  $t_{+15}$  would try to explain the drop in transaction data of  $t_{-15}$  days previously based on the hospitalized Covid-19 cases at  $t$ , where a causative relationship would not seem possible. Moreover, as only few patients infected with covid-19 patient are actually hospitalized (our explanatory variable  $X_{it}$ ) the local spread may have already taken off the moment people are actually admitted to the hospital. Figure 18 shows the p-value of ( $X_{it}$ ) in the second-stage residual regression. The horizontal axis  $t$  indicates the time in days. This figure shows that the explanatory variable ( $X_{it}$ ) becomes non-significant when the time is shifted towards  $t_{-45}$ . This makes sense as the amount of Covid-19 cases was zero for all municipalities before the

first Covid-19 case was confirmed on 27 February 2020. In general, these results show that our variable of interest is robust to shifts in time.

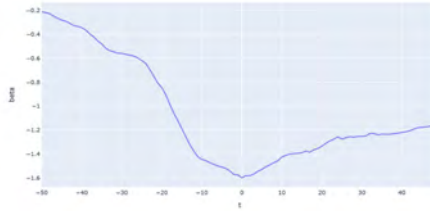


Figure 17: The development of the beta coefficient of the explanatory variable ( $X_{it}$ ), the new amount of hospitalized Covid-19 cases, shifted over time. We use the second-stage regression (the regression of the residuals) to show the evolution of the beta coefficient. The horizontal axis  $t$  indicates the time in days and the vertical axis shows the beta coefficient of ( $X_{it}$ ).

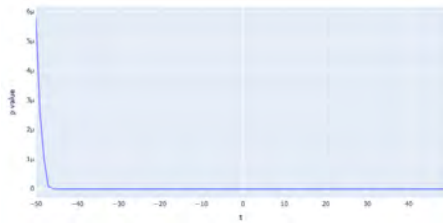


Figure 18: The development of the p-value of the explanatory variable ( $X_{it}$ ), the new amount of hospitalized Covid-19 cases, shifted over time. We use the second-stage regression (the regression of the residuals) to show the evolution of the beta coefficient. The horizontal axis  $t$  indicates the time in days and the vertical axis shows the p-value of the explanatory variable ( $X_{it}$ ).

## 5.2 The effect of the lockdown

One may argue that the difference between municipalities may not be the result of the number of local Covid-19 cases, but rather the result of “disobedience” or the lack of “enforcement” of the lockdown rules. In our research we take the assumption that the lockdown measures—as they were implemented nationwide—are similar across municipalities. While this should be true theoretically, in practice some municipalities may be stricter in following the national government rules than others. For example, Amsterdam might have been much more strict in terms of checking whether

people actually obey the rules compared to, for example, a small municipality in the North. Figure 19 shows that the variance in closed sectors between big cities is very small and largely constant over time. We test this further by regressing the stringency index on the total transactions in closed sectors. Under this category we take all sectors that were subject to restrictions and were either forced to fully close or continue with very limited capacity, for instance, restaurants that were permitted only to provide takeaway goods (see Table 2 for a list of consumer categories that we include in the subset of closed sectors). As expected (see Table 5, column (1)) the stringency level is an extremely good predictor of the drop in transactions in the closed sector, with an  $R^2$  of 0.45<sup>11</sup>. Table 5 column (2) shows the same regression but including the Covid-19 variable ( $X_{it}$ ). For completeness, we include the residual regressions in Table 7, which includes stringency in the first-stage regression of equation (3), and also show a statistically significant result for the coefficient on hospitalized Covid-19 cases in equation (4). It is interesting to see that the variable is still significant at the 1% confidence level, which indicates that the small differences between municipalities in supermarket visits are the result of the severity of the local Covid-19 outbreak. Table 6 validates this conclusion. Here, we regress the Covid-19 variable on the variance between municipalities in transactions in the closed sectors. Again the coefficient on the Covid-19 variable is statistically significant, albeit at the 5% level. Intuitively, these results make sense. People are less likely to follow lockdown rules if they don't see the benefit or purpose of these rules. Similarly, local municipalities may be less strict in enforcing the national rules if they have few or no Covid-19 cases in their community. This also tells us that even for the sectors that may feel their loss in revenues is fully caused by the lockdown measures, it does also matter how severely their local community has been hit by the virus. The effect is actually quite strong: With every additional hospitalised Covid-19 case in the municipality, closed sectors see their pin transactions drop (year on year) by 3.2%. If the lockdown measures had been made tougher, for example during April to the level that Italy faced at the time (a stringency level of 93.5 out of 100), this would have resulted in an additional 10% decrease in pin transactions (year on year) in the closed sectors.

<sup>11</sup>Note that this panel regression only includes entity effects because stringency is constant for each entity  $i$  over time.

Table 5: Dependent Variable: Percentage change in closed sectors year on year

Regressor	Column 1	Column 2
Stringency	-0.7836*** (0.0025)	-0.7662*** (0.0026)
Covid-19 cases		-3.2599*** (0.1160)
<i>N</i>	299	299
<i>T</i>	386	386
<i>FE</i>	Entity	Entity
<i>R</i> <sup>2</sup>	0.4585	0.4622

(Standard errors in parentheses)  
 \*\*\*  $p < 0.01$ ; \*\*  $p < 0.05$ ; \*  $p < 0.1$

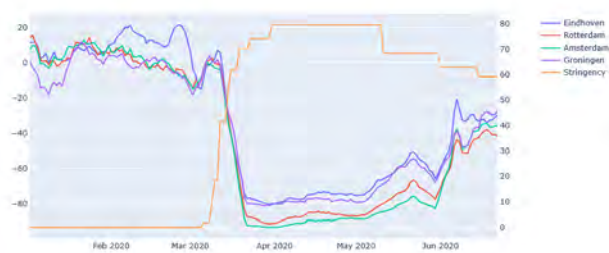


Figure 19: Year on year change in transactions in sectors that were forced to close during the lockdown in four large cities. Stringency is a proxy of the lockdown.

Table 6: Dependent Variable: Variance between municipalities in percentage change in transactions in closed sectors year on year

Regressor	Column 1
Covid-19 cases	-0.2525** (0.1038)
<i>N</i>	299
<i>T</i>	386
<i>FE</i>	Entity and Time
<i>R</i> <sup>2</sup>	0.001

(Standard errors in parentheses)  
 \*\*\*  $p < 0.01$ ; \*\*  $p < 0.05$ ; \*  $p < 0.1$

### 5.3 The effect of the unwillingness to go outside

Our results show a strong negative sensitivity of consumption to within-municipality changes in the outbreak's severity. The reason why people start to spend less when the virus outbreak surges is

Table 7: Dependent Variable: Residuals for percentage change in closed sectors year on year

Regressor	Column 1
Residual Covid-19 cases	-1.2147*** (0.1317)
<i>N</i>	299
<i>T</i>	386
<i>FE</i>	NO
<i>R</i> <sup>2</sup>	0.0007

(Standard errors in parentheses)  
 \*\*\*  $p < 0.01$ ; \*\*  $p < 0.05$ ; \*  $p < 0.1$

hard to tell: it could be fear of getting the virus (I), or due to the fact that a considerable part of the population gets sick (II). Alternatively, some may be afraid of having the virus (while showing little or no symptoms) and don't want to go outside to prevent spreading (III). Another possible reason is that the local virus outbreak adds to the negative sentiment, or reminds people that tough economic times are about to come and therefore they increase their precautionary savings at the expense of spending (IV). We define two reasons:

**Reason 1:** I, II and III can be summarised by: the unwillingness to go outside

**Reason 2:** IV can be summarised by: the unwillingness to spend

**Reason 2**, the unwillingness to spend, is not unique to the Covid-19 epidemic, as during a crisis or recession precautionary savings normally go up and spending goes down as people anticipate negative income or welfare shocks. Therefore this particular behavioral aspect may not be specific for the Covid-19 crisis. **Reason 1**, the unwillingness to go outside, is a Covid-19 specific effect.

To investigate **Reason 1**, the unwillingness to go outside, is a reasonable assumption, we look at the frequency of visits in supermarkets. Given that supermarkets are generally crowded places and a potential source of Covid-19 contamination, we hypothesize that consumers would want to avoid these places more if they live in a municipality that experiences a larger Covid-19 outbreak. We choose supermarket visits specifically because they are not impacted by the lockdown measures, because supermarkets, convenience stores and other "vital" food retailers were allowed to stay open. Moreover, supermarkets are likely to be situated close to costumers, generally within

the same municipality, which minimizes any spatial effects that may occur. CBS data show that, on average, there is a supermarket around 1 kilometre away from every Dutch household.

Aggregate data show that spending in supermarkets was not negatively impacted by the Covid-19 crisis. Figure 7 shows that despite the initial spike in expenditure on groceries, spending in this category remained high throughout the lockdown period. From March 13 until the beginning of July, the expenditure in this category increased, on average, by 25% compared to the previous year. This is partly explained by the substitution effect, as consumers spend less on restaurants, bars and catering at work. However, the frequency with which consumers visited supermarkets did decline and hence, on average, consumers spent more during each visit. Figure 20 shows that the average amount spent in supermarkets (in euros) was substantially higher throughout the Covid-19 crisis.<sup>12</sup> Before the Covid-19 crisis, consumers spent around 18.5 euros at every supermarket visit, and this number increased to around 22.5 euros during the Covid-19 crisis.

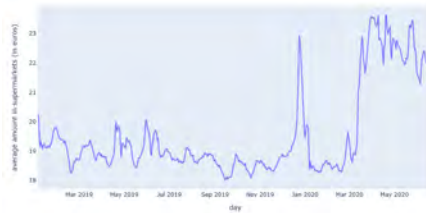


Figure 20: Average amount in euros per transaction spent with debit cards in supermarkets in the Netherlands, 7-days rolling average

In Table 8 we investigate whether Covid-19 had a statistically significant impact on the number of visits to supermarkets. Similar to Table 3, we perform a panel regression with fixed effects (see equations (2), (5) and (6) and a two-stage panel regression with the residuals (see equation (4)). The fixed effects regressions in Table 8 show that the amount of new hospitalized Covid-19 cases has a strong and statistically significant negative effect on the number of supermarket visits. This result shows that every additional hospitalized Covid-19 case reduces year on year supermarket visits by -1.09%, on average. This beta coefficient becomes slightly larger if we add other control

<sup>12</sup>This also holds for online grocery shopping. Figure 21 shows that the average amount people spent on online groceries increased from around 50 euros to an average of 67 euros in the period from mid-March until July.



Figure 21: Average amount in euros per order spent on online groceries in the Netherlands, 7-days rolling average

variables and eliminate time effects. Table 8 shows that adding control variables does not change the significance nor the sign of the coefficient on the Covid-19 variable  $X_{it}$ . Also, if we regress the two-stage residuals regression (see Table 9) the results do not change. This finding indicates that whereas total spending in supermarkets was not negatively effected by the Covid-19 outbreak, people living in municipalities that have seen a bigger spread of the virus did visit supermarkets less often. These results suggest that the day-to-day change in the within-municipality Covid-19 intensity affects daily supermarket visits, beyond the effect of physical constrains imposed by the government’s lockdown measures. On the basis of these results, we can reasonably argue that people living in badly affected areas were more afraid of going outside than people that live in areas that were little affected by the virus. Therefore, **Reason 1**, the unwillingness to go outside, seems to be reasonable explanation of why people curtail their pysical spending.

Table 8: Dependent Variable: Percentage change in supermarket visits year on year

Regressor	Column 1	Column 2	Column 3
Covid-19 cases	-1.087*** (0.1179)	-1.4899*** (0.1133)	-1.6376*** (0.1135)
Stringency		-0.0912*** (0.0025)	-0.1237*** (0.0047)
AEX			-0.0150*** (0.0026)
EURIBOR			-36.220*** (1.9265)
<i>N</i>	299	299	299
<i>T</i>	386	386	386
<i>FE</i>	Entity and Time	Entity	Entity
<i>R</i> <sup>2</sup>	0.0007	0.0115	0.0153

(Standard errors in parentheses)  
 \*\*\*  $p < 0.01$ ; \*\*  $p < 0.05$ ; \*  $p < 0.1$

Table 9: Dependent Variable: Residuals for percentage change in supermarket visits year on year

Regressor	Column 1
Residual Covid-19 cases	-1.3375*** (0.1553)
$N$	299
$T$	386
$FE$	NO
$R^2$	0.0006

(Standard errors in parentheses)  
 \*\*\*  $p < 0.01$ ; \*\*  $p < 0.05$ ; \*  $p < 0.1$

We further examine **Reason 1** by looking at the online ordering of groceries. Aside from people going to supermarkets less often, buying more at each visit (as Figure 20 shows), they could also choose to fully self-isolate by ordering groceries online. We hypothesise that if people are afraid to go outside because they live in an area that has seen a large virus outbreak, they will be more inclined to order groceries online and get them delivered to their home address. Whereas online ordering of groceries was a relatively small market in the Netherlands<sup>13</sup> before the Covid-19 outbreak, the country has seen an enormous increase during the epidemic crisis. Figure 8 shows the increase in online grocery shopping during the crisis, which on average more than doubled compared to the period before the crisis.

In Table 10, column (1) we regress the measure of Covid-19 ( $X_{it}$ ) on the year on year change of the volume<sup>14</sup> in online grocery shopping ( $Y_{it}$ ) for every municipality (see equation (2)). We find a strong statistically significant effect of the Covid-19 variable ( $X_{it}$ ). The coefficient is positive, which supports our hypothesis that people living in areas that see larger Covid-19 outbreaks order more online in order to avoid going outside. Table 10, columns (2) and (3), show the regression results from equation (6), including the control variables  $X_t$  (stringency, AEX and EURIBOR). Again, these variables seem to capture some of the fixed effects that change over time but stay constant over municipality. Table 11 shows the regression results with the residuals (equation (4)). Again, the coefficient on Covid-19 is statistically significant and positively correlated with the dependent variable online grocery expenditure. These results further strengthen our view that **Reason 1**, is

<sup>13</sup>Exact figures are not available for the Netherlands, but on the basis of survey data it is estimated that online grocery orders amount to around 5% of the total expenditure on groceries, see <https://insights.abnamro.nl/2020/04/waar-halen-we-ons-eten-in-de-anderhalve-meter-samenleving/>

<sup>14</sup>volume is measured as the amount of times that people ordered online



important in people’s decision to change their behavior and switch from offline to online grocery shopping.

Table 10: Dependent Variable: Percentage change in online groceries year on year

Regressor	Column 1	Column 2	Column 3
Covid-19 cases	5.0367*** (0.8726)	-5.5437*** (0.8345)	-3.1878*** (0.8340)
Stringency		2.0882*** (0.0185)	2.2304*** (0.0346)
AEX			0.4589*** (0.0192)
EURIBOR			240.54*** (14.152)
<i>N</i>	299	299	299
<i>T</i>	386	386	386
<i>FE</i>	Entity and Time	Entity	Entity
<i>R</i> <sup>2</sup>	0.0003	0.1024	0.1107

(Standard errors in parentheses)  
 \*\*\*  $p < 0.01$ ; \*\*  $p < 0.05$ ; \*  $p < 0.1$

Table 11: Dependent Variable: Residuals for percentage change in online grocery volume year on year

Regressor	Column 1
Residual Covid-19 cases	16.175*** (1.1305)
<i>N</i>	299
<i>T</i>	386
<i>FE</i>	NO
<i>R</i> <sup>2</sup>	0.0018

(Standard errors in parentheses)  
 \*\*\*  $p < 0.01$ ; \*\*  $p < 0.05$ ; \*  $p < 0.1$

### 5.4 Do people stay inside for a reason?

One can wonder how “rational” it is for people to stay inside. Research has shown that people are very much influenced by the media (Akerlof and Shiller, 2010 [16]; Baker et al., 2014 [6]; Beaudry and Portier, 2004 [8]; Soroka, 2006 [27]; Tetlock, 2007 [28]). So the fear of going outside may not necessarily be caused by the absolute size of the local outbreak, but rather by the “perception” of the magnitude of the outbreak. People living in the province of Brabant, which was known as the “epicentre” of the Netherlands’ outbreak, may simply change their behavior because they feel the virus to be present, whereas some municipality in Brabant had very little to no Covid-19 cases. Did

these people that live in in heavy effected provinces, but in a municipalities that saw little to no Covid-19 cases, also stayed inside?

In order to disentangle these two effects, we use an identification strategy that considers the amount of Covid-19 cases in the province (denoted by  $p$ ) where municipality  $i$  is located. The Netherlands consists of 12 provinces. We include a variable that distinguishes the Covid-19 outbreak in municipality  $i$  from the cross-sectional average over the province ( $\bar{X}_{pt}$ ), weighed by population size (expressed as a figure for hospitalized cases per 1000 people). We do this specifically for the regression on supermarket visits, because these should not be impacted by the amount of Covid-19 cases on a province level. Other transactions, such as spending on clothing, books or hardware could potentially be affected by the scale of the virus outbreak at the province level because some of these shops are not available within a close distance, causing people to travel to different municipalities (that may have seen different levels of Covid-19 cases). In the latter case, staying inside may actually be “rational” behavior, despite a low number of Covid-19 cases in their own municipality cases. As previously noted, the average travel distance for supermarkets is small, which eliminates potential spatial issues. Table 12 shows the results of the fixed effects regression. Whereas the Covid-19 variable is still significant at the 5% level, the variable that measures the difference to the amount of cases on the province level is not statistically significant. We also perform the two-stage residual regression. In the first-stage (equation (3)) we perform three regressions, on  $Y_{it}$ ,  $X_{it}^1$  and  $X_{it}^2$ , with Covid-19 cases by municipality denoted by  $X_{it}^1$  and the Covid-19 outbreak in municipality  $i$  minus the cross-sectional average for the province ( $\bar{X}_{pt}$ ) denoted by  $X_{it}^2$ . In equation (4) we perform the regression  $e_{it}^y = e_{it}^{x1} + e_{it}^{x2} + w_{it}$ . Table 13 shows the results and again, the Covid-19 cases by municipality is the only statistically significant variable.

From the regression in Table 12 we can conclude that it is not the average level of the Covid-19 outbreak in the province that make people change their physical consumer behavior, but rather the amount of Covid-19 cases in close proximity to them. Therefore, **Reason 1**, the unwillingness to go outside, may actually be provoked by “rational” behavior. Although further research is needed to look deeper into how people experience anxiety due to virus outbreaks and how this may result

Table 12: Dependent Variable: Percentage change in supermarket visits year on year

Regressor	Column 1
Covid-19 cases	-39.272** (16.108)
Province Covid-19 cases minus municipality Covid-19 cases	-21.218 (17.433)
<i>N</i>	299
<i>T</i>	386
<i>FE</i>	Entity and time
<i>R</i> <sup>2</sup>	0.0001

(Standard errors in parentheses)

\*\*\*  $p < 0.01$ ; \*\*  $p < 0.05$ ; \*  $p < 0.1$ 

Table 13: Dependent Variable: Residuals for percentage change in supermarket visits year on year

Regressor	Column 1
Covid-19 cases	-74.345*** (21.345)
Province Covid-19 cases minus municipality Covid-19 cases	-37.192 (23.146)
<i>N</i>	299
<i>T</i>	386
<i>FE</i>	NO
<i>R</i> <sup>2</sup>	0.0002

(Standard errors in parentheses)

\*\*\*  $p < 0.01$ ; \*\*  $p < 0.05$ ; \*  $p < 0.1$ 

in changing physical spending behavior, our results show that people's spending behavior may be driven by the developments of the Covid-19 virus on their local community.

## 6 Conclusion and discussion

From our regression results described in section , we find that the amount of new hospitalized Covid-19 cases in a municipality has a strong and statistically significant negative effect on the change in physical transactions by consumers. In other words, municipalities that have seen a large Covid-19 outbreak have struggled more in economic terms than municipalities that seen few or no Covid-19 cases. This finding holds even for sectors that were subject to restrictions due to the lockdown measures. We find that spending on necessities, proxied by supermarket expenditure, were barely hit by the Covid-19 crisis. However, the number of supermarket visits was reduced, especially in those municipalities that saw a large Covid-19 spread. This suggests that people living in badly affected areas altered their economic behavior differently to people living in little affected areas. This finding was further confirmed by the evidence that people were ordering more groceries online if their area was badly affected. Moreover, we find that it is not the perception of the outbreak that results into people changing their behavior, but rather the real magnitude of the local outbreak. Therefore, we conclude that the only path to full economic recovery in the long run is to diminish the effect of fear and restore consumer confidence by addressing the virus spread itself.

Our research has several policy implications. Our findings show that to in order to minimize the economic impact of the Covid-19 pandemic, governments should balance the negative economic effects of lockdown measures with the negative effects and the behavioral reaction function of consumers to the virus itself. Measures that effectively contain the virus, but have little direct negative economic impact (such as as social distancing and contact tracing) may therefore be the most effective from an economic point of view.<sup>15</sup> Many other authors have focused on researching the effectiveness of different policies on containing the virus (see, for example, Fang, Yiting and Marshare (2020) [25]; Hou et al. (2020) [22] and Alvarez, Argente and Lippi (2020) [3]).

Our research also shows that consumption in sectors that faced restrictions during the nationwide lockdown differs in accordance with the magnitude of the local virus outbreak. Therefore, local lockdowns may prove to be more effective than nationwide lockdowns, because people tend to

---

<sup>15</sup>Aum, Lee and Shin (2020) [5] provide a good overview of the economic effect of intensive testing and contact tracing in South Korea.

be more strict in following the rules and/or local enforcement is tougher in areas where there is a severe local outbreak.

Our research could potentially also have implications for the distribution of national funds to local governments. Our research indicates that some municipalities have been hit substantially harder by the drop in transactions than others, which could be used as an argument to reallocate budgets according to the extent to which a municipality has been hit by the Covid-19 crisis.

Measuring physical transactions is not a perfect substitute for economic activity. The drop in physical transactions can be partly offset by an increase in online transactions. Also, our regression results (section 6) show that the incidence of Covid-19 has a large positive correlation with online grocery spending. Further research could investigate to what extent online consumption substitutes the reduction in offline consumption. Also relevant in this respect is the reallocation from spending at local businesses to online retail businesses. The local community does not necessarily profit from an increase in online consumption at the expense of offline consumption, because many of the online retailers may not be located within the same municipality.

Moreover, it would be interesting to further research the impact of loss of income on consumer expenditure. In section 5.3 we found that **Reason 1**, the unwillingness to go outside, is a credible reason for people to spend less when they live in highly affected areas. This is confirmed by Cajner et al. (2020) [10] and Ganong, Noel and Vavra (2020) [17], who found that spending fell in the early stages of the pandemic primarily because of health concerns rather than a loss of current or expected income. They argue that income losses were relatively modest because relatively few high-income individuals lost their jobs and lower-income households who experienced job losses had their loss in income offset by unemployment benefits. This also holds for the Netherlands, where Covid-19 crisis measures provided financial support to around 2.9 million workers (out of a labour force of about 9 million).<sup>16</sup> However, **Reason 2**, the unwillingness to spend, may become more relevant as the time passes. When companies lose customers and revenue, they may be forced to cut costs, including labour costs. Municipalities that have seen larger virus outbreaks may also experience a higher increase in local unemployment. Such a negative income shock could further deteriorate the

<sup>16</sup>[https://www.tweedekamer.nl/debat\\_en\\_vergadering/plenaire\\_vergaderingen/details?date=24-06-2020](https://www.tweedekamer.nl/debat_en_vergadering/plenaire_vergaderingen/details?date=24-06-2020)

economic situation at the local level. Further research into the dynamics of the labour market and consumer spending at the local level in relation to the Covid-19 outbreak is needed to understand its full economic impact.

Also, in relation to our findings in section 5.3 and section 5.4, it would be interesting to further look into the reaction function of consumers to the virus. Behavior toward the virus is not static. We have seen that before the lockdown was eased, consumer spending in many categories had already started to recover. People's perception towards the virus may change throughout time. Some may get used to the situation while others may experience more distress as the virus lingers on. Especially relevant in this respect is the interaction between the reaction of consumers to the virus outbreak and the reaction of the government. Strict (local) government measures may diminish fear, as people may feel the government is in control and are more confident about a positive outcome. On the other hand, government interventions may actually reinforce the effect of fear. People may interpret the strictness of the lockdown measures as a signalling function of how bad it is. After the second-wave has passed, researchers may be able to form a more definite answer on how people react to the Covid-19 virus outbreak.

# Appendices

## A Appendix

To determine geolocations for physical pin transactions we use an unsupervised model. Given that we want to determine dense clusters and classify all other points as outliers, a density-based method is the most suitable approach. As the dataset is rather large and clustering will need to happen for many sets of points, a less computationally expensive algorithm is preferred, and hence DBSCAN was selected as the clustering algorithm for this problem.

**Parameter selection** The DBSCAN clustering algorithm requires two main parameters to be set. The first,  $\epsilon$ , is the maximum distance that two points can be from each other whilst still belonging to the same cluster. The second, *min\_samples*, is the minimum number of samples required for a group of points to become a cluster in the final results. As there are many varieties of payment points in the data, there is no 'one size fits all' approach. The goal with the setting of these parameters is to find the optimal (most dense whilst including the most samples) cluster for a set of home locations associated with a payment point, in order to be able to remove points which are outliers or do not improve the location prediction. The initial parameters are set at very ambitious levels based on the label of the payment point and the total amount of samples there are. When no cluster is found, the parameters are widened until either a cluster has been found or the parameter limit has been reached, and thus, hypothetically, no dense enough cluster exists in the samples to make a good prediction for the payment point.

**Transaction weighting** The distance between a customer's home and the payment point can differ according to the time of the day, month of the year and total amount spent. Therefore we introduce heuristic transaction weighting, also called transaction-weighted dynamic-parameter DBSCAN (TWDP-DBSCAN). These heuristics determine the weight of a transaction, which can vary between 0 and 2. This weight is used to determine how strongly the transaction influences the final predicted location of the payment point. The final location (after clustering) is calculated as follows (for latitude and longitude separately):

$$location = \frac{\sum_{i=1}^N location_i * weight_i}{\sum_{i=1}^N weight_i}$$

where  $N$  is the amount of samples after clustering. Although this is based on analysis of a smaller sample, Van der Cruijssen (2018) [30] suggests that payment behaviors tend to be consistent across different groups of people and thus this sample is assumed to generalize well to the full dataset.

After the implementation the transaction-weighted dynamic-parameter DBSCAN (TWDP-DBSCAN), it was found that certain labels (categories) of payment points, such as hotels, did not

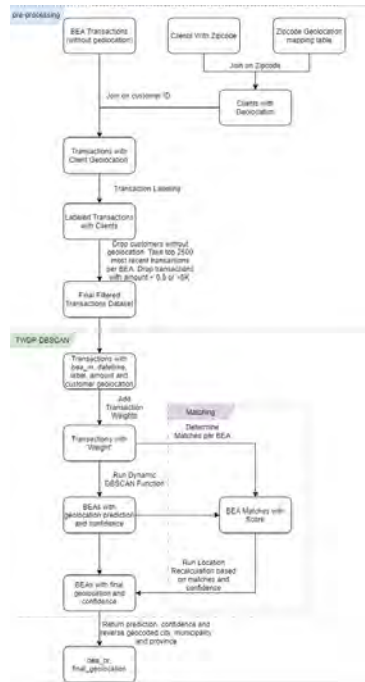


Figure 22: Transaction-weighted dynamic-parameter DBSCAN

perform well. This can be explained by the fact that consumers usually stay in hotels far from their home address. In order to account for the harder-to-predict categories, payment point matching was introduced, where each prediction was assigned a confidence based on the heuristics of the category, number of samples and cluster size. Payment points were then matched according to the following routine:

1. Partition the transactions by customer
2. Sort the transactions by transaction date and time
3. For each transaction, calculate the time delta between it and the customer’s previous transaction
4. If this time delta is smaller than the threshold level, add the previous payment point with its predicted location and confidence as a ‘match’



Finally, the lower confidence payment point locations are recalculated based on their own location and the locations of the matched payment points using an algorithm that takes into account the confidence of all predictions, and the time delta of all the matches.

**Implementation details** The TWDP-DBSCAN algorithm is implemented as a class in PySpark for parallel processing and it implements two public methods, *preprocess* and *predict*. After performing pre-processing, a column with the transaction weights is added and matches are calculated. Then TWDP-DBSCAN is executed for the first location prediction and if selected, the location is recalculated based on the matches. Next the locations are returned or city, municipality and province columns are added and returned. Finally, the predicted geolocations are coded to the respective cities/municipalities/provinces using the reverse geocoder library<sup>17</sup>, which takes latitude/longitude pairs and returns the nearest respective town/city.

The GeoNames<sup>18</sup> dataset was used for zipcode geolocation mapping. Although Ahlers (2013) [1] has determined that GeoNames is not perfect, and certainly has limitations regarding shortening of latitudes/longitudes and imperfections in the data, this is the main widely accessible resource able to map almost all of the Dutch zipcodes to a geolocation.

**Validation** The testing results displayed in Table 15 and Table 16 are on a transaction level and not on a payment point level. This is done for the reason that payment points with very few transactions are less relevant in the final result, as the number and value of transactions are what drive the correctness of the measures of consumption.

Year	Transactions	Payment Points	Customers	Label Source
2015	64M	54,700	2.7M	Ground-truth dataset
2020	393M	1.88M	3.24M	Description (fuzzy city matching)

Table 14: The two test sets used for evaluation

Table 14 describes the test sets that were used for the final testing, the size of the datasets and how the label (location) was obtained. As there is no training with unsupervised learning (clustering), there is no need to split the dataset into training and testing samples, and the full dataset can be used for final tests. Also, both test sets went through the same pre-processing function where payment points with less than 10 or more than 50,000 transactions were removed and transactions with a value under 0.5 euros or over 5,000 euros were removed. This is done to remove non-significant transactions and outliers.

Model	MHE	CA	PA	Run-time
Baseline	4,213 m	34.88%	85.05%	4 mins
TWDP-DBSCAN	981 m	71.03%	91.71%	39 mins
TWDP-DBSCAN with matching	981 m	71.03%	91.71%	94 mins

Table 15: Results on 2015 test set (N=64,000,000)

<sup>17</sup>[https://pypi.org/project/reverse\\_geocoder/](https://pypi.org/project/reverse_geocoder/)

<sup>18</sup><http://geonames.org>

The results on the 2015 test data can be found in Table 15. In this table, MHE represents the *Mean Haversine Error*, CA is the *City Accuracy* and PA is the *Province Accuracy*. Also, the run-time of each model is included. The algorithm was run with all transactions, but only the results for the smaller subset reported in Table 14 are reported as these are the only payment points which have an available ground-truth location.

Model	MHE	CA	PA	Run-time
Baseline	N.A.*	33.66%	85.0%	8 mins
TWDP-DBSCAN	N.A.*	67.63%	94.56%	30 mins
TWDP-DBSCAN with matching	N.A.*	67.61%	94.55%	104 mins

Table 16: Results on 2020 test set (N=393,000,000)

*\*Not Available because the test set only contains cities, not exact locations. Cities are as large as 220km<sup>2</sup>, and so would yield a very imprecise estimate.*

As the method has been developed primarily with exploratory data analysis on the 2015 dataset (as specific geolocations of payment points were available here), a good method of validation is to test the method on more recent data without changing the implementation or heuristics. The results, for the first five months of transactions of 2020, are presented in Table 16. On this much larger, diverse and high-quality sample, it is found that the baseline and TWDP-DBSCAN (with or without matching) results are similar to the 2015 results. This shows that the method is built in a robust way and generalizes well over time, as the samples are 5 years apart and no modifications to the method have been made prior to testing.

**Limitations** The validation data used are from 2015 and only represent a limited sub-sample of all payment points. They thus only contain small numbers of observations for certain labels and areas. This means that the validation set is biased towards certain labels and areas in the Netherlands. Nothing can be done about this limitation, except for manually creating more validation data. For this reason, 2020 transaction data has also been used, where the exact geolocation is not known but the city can be extracted from the transaction description.

## B Appendix

Using a fixed effects model allows us to control for all time-invariant characteristics of an entity. As these factors do not change over time, the fixed effects absorb this variation.<sup>19</sup> To investigate whether the above mentioned factors may impact the data on changes in transaction levels, we run

<sup>19</sup>The fixed effects specification accounts for differences in municipalities that cannot be explained by the control variables. Statistically, time-invariant characteristics are perfectly collinear with the dummy, so their effect cannot be estimated in the model. These differences between municipalities could reveal idiosyncrasies that are hard to capture using additional regressors varying at the municipality level

the panel OLS model specified in equation (5), allowing time-invariant variables to be included ( $X_i$ ). Table 17 shows the results. In the regression we include several variables that measure the average proximity of various public services. Proximity figures measure the average distance in kilometres of all citizens in a municipality to a given public service. We have included the proximity to a general practitioner (GP), hospital, supermarket, restaurant, cultural building (museums, theaters and cinemas) and public transport hub. Table 17 shows that target variable ( $X_{it}$ ) is strong and statistically significant. From the control variables, the average distance to a GP is the only variable that is not statistically significant. However, the beta coefficients on the other variables do differ substantially. Table 17 indicates that in particular, the proximity to a restaurant and supermarket explain our dependent variable. This is probably because these two variables best capture the “big city” effect. In general, big cities have seen larger outbreaks of the Covid-19 virus and consumers have withheld spending in these places because they are generally crowded and a potential source of contamination. Moreover, the proximity of restaurants may partly capture the lockdown effect, because restaurants were not allowed to let costumers in, but only to serve take-away orders.

Table 17: Dependent Variable: Percentage change in transactions year on year

Regressor	Column 1
Covid-19 cases	-1.3986*** (0.0463)
Proximity to GP	-0.1127 (0.1343)
Proximity to hospital	0.5934*** (0.0058)
Proximity to supermarket	-1.3413*** (0.1467)
Proximity to restaurant	-2.8558*** (0.1270)
Proximity to culture	-0.0215*** (0.0077)
Proximity to public transport hub	-0.1582*** (0.0057)
<i>N</i>	299
<i>T</i>	386
<i>FE</i>	Time
<i>R</i> <sup>2</sup>	0.1521

(Standard errors in parentheses)

\*\*\*  $p < 0.01$ ; \*\*  $p < 0.05$ ; \*  $p < 0.1$

## References

- [1] Dirk Ahlers. Assessment of the accuracy of geonames gazetteer data. In Proceedings of the 7th workshop on geographic information retrieval, pages 74–81, 2013.
- [2] David Altig, Scott R Baker, Jose Maria Barrero, Nicholas Bloom, Philip Bunn, Scarlet Chen, Steven J Davis, Julia Leather, Brent H Meyer, Emil Mihaylov, Paul Mizen, Nicholas B Parker, Thomas Renault, Pawel Smietanka, and Greg Thwaites. Economic uncertainty before and during the covid-19 pandemic. Working Paper 27418, National Bureau of Economic Research, June 2020.
- [3] Fernando E Alvarez, David Argente, and Francesco Lippi. A simple planning problem for covid-19 lockdown. Working Paper Covid Economics 14, C.E.P.R Discussion Papers, 2020.
- [4] Asger Andersen, Emil Toft Hansen, Niels Johannesen, and Adam Sheridan. Consumer Responses to the COVID-19 Crisis: Evidence from Bank Account Transaction Data. Covid economics 7, C.E.P.R. Discussion Papers, 2020.
- [5] Sangmin Aum, Sang Yoon (Tim) Lee, and Yongseok Shin. Covid-19 doesn't need lockdowns to destroy jobs: The effect of local outbreaks in korea. Working Paper 27264, C.E.P.R discussion papers, May 2020.
- [6] Collin Baker. FrameNet: A knowledge base for natural language processing. In Proceedings of Frame Semantics in NLP: A Workshop in Honor of Chuck Fillmore (1929-2014), pages 1–5, Baltimore, MD, USA, June 2014. Association for Computational Linguistics.
- [7] Scott R Baker, R. A Farrokhnia, Steffen Meyer, Michaela Pagel, and Constantine Yannelis. Income, liquidity, and the consumption response to the 2020 economic stimulus payments. Working paper, Centre for Economic policy Research, May 2020.
- [8] Paul Beaudry and Franck Portier. Stock prices, news and economic fluctuations. Working Paper 10548, National Bureau of Economic Research, June 2004.
- [9] Abel Brodeur, David M. Gray, Anik Islam, and Suraiya Jabeen Bhuiyan. A Literature Review of the Economics of COVID-19. IZA Discussion Papers 13411, Institute of Labor Economics (IZA), June 2020.
- [10] Tomaz Cajner, Leland Crane, Ryan Decker, John Grigsby, Adrian Hamins-Puertolas, Erik Hurst, Christopher Kurz, and Ahu Yildirmaz. The u.s. labor market during the beginning of the pandemic recession. SSRN Electronic Journal, 01 2020.
- [11] Vasco M Carvalho, Juan R Garcia, Hansen Álvaro, Ortiz Tomasa, Stephen Hansen, and Tomasa Rodrigo. Tracking the COVID-19 Crisis with High- Resolution Transaction Data. (April), 2020.

- [12] Vasco M Carvalho, Juan Ramon Garcia, Stephen Hansen, Alvaro Ortiz, Tomasa Rodrigo, Jose v. Rodriguez Mora, and pep ruiz. Tracking the covid-19 crisis with high-resolution transaction data, April 2020.
- [13] Haiqiang Chen, Wenlan Qian, and Qiang Wen. The impact of the covid-19 pandemic on consumption: Learning from high frequency transaction data. Working paper, SSRN.
- [14] Raj Chetty, John N Friedman, Nathaniel Hendren, Michael Stepner, and The Opportunity Insights Team. How did covid-19 and stabilization policies affect spending and employment? a new real-time economic tracker based on private sector data. Working Paper 27431, National Bureau of Economic Research, June 2020.
- [15] Jerry Coakley, Ana-Maria Fuertes, and Ronald Smith. A principal components approach to cross-section dependence in panels. 10th International Conference on Panel Data, Berlin, July 5-6, 2002 B5-3, International Conferences on Panel Data, 2002.
- [16] Selwyn Cornish. George A. Akerlof and Robert J. Shiller, *Animal Spirits. How Human Psychology Drives The Economy, And Why It Matters For Global Capitalism* (Princeton University Press, 2009). *Agenda - A Journal of Policy Analysis and Reform*, 16(4):117-122, 2009.
- [17] Peter Ganong, Pascal J Noel, and Joseph S Vavra. Us unemployment insurance replacement rates during the pandemic. Working Paper 27216, National Bureau of Economic Research, May 2020.
- [18] Austan Goolsbee and Chad Syverson. Fear, Lockdown, and Diversion: Comparing Drivers of Pandemic Economic Decline 2020. NBER Working Papers 27432, National Bureau of Economic Research, Inc, June 2020.
- [19] Sumedha Gupta, Thuy D. Nguyen, Felipe Lozano Rojas, Shyam Raman, Byungkyu Lee, Ana Bento, Kosali I. Simon, and Coady Wing. Tracking Public and Private Responses to the COVID-19 Epidemic: Evidence from State and Local Government Actions. NBER Working Papers 27027, National Bureau of Economic Research, Inc, April 2020.
- [20] Sinem Hacioglu, Diego R Känzig, and Paolo Surico. Consumption in the time of Covid-19: Evidence from UK transaction data. CEPR Discussion Papers 14733, C.E.P.R. Discussion Papers, May 2020.
- [21] Inoue Hiroyasu and Todo Yasuyuki. The Propagation of Economic Impacts through Supply Chains: The Case of a Mega-city Lockdown to Prevent the Spread of COVID-19. Working paper Covid Economics 2, C.E.P.R Discussion papers, April 2020.

- [22] Can Hou, Jiaxin Chen, Yaqing Zhou, Lei Hua, Jinxia Yuan, Shu He, Yi Guo, Sheng Zhang, Qiaowei Jia, Chenhui Zhao, Jing Zhang, Guangxu Xu, and Enzhi Jia. The effectiveness of quarantine of wuhan city against the corona virus disease 2019 (covid-19): A well-mixed seir model analysis. Journal of Medical Virology, 92(7):841–848, 2020.
- [23] Nicole Jonker, Lola Hernandez, Renate de Vree, and Patricia Zwaan. From cash to cards: how debit card payments overtook cash in the Netherlands. 2017.
- [24] George Kapetanios and Hashem Pesaran. Alternative approaches to estimation and inference in large multifactor panels: Small sample results with an application to modelling of asset returns. The Refinement of Econometric Estimation and Test Procedures: Finite Sample and Asymptotic Analysis, 06 2005.
- [25] M. Hashem Pesaran. Estimation and inference in large heterogeneous panels with a multifactor error structure. Econometrica, 74(4):967–1012, 2006.
- [26] Stanislav Sobolevsky, Emanuele Massaro, Iva Bojic, Juan Murillo Arias, and Carlo Ratti. Predicting regional economic indices using big data of individual bank card transactions. Proceedings - 2017 IEEE International Conference on Big Data, Big Data 2017, 2018-January:1313–1318, 2017.
- [27] Stuart N. Soroka. Good news and bad news: Asymmetric responses to economic information. Journal of Politics, 68(2):372–385, 2006.
- [28] PAUL C. TETLOCK. Giving content to investor sentiment: The role of media in the stock market. The Journal of Finance, 62(3):1139–1168, 2007.
- [29] Nederlandse Vereniging van Banken. Betalingsverkeer (<https://www.bankinbeeld.nl/thema/betalingsverkeer/>).
- [30] Carin van der Cruijssen and Joris Knobens. Ctrl C Ctrl Pay: Do People Mirror Payment Behaviour of Their Peers? SSRN Electronic Journal, (611), 2018.

# Preventing COVID-19 fatalities: State versus federal policies<sup>1</sup>

Jean-Paul Renne,<sup>2</sup> Guillaume Roussellet,<sup>3</sup> and Gustavo Schwenkler<sup>4</sup>

Date submitted: 29 October 2020; Date accepted: 30 October 2020

*Are COVID-19 fatalities large when a federal government does not impose containment policies and instead allow states to implement their own policies? We answer this question by developing a stochastic extension of a SIRD epidemiological model for a country composed of multiple states. Our model allows for interstate mobility. We consider three policies: mask mandates, stay-at-home orders, and interstate travel bans. We fit our model to daily U.S. state-level COVID-19 death counts and exploit our estimates to produce various policy counterfactuals. While the restrictions imposed by some states inhibited a significant number of virus deaths, we find that more than two-thirds of U.S. COVID-19 deaths could have been prevented by late September 2020 had the federal government imposed federal mandates as early as some of the earliest states did. Our results highlight the need for early actions by a federal government for the successful containment of a pandemic.*

- 1 We are grateful to Andrea Vedolin, Charles Wyplosz, and seminar participants at Santa Clara University for useful comments and suggestions. The latest version of the codes used in this paper can be found at [https://github.com/guillaume-roussellet/RRS\\_Covid\\_2020](https://github.com/guillaume-roussellet/RRS_Covid_2020).
- 2 Professor of Economics, University of Lausanne.
- 3 Assistant professor of Finance, Desautels School of Management, McGill University.
- 4 Associate Professor of Finance, Leavey School of Business, Santa Clara University.

Copyright: Jean-Paul Renne, Guillaume Roussellet and Gustavo Schwenkler

## 1 Introduction

COVID-19 is a rampant disease that has affected the world population to an unprecedented scale. This experience has pushed state and federal governments to implement drastic regulatory policies to contain the spread of the disease. In many countries, such as the United States, state governments can independently implement policies while other states or the federal government do not impose any restrictions. This begets the questions: how effective are policies implemented at a local level? And what could be gained from unified containment policies at the federal level?

We answer these questions by developing an extension of the standard SIRD model of [Kermack et al. \(1927\)](#) that allows for travel and commuting across states within a country.<sup>1</sup> In our model, the government of a state can impose three types of regulations. It can impose a mask mandate that shrinks the transmission rate in the state. It can impose a stay-at-home order that shrinks the transmission rate in the state as well as the inflow of out-of-state commuters and travelers. Or it can also issue a travel ban that shrinks the inflow of out-of-state travelers. The federal government can force all states to implement the same policies or allow states to decide individually what policies to implement, if any at all. We assume that a coronavirus infection takes on average 14 days to resolve and that the fatality rate of the disease is 0.6%.<sup>2</sup> To incorporate uncertainty about the contagiousness of COVID-19, we assume that the transmission rates in individual states vary randomly over time and are not directly observable. They fluctuate around a natural mean rate but can be substantially higher or lower at times. We fit our model to data on state-level COVID-19 fatalities from the United States between February 12 and September 30, 2020. We then run counterfactual experiments using the estimated model under the assumption that states implemented policies different than the ones they adopted in reality. We measure the effectiveness of the different policies by looking at the difference between the observed and counterfactual numbers of virus deaths on September 30. All of our results are replicable by using our codes that are available on [Github](#).

Our results show that a lack of unified policies at the federal level results in significantly elevated virus deaths nationally. We estimate that more than 136,000 deaths could have been prevented by September 30, 2020 – over two-thirds of all death cases recorded in the U.S. by

<sup>1</sup>We are inspired by mean-field models that are commonly used in the financial economics literature to model credit risk contagion across financial institutions; see [Cvitanic et al. \(2012\)](#), [Giesecke et al. \(2015\)](#), [Giesecke et al. \(2020\)](#), and others.

<sup>2</sup>These assumptions are consistent with [Fernández-Villaverde and Jones \(2020\)](#), [Perez-Saez et al. \(2020\)](#), and [Stringhini et al. \(2020\)](#), and are benchmarked against alternatives in a sensitivity study.



that date – if the federal government had imposed federal policies that mirrored those of the earliest and strictest states. Our results also show that containment policies implemented by individual states are effective. We find that the U.S. would have recorded more than 1,000,000 additional virus deaths if states had not implemented any containment policies at all.

Our study suggests that a large number of COVID-19 deaths could have been prevented if the federal government had imposed stay-at-home orders or mask mandates that followed the leads taken by the different states. We estimate that more than 110,000 deaths could have been prevented if the federal government had imposed a federal stay-at-home order that had gone into effect on March 20, 2020, corresponding to the start of the stay-at-home order in California. Imposing a federal mask mandate as early as Connecticut did on April 17, 2020, would have prevented more than 96,000 deaths. Considering that shutting down the national economy with a federal stay-at-home order carries significant economic costs, which we do not consider in this paper, a federal mask mandate would likely be preferred over a federal stay-at-home order. Our counterfactuals suggest that between 96,000 and 183,000 virus deaths could have been prevented if the federal government had enacted a federal mask mandate sometime between March 17 and April 17, 2020, on top of the stay-at-home and travel ban policies adopted by the different states. An early federal mask mandate would have contributed to slowing down the transmission of the virus early in the Spring of 2020, when we estimate the reproduction numbers to have been the highest.<sup>3</sup> While it is questionable whether an early mask mandate would have been realistic or whether there existed political or even scientific consensus for enacting such a policy, what our results indicate is that early action by the federal government that complemented the steps taken by state governments could have resulted in significantly less virus deaths.<sup>4</sup> These results provide an important policy lesson for future waves of the pandemic by highlighting that early action by a federal regulator when the reproduction rates are high is key to prevent virus deaths.

We find that interstate travel bans do not accomplish significant virus death prevention, mostly for two reasons. First, travel bans are often imposed once a regulator becomes aware of

---

<sup>3</sup>By matching death counts only, we estimate that the effective reproduction numbers of the virus in the different states during the Spring of 2020 must have been up to two-times higher than prevailing estimates that are based on infection cases, which are likely under-measured due to the large number of undetected infections and asymptomatic individuals. Since our estimates depend on our modeling and parametric assumptions, we carry out several experiments that assess how sensitive our findings are to our assumed parameter values. These experiments corroborate our findings.

<sup>4</sup>During the month of March, the WHO recommended masks be reserved to medical staff and discouraged a widespread use to the general public (see WHO interim guidance of [April 6, 2020](#)). As noted by [Feng et al. \(2020\)](#), the rationale underlying the discouragement of mask use was to preserve the limited supplies of masks in countries where the health-care system and ICU use was under pressure.

the virus, at which point the virus has already penetrated and spread in the states. The first travel ban in the U.S. went into effect in Hawaii on March 17, 2020. Our counterfactuals indicate that only around 5,100 U.S. virus deaths could have been avoided if the federal regulator had imposed a nationwide ban of interstate travel on the same day as Hawaii and maintained it through September 30. In contrast, we find that close to 6,000 deaths could have been prevented if the nationwide interstate travel ban had begun by the start of our sample on February 12. Such an early ban of interstate travel is unrealistic given that the severity of the virus was not perceived to be as serious at that point of time as to justify such a drastic policy.

Second, interstate mobility scatters virus cases across state lines and this may slow down the spread of the virus within a country. In our model, states that are net importers of individuals record higher numbers of infections than they would in the absence of interstate movement while states that are net exporters of individuals record lower number of infections. When interstate mobility is restricted, infected population that would otherwise disperse out-of-state is forced to stay in-state. The higher concentration of infected population in some states can result in accelerated virus transmission in those states and worse death outcomes at the federal level. Our counterfactuals suggest that this is only a minor effect, nonetheless. For example, we find that only around 860 of the more than 110,000 virus deaths that could have been prevented with a federal stay-at-home order on March 20 are explained by the fact that interstate commuting and traveling are discouraged when individuals are required to stay at home.

Our results suggest that policies that restrict cross-border mobility accomplish little in preventing COVID-19 deaths unless they are imposed so early and for so long that they prevent the virus from initially taking hold in a population. To the extent that our results can be extrapolated to a global setting with multiple countries, they suggest that the late banning of international travel may be an ineffective tool in combating COVID-19.

Finally, we focus on individual states and find that the states that imposed some of the strictest containment policies were able to reduce the spread of the disease. Our counterfactuals suggest that New York would have only recorded 17% fewer death cases if all states had imposed strict containment policies, while California would have recorded close to 200,000 additional deaths if the state government had not imposed any containment policies at all. These results suggest that strict-policy states, such as New York and California, were protected by their policies even when other states implemented weaker policies. On other end of the spectrum, we find that states that adopted weak or no containment policies could have prevented a significant

number of COVID-19 deaths by adopting stricter policies. Our results suggest that over 29,000 deaths could have been prevented if Florida and Texas had adopted strict containment policies. We also find that the four states that adopted no containment policies in our sample—Iowa, Nebraska, South Dakota, and Utah—could have prevented more than 70% of their death cases by adopting early mask mandates.

Our results hinge on modeling choices and assumed parameter values. To understand how sensitive our findings are to our choices, we carry out several sensitivity analyses that assume alternative parametric values and provide a reasonable set of bounds for our results. We find, for example, that the number of preventable deaths is higher if we assume that it takes less times for a virus infection to resolve; i.e., if the virus is less severe. This is because, if a virus infection is less severe, there must have been many more infections early on in the sample to match the observed death data. Therefore, early action by the federal regulator would have been even more impactful. The sensitivity analyses highlight a key benefit of our approach. By relying on death counts only, we allow our methodology to infer how many infections there must have been to justify the death data. This enables us to make data-driven inferences on how many infections and ultimate deaths could have been prevented through regulatory actions.

Our contributions are methodological and normative. On the methodological front, we develop a novel model for infectious disease transmission within a country composed of multiple states. Our model incorporates the effects of interstate traveling and commuting, as well as uncertain transmission rates.<sup>5</sup> It also allows for independent regulatory policies across states.<sup>6</sup> Our methodology delivers daily estimates of the transmission rates and effective reproduction numbers ( $\mathcal{R}_0$ ); these objects are jointly estimated for 51 U.S. states based solely on death cases.<sup>7</sup> On the normative side, we show that early actions by a federal government that complement state-level policies result in significantly reduced virus deaths during a pandemic.<sup>8</sup> Our results hint that more than 135,000 COVID-19 deaths could have been prevented if the federal govern-

<sup>5</sup>Stochastic SIR models of COVID-19 have recently been used by [Fernández-Villaverde and Jones \(2020\)](#) and [Hong et al. \(2020\)](#). Deterministic mean-field models of infection rates have been considered by [Read and Keeling \(2003\)](#), [Youssef and Scoglio \(2011\)](#), [Zhang et al. \(2015\)](#), and others.

<sup>6</sup>[Brady et al. \(2020\)](#) study an SIR model with spatial interaction of susceptible and infected people across neighboring states and allow for independent social distancing policies across states. This model, however, does not account for interstate travel. It also does not account for the effects of mask mandates.

<sup>7</sup>For single-state models, a related methodology is discussed in [Gouriéroux and Jasiak \(2020\)](#) and implemented in [Arroyo Marioli et al. \(2020\)](#), [Hasan et al. \(2020\)](#), and [Hasan and Nasution \(2020\)](#) using infections data. [Fernández-Villaverde and Jones \(2020\)](#) develop an alternative filtering-based methodology to obtain time-varying estimates of the  $\mathcal{R}_0$  using death counts only but it requires extensive smoothing of the data.

<sup>8</sup>Studying the economic impact of state-level stay-at-home orders, [Rothert \(2020\)](#) document that externalities arise if the federal government does not coordinate policies across states.

ment in the United States had followed the lead of some of the states that took early actions to contain the virus.<sup>9</sup> We also show that early mask mandates are highly effective, while travel restrictions create distortions at the state level and have small benefits at the federal level.<sup>10</sup>

While the results of this paper are compelling, it is important to keep in mind several caveats that confound our findings. First, we do not consider that changes in federal policies may have resulted in different strategies implemented in the states and different reactions by the U.S. population. This is difficult to control in counterfactual experiments. Second, we do not consider whether federal mask, stay-at-home, or travel ban policies are feasible from a legal point of view. The legality of some of these policies is beyond the scope of our paper. Finally, our results about the number of preventable deaths are based on a hindsight approach that assumes that some information about the effect of different regulatory policies may have already been known at the beginning of the pandemic. Looking forward to future pandemics, or even future waves of the current COVID-19 pandemic, our results highlight the benefits of early actions by federal and state regulators.

## 2 Model description

We briefly describe our model here and provide a detailed model formulation in Appendix A. We assume that a unit of time is one day and that a country is composed of several states. We model the number of people in each state that are *(i)* susceptible to the virus (i.e., have never been infected), *(ii)* infected by the virus, *(iii)* recovered from the virus (and immune to subsequent infections), and *(iv)* deceased due to the virus.<sup>11</sup> Our model explicitly takes into account the impact of different containment policies on the transmission of the disease. We consider three different types of containment policies: mask mandates, travel bans, and stay-at-home orders. Our model also accounts for the effects of traveling and commuting across state lines.

Each state is endowed with a certain number of inhabitants. On any given day in a given state, the number of people that are contaminated by an infected person is assumed to be

<sup>9</sup>Redlener et al. (2020) establish a similar number of preventable deaths through a comparison of international policy responses. As Shefrin (2020) argues, however, cultural and ideological differences may have prevented the U.S. government from adopting international policies. We show that a large number of COVID-19 deaths could have been prevented by following policies that were already implemented domestically in the states.

<sup>10</sup>Our results are consistent with the findings of Eikenberry et al. (2020), Ngonghala et al. (2020), and Stutt et al. (2020), who highlight the benefits of a federal mask mandate in single-state models. Other studies that consider the impact of different federal containment policies include Alfaro et al. (2020), Alvarez et al. (2020), Ferguson et al. (2020), Flaxman et al. (2020), and Fowler et al. (2020), among others.

<sup>11</sup>Our assumption on immunity post-infection is merely a simplification given that current evidence on re-infections from COVID-19 is thin and mixed, see, e.g., Iwasaki (2020).

a random draw from a Poisson distribution whose rate is the product of the policy-adjusted transmission rate in the state and the fraction of the state's population that is susceptible to the virus. If a person is infected on any given day, that person either dies, recovers, or continues to be infected in the next day with certain probabilities. We assume that it takes on average 14 days for an infection to resolve and that the fatality rate by the end of this time period is 0.6%. All in one, on aggregate in a state, the net number of new infections in a day is Poisson distributed with rate equal to the product of the policy-adjusted transmission rate, the ratio of susceptible population, and the number of infected inhabitants of the state, after subtracting the number of infected individuals that recover or die from the disease.

We assume that the transmission rates in the different states are unobservable and evolve stochastically from day to day. They are positively correlated across states and time.

We account for interstate commuting and traveling as follows. Each day, an inhabitant of a state can commute to another state, travel to another state, or remain in the home state with given probabilities. Inhabitants that stay in their home states contribute to the disease transmission in their home states. Commuters travel during parts of the day and return to their home states at the end of a day. They contribute to the transmission of the disease in their home states and the visited states. Travelers spend several days in the visited state. They only contribute to the transmission of the disease in the state they visit.

The transmission rates in each state, as well as the travel and commuting probabilities across states, are adjusted to reflect the containment policies adopted by the different states. The effects of the different policies are modeled by shrinking the transmission rates or the inflows of travelers and commuters when the policies are active. We assume that a mask mandate in a given state shrinks the transmission rate in that state by 42% but does not affect the inflow or outflow of travelers and commuters.<sup>12</sup> A travel ban in a given state shrinks the inflow of travelers by 90%, but does not affect the transmission rate or the inflow of commuters in that state.<sup>13</sup> Finally, a stay-at-home order shrinks both the transmission rate and the inflow of commuters and travelers in that state by 36%.<sup>14</sup> Appendix E considers variations of these parameters and

<sup>12</sup>We justify this value as follows. Based on the estimates of Fischer et al. (2020), we assume that a typical mask worn in the U.S. filters out particles by a median value of 85%. We assume that only half of the population wears masks as suggested by data from the Institute of Health Metrics and Evaluation, justifying a reduction factor of approximately 42%.

<sup>13</sup>We estimate the 90% impact of travel bans as the reduction factor in the average number of daily trips of more than 100 miles that were taken in the U.S. between March 15 and April 30, 2020, compared to 2019. We assume that travel bans do not reduce the inflow of commuters into a state because travel bans were often accompanied by exemptions for commuters.

<sup>14</sup>We estimate the impact of stay-at-home orders on transmission rates as the reduction factor in the average

measures the sensitivity of our results to our assumptions.

We use mobility, travel, and state-level policy data from the United States to calibrate most of the parameters of our model. We develop a filtering-based maximum likelihood methodology to estimate some of the parameters governing the transmission rates of the different states. We rely on daily state-level death counts from The COVID Tracking Project since they are the least likely to be contaminated with substantial measurement issues (compared to the number of infections, for instance).<sup>15</sup> The sample period is February 12 through September 30, 2020. Appendix B provides details of the approach we take to fit our model to the data.

Figure 5 in Appendix B shows the death counts in the data as well as the posterior mean of the death counts in our model. The figure shows that our model performs well at matching state-level and aggregate death counts. We show in Appendix B that our model implies that, in order to match the levels of fatalities we observed over the sample period in U.S. states, the effective  $\mathcal{R}_0$  of the disease in the different states must have been substantially higher than 1 through April 2020 for the majority of the states. We also show that the  $\mathcal{R}_0$  grew larger than 1 in several states over the summer. Our estimates suggest that the number of infections in the different states required to match the history of COVID-19 fatalities in the U.S. must have been substantially higher than recorded in the data. Unreported model outcomes show that the estimated number of infected individuals in mid March was about 50-times larger than data records show, while it was about 5-time as large as in the data by late September. Our results imply that many infected people remained undiagnosed and contributed to the spread of the disease early in the sample.

### 3 Results

We run counterfactual experiments in our model to study the effectiveness of the different containment policies. The underlying assumption of our counterfactuals is that states deviate from the policies they enacted in reality by imposing stricter or looser restrictions in a hypothetical world. We ask: what would have happened to the death count of a state if it had enacted a

---

number of daily trips of less than 10 miles taken in 2019 versus those taken between March 15 and April 30, 2020, which is the period in which most stay-at-home orders were active in the United States. Because stay-at-home orders were often accompanied by lockdowns which closed out office buildings, we assume that stay-at-home orders also reduce the inflow of commuters into a state. Finally, because stay-at-home orders were also associated with closed out tourist attractions, we also assume that stay-at-home orders reduce the inflow of travelers into a state.

<sup>15</sup>The fact that our estimation approach relies on death counts data only, as in [Flaxman et al. \(2020\)](#), is an advantage over standard approaches to estimate time-varying reproduction numbers (e.g. [Bettencourt and Ribeiro \(2008\)](#), [Cori et al. \(2013\)](#), [Thompson et al. \(2019\)](#)), as these approaches necessitate data on infection cases.

stricter containment policy than it actually did? What would have happened if it had adopted a policy that it did not enact in reality? And how would these deviations have impacted the aggregate death count in the U.S. by the end of our sample? We answer these questions for mask mandates, stay-at-home orders, and travel ban policies.

We assume that a state adopts a *loose* policy if it does not impose that policy at all over our sample period. In contrast, we assume that a state adopts a *strict* policy if it adopts that policy as early as the earliest state adopted the policy in the data, and keeps the policy active until the last state in our sample shuts off that policy. Our strict policy scenario therefore avoids forward-looking biases. Any regulator could have adopted a strict policy scenario in real life by moving along with the first state that adopted a policy and ending the policy as soon as no other state had the policy in place.<sup>16</sup> The strict scenarios for the different policies are:

- **Stay-at-Home:** Start on March 20, 2020 (the day when California activated its stay-at-home mandate) and keep it active through September 30, 2020 (the last day in our sample in which the stay-at-home order was still active in California).
- **Travel ban:** Start on March 17, 2020 (the day the first interstate travel ban in the U.S. went into effect in Hawaii) and keep it active through September 30, 2020 (the last day in our sample in which an interstate travel ban was still active in Alaska).
- **Mask mandate:** Start on April 17, 2020 (the day the first mask mandate in the U.S. went into effect in Connecticut) and keep it active through September 30, 2020 (the last day in our sample in which several states had mask mandates in place).

We consider two variations of our counterfactual experiments. One in which only one state at a time deviates from its actual policies at a time, and another one in which all states take on the same policy jointly at the same time. With the first set of experiments we seek to answer how impactful deviations at the state level would have been. The second set of counterfactuals studies how impactful federally mandated policies would have been. To evaluate the effectiveness of the different policies, we compare the number of deaths at the state and federal levels in the different counterfactual experiments to the baseline levels in the data. Appendix C provides details of our approach to computing counterfactual results.

Table 1 shows the results of the counterfactual experiments in which we assume that all states deviate jointly. Figure 1 breaks down the number of deaths that could have been prevented

<sup>16</sup>The legality of such federal mandates are outside of the scope of this paper.

Counterfactual assumption	Federal mandate active on:			Deaths in excess of baseline
	Stay-at-home	Mask	Travel ban	
Strict stay-at-home orders, mask mandates, and travel bans for all states.	3/20	4/17	3/17	-136,514 [-162,029; -105,168]
Strict stay-at-home orders in all states, and all other state-level policies remain as in the data.	3/20			-110,129 [-136,201; -78,960]
Strict mask mandates in all states, and all other state-level policies remain as in the data.		4/17		-96,515 [-116,362; -67,520]
Strict travel bans in all states, and all other state-level policies remain as in the data.			3/17	-5,148 [-5,435; -2,557]
No stay-at-home order, mask mandate, or travel ban in any state.				+1,012,053 [+379,784; +1,600,955]
No stay-at-home order in any state, but all other policies remain as in the data.				+657,949 [+253,519; +1,483,567]
No mask mandate in any states, but all other policies remain as in the data.				+439,193 [+78,136; +1,290,944]
No travel ban in any states, but all other policies remain as in the data.				+2,286 [+1,061; +2,433]
Mask mandate in all states on March 20, 2020, while no state adopts any state-level policies.		3/20		-78,136 [-188,723; 181,526]
Strict travel bans in all states by February 12, 2020, while all other state-level policies remain as in the data.			2/12	-5,986 [-6,265; -2,983]

Table 1: Results of the counterfactual experiments in which we assume that all states jointly deviate from their enacted policies and adopt either strict or loose versions of the policies instead. The reported values are excess deaths relative to the number of U.S. deaths recorded in our data on September 30, 2020. In the counterfactuals, we compute the trajectories of death counts per state under the alternative policy scenarios that are consistent with the susceptible, infected, recovered, and dead populations as well as the transmission rates filtered from the observed data. The values in brackets give confidence bounds based on a sensitivity analysis of the estimates of the impact of the different policies on transmission rates and traveler and commuter inflow. The lower bounds assume that any policy that deviates from what it was in the data is half as impactful, while the upper bound assumes that any policy that deviates is twice as impactful. Table 2 in Appendix E provides the parameter values used for the sensitivity analyses. In the sensitivity analysis, we proceed in a similar way as for the counterfactuals and first compute posterior means of the state-level transmission rates that would explain the observed death counts under the assumption of alternative effectiveness for the different policies. We then compute the number of death that would have been observed if the policies had changed while keeping the recomputed trajectories of the transmission rates fixed.



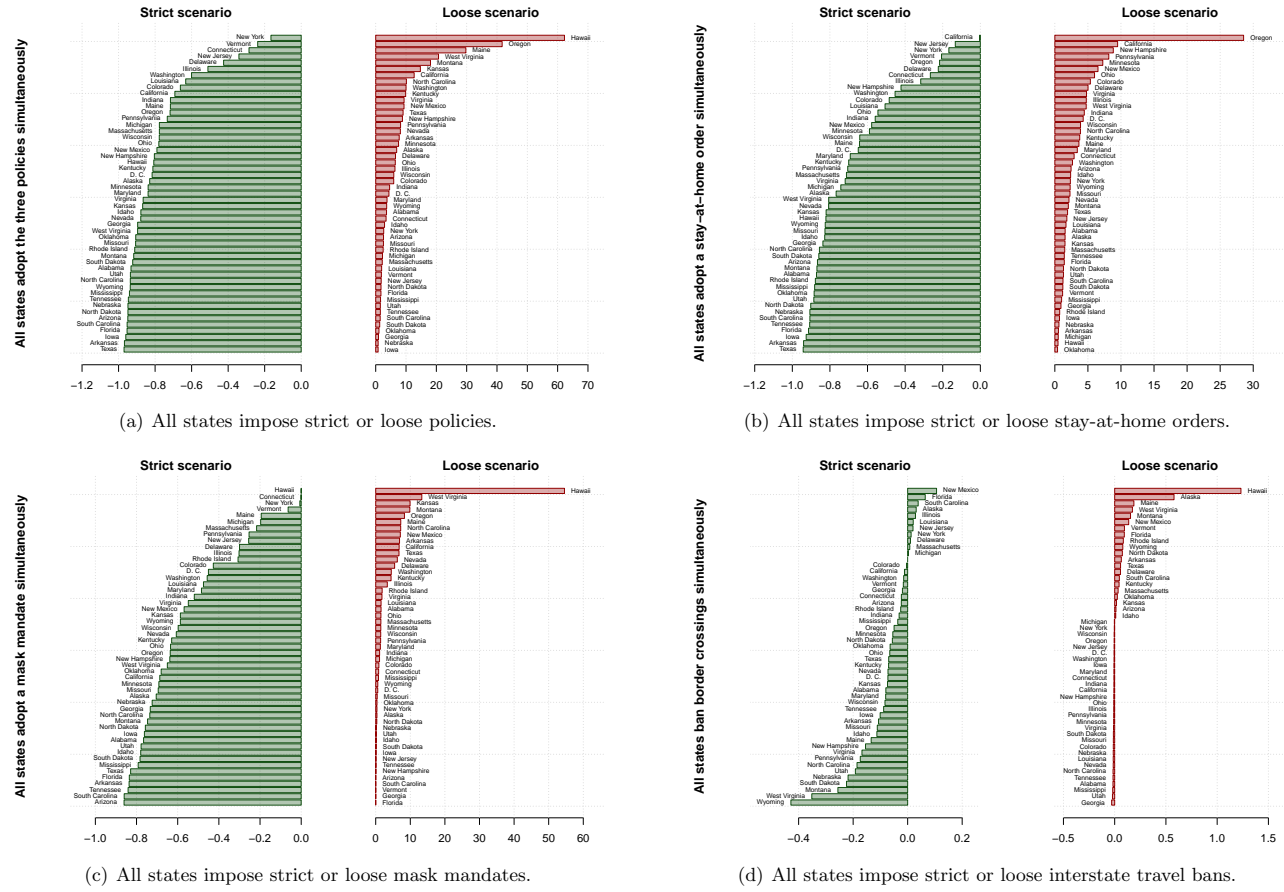


Figure 1: State-by-state breakdown of excess deaths relative to the baseline in the different counterfactual scenarios in which all states jointly deviate from their implemented policies. The excess death values are measured as proportions of the death cases in the data for each state. Policies are divided into stay-at-home order (b), mask mandates (c), travel bans (d), and all three policies together (a). Counterfactual policies are divided into a *strict* scenario in which all states implement a policy as long as at least one state decides to do so, and a *loose* scenario in which no state implements a particular policy. Counterfactual death counts are computed through the methodology detailed in Appendix C.

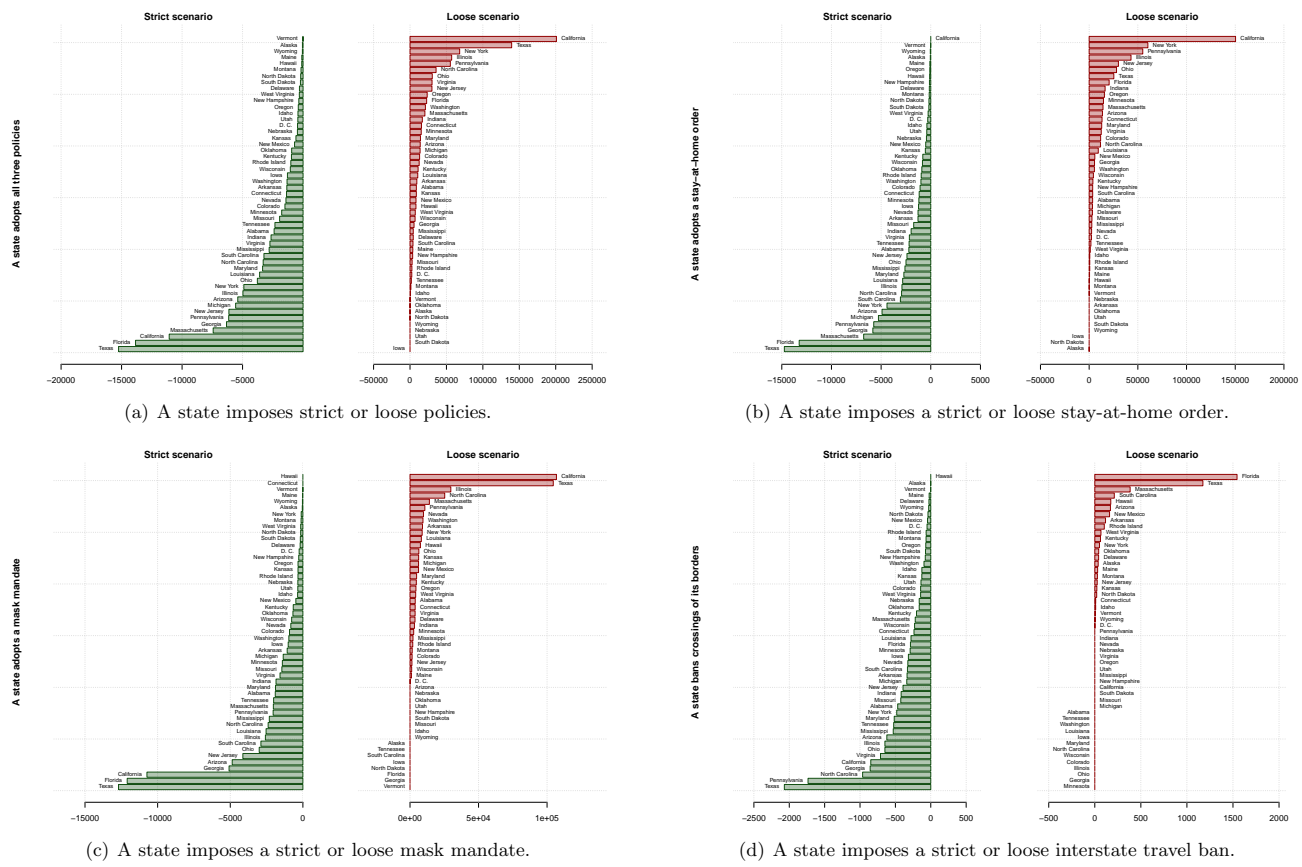


Figure 2: State-by-state breakdown of excess deaths relative to the baseline in the different counterfactual scenarios in which states deviate individually from their implemented policies. Policies are divided into stay-at-home order (b), mask mandates (c), travel bans (d), and all three policies together (a). Counterfactual policies are divided into a *strict* scenario in which a particular state implements a policy as long as at least one state decides to do so, and a *loose* scenario in which a state does not implement a particular policy. Counterfactual death counts are computed through the methodology detailed in Appendix C.

through federal mandates by states and displays these in proportion to the number of death in the data of the individual states. Figure 2 shows the number of deaths that could have been prevented in the different states if individual states had deviated from their implemented policies while all other states kept their policies untouched. The time series of cumulative virus deaths in the different counterfactual scenarios are given in Figure 8 of Appendix C. We carry out several robustness checks that re-evaluate the number of preventable deaths in the different scenarios under alternative assumptions of the impact of the different policies on transmission rates and traveler and commuter flows, as well as the fatality rate of the disease and the number of days it takes for an infection to resolve. The results of these sensitivity analyses are summarized in Table 1 and further elaborated in Appendix E. The additional sensitivity analyses are consistent with our main conclusions and provide validity for our results.

### 3.1 Federal mandates

Table 1 suggests that 136,514 virus deaths could have been prevented if the U.S. government had mandated federal containment policies as early as the earliest state did and maintained the policies for as long as the strictest states did. Our results indicate that 110,129 deaths could have been prevented had the federal government moved along with California and mandated a federal stay-at-home order on March 20, 2020 that remained active throughout our sample. The results also indicate that 96,515 deaths could have been prevented if the federal government had issued a federal mask mandate as early as Connecticut did on April 17, 2020, and kept the mandate active through September 30. In contrast, we find that only 5,148 deaths could have been prevented had the federal government banned all interstate travel by March 17, 2020 – the day in which Hawaii banned inbound interstate travel.

Figure 1 hints that strict federal mandates could have been highly effective at preventing death in states that adopted weak containment policies. Over 95% of all death cases in Arkansas, Florida, Iowa, South Carolina, and Texas – corresponding to close to 35,000 fatalities – could have been prevented if the federal government had imposed strict stay-at-home orders, mask mandates, and interstate travel bans. These states adopted some of the weakest containment policies during our sample period.

Although Table 1 suggests the biggest reduction of fatalities could be achieved through a federal stay-at-home mandate, this comes at the cost of shutting down the national economy. The potential substantial economic costs inherent to that policy cast doubt on whether the federal

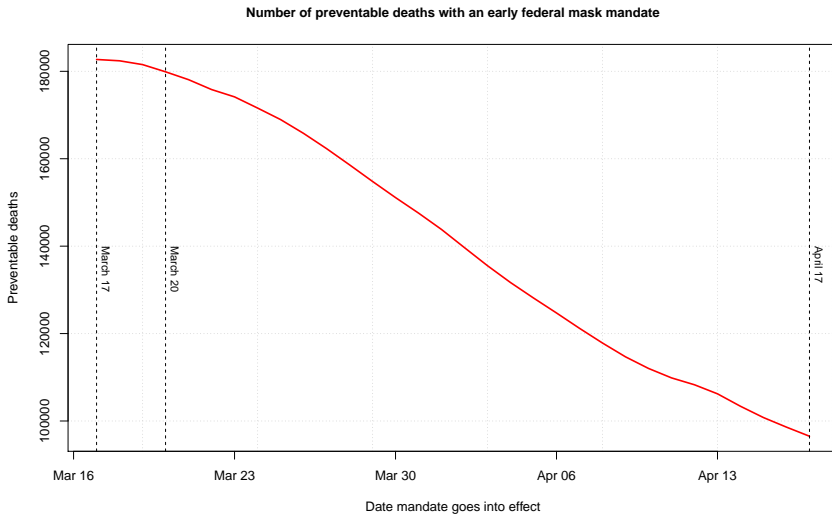


Figure 3: Number of deaths that could have been prevented through an early federal mask mandate. The  $x$ -axis indicates the date in which we assume a federal mask mandate had gone into effect, while the  $y$ -axis gives the number of deaths that could have been prevented had a federal mask mandate gone into effect on that date. We assume that state-level stay-at-home and travel ban policies remain as in the data, and that a federal mask mandate supersedes the state-level mask policies.

government would have been persuaded to carry out such a drastic step. Instead, imposing a federal mask mandate could have been a cost-effective option. We ask: how many deaths could have been prevented if the federal government had imposed an early federal mask mandate sometime between March 17 and April 17 that complemented the stay-at-home and interstate travel policies that were in effect in the different states? We run an additional counterfactual experiment to answer this question; Figure 3 summarizes our findings.

Our results indicate that between 96,515 and 182,710 deaths could have been prevented if a federal mask mandate that complemented the state-level stay-at-home and travel ban policies went into effect sometime between mid March and mid April. What drives our findings is that an early federal mask mandate could have provided a significant boost in reducing the potential for infections. As Figure 6 in Appendix B shows, the effective reproduction number ( $\mathcal{R}_0$ ) of the virus was substantially high – much higher than 1 – in all states through April 2020 even while stay-at-home orders were in place in the different states. By imposing an early mask mandate, the federal regulator could have contributed to drastically reducing the infection potential in all states early in the sample. This would have contributed to slowing down new infections

over time even while some state-level policies were relaxed. Indeed, Table 1 shows that, in a counterfactual world in which a federal mask mandate had gone into effect on March 20 while no state-level policies had been enacted, only 78,136 virus deaths would have been prevented. This result suggests that the key step for the federal regulator would have been to issue an early federal mask mandate that complemented, but did not replace, the state-level stay-at-home and travel ban policies that were enacted over time.

The number of deaths that could have been prevented with early federal policies depends on our assumptions on how fatal COVID-19 is and how long it takes for an infection to resolve. We run sensitivity analyses in Appendix E to verify that our results are robust to different calibrations. The results of Appendix E are generally consistent with Table 1 and Figures 1 through 3. They also highlight an important benefit of our methodology. Appendix E establishes that the number of preventable deaths is higher if we assume that it takes only 10 days for an infection to resolve.<sup>17</sup> We find that this is the case because, in order to match the number of deaths observed in the data if the virus were less severe, the methodology infers that there must have been many more infected individuals early in the sample so that early federal action would have been even more impactful. We obtain these results because we rely only on death counts to make our inferences and allow the methodology to estimate how many infections there must have been to match the data. This highlights a fundamental benefit of our approach relative to alternative approaches that rely on infection cases, which may be under-counted in the data due to the large number of asymptomatic cases or undetected infections,

Looking forward to future waves of the COVID-19 pandemic, our results suggest that early actions by the federal government when the reproduction numbers are high could have a great impact on preventing virus deaths.

### 3.2 State mandates

Our counterfactual experiments indicate that the actions taken by individual states benefited both the states that implemented the policies and the U.S. as a nation. We find that the U.S. would have been much worse off if no state had adopted any containment policies. In a hypothetical scenario in which no state had imposed any policies, Table 1 indicates that the U.S. would have observed 1,012,053 additional deaths due to COVID-19. Our results show that states that

---

<sup>17</sup>We find that the fatality rate has little impact on the number of preventable deaths, and instead mostly affects the number of deaths that would have been observed if no state adopted any policy.

implemented strict containment policies were able to contain the spread of the disease. Figure 1 shows that a state like New York, which had one of the longest running stay-at-home and mask mandates, would have experienced only 17% fewer death cases if all states had imposed all three strict policies simultaneously. Figure 2 also shows that a state like California, which imposed the strictest stay-at-home policy in the country, would have recorded around 200,000 additional COVID-19 deaths, or 13-times its end-of-September toll, if it had not imposed any containment policies at all. These results suggest that the measures adopted by individual states to contain the disease were highly effective and shielded states from inaction from other states.

Figure 2 also shows that states that imposed weak containment policies could have prevented a substantial number of COVID-19 fatalities by imposing stricter policies. Two states in particular stand out: Florida and Texas. These states could have prevented 13,846 deaths (95% of all death cases in Florida) and 15,250 (97% of all death cases in Texas), respectively, if they had implemented strict versions of the containment policies we consider in this paper. While it may be unrealistic to have expected most states to enact strict stay-at-home orders and interstate travel bans because these policies carry heavy economic burdens, mask mandates could have been enacted without concerns about economic consequences. We find that Texas could have prevented 81% of its COVID-19 fatalities, while Florida could have prevented 83% of its COVID-19 fatalities, if the states had enforced mask mandates as early as Connecticut did on April 17, 2020. Even some states that otherwise had strict policies in place suffered from not adopting a mask mandate early enough. Our counterfactuals suggest that California, whose mask mandate went into effect on June 19, could have prevented 10,736 virus deaths if it had adopted a mask mandate as early as Connecticut did on April 17.

We find that the four states that implemented no containment policies at all during our sample period—Iowa, Nebraska, South Dakota, and Utah – could have benefited if they had implemented mask mandates by April 17 without forcing stay-at-home orders or interstate travel bans. Figure 2 suggests that strict mask mandates could have prevented as many COVID-19 deaths as -1,011 in Iowa (75% of all COVID-19 deaths in the state), 347 in Nebraska (70%), 177 in South Dakota (75%), and 350 in Utah (75%). These results corroborate our findings on the effectiveness of mask mandates for preventing COVID-19 transmission and deaths, both at the federal and the state levels.

### 3.3 Interstate mobility

The results of Table 1 and Figures 1 and 2 suggest that interstate travel bans are not very effective in preventing COVID-19 deaths. We find that there are two reasons driving the low impact of interstate travel bans.

First, interstate travel bans were often imposed late, only once the state regulator became aware of the virus and the virus had already taken hold in the state's population. Table 1 shows that only 5,148 deaths could have been prevented in the U.S. if all interstate travel had been banned by March 17, 2020. At that point, however, Figure 7 in Appendix B shows that most states must have already had several infected individuals so that the virus was already spreading in the states. Banning interstate travel at that point would not have prevented the spread of the virus. It may have been different, however, if interstate travel bans were enacted earlier. Early enough that they prevented the virus from entering certain states. We run an additional counterfactual in which we ask how many virus deaths could have been prevented if the federal regulator banned all interstate travel on the first day of our sample, namely February 12. The results, summarized in Table 1, show that an additional 838 deaths could have been prevented with such an early interstate travel ban. This result indicates that travel bans are more effective if they are implemented early on.

Second, some externalities arise when individuals can move across state lines and these externalities reduce the effectiveness of travel bans. In our model, interstate travel allows for the transfer of infected population across states. Consider South Carolina, for example. On an average day, our estimates suggest that 96,242 South Carolinians travel or commute out-of-state while 83,572 out-of-state residents travel or commute into South Carolina. As a result, South Carolina is a net exporter of individuals in our model. Now, Figure 1 suggests that South Carolina would have recorded 4% more virus death cases if all interstate travel had been banned on March 17. Why is this the case? We find that this is driven by the fact that, when population is not allowed to cross state borders, infected individuals are forced to stay within the home state. The higher concentration of infected population in those state leads to an accelerated spread of the disease and therefore also to higher infections and death cases. This is showcased in Figure 9 of Appendix D, in which we plot the estimated cumulative number of infections in South Carolina both under the baseline and in the counterfactual in which a strict federal interstate travel ban is imposed.

Consider Wyoming, on the other hand. Wyoming is a net importer of travelers and com-

muters, receiving on an average day a net inflow of around 8,750 out-of-state individuals. Figure 1 indicates that Wyoming would have recorded 43% fewer death cases if a federal ban of interstate travel had gone into effect on March 17. Figure 9 of Appendix D suggests a similar mechanism in this case. Without a travel ban, Wyoming received infected population from other states and this resulted in a higher number of infections in the state. If the federal government had imposed a strict interstate travel ban, then the out-of-state infected population would not have easily reached Wyoming. This would have resulted in a lower number of in-state infections and ultimate virus deaths.

All in one, our experiments indicate that interstate travel makes it possible that states that are net importers of travelers record higher numbers of death cases than they would in the absence of travel, while states that are net exporters of travelers record lower number of virus fatalities. Policies that restrict interstate mobility do not resolve this externality because they only redistribute infection cases among states. Our results also suggest that late restrictions of interstate mobility can be counterproductive because they allow for the virus to spread in an accelerated fashion in some states rather than allowing for a balanced distribution of the virus across states. However, we find this is only a minor adverse consequence of policies that restrict interstate mobility. We find that interstate travel bans account only for a couple of thousand preventable deaths in our counterfactual analyses. In additional unreported experiments, we also find only 861 additional virus deaths could have been prevented through a strict federal stay-at-home order on March 20, 2020, if interstate traveling and commuting were not discouraged by the order. Putting everything together, our study shows that the ban of interstate travel can be an effective tool to prevent the spread of a virus if the ban is enacted early enough to prevent the virus from taking hold in a population.

## 4 Conclusion

We show that more than two-thirds of all COVID-19 death cases in the U.S. were preventable had the federal government followed the leads of several states that took early actions to contain the virus. Our results indicate that, in the absence of a unified federal approach, the policies enacted in individual states were effective and resulted in reduced virus fatalities. This benefited both the individual states and the U.S. as a whole. As a lesson for future waves of the COVID-19 pandemic, as well as future pandemics, our results highlight the need for decisive and impactful



early actions by a federal regulator to complement actions taken by state regulators, especially at times when the reproduction numbers are substantially large.

## — Appendix —

### A Model

#### A.1 Single-state model

We first introduce a single-state model to provide an overview of the assumptions underlying the stochastic evolution of the COVID-19 disease. This provides a basis that we extend in the following section to account for a network of  $N$  states.

##### A.1.1 From micro assumptions to aggregate dynamic equations

Consider individual  $j$  that was infected on date  $t - 1$  (i.e.,  $j \in \{1, \dots, I_{t-1}\}$ ). We assume that the number of people infected by this individual between dates  $t - 1$  and  $t$  follows a Poisson distribution:  $i_{j,t} \sim i.i.d. \mathcal{P}\left(\frac{S_{t-1}}{N}\beta_{t-1}\right)$ . Using the fact that a sum of Poisson-distributed variables is Poisson, the total number of people infected between dates  $t - 1$  and  $t$  is  $i_t \sim i.i.d. \mathcal{P}\left(\frac{S_{t-1}}{N}I_{t-1}\beta_{t-1}\right)$ .

If  $j$  is infected on date  $t$ , then the probability that she dies between dates  $t$  and  $t + 1$  is  $\delta$  (i.i.d. Bernoulli) and, if she does not die, the probability she recovers between dates  $t$  and  $t + 1$  is  $\gamma/(1 - \delta)$ . (In such a way that the probability she recovers if  $\gamma$ .)

The cumulated number of dead people on date  $t$  ( $D_t$ ) is given by  $D_t = D_{t-1} + d_t$ , where  $d_t$  is the number of deaths taking place on date  $t$ . Under the assumptions stated above,  $d_t$  follows a binomial distribution:  $d_t \sim \mathcal{B}(I_{t-1}, \delta)$ . Moreover, the number of people who recover between dates  $t - 1$  and  $t$  is  $r_t \sim \mathcal{B}\left(I_{t-1} - d_t, \frac{\gamma}{1-\delta}\right)$ .

We have  $S_t = S_{t-1} - i_t$ ,  $I_t = I_{t-1} + i_t - d_t - r_t$ , and  $R_t = R_{t-1} + r_t$ , where  $S_t$  and  $R_t$  respectively denote the number of susceptible and recovered persons as of date  $t$ . (It is easily checked that  $S_t + I_t + R_t + D_t = S_{t-1} + I_{t-1} + R_{t-1} + D_{t-1}$ .)

**A.1.2 Transmission rate dynamics**

The transmission rate  $\beta_t$  is assumed to follow a non-negative square root process whose Euler discretization reads:

$$\beta_t = \mathbb{E}_{t-1}(\beta_t) + \sigma \sqrt{\Delta t \mathbb{E}_{t-1}(\beta_t)} \varepsilon_{\beta,t}, \tag{1}$$

where  $\varepsilon_{\beta,t} \sim \mathcal{N}(0, 1)$  and  $\mathbb{E}_{t-1}(\beta_t) = \beta_{t-1} + \kappa(\beta - \beta_{t-1})$ .

**A.1.3 State-space model**

Let us now write the state-space representation of the model in a context where only  $D_t$  is observed. The vector of latent variables is  $[\beta_t, S_t, I_t, R_t]'$ .

The measurement equation is  $\Delta D_t = \delta I_{t-1} + \varepsilon_{D,t}$ . The transition equations are:

$$\begin{bmatrix} S_t \\ I_t \\ R_t \\ \beta_t \end{bmatrix} = \begin{bmatrix} 1 & 0 & 0 & 0 \\ 0 & 1 - \delta - \gamma & 0 & 0 \\ 0 & \gamma & 1 & 0 \\ 0 & 0 & 0 & 1 - \kappa \end{bmatrix} \begin{bmatrix} S_{t-1} \\ I_{t-1} \\ R_{t-1} \\ \beta_{t-1} \end{bmatrix} + \begin{bmatrix} -\frac{S_{t-1}}{N} \beta_{t-1} I_{t-1} \\ +\frac{S_{t-1}}{N} \beta_{t-1} I_{t-1} \\ 0 \\ \kappa \beta \end{bmatrix} + \begin{bmatrix} \varepsilon_{S,t} \\ \varepsilon_{I,t} \\ \varepsilon_{R,t} \\ \sigma \sqrt{\beta_{t-1} \Delta t} \varepsilon_{\beta,t} \end{bmatrix} \tag{2}$$

with  $\varepsilon_{\beta,t} \sim i.i.d. \mathcal{N}(0, 1)$  and

$$\begin{bmatrix} \varepsilon_{D,t} \\ \varepsilon_{S,t} \\ \varepsilon_{I,t} \\ \varepsilon_{R,t} \end{bmatrix} = \begin{bmatrix} d_t - \delta I_{t-1} \\ -i_t + \frac{S_{t-1}}{N} I_{t-1} \beta_{t-1} \\ i_t - d_t - r_t - \frac{S_{t-1}}{N} I_{t-1} \beta_{t-1} + (\delta + \gamma) I_{t-1} \\ r_t - \gamma I_{t-1} \end{bmatrix}.$$

Appendix F shows that  $\text{Var}_{t-1}([\varepsilon_{D,t}, \varepsilon_{S,t}, \varepsilon_{I,t}, \varepsilon_{R,t}, \varepsilon_{\beta,t}])$  is equal to

$$I_{t-1} \begin{bmatrix} \delta(1-\delta) & 0 & -\delta(1-\delta-\gamma) & -\delta\gamma & 0 \\ 0 & \frac{S_{t-1}}{N}\beta_{t-1} & -\frac{S_{t-1}}{N}\beta_{t-1} & 0 & 0 \\ -\delta(1-\delta-\gamma) & -\frac{S_{t-1}}{N}\beta_{t-1} & \frac{S_{t-1}}{N}\beta_{t-1} + \nu & -\gamma(1-\gamma-\delta) & 0 \\ -\delta\gamma & 0 & -\gamma(1-\gamma-\delta) & \gamma-\gamma^2 & 0 \\ 0 & 0 & 0 & 0 & 1 \end{bmatrix}, \quad (3)$$

where  $\nu = \frac{(1-\delta-\gamma)^2\delta + \gamma(1-\delta-\gamma)}{1-\delta}$ .

## A.2 Multi-state model

We now consider a  $N$ -state model. Inhabitants may travel across states for commuting or other reasons – we refer to the latter as “traveling.” In terms of notations, superscript  $j$  refers to a given state. Variables without superscripts denote  $N$ -dimensional vectors. We denote by  $\mathbf{p} = [p_1, \dots, p_N]'$  the vector of the state population sizes.  $S_t, I_t, R_t$  and  $D_t$  are  $N$ -dimensional vectors gathering the number of susceptible, infected, recovered, and deceased people in each state.

### A.2.1 Policy restrictions

The transmission rates  $\beta_{j,t}$  and the flow probabilities are impacted by the containment policies implemented in the different states. We consider three containment policies: mask mandates, stay-at-home orders, and travel bans. The effect of each policy is captured through the binary variables  $\theta_{t,M}^j, \theta_{t,S}^j$  and  $\theta_{t,T}^j$ , respectively valued in  $\{\theta_M^{low}, 1\}, \{\theta_S^{low}, 1\}$ , and  $\{\theta_T^{low}, 1\}$ . The parameters  $\theta_M^{low}, \theta_S^{low}$ , and  $\theta_T^{low}$  are strictly lower than one; they reflect the effects of the containment policies. More precisely:

- The transmission rate  $\beta_{j,t}$  is reduced when mask mandates or stay-at-home policies are implemented. Formally, it is of the form  $\beta_{j,t}^0 \theta_{t,M}^j \theta_{t,S}^j$ , where  $\beta_{j,t}^0$  is an exogenous transmission rate following the dynamics depicted by (1). Given that the  $\theta$  variables are equal to one when the policies are not in place, it follows that  $\beta_{j,t}^0$  coincides with the effective transmission rate ( $\beta_{j,t}$ ) when mask mandates and stay-at-home policies are not implemented.
- The probability that a given inhabitant of State  $j$  commutes to State  $k$ , that is  $w_{j,k,t}^{com}$ , is of the form  $w_{j,k}^{com} \theta_{S,t}^k$ . Similarly, the travel probability is given by  $w_{j,k,t}^{trav} = w_{j,k}^{trav} \theta_{T,t}^k$ . These

probabilities are therefore lower when (i) stay-at-home orders are in place or (ii) when travel bans are enforced in the visited state.

**A.2.2 Traveler flows**

The variables  $\text{Flow}_{trav,S,t}^j$ ,  $\text{Flow}_{trav,I,t}^j$ , and  $\text{Flow}_{trav,R,t}^j$  are net travel inflows of susceptible, infected, and recovered populations, respectively.

We denote by  $w_{trav,t}^{k,j}$  the average fractions of the date- $t$  population of State  $k$  that travels to State  $j$ ;  $\mathbf{e}_j$  is the  $j^{\text{th}}$  column of the  $N \times N$  identity matrix;  $\mathbf{1}$  is a  $N \times 1$  vector of ones;  $w_{trav,t}^{j,\bullet}$  and  $w_{trav,t}^{\bullet,j}$  respectively denote the  $j^{\text{th}}$  row vector and column vector of  $W_{trav,t}$ . Consistent with the assumptions made in A.2.1, we have:

$$W_{trav,t} = \tau_{trav} W_{trav} \mathbf{d}(\theta_{T,t}) \mathbf{d}(\theta_{S,t}). \tag{4}$$

Here,  $\tau_{trav}$  measures the average number of days that a traveler spends in the visited states. Using the Poisson approximation of the binomial distribution, we consider that the number of outward travelers is drawn from Poisson distributions. For example, the number of susceptible individuals traveling from State  $k$  to State  $j$  between dates  $t$  and  $t + 1$  is:

$$\text{Flow}_{trav,S,t}^{k,j} \sim i.i.d. \mathcal{P}(w_{trav,t}^{k,j} S_t^k). \tag{5}$$

This implies in particular that the net number of inhabitants traveling into State  $j$  between dates  $t$  and  $t + 1$  (denoted by  $\text{Flow}_{trav,S,t}^j$ ) is such that:

$$\begin{aligned} \phi_{trav,S,t}^j &:= \mathbb{E}(\text{Flow}_{trav,S,t}^j | S_t) = \left( \sum_{k \neq j} w_{trav,t}^{k,j} S_t^k \right) - \left( \sum_{j \neq k} w_{trav,t}^{j,k} \right) S_t^j \\ &= \left( w_{trav,t}^{\bullet,j} - (w_{trav,t}^{j,\bullet} \mathbf{1}) \mathbf{e}_j \right)' S_t. \end{aligned}$$

Using the convention  $w_{trav,t}^{j,j} = 0$ , it follows that the  $N$ -dimensional vector  $\phi_{trav,S,t}$  is given by  $\phi_{trav,S,t} = \Omega_{trav,t} S_t$ , where

$$\Omega_{trav,t} = W'_{trav,t} - \mathbf{d}(W_{trav,t} \mathbf{1}). \tag{6}$$

By the same token, and with obvious notations for  $\phi_{trav,I,t}$  and  $\phi_{trav,R,t}$ :  $\phi_{trav,I,t} = \Omega_{trav,t} I_t$  and  $\phi_{trav,R,t} = \Omega_{trav,t} R_t$ .

**A.2.3 Commuter flows**

Interstate commuters are people who spend a fraction  $\tau$  of each day in another state. Consider the infected inhabitants of State  $k$  working in State  $j$ . They contaminate less people in State  $k$  because they spend less time in that state. But they may also contaminate people in State  $j$  because they spend some time in that state while commuting. We respectively denote by  $\text{Flow}_{com,S,t}^{j\leftarrow}$ ,  $\text{Flow}_{com,I,t}^{j\leftarrow}$ , and  $\text{Flow}_{com,R,t}^{j\leftarrow}$  the commuting inflows of susceptible, infected and recovered people in State  $j$ . Outflows are given by  $\text{Flow}_{com,S,t}^{j\rightarrow}$ ,  $\text{Flow}_{com,I,t}^{j\rightarrow}$  and  $\text{Flow}_{com,R,t}^{j\rightarrow}$ .

Let us denote by  $W_{com,t}$  the “commute” matrix; that is, the matrix whose component  $(i, j)$ , denoted by  $w_{com,t}^{i,j}$ , is the fraction of the date- $t$  population of State  $k$  that commutes to State  $j$ . On date  $t$ , the number of susceptible people commuting from State  $k$  to State  $j$  is:

$$\text{Flow}_{com,S,t}^{k,j} \sim i.i.d. \mathcal{P}(w_{com,t}^{k,j} S_t^k). \tag{7}$$

This implies in particular, with obvious vectorial notations, that:

$$\phi_{com,S,t}^{\leftarrow} := \mathbb{E}(\text{Flow}_{com,S,t}^{\leftarrow} | S_t) = W'_{com,t} S_t, \tag{8}$$

with (consistently with the assumptions made in A.2.1):

$$W_{com,t} = W_{com} \mathbf{d}(\theta_{S,t}). \tag{9}$$

where  $W_{com}$  is the commute matrix that would prevail under no containment policies.

By the same token:

$$\phi_{com,S,t}^{\rightarrow} := \mathbb{E}(\text{Flow}_{com,S,t}^{\rightarrow} | S_t) = \mathbf{d}(W_{com,t} \mathbf{1}) S_t. \tag{10}$$

All in all, if we denote by  $\text{Flow}_{com,S,t}$  the vector of time-weighted commuters net inflows, we have:

$$\mathbb{E}(\text{Flow}_{com,S,t} | S_t) = \Omega_{com,t} S_t, \tag{11}$$

with

$$\Omega_{com,t} = \tau_{com} W'_{com,t} - \tau_{com} \mathbf{d}(W_{com,t} \mathbf{1}). \tag{12}$$

**A.2.4 Transmission rate dynamics**

Each state  $j$  features an autonomous  $\beta_{j,t}^0$  process (see A.2.1). These variables, gathered in vector  $\beta_t^0$ , follow non-negative square-root processes whose dynamics is approximated by:

$$\beta_{j,t}^0 \approx \beta_{j,t-1}^0 + \kappa(\beta - \beta_{j,t-1}^0)\Delta t + \sigma\sqrt{\Delta t\beta_{j,t-1}^0}\varepsilon_t^j,$$

with  $\varepsilon_t \sim i.i.d. \mathcal{N}(0, \Sigma)$ , where the diagonal elements of  $\Sigma$  are ones and the extra-diagonal entries are set to  $\rho$ .

**A.2.5 State-space model**

The state-space model is characterized by

$$\mathbb{E}_{t-1} \begin{pmatrix} D_t \\ S_t \\ I_t \\ R_t \\ \beta_t^0 \end{pmatrix} \quad \text{and} \quad \text{Var}_{t-1} \begin{pmatrix} D_t \\ S_t \\ I_t \\ R_t \\ \beta_t^0 \end{pmatrix}.$$

We have:

$$\mathbb{E}_{t-1} \begin{pmatrix} D_t \\ S_t \\ I_t \\ R_t \\ \beta_t^0 \end{pmatrix} = \begin{bmatrix} 0 \\ 0 \\ 0 \\ 0 \\ \kappa\beta\mathbf{1} \end{bmatrix} + \begin{bmatrix} \mathbf{Id} & 0 & \delta\mathbf{Id} & 0 & 0 \\ 0 & \mathbf{Id} & 0 & 0 & 0 \\ 0 & 0 & (1 - \delta - \gamma)\mathbf{Id} & 0 & 0 \\ 0 & 0 & \gamma\mathbf{Id} & \mathbf{Id} & 0 \\ 0 & 0 & 0 & 0 & (1 - \kappa)\mathbf{Id} \end{bmatrix} \begin{bmatrix} D_{t-1} \\ S_{t-1} \\ I_{t-1} \\ R_{t-1} \\ \beta_{t-1}^0 \end{bmatrix} + \begin{bmatrix} 0 \\ -\mathbf{Id} \\ +\mathbf{Id} \\ 0 \\ 0 \end{bmatrix} \left( \theta_{S,t-1} \odot \theta_{M,t-1} \odot \beta_{t-1}^0 \odot \frac{1}{\mathbf{p}} \odot ([\mathbf{Id} + \Omega_{t-1}]I_{t-1}) \odot ([\mathbf{Id} + \Omega_{t-1}]S_{t-1}) \right), \quad (13)$$

where  $\Omega_{t-1} = \Omega_{com,t-1} + \Omega_{trav,t-1}$ , where the latter two matrices are respectively defined in equations (6) and (12). Notice that the state-space ends up being of size  $5 \times N$ , where  $N$  is the

$\gamma$	0.07 [0.05, 0.1]	$\delta$	0.0004 [0.0003, 0.0007]	$\kappa$	0.001
$\beta$	0.16	$\sigma$	0.05	$\rho$	0.49
$\theta_S^{low}$	0.64 [0.32, 0.82]	$\theta_T^{low}$	0.10 [0.05, 0.55]	$\theta_M^{low}$	0.58 [0.29, 0.79]
$\tau_{com}$	0.36			$\tau_{trav}$	4.00

Table 2: Parameter values. The values in bracket give alternative parametrizations used for a sensitivity analysis of our results in Appendix E.

number of states, so 255 in our application.

Appendix G details the computation of the conditional variance of  $[D_t, S_t, I_t, R_t, \beta_t^0]$  (see equation 28 in G.4).

The previous equations constitute the set of transition equations of the state-space. We complete the formulation with the measurement equations being only the (seasonally adjusted) time series of fatalities per day, for each state, which we denote by  $D_t^{obs}$ . We assume that the number of deaths per day is measured nearly perfectly, such that:

$$D_t^{obs} = D_t + \eta_t, \quad \text{where } \eta_t \sim \mathcal{N}(0, 0.001^2 \mathbf{Id}). \tag{14}$$

Since the state-space is non-linear, we resort to the extended Kalman filter for estimation. This requires the computation of the Jacobian matrix of  $\mathbb{E}_{t-1}[D_t, S_t, I_t, R_t, \beta_t^0]$  with respect to  $[D_{t-1}, S_{t-1}, I_{t-1}, R_{t-1}, \beta_{t-1}^0]$ , which is closed-form and detailed in Appendix H. We then apply a fixed-interval Rauch-Tung-Striebel smoother (backward filter) with the estimated trajectories produced by the filter.

## B Data & estimates

Our model features several parameters that we need to fix: The death rate  $\delta$ , the recovery rate  $\gamma$ , the parameters  $\beta$ ,  $\kappa$ ,  $\sigma$ , and  $\rho$  governing the dynamics of transmission rates in the states, the effects  $\theta_M^{low}$ ,  $\theta_S^{low}$ , and  $\theta_T^{low}$  of the different containment policies, and the average traveling and commuting flows across states. We proceed as follows to select parameter values. We summarize our parameter estimates in Table 2.

We follow Fernández-Villaverde and Jones (2020), Perez-Saez et al. (2020), and Stringhini et al. (2020) and assume that it takes on average 14 days for an infection to resolve. We assume that after this period, an infected person either recovers and becomes immune, or dies with a

probability of 0.6%. These assumptions imply that  $\gamma = \frac{1}{14}$  and  $\delta = \frac{0.06\%}{14} = 0.0004$ .

We estimate average interstate travel flows from travel and mobility data in the United States. We collect data on interstate travels from the Traveler Analysis Framework published by the Federal Highway Administration (<https://www.fhwa.dot.gov/policyinformation/analysisframework/01.cfm>). We also collect data on state-level mobility and staying-at-home from the Trips by Distance database of the Bureau of Transportation Statistics (<https://www.bts.gov/distribution-trips-distance-national-state-and-county-level>). We combine these two databases to compute the percentage of a state's population that stays home before and during the pandemic, as well as the percentage of a state's population that traveled across state boundaries before and during the pandemic. We use these data to determine the travel matrix  $W_{trav}$  of Appendix A.2.2. We illustrate the estimated interstate travel network in Figure 4(a). The size of a node is proportional to the percentage of a state's population that travels outwards and the width of a link is proportional to the percentage of a state's population that travel to the linked state. We assume that an average traveler spends 4 days on vacation. This implies that  $\tau_{trav} = 4$ .

We measure commuting flows from the 2011-2015 5-Year ACS Commuting Flows table of the U.S. Census (<https://www.census.gov/data/tables/2015/demo/metro-micro/commuting-flows-2015.html>). We use these data to estimate the commuter matrix  $W_{com}$  of Appendix A.2.3. Figure 4(b) shows the implied commuting travel network. In this figure, however, the size of a node is proportional to the logarithm of the percentage of a state's population that commutes outwards. We assume that out-of-state commuters spend 8 hours each business day and no time during a weekend in the visited state. We also assume that commuters sleep 8 hours a day and during that time infections are not possible. As a result, we set  $\tau_{trav} = 0.36 \approx \frac{8 \times 5}{16 \times 7}$ .

We calibrate the parameters  $\theta_M^{low}$ ,  $\theta_S^{low}$ , and  $\theta_T^{low}$  to match mobility and mask usage data from the United States. We collect data on when the different policies were active in the different states from the National Academy for State Health Policy (<https://www.nashp.org/governors-prioritize-health-for-all/>) and the Steptoe COVID-19 State Regulatory Tracker (<https://www.steptoe.com/en/news-publications/covid-19-state-regulatory-tracker.html>). Figure 6 showcases the time periods in which policies were active in the different states. We also collect data on average mask adoption across U.S. states from the Institute of Health Metrics and Evaluation (<https://covid19.healthdata.org/united-states-of-america>). We assume that a stay-at-home policy is in place for the time period that covers





any order for staying at home, sheltering at home, or being safer at home issued by a state governor. We neglect any stay-at-home advisories that are not strictly enforced by law officials. We estimate  $\theta_S^{low} = 0.64$  as the reduction factor in the number of short trips taken during the pandemic versus before the pandemic.<sup>18</sup> We consider a travel ban to be active when a state requires inbound travelers to self-quarantine for an extended period of time. Travel bans are active in our model only if they apply for all states. That is, we neglect any travel ban that only applies for travelers from selected states. We estimate  $\theta_T^{low} = 0.10$  as the reduction factor in the number of long trips taken during the pandemic versus before the pandemic.<sup>19</sup> Finally, we assume that a mask mandate is active if a state requires the use of masks indoors in public places. We do not consider mask mandates to be active if mask wearing is only recommended or only required outdoors. We estimate  $\theta_M^{low} = 0.58$  by assuming that only half of the population adopts mask usage (as suggested by the Institute of Health Metrics and Evaluation) and that an average mask used in the U.S. reduces COVID-19 transmission by 85% (as suggested by Fischer et al. (2020)).

We develop a quasi maximum likelihood methodology to estimate the parameters governing the dynamics of the transmission rates  $\beta_{j,t}$  from daily data on state-level deaths in the United States for the time period between February 12 through September 30, 2020. We remove weekly seasonality patterns observed in COVID-19 fatality records using an STL approach. Our methodology assumes that daily death counts at the state-level are measures with small measurement errors. We take into account all state-level containment policies that were observed over the sample period. We write a non-linear state-space representation of the model, gathering  $S_t^j$ ,  $I_t^j$ ,  $R_t^j$ ,  $D_t^j$ , and  $\beta_{j,t}$  for all states simultaneously (255 variables). Filtering is easily performed through the first order extended Kalman filter algorithm. While we could estimate the speed of reversion  $\kappa$  with our methodology, we find that the data prefers to set  $\kappa$  arbitrarily close to zero, implying an extremely high persistence for the  $\beta_{j,t}$ . This results in numerical instabilities. To avoid these issues, we fix  $\kappa = 0.001$  so that the first-order autocorrelation of the  $\beta_{j,t}$  is 0.999. We then estimate the remaining parameters  $\beta$ ,  $\sigma$ , and  $\rho$  using our quasi maximum likelihood methodology. The estimates are provided in Table 2. We find that our parameter estimates are

<sup>18</sup>More precisely, for each state we evaluate the average number of daily trips of less than 10 miles taken in 2019 and compare that number to the average number of daily trips of less than 10 miles taken during the time frame March 15 through April 30, 2020. We compute  $\theta_S^{low}$  as the average reduction factor across states.

<sup>19</sup>We evaluate the average number of daily trips of more than 100 miles taken in 2019 and compare that number to the average number of daily trips of more than 100 miles taken during the time frame March 15 through April 30, 2020. We compute  $\theta_T^{low}$  as the average reduction factor across states.

not very sensitive to alternative choices for the value of  $\kappa$ .

Figure 5 shows the data-implied death counts in each state as well as the smoothed model-implied death counts. We see that our model performs well at fitting the state-level data. The estimated measurement errors are fairly small. Figures 6 and 7 show the smoothed model-implied effective  $\mathcal{R}_0$  and cumulated infections for each state. The data pushes our model to showcase high  $\mathcal{R}_0$  in the different states.<sup>20</sup> The highest  $\mathcal{R}_0$  were observed in New Jersey, New York, and Washington in February and March, reaching levels of more than 8.<sup>21</sup> Indeed, we find that the state-level  $\mathcal{R}_0$  must have been substantially higher than 1 for most states through April 2020. Several states, like Delaware, Hawaii, Idaho, Montana, Oklahoma, South Carolina, Texas, and West Virginia, experienced significant upticks in their Coronavirus  $\mathcal{R}_0$  in the summer. There have also been upticks in the  $\mathcal{R}_0$  in September in states like Arkansas, Florida, Kansas, Michigan, Missouri, North Dakota, Rhode Island, South Dakota, and Virginia. Some states have been successful at maintaining their  $\mathcal{R}_0$  values consistently at or below 1. The list of states that have accomplished this task include California, D. C., Illinois, Indiana, Maine, Maryland, Massachusetts, Minnesota, New Hampshire, New Mexico, New York, Oregon, and Vermont. Overall, our findings suggest that the virus spread drastically in the U.S. through the Fall of 2020. In fitting the data, our model estimates that the number of infections in the different states must have been significantly higher than recorded in the data. These observations suggest that there must have been many undiagnosed infections that facilitated the spread of the disease throughout our sample period. Note that we never use infections data for the estimation or calibration of our model parameters.

## C Counterfactual experiments

This section details how our counterfactual experiments are conducted.

<sup>20</sup>The  $\mathcal{R}_0$  of State  $j$  in our model is given by  $\theta_{i,M}^j \theta_{i,S}^j \beta_{j,t}^0 / (\delta + \gamma)$ .

<sup>21</sup>Our estimates of the effective reproduction numbers are one-and-a-half to two-times larger than prevailing estimates in Fernández-Villaverde and Jones (2020). We find that this is driven by a key difference in our models. Fernández-Villaverde and Jones (2020) assume that, while it take two weeks for an infection to resolve, an infected individual is only contagious for the first 5 days of an infection. We, instead, assume that an infected individual is contagious during the whole infection period. We run several experiments in Appendix E in which we study whether are results are sensitive to this assumption, and we find that this is not the case.

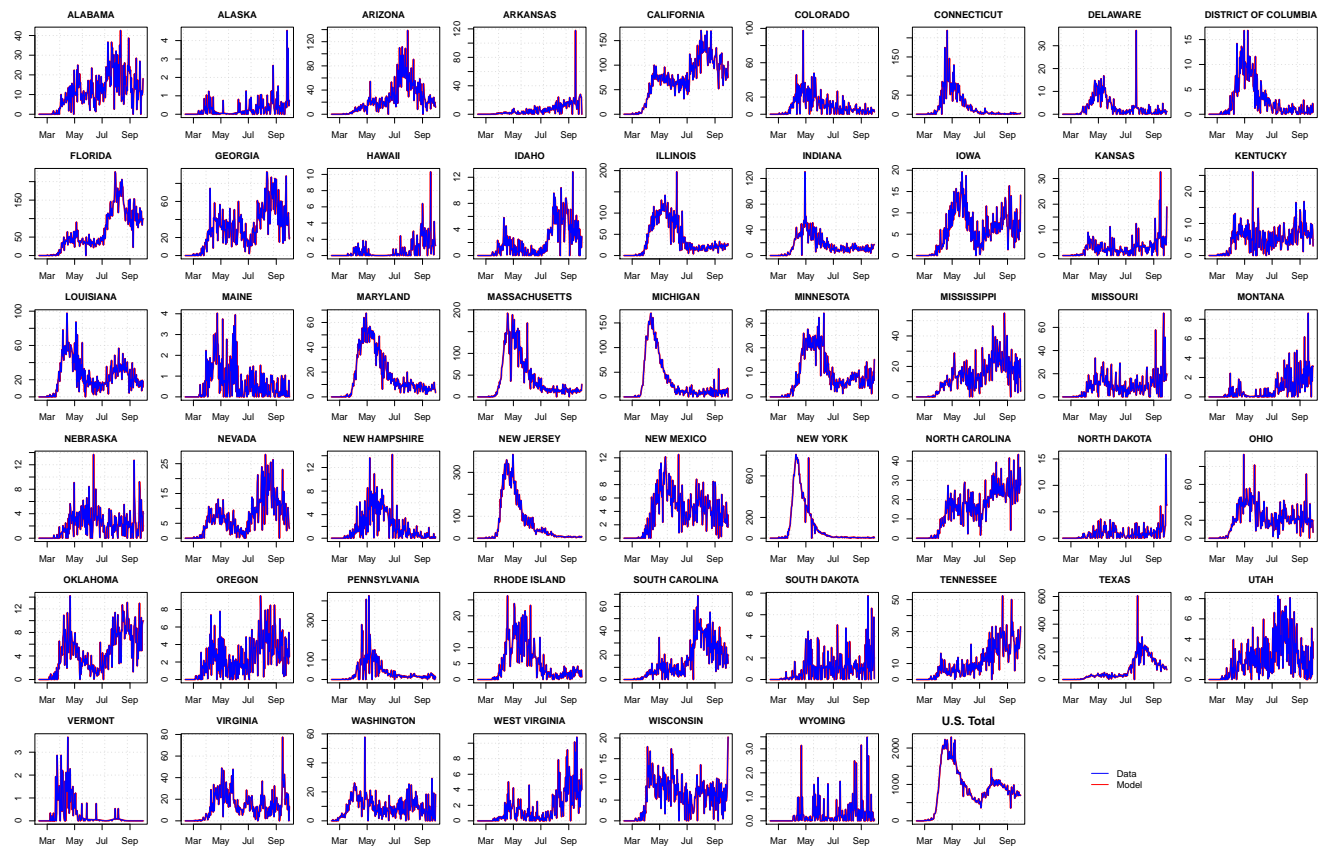


Figure 5: Data and model-implied death counts across states. The model-implied death counts correspond to the number of fatalities that needed to have been recorded in our model to match the total number of deaths in a state at the end of the sample period (i.e., the smoother). Estimation is performed through forward/backward extended Kalman filtering, using the time series of death counts per state from February 12 to September 30, 2020. Our estimation methodology is detailed in Appendix B.

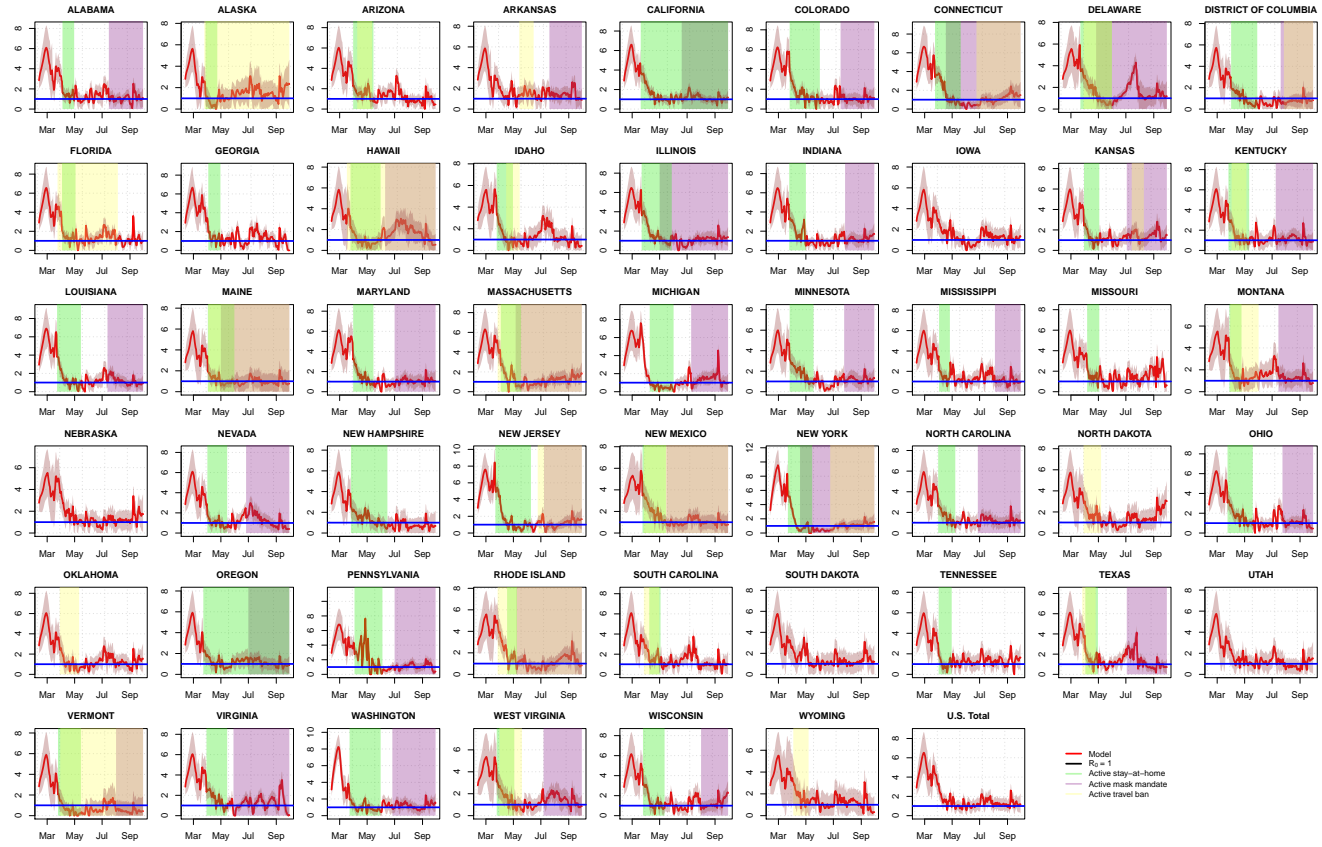


Figure 6: Smoothed means of the model-implied effective  $\mathcal{R}_0$  of COVID-19 in U.S. states. The shaded red areas denote 2-standard-deviation confidence bands. Estimation is performed through forward/backward extended Kalman filtering, using the time series of death counts per state from February 12 to September 30, 2020. Our estimation methodology is detailed in Appendix B. The  $\mathcal{R}_0$  estimates correspond to the ratios of estimated  $\beta_0^d$  multiplied by the policy dummies and divided by the sum of the daily fatality and recovery rates ( $\gamma + \delta$ ). The figure also shows the periods of time in which the different containment policies were active. Green shaded areas correspond to active stay-at-home policies, purple areas to active mask mandates, and yellow areas to active travel bans. Horizontal blue lines correspond the standard value of  $\mathcal{R}_0 = 1$ , below which the virus does not reproduce itself indefinitely.

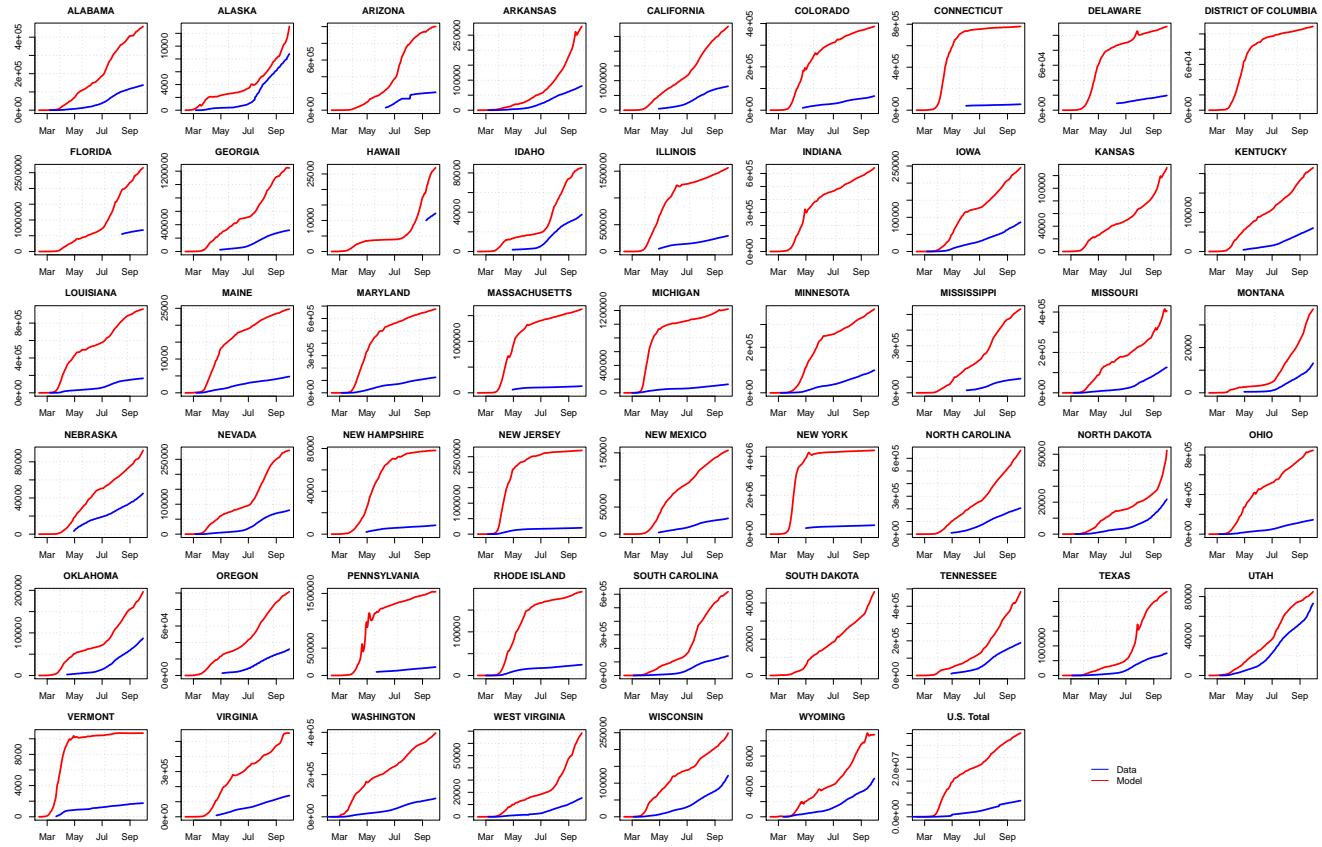


Figure 7: Smoothed means of the model-implied cumulative number of COVID-19 infections in U.S. states. The figures also shows the number of infections that are recorded in state-level data from JHU. We obtain the cumulative number of infections by summing all populations per states except the susceptible. Estimation is performed through forward/backward extended Kalman filtering, using the time series of death counts per state from February 12 to September 30, 2020. Our estimation methodology is detailed in Appendix B.

### C.1 Baseline scenario

The estimated dynamics constitutes our baseline scenario. All of our results are presented as a difference with respect to this baseline scenario. We compare the outcomes in terms of fatalities.

### C.2 “Strict” and “loose” counterfactuals

We consider two types of experiments, which we call strict and loose, respectively:

- In the strict scenario, we assume that the states start adopting the same policy as that implemented by the earliest state during the sample period and relax it when the latest state does so. The scenarios are as follows:
  - **Stay-at-Home:** Start on March 20, 2020 (the day when California activated its stay-at-home mandate) and keep it active through September 30, 2020 (the last day in our sample in which the stay-at-home order was still active in California).
  - **Travel ban:** Start on March 17, 2020 (the day the first interstate travel ban in the U.S. went into effect in Hawaii) and keep it active through September 30, 2020 (the last day in our sample in which an interstate travel ban was still active in Alaska).
  - **Mask mandate:** Start on April 17, 2020 (the day the first mask mandate in the U.S. went into effect in Connecticut) and keep it active through September 30, 2020 (the last day in our sample in which several states had mask mandates in place).
- For the loose scenario, we assume that states do not implement a specific policy at all. We then re-propagate the model with these counterfactual policies according to the methodology described below.

We conduct these two types of experiments one policy at a time, and one last time all together.

### C.3 Joint and state-by-state counterfactuals

Our analysis is split into joint and state-by-state experiments. For the former, we assume that the federal government imposes on all states the counterfactual policy (strict federal mandate), i.e. to be as strict as the strictest or to do nothing (loose federal mandate). For the latter, we take each state one at a time and assume that only this state follows the strict or loose scenario and compute the counterfactual outcomes one state at a time.

C.4 Computation of counterfactual scenarios

Recall that the model parameters and the latent variables ( $S_t, I_t, R_t$  and  $\beta_t^0$ ) are estimated by employing the extended Kalman filter. The observed variables are the numbers of deaths  $D_t^{obs.}$ , as well as the observed implemented policies  $\theta_{obs.}$ .

In order to derive our counterfactual outcomes, we also extend our filtering approach. The broad idea is the following: We augment the state vector used at the estimation step – i.e.  $X_t = [D_t, S_t, I_t, R_t, \beta_t^0]$  – with a similar state vector for a fictitious country (*fict.*), with the same number of states, where the counterfactual policies would be implemented. Critically, we assume that the basic, standardized, shocks affecting the two countries are almost perfectly correlated, implying in particular that the  $\beta_t^0$ 's are the same for the baseline and fictitious countries.

Specifically, let us denote by  $X_t^*$  the state vector corresponding to the fictitious country. The transition equation of the augmented state-space model are:

$$\begin{bmatrix} X_t \\ X_t^* \end{bmatrix} = \begin{bmatrix} \mathcal{E}(X_{t-1}, \theta_{obs.}) \\ \mathcal{E}(X_{t-1}^*, \theta_{fict.}) \end{bmatrix} + \begin{bmatrix} \mathcal{V}^{1/2}(S_{t-1}, I_{t-1}, \theta_{obs.})\varepsilon_{True,t} \\ \mathcal{V}^{1/2}(S_{t-1}^*, I_{t-1}^*, \theta_{fict.})\varepsilon_{fict.,t} \end{bmatrix}, \tag{15}$$

where  $\theta_{obs.}$  and  $\theta_{fict.}$  contain the full trajectories of observed and fictitious policies, respectively; where  $\varepsilon_{True,t}$  and  $\varepsilon_{fict.,t}$  denote differences of martingale sequence; and where  $\mathcal{V}^{1/2}(S, I, \theta)$  is such that  $(\mathcal{V}^{1/2}(S, I, \theta))(\mathcal{V}^{1/2}(S, I, \theta))' = \mathcal{V}(S, I, \theta)$ , with the function  $\mathcal{V}$  defined in (28). To capture the idea that the two countries are affected by very similar standardized shocks, which are the  $\varepsilon_{True,t}$ 's and the  $\varepsilon_{fict.,t}$ 's, we further assume that:

$$\text{Var}_t \left( \begin{bmatrix} \varepsilon_{True,t} \\ \varepsilon_{fict.,t} \end{bmatrix} \right) \approx \begin{bmatrix} \mathbf{Id} & \mathbf{Id} \\ \mathbf{Id} & \mathbf{Id} \end{bmatrix}.$$

On top of the transition equation (15), the state-space model comprehends the following measurement equation:

$$D_t^{obs.} = D_t, \tag{16}$$

where  $D_t^{obs.}$  is the observed vector of numbers of deaths (in the “observed” country). By construction, the filtered variables  $X_t$  resulting from this augmented state-space framework are exactly equal the the ones of the regular state-space. Indeed, it produces the moment  $\mathbb{E}(X_t | D_t^{obs.}, D_{t-1}^{obs.}, \dots)$ , which is the same in both state-space models. However,  $X_t^*$  will be differ-



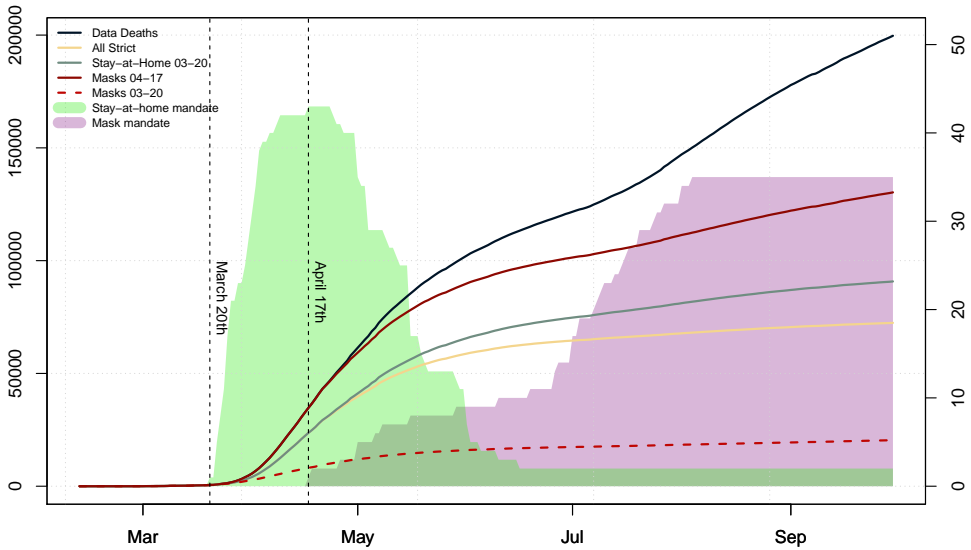


Figure 8: Time series of counterfactual death counts in which the federal government imposes strict joint mandates (left axis), along with the number of states that adopted stay-at-home or mask mandates in the data (right axis). The black solid line provides the death count obtained from the original data. The grey, red, and beige solid lines provide the time series of deaths that would have been observed if the federal government had imposed strict stay-at-home, masks, and all policies together on all states, respectively. The *strict* mandates start as early as the earliest state in the sample, that is March 20, 2020 for stay-at-home, and April 17, 2020 for mask mandates. The red dashed line presents a counterfactual scenario where masks are imposed as early as March 17, 2020. Green and purple-shaded areas provide the number of states that implemented stay-at-home policies and mask mandates in the data, with respect to time. Their units are presented on the right axis.

ent from  $X_t$  since the implemented policies are different, and their impacts are non-trivial since they are non-linearly propagated in the state-space.

As a last step, we provide backward path estimates using the Bryson-Frazier smoother and compare the paths of  $D_t$  and  $D_t^*$  produced by the smoother. We used Bryson-Frazier rather than Rauch-Tung-Striebel because the latter requires to invert the conditional variance-covariance matrices of the transition equations, which are of size  $(9N \times 9N)$ . In our empirical application (51 states), this results in matrices of size  $(459 \times 459)$  that have to be inverted for each day of data. This results in a large numerical instability. Instead, the Bryson-Frazier smoother only requires the inversion of the variance-covariance matrix of the observables, that is of matrices of size  $(N \times N)$ . The time series dynamics of the federal counterfactuals are presented on Figure 8.

## D Infected populations in travel ban counterfactual

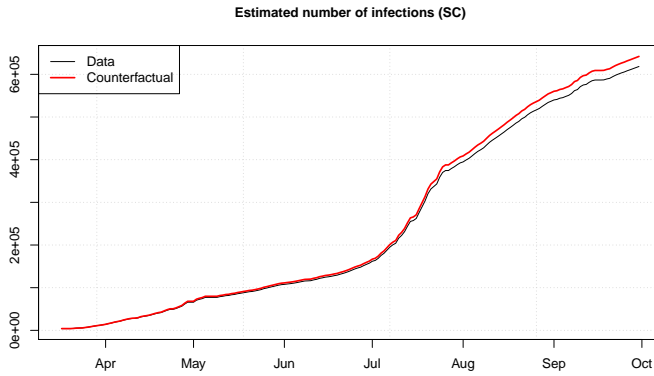
Figure 9 showcases the posterior (smoothed) mean of the cumulative number of infected individuals in the baseline scenario for some select states. The figure also shows the smoothed mean of the cumulative number of infected individuals in the counterfactual in which a federal interstate travel ban goes into effect on March 17, 2020.

## E Sensitivity analysis

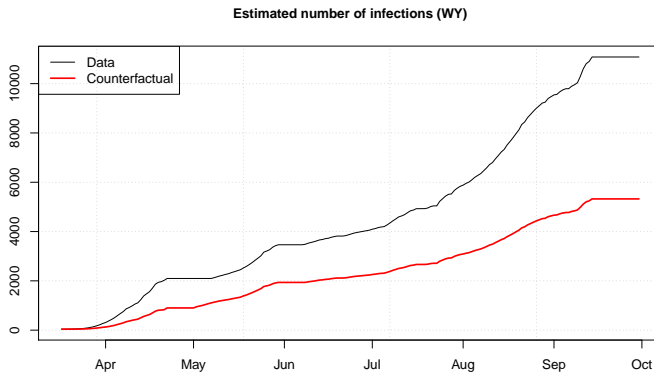
We run several analyses to understand how sensitive our results are with respect to changes in our parameter values. Table 1 shows confidence bands that are derived from re-estimating the number of preventable deaths if the policy that deviated from the data was either twice or half as impactful. What we mean in precise terms by this is that if, for example, we assume that a counterfactual is carried out with respect to changes in a mask mandate, we would evaluate the number of preventable deaths by assuming that  $\theta_M^{low}$  is either half or twice as large as indicated in Table 2. This sensitivity analysis provides confidence bands for our estimates of the number of deaths that could have been prevented by adopting policies different than the ones that were adopted in reality by considering that the policies may have a different impact on reducing transmission rates and traveler and commuter inflows than what we assume in our study.

We also carry out additional sensitivity analyses with respect to two key parameters in our model: the number of days that it takes for an infection to resolve, and the fatality rate of the disease. Tables 3 through 6 repeat the experiments of Table 1 by assuming that it either takes 10 or 20 days for an infection to resolve, or that the fatality rate of the disease is 0.4% or 1%. To obtain the results, we re-estimate the parameters  $\beta$ ,  $\sigma$ , and  $\rho$  that would be necessary under the new assumptions for the fatality rate or the number of days for infection resolution. The sensitivity analyses are carried out one-by-one.

We find that adopting early federal containment policies would have been less impactful and prevented less deaths if an infection took longer time to resolve. Vice versa, we find that early federal action would have been more impactful if an infection took less time to resolve. This is primarily because, if the disease were less severe than we assumed and it took less time to resolve an infection, then the methodology estimates that there must have been many more infections early on in the sample to match the number of deaths observed throughout the sample. That means that early action would have been more impactful if the disease is less severe than we



(a) South Carolina.



(b) Wyoming.

Figure 9: Time series of estimated number of infected individuals in select states. The grey line marks the posterior (smoothed) mean of the cumulative number of infections in the baseline. The red line denotes the posterior (smoothed) mean of the cumulative number of infections in the counterfactual in which a federal interstate travel ban goes into effect on March 17, 2020. Estimation is performed through forward/backward extended Kalman filtering, using the time series of death counts per state from February 12 to September 30, 2020. Our estimation methodology is detailed in Appendix B.

Counterfactual assumption ( $\gamma = 0.1$ )	Federal mandate active on:			Deaths in excess of baseline
	Stay-at-home	Mask	Travel ban	
Strict stay-at-home orders, mask mandates, and travel bans for all states.	3/20	4/17	3/17	-145,158
Strict stay-at-home orders in all states, and all other state-level policies remain as in the data.	3/20			-115,868
Strict mask mandates in all states, and all other state-level policies remain as in the data.		4/17		-109,675
Strict travel bans in all states, and all other state-level policies remain as in the data.			3/17	-5,447
No stay-at-home order, mask mandate, or travel ban in any state.				+1,055,371
No stay-at-home order in any state, but all other policies remain as in the data.				+711,567
No mask mandate in any states, but all other policies remain as in the data.				+687,774
No travel ban in any states, but all other policies remain as in the data.				+2,501
Mask mandate in all states on March 20, 2020, and all other state-level policies remain as in the data.		3/20		-185,023
Mask mandate in all states on March 20, 2020, while no state adopts any state-level policies.		3/20		-39,228
Strict travel bans in all states by February 12, 2020, while all other state-level policies remain as in the data.			2/12	-6,063

Table 3: Results of the counterfactual experiments in which we assume that all states jointly deviate from their enacted policies and adopt either strict or loose versions of the policies instead. Here, we assume that it takes on average 10 days for an infection to resolve, while keeping the fatality rate of the disease fixed at 0.6%. The reported values are excess deaths relative to the number of U.S. deaths recorded in our data on September 30, 2020. In the counterfactuals, we compute the trajectories of death counts per state under the alternative policy scenarios that are consistent with the susceptible, infected, recovered, and dead populations as well as the transmission rates filtered from the observed data. The values in brackets give confidence bounds based on a sensitivity analysis of the estimates of the impact of the different policies on transmission rates and traveler and commuter inflow. The lower bounds assume that any policy that deviates from what it was in the data is half as impactful, while the upper bound assumes that any policy that deviates is twice as impactful. Table 2 in Appendix E provides the parameter values used for the sensitivity analyses. In the sensitivity analysis, we proceed in a similar way as for the counterfactuals and first compute posterior means of the state-level transmission rates that would explain the observed death counts under the assumption of alternative effectiveness for the different policies. We then compute the number of death that would have been observed if the policies had changed while keeping the recomputed trajectories of the transmission rates fixed.

Counterfactual assumption ( $\gamma = 0.05$ )	Federal mandate active on:			Deaths in excess of baseline
	Stay-at-home	Mask	Travel ban	
Strict stay-at-home orders, mask mandates, and travel bans for all states.	3/20	4/17	3/17	-126,471
Strict stay-at-home orders in all states, and all other state-level policies remain as in the data.	3/20			-103,321
Strict mask mandates in all states, and all other state-level policies remain as in the data.		4/17		-81,338
Strict travel bans in all states, and all other state-level policies remain as in the data.			3/17	-4,785
No stay-at-home order, mask mandate, or travel ban in any state.				+910,918
No stay-at-home order in any state, but all other policies remain as in the data.				+592,475
No mask mandate in any states, but all other policies remain as in the data.				+249,573
No travel ban in any states, but all other policies remain as in the data.				+2,052
Mask mandate in all states on March 20, 2020, and all other state-level policies remain as in the data.		3/20		-173,620
Mask mandate in all states on March 20, 2020, while no state adopts any state-level policies.		3/20		-97,146
Strict travel bans in all states by February 12, 2020, while all other state-level policies remain as in the data.			2/12	-5,385

Table 4: Results of the counterfactual experiments in which we assume that all states jointly deviate from their enacted policies and adopt either strict or loose versions of the policies instead. Here, we assume that it takes on average 20 days for an infection to resolve, while keeping the fatality rate of the disease fixed at 0.6%. The reported values are excess deaths relative to the number of U.S. deaths recorded in our data on September 30, 2020. In the counterfactuals, we compute the trajectories of death counts per state under the alternative policy scenarios that are consistent with the susceptible, infected, recovered, and dead populations as well as the transmission rates filtered from the observed data. The values in brackets give confidence bounds based on a sensitivity analysis of the estimates of the impact of the different policies on transmission rates and traveler and commuter inflow. The lower bounds assume that any policy that deviates from what it was in the data is half as impactful, while the upper bound assumes that any policy that deviates is twice as impactful. Table 2 in Appendix E provides the parameter values used for the sensitivity analyses. In the sensitivity analysis, we proceed in a similar way as for the counterfactuals and first compute posterior means of the state-level transmission rates that would explain the observed death counts under the assumption of alternative effectiveness for the different policies. We then compute the number of death that would have been observed if the policies had changed while keeping the recomputed trajectories of the transmission rates fixed.

Counterfactual assumption ( $\delta = 0.0003$ )	Federal mandate active on:			Deaths in excess of baseline
	Stay-at-home	Mask	Travel ban	
Strict stay-at-home orders, mask mandates, and travel bans for all states.	3/20	4/17	3/17	-135,805
Strict stay-at-home orders in all states, and all other state-level policies remain as in the data.	3/20			-109,118
Strict mask mandates in all states, and all other state-level policies remain as in the data.		4/17		-95,703
Strict travel bans in all states, and all other state-level policies remain as in the data.			3/17	-5,965
No stay-at-home order, mask mandate, or travel ban in any state.				+673,173
No stay-at-home order in any state, but all other policies remain as in the data.				+463,490
No mask mandate in any states, but all other policies remain as in the data.				+338,903
No travel ban in any states, but all other policies remain as in the data.				+2,002
Mask mandate in all states on March 20, 2020, and all other state-level policies remain as in the data.		3/20		-178,419
Mask mandate in all states on March 20, 2020, while no state adopts any state-level policies.		3/20		-78,541
Strict travel bans in all states by February 12, 2020, while all other state-level policies remain as in the data.			2/12	-3,719

Table 5: Results of the counterfactual experiments in which we assume that all states jointly deviate from their enacted policies and adopt either strict or loose versions of the policies instead. Here, we assume that the fatality rate of the disease is 0.4% instead of 0.6%, and keep the number of days that it take for an infection to resolve at 14 days. The reported values are excess deaths relative to the number of U.S. deaths recorded in our data on September 30, 2020. In the counterfactuals, we compute the trajectories of death counts per state under the alternative policy scenarios that are consistent with the susceptible, infected, recovered, and dead populations as well as the transmission rates filtered from the observed data. The values in brackets give confidence bounds based on a sensitivity analysis of the estimates of the impact of the different policies on transmission rates and traveler and commuter inflow. The lower bounds assume that any policy that deviates from what it was in the data is half as impactful, while the upper bound assumes that any policy that deviates is twice as impactful. Table 2 in Appendix E provides the parameter values used for the sensitivity analyses. In the sensitivity analysis, we proceed in a similar way as for the counterfactuals and first compute posterior means of the state-level transmission rates that would explain the observed death counts under the assumption of alternative effectiveness for the different policies. We then compute the number of death that would have been observed if the policies had changed while keeping the recomputed trajectories of the transmission rates fixed.

Counterfactual assumption ( $\delta = 0.0007$ )	Federal mandate active on:			Deaths in excess of baseline
	Stay-at-home	Mask	Travel ban	
Strict stay-at-home orders, mask mandates, and travel bans for all states.	3/20	4/17	3/17	-137,349
Strict stay-at-home orders in all states, and all other state-level policies remain as in the data.	3/20			-111,536
Strict mask mandates in all states, and all other state-level policies remain as in the data.		4/17		-95,924
Strict travel bans in all states, and all other state-level policies remain as in the data.			3/17	-5,152
No stay-at-home order, mask mandate, or travel ban in any state.				+1,660,900
No stay-at-home order in any state, but all other policies remain as in the data.				+1,009,853
No mask mandate in any states, but all other policies remain as in the data.				+572,851
No travel ban in any states, but all other policies remain as in the data.				+2,524
Mask mandate in all states on March 20, 2020, and all other state-level policies remain as in the data.		3/20		-180,651
Mask mandate in all states on March 20, 2020, while no state adopts any state-level policies.		3/20		-77,375
Strict travel bans in all states by February 12, 2020, while all other state-level policies remain as in the data.			2/12	-6,017

Table 6: Results of the counterfactual experiments in which we assume that all states jointly deviate from their enacted policies and adopt either strict or loose versions of the policies instead. Here, we assume that the fatality rate of the disease is 1% instead of 0.6%, and keep the number of days that it take for an infection to resolve at 14 days. The reported values are excess deaths relative to the number of U.S. deaths recorded in our data on September 30, 2020. In the counterfactuals, we compute the trajectories of death counts per state under the alternative policy scenarios that are consistent with the susceptible, infected, recovered, and dead populations as well as the transmission rates filtered from the observed data. The values in brackets give confidence bounds based on a sensitivity analysis of the estimates of the impact of the different policies on transmission rates and traveler and commuter inflow. The lower bounds assume that any policy that deviates from what it was in the data is half as impactful, while the upper bound assumes that any policy that deviates is twice as impactful. Table 2 in Appendix E provides the parameter values used for the sensitivity analyses. In the sensitivity analysis, we proceed in a similar way as for the counterfactuals and first compute posterior means of the state-level transmission rates that would explain the observed death counts under the assumption of alternative effectiveness for the different policies. We then compute the number of death that would have been observed if the policies had changed while keeping the recomputed trajectories of the transmission rates fixed.

assumed. Note that this is always a conclusion based on matching the amount of death cases that we observe in the data. If the disease were less severe and we still observed as many deaths as in the data, then the only possible explanation is that there must have been more infections early on in the sample. As a result, early action would have been the more impactful.

We find that the number of preventable deaths would not be much different if the virus were less lethal. However, we find that the costs of inaction at the state level would be much higher if the virus were more lethal. We find that close to 2,000,000 additional deaths would have been observed if no state enacted any policy and if the lethality rate of the virus were 1%. These observations further corroborate our findings of the success of the policies enacted by the individual states to prevent COVID-19 deaths both at the state and federal levels.

## F Conditional covariances for the single-state model

We have:

$$\begin{aligned} \mathbb{E}_{t-1}(r_t + d_t) &= \mathbb{E}_{t-1}(d_t + \mathbb{E}_{t-1}(r_t|d_t)) - (\gamma + \delta)I_{t-1} & (17) \\ \text{Var}_{t-1}(r_t + d_t) &= \text{Var}_{t-1}(d_t + \mathbb{E}_{t-1}(r_t|d_t)) + \mathbb{E}_{t-1}(\text{Var}_{t-1}(d_t + r_t|d_t)) \\ &= \text{Var}_{t-1}\left(\frac{1 - \delta - \gamma}{1 - \delta}d_t\right) + \mathbb{E}_{t-1}\left((I_{t-1} - d_t)\frac{\gamma(1 - \delta - \gamma)}{(1 - \delta)^2}\right) \\ &= \left(\frac{1 - \delta - \gamma}{1 - \delta}\right)^2 I_{t-1}\delta(1 - \delta) + \mathbb{E}_{t-1}\left((I_{t-1} - d_t)\frac{\gamma(1 - \delta - \gamma)}{(1 - \delta)^2}\right) \\ &= \underbrace{\frac{(1 - \delta - \gamma)^2\delta + \gamma(1 - \delta - \gamma)}{1 - \delta}}_{=: \nu} I_{t-1}. & (18) \end{aligned}$$

Because  $d_t + r_t$ , on the one hand, and  $i_t$ , on the other hand, are independent conditional on the information available on date  $t - 1$ , it follows that:

$$\mathbb{E}_{t-1}(\Delta I_t) = \frac{S_{t-1}}{N}I_{t-1}\beta_{t-1} - (\gamma + \delta)I_{t-1} \tag{19}$$

$$\text{Var}_{t-1}(\Delta I_t) = \frac{S_{t-1}}{N}I_{t-1}\beta_{t-1} + \nu I_{t-1}. \tag{20}$$

**Remark:** Let us introduce  $Z_t \equiv \Delta I_t - \mathbb{E}_{t-1}(\Delta I_t)$ . By construction,  $\mathbb{E}_{t-1}(Z_t) = 0$ . It can be seen that  $Z_t$  is the sum of  $I_{t-1}$  i.i.d. random variables. Hence, if  $I_{t-1}$  is large, we approximately



have:

$$Z_t \sim \mathcal{N}\left(0, \frac{S_{t-1}}{N} I_{t-1} \beta_{t-1} + \nu I_{t-1}\right),$$

conditional on the information available on  $t - 1$ . This is also true for  $i_t$ ,  $r_t$  and  $d_t + r_t$ . Because the conditional variances of these variables are in  $I_{t-1}$  (and not in  $I_{t-1}^2$ ), it follows that, when  $I_{t-1}$  is large, the deterministic version of the SIR model provides a good approximation of the dynamics of  $(S, I, R, D)$  – at least up to potential stochastic variation of  $\beta_t$ .

In the remaining of this appendix, we detail the computation of some of the covariances appearing in equation (3)

$$\begin{aligned} \text{Cov}_{t-1}(\varepsilon_{D,t}, \varepsilon_{R,t}) &= \text{Cov}_{t-1}(r_t, d_t) = \text{Cov}_{t-1}(\mathbb{E}_{t-1}(r_t|d_t), d_t) \\ &= \text{Cov}_{t-1}\left(\frac{(I_{t-1} - d_t)\gamma}{1 - \delta}, d_t\right) \\ &= -\frac{\gamma}{1 - \delta} \text{Var}_{t-1}(d_t) = -\gamma\delta I_{t-1}. \end{aligned}$$

$$\begin{aligned} \text{Cov}_{t-1}(\varepsilon_{D,t}, \varepsilon_{I,t}) &= -\text{Cov}_{t-1}(d_t, d_t + r_t) = -(\mathbb{E}_{t-1}(d_t(d_t + r_t)) - \mathbb{E}_{t-1}(d_t)\mathbb{E}_{t-1}(d_t + r_t)) \\ &= -\text{Var}_{t-1}(d_t) - \text{Cov}_{t-1}(r_t, d_t) \\ &= -\delta(1 - \delta)I_{t-1} + \gamma\delta I_{t-1} \\ &= -\delta(1 - \delta - \gamma)I_{t-1}. \end{aligned}$$

$$\begin{aligned} \text{Var}_{t-1}(r_t) &= \text{Var}_{t-1}(\mathbb{E}_{t-1}(r_t|d_t)) + \mathbb{E}_{t-1}(\text{Var}_{t-1}(r_t|d_t)) \\ &= \text{Var}_{t-1}\left(\frac{(I_{t-1} - d_t)\gamma}{1 - \delta}\right) + \mathbb{E}_{t-1}\left((I_{t-1} - d_t)\frac{\gamma(1 - \delta - \gamma)}{(1 - \delta)^2}\right) \\ &= \frac{\gamma^2\delta}{1 - \delta} I_{t-1} + \frac{\gamma(1 - \delta - \gamma)}{1 - \delta} I_{t-1} = (\gamma - \gamma^2)I_{t-1}. \end{aligned}$$

$$\text{Cov}_{t-1}(\varepsilon_{R,t}, \varepsilon_{I,t}) = -\text{Cov}_{t-1}(r_t, d_t + r_t) = -(\mathbb{E}_{t-1}(r_t(d_t + r_t)) - \mathbb{E}_{t-1}(r_t)\mathbb{E}_{t-1}(d_t + r_t))$$

$$\begin{aligned}
 &= -\text{Var}_{t-1}(r_t) - \text{Cov}_{t-1}(r_t, d_t) \\
 &= -(\gamma - \gamma^2)I_{t-1} + \gamma\delta I_{t-1} \\
 &= -\gamma(1 - \gamma - \delta)I_{t-1}.
 \end{aligned}$$

## G Conditional means and variances in the multi-state model

### G.1 Conditional variance of commute and travel flows

Let us denote by  $\text{Flow}_{com,I,t}$  the vector whose  $i^{th}$  component is the time-weighted net inflow of infected commuters in state  $i$ . (Remember that  $\tau$  is the fraction of time spent by commuters in the state where they work.) We have:

$$\text{Flow}_{com,I,t} = \tau \text{Flow}_{com,I,t-1}^{\leftarrow} - \tau \text{Flow}_{com,I,t-1}^{\rightarrow}.$$

Using equations (8) to (12), we have, in particular:

$$\mathbb{E}(\text{Flow}_{com,I,t}|I_t) = \tau \phi_{com,I,t}^{\leftarrow} - \tau \phi_{com,I,t}^{\rightarrow} = \Omega_{com,t} I_t.$$

We also have

$$\text{Cov}(\text{Flow}_{com,I,k,t}, \text{Flow}_{com,I,j,t}|I_t) = \begin{cases} -\tau^2 w_{com,t}^{k,j} I_t^k - \tau^2 w_{com,t}^{j,k} I_t^j & \text{if } j \neq k \\ \tau^2 \left( \sum_{k \neq j} w_{com,t}^{k,j} I_t^k \right) + \tau^2 \left( \sum_{j \neq k} w_{com,t}^{j,k} I_t^j \right) & \text{if } j = k, \end{cases}$$

that is, in vectorial form:

$$\begin{aligned}
 \text{Var}(\text{Flow}_{com,I,t}|I_t) &= \\
 &-\tau^2 W_{com,t} \odot (I_t \mathbf{1}') - \tau^2 W'_{com,t} \odot (\mathbf{1} I_t') + \mathbf{d}(\tau^2 W'_{com,t} I_t + \tau^2 (W_{com,t} \mathbf{1}) \odot I_t),
 \end{aligned}$$

which we denote by

$$\text{Var}(\text{Flow}_{com,I,t}|I_t) = \mathcal{C}(W_{com,t}, I_t, \tau), \tag{21}$$

where function  $\mathcal{C}$  is defined by

$$\mathcal{C}(W, Z, \tau) = \tau^2 \{ -W \odot (Z \mathbf{1}') - W' \odot (\mathbf{1} Z') + \mathbf{d}(W' Z + (W \mathbf{1}) \odot Z) \}. \tag{22}$$

The same type of computation leads to

$$\text{Var}(\text{Flow}_{com,S,t}|S_t) = \mathcal{C}(W_{com,t}, S_t, \tau) \tag{23}$$

$$\text{Var}(\text{Flow}_{trav,I,t}|I_t) = \mathcal{C}(W_{trav,t}, I_t, 1) \tag{24}$$

$$\text{Var}(\text{Flow}_{trav,S,t}|S_t) = \mathcal{C}(W_{trav,t}, S_t, 1). \tag{25}$$

### G.2 Conditional variance of new infections

For any pair of independent random vectors  $X$  and  $Y$ , we have

$$\begin{aligned} \text{Var}(X \odot Y) &= \mathbb{E}(XX') \odot \mathbb{E}(YY') - \mathbb{E}(X)\mathbb{E}(X)' \odot \mathbb{E}(Y)\mathbb{E}(Y)' \\ &= \text{Var}(X) \odot \text{Var}(Y) + \text{Var}(X) \odot \mathbb{E}(Y)\mathbb{E}(Y)' + \text{Var}(Y) \odot \mathbb{E}(X)\mathbb{E}(X)'. \end{aligned}$$

Therefore:

$$\begin{aligned} &\text{Var}\left((I_{t-1} + \text{Flow}_{com,I,t-1} + \text{Flow}_{trav,I,t-1}) \odot (S_{t-1} + \text{Flow}_{com,S,t-1} + \text{Flow}_{trav,S,t-1}) \middle| I_{t-1}, S_{t-1}\right) \\ = &\text{Var}\left(\text{Flow}_{com,I,t-1} + \text{Flow}_{trav,I,t-1} \middle| I_{t-1}\right) \odot \text{Var}\left(\text{Flow}_{com,S,t-1} + \text{Flow}_{trav,S,t-1} \middle| S_{t-1}\right) + \\ &\text{Var}\left(\text{Flow}_{com,I,t-1} + \text{Flow}_{trav,I,t-1} \middle| I_{t-1}\right) \odot \left((\mathbf{Id} + \Omega_{t-1})S_{t-1}S'_{t-1}(\mathbf{Id} + \Omega_{t-1})'\right) + \\ &\text{Var}\left(\text{Flow}_{com,S,t-1} + \text{Flow}_{trav,S,t-1} \middle| S_{t-1}\right) \odot \left((\mathbf{Id} + \Omega_{t-1})I_{t-1}I'_{t-1}(\mathbf{Id} + \Omega_{t-1})'\right) \\ = &\left(\mathcal{C}(W_{com,t-1}, I_{t-1}, \tau) + \mathcal{C}(W_{trav,t-1}, I_{t-1}, 1)\right) \odot \left(\mathcal{C}(W_{com,t-1}, S_{t-1}, \tau) + \mathcal{C}(W_{trav,t-1}, S_{t-1}, 1)\right) + \\ &\left(\mathcal{C}(W_{com,t-1}, I_{t-1}, \tau) + \mathcal{C}(W_{trav,t-1}, I_{t-1}, 1)\right) \odot \left((\mathbf{Id} + \Omega_{t-1})S_{t-1}S'_{t-1}(\mathbf{Id} + \Omega_{t-1})'\right) + \\ &\left(\mathcal{C}(W_{com,t-1}, S_{t-1}, \tau) + \mathcal{C}(W_{trav,t-1}, S_{t-1}, 1)\right) \odot \left((\mathbf{Id} + \Omega_{t-1})I_{t-1}I'_{t-1}(\mathbf{Id} + \Omega_{t-1})'\right) \\ =: &\mathcal{D}(W_{com,t-1}, W_{trav,t-1}, S_{t-1}, I_{t-1}, \tau, \Omega_{t-1}), \end{aligned}$$

where  $\Omega_{t-1} = \Omega_{trav,t-1} + \Omega_{com,t-1}$  and where

$$\begin{aligned} \mathcal{D}(W_1, W_2, S, I, \tau, \Omega) &= \left(\mathcal{C}(W_1, I, \tau) + \mathcal{C}(W_2, I, 1)\right) \odot \left(\mathcal{C}(W_1, S, \tau) + \mathcal{C}(W_2, S, 1)\right) + \\ &\left(\mathcal{C}(W_1, I, \tau) + \mathcal{C}(W_2, I, 1)\right) \odot \left((\mathbf{Id} + \Omega)SS'(\mathbf{Id} + \Omega)'\right) + \\ &\left(\mathcal{C}(W_1, S, \tau) + \mathcal{C}(W_2, S, 1)\right) \odot \left((\mathbf{Id} + \Omega)II'(\mathbf{Id} + \Omega)'\right), \tag{26} \end{aligned}$$

function  $\mathcal{C}$  being defined in (22).

### G.3 Conditional variance of susceptibles

Let us use the notation:

$$I_t^* = I_t + \text{Flow}_{com,I,t} + \text{Flow}_{trav,I,t} \quad \text{and} \quad S_t^* = S_t + \text{Flow}_{com,S,t} + \text{Flow}_{trav,S,t}.$$

Using the law of total variance:

$$\begin{aligned} & \text{Var}_{t-1}(S_t) \\ &= \text{Var}_{t-1}(\mathbb{E}_{t-1}(S_t | I_{t-1}, S_{t-1}, \text{Flow}_{com,I,t-1}, \text{Flow}_{com,S,t-1}, \text{Flow}_{trav,I,t-1}, \text{Flow}_{trav,S,t-1})) + \\ & \quad \mathbb{E}_{t-1}(\text{Var}_{t-1}(S_t | I_{t-1}, S_{t-1}, \text{Flow}_{com,I,t-1}, \text{Flow}_{com,S,t-1}, \text{Flow}_{trav,I,t-1}, \text{Flow}_{trav,S,t-1})) \\ &= \text{Var}_{t-1}\left(\theta_{\beta,t-1} \odot \beta_{t-1} \odot \frac{1}{\mathbf{p}} \odot I_{t-1}^* \odot S_{t-1}^*\right) + \mathbb{E}_{t-1}\left(\mathbf{d}\left(\theta_{\beta,t-1} \odot \beta_{t-1} \odot \frac{1}{\mathbf{p}} \odot I_{t-1}^* \odot S_{t-1}^*\right)\right) \\ &= \left[\left(\theta_{\beta,t-1} \odot \beta_{t-1} \odot \frac{1}{\mathbf{p}}\right)\left(\theta_{\beta,t-1} \odot \beta_{t-1} \odot \frac{1}{\mathbf{p}}\right)'\right] \odot \mathcal{D}(W_{com,t-1}, W_{trav,t-1}, S_{t-1}, I_{t-1}, \tau, \Omega_{t-1}) + \\ & \quad \mathbf{d}\left(\theta_{\beta,t-1} \odot \beta_{t-1} \odot \frac{1}{\mathbf{p}} \odot [(\mathbf{Id} + \Omega_{t-1})I_{t-1}] \odot [(\mathbf{Id} + \Omega_{t-1})S_{t-1}]\right), \end{aligned}$$

Let's denote the previous conditional variance by  $\Theta_{t-1}$ . We have:

$$\begin{aligned} \Theta_{t-1} &= \text{Var}_{t-1}(S_t) \\ &:= \left[\left(\theta_{\beta,t-1} \odot \beta_{t-1} \odot \frac{1}{\mathbf{p}}\right)\left(\theta_{\beta,t-1} \odot \beta_{t-1} \odot \frac{1}{\mathbf{p}}\right)'\right] \odot \mathcal{D}(W_{com,t-1}, W_{trav,t-1}, S_{t-1}, I_{t-1}, \tau, \Omega_{t-1}) + \\ & \quad \mathbf{d}\left(\theta_{\beta,t-1} \odot \beta_{t-1} \odot \frac{1}{\mathbf{p}} \odot [(\mathbf{Id} + \Omega_{t-1})I_{t-1}] \odot [(\mathbf{Id} + \Omega_{t-1})S_{t-1}]\right), \end{aligned} \tag{27}$$

where  $\Omega_{t-1} = \Omega_{com,t-1} + \Omega_{trav,t-1}$  and function  $\mathcal{D}$  is defined by (26).

G.4 Conditional variance of the state vector

What precedes implies that:

$$\mathcal{V}(S_{t-1}, I_{t-1}) := \text{Var}_{t-1} \left( \begin{bmatrix} D_t \\ S_t \\ I_t \\ R_t \\ \beta_t \end{bmatrix} \right) = \tag{28}$$

$$\begin{bmatrix} \delta(1-\delta)\mathbf{d}(I_{t-1}) & \mathbf{0} & -\delta(1-\delta-\gamma)\mathbf{d}(I_{t-1}) & -\delta\gamma\mathbf{d}(I_{t-1}) & \mathbf{0} \\ \mathbf{0} & \Theta_{t-1} & -\Theta_{t-1} & \mathbf{0} & \mathbf{0} \\ -\delta(1-\delta-\gamma)\mathbf{d}(I_{t-1}) & -\Theta_{t-1} & \Theta_{t-1} + \nu\mathbf{d}(I_{t-1}) & -\gamma(1-\gamma-\delta)\mathbf{d}(I_{t-1}) & \mathbf{0} \\ -\delta\gamma\mathbf{d}(I_{t-1}) & \mathbf{0} & -\gamma(1-\gamma-\delta)\mathbf{d}(I_{t-1}) & (\gamma-\gamma^2)\mathbf{d}(I_{t-1}) & \mathbf{0} \\ \mathbf{0} & \mathbf{0} & \mathbf{0} & \mathbf{0} & \Omega_{\beta,t-1} \end{bmatrix},$$

with

$$\Omega_{\beta,t-1} = \sigma^2 \Delta t \mathbf{d}(\sqrt{\beta_{t-1}}) \cdot \Sigma \cdot \mathbf{d}(\sqrt{\beta_{t-1}}),$$

and where  $\Theta_t$  is defined by equations (27), and  $\nu$  is defined in equation (18).

H Jacobian matrix for extended Kalman filter implementation

We hereby provide the formulas for the Jacobian computation in the extended Kalman filter recursions. Denoting by  $J = \partial \mathbb{E}_{t-1}[D_t, S_t, I_t, R_t, \beta_t^0] / \partial [D_{t-1}, S_{t-1}, I_{t-1}, R_{t-1}, \beta_{t-1}^0]$ , we have:

$$J = \begin{bmatrix} \mathbf{Id} & \mathbf{0} & \delta\mathbf{Id} & \mathbf{0} & \mathbf{0} \\ \mathbf{0} & \mathbf{Id} & \mathbf{0} & \mathbf{0} & \mathbf{0} \\ \mathbf{0} & \mathbf{0} & (1-\delta-\gamma)\mathbf{Id} & \mathbf{0} & \mathbf{0} \\ \mathbf{0} & \mathbf{0} & \gamma\mathbf{Id} & \mathbf{Id} & \mathbf{0} \\ \mathbf{0} & \mathbf{0} & \mathbf{0} & \mathbf{0} & (1-\kappa)\mathbf{Id} \end{bmatrix} +$$

$$\begin{bmatrix} 0 \\ -\mathbf{Id} \\ +\mathbf{Id} \\ 0 \\ 0 \end{bmatrix} \frac{\partial \left( \theta_{S,t-1} \odot \theta_{M,t-1} \odot \beta_{t-1}^0 \odot \frac{1}{\mathbf{p}} \odot ([\mathbf{Id} + \Omega_{t-1}]I_{t-1}) \odot ([\mathbf{Id} + \Omega_{t-1}]S_{t-1}) \right)}{\partial [D_{t-1}, S_{t-1}, I_{t-1}, R_{t-1}, \beta_{t-1}^0]} \quad (29)$$

The matrix of partial derivatives is given by:

$$\begin{aligned} & \frac{\partial \left( \theta_{S,t-1} \odot \theta_{M,t-1} \odot \beta_{t-1}^0 \odot \frac{1}{\mathbf{p}} \odot ([\mathbf{Id} + \Omega_{t-1}]I_{t-1}) \odot ([\mathbf{Id} + \Omega_{t-1}]S_{t-1}) \right)}{\partial [D_{t-1}, S_{t-1}, I_{t-1}, R_{t-1}, \beta_{t-1}^0]} \\ &= \begin{bmatrix} 0 \\ (\mathbf{Id} + \Omega_{t-1}) \times \mathbf{d} \left( \theta_{S,t-1} \odot \theta_{M,t-1} \odot \beta_{t-1}^0 \odot \frac{1}{\mathbf{p}} \odot ([\mathbf{Id} + \Omega_{t-1}]I_{t-1}) \right) \\ (\mathbf{Id} + \Omega_{t-1}) \times \mathbf{d} \left( \theta_{S,t-1} \odot \theta_{M,t-1} \odot \beta_{t-1}^0 \odot \frac{1}{\mathbf{p}} \odot ([\mathbf{Id} + \Omega_{t-1}]S_{t-1}) \right) \\ 0 \\ \mathbf{d} \left( \theta_{S,t-1} \odot \theta_{M,t-1} \odot \frac{1}{\mathbf{p}} \odot ([\mathbf{Id} + \Omega_{t-1}]I_{t-1}) \odot ([\mathbf{Id} + \Omega_{t-1}]S_{t-1}) \right) \end{bmatrix}' \quad (30) \end{aligned}$$

### References

Alfaro, Laura, Ester Faia, Nora Lamersdorf and Farzad Saidi (2020), Social Interactions in Pandemics: Fear, Altruism, and Reciprocity. NBER Working Paper No. 27134.

Alvarez, Fernando E., David Argente and Francesco Lippi (2020), ‘A Simple Planning Problem for COVID-19 Lockdown’, *Covid Economics* **14**, 1–32.

Arroyo Marioli, Francisco, Francisco Bullano, Simas Kucinskas and Carlos Rondón-Moreno (2020), ‘Tracking R of COVID-19: A New Real-Time Estimation Using the Kalman Filter’, *medRxiv*.

Bettencourt, Luis M. A. and Ruy M. Ribeiro (2008), ‘Real Time Bayesian Estimation of the Epidemic Potential of Emerging Infectious Diseases’, *Plos One* **5**(1), 1–9.

Brady, Ryan, Michael Insler and Jacek Rothert (2020), ‘The Fragmented United States of America: The Impact of Scattered Lock-down Policies on Country-wide Infections’, *Covid Economics*, **43**.

Cori, Anne, Neil M. Ferguson, Christophe Fraser and Simon Cauchemez (2013), ‘A New Frame-

work and Software to Estimate Time-Varying Reproduction Numbers During Epidemics', *American Journal of Epidemiology* **178**(9), 1505–1512.

Cvitanic, Jaksa, Jin Ma and Jianfeng Zhang (2012), 'The Law of Large Numbers for Self-exciting Correlated Defaults', *Stochastic Processes and their Applications* **122**(8), 2781–2810.

Eikenberry, Steffen E., Marina Mancuso, Enahoro Iboi, Tin Phan, Keenan Eikenberry et al. (2020), 'To Mask or not to Mask: Modeling the Potential for Face Mask Use by the General Public to Curtail the COVID-19 Pandemic', *Infectious Disease Modelling* **5**, 293 – 308.

Feng, Shuo, Chen Shen, Nan Xia, Wei Song, Mengzhen Fan and Benjamin Cowling (2020), 'Rational use of face masks in the covid-19 pandemic', *The Lancet Respiratory Medicine* **8**(5), 434–436.

Ferguson, Neil M, Daniel Laydon, Gemma Nedjati-Gilani, Natsuko Imai, Kylie Ainslie et al. (2020), Impact of Non-pharmaceutical Interventions (NPIs) to Reduce COVID-19 Mortality and Healthcare Demand. Technical Report, Imperial College London.

Fernández-Villaverde, Jesús and Charles I. Jones (2020), Estimating and Simulating a SIRD Model of COVID-19 for Many Countries, States, and Cities, NBER Working Papers 27128, National Bureau of Economic Research, Inc.

Fischer, Emma P., Martin C. Fischer, David Grass, Isaac Henrion, Warren S. Warren et al. (2020), 'Low-cost Measurement of Face Mask Efficacy for Filtering Expelled Droplets During Speech', *Science Advances* **6**(36).

Flaxman, Seth, Swapnil Mishra, Axel Gandy, H. Juliette T. Unwin, Thomas A. Mellan et al. (2020), 'Estimating the Effects of Non-pharmaceutical Interventions on COVID-19 in Europe', *Nature* **584**(7820), 257–261.

Fowler, James H., Seth J. Hill, Nick Obradovich and Remy Levin (2020), 'The Effect of Stay-at-Home Orders on COVID-19 Cases and Fatalities in the United States', *medRxiv*.

Giesecke, K., K. Spiliopoulos, R.B. Sowers and J.A. Sirignano (2015), 'Large Portfolio Asymptotics for Loss from Default', *Mathematical Finance* **25**(1), 77–114.

Giesecke, Kay, Gustavo Schwenkler and Justin A. Sirignano (2020), 'Inference for Large Financial Systems', *Mathematical Finance* **30**(1), 3–46.

- Gouriéroux, C. and J. Jasiak (2020), Analysis of Virus Propagation: A Transition Model Representation of Stochastic Epidemiological Models. Working Paper.
- Hasan, Agus, Hadi Susanto, Venansius Tjahjono, Rudy Kusdiantara, Endah Putri et al. (2020), ‘A New Estimation Method for COVID19 Time-varying Reproduction Number Using Active Cases’, *medRxiv* .
- Hasan, Agus and Yuki Nasution (2020), ‘A Compartmental Epidemic Model Incorporating Probable Cases to Model COVID19 Outbreak in Regions with Limited Testing Capacity’, *medRxiv* .
- Hong, Harrison, Neng Wang and Jinqiang Yang (2020), Implications of stochastic transmission rates for managing pandemic risks. NBER Working Paper 27218.
- Iwasaki, Akiko (2020), ‘What reinfections mean for covid-19’, *The Lancet Infectious Diseases* **in press**.
- Kermack, William Ogilvy, A. G. McKendrick and Gilbert Thomas Walker (1927), ‘A Contribution to the Mathematical Theory of Epidemics’, *Proceedings of the Royal Society of London. Series A, Containing Papers of a Mathematical and Physical Character* **115**(772), 700–721.
- Ngonghala, Calistus N., Enahoro A. Iboi and Abba B. Gumel (2020), ‘Could Masks Curtail the Post-lockdown Resurgence of COVID-19 in the US?’, *Mathematical Biosciences* **329**, 108452.
- Perez-Saez, Javier, Stephen A Lauer, Laurent Kaiser, Simon Regard, Elisabeth Delaporte et al. (2020), ‘Serology-Informed Estimates of SARS-CoV-2 Infection Fatality Risk in Geneva, Switzerland’, *The Lancet Infectious Diseases* .
- Read, Jonathan M. and Matt J. Keeling (2003), ‘Disease evolution on networks: the role of contact structure’, *Proceedings of the Royal Society of London. Series B: Biological Sciences* **270**(1516), 699–708.
- Redlener, Irwin, Jeffrey D. Sachs, Sean Hansen and Nathaniel Hupert (2020), 130,000 – 210,000 Avoidable COVID-19 Deaths – And Counting – In The U.S. Working Paper, Columbia University.
- Rothert, Jacek (2020), Optimal Federal Redistribution During the Uncoordinated Response to a Pandemic. United States Naval Academy Working Papers 64.



- Shefrin, Hersh (2020), 'The psychology underlying biased forecasts of covid-19 cases and deaths in the united states', *Frontiers in Psychology* . Forthcoming.
- Stringhini, Silvia, Ania Wisniak, Giovanni Piumatti, Andrew S Azman, Stephen A Lauer et al. (2020), 'Seroprevalence of Anti-SARS-CoV-2 IgG Antibodies in Geneva, Switzerland (SEROCoV-POP): a Population-based Study', *The Lancet* **396**(10247), 313 – 319.
- Stutt, Richard O. J. H., Renata Retkute, Michael Bradley, Christopher A. Gilligan and John Colvin (2020), 'A Modelling Framework to Assess the Likely Effectiveness of Facemasks in Combination with 'Lock-down' in Managing the COVID-19 Pandemic', *Proceedings of the Royal Society A: Mathematical, Physical and Engineering Sciences* **476**(2238), 20200376.
- Thompson, R.N., J.E. Stockwin, R.D. van Gaalen, J.A. Polonsky, Z.N. Kamvar et al. (2019), 'Improved Inference of Time-varying Reproduction Numbers During Infectious Disease Outbreaks', *Epidemics* **29**, 1–11.
- Youssef, Mina and Caterina Scoglio (2011), 'An Individual-based Approach to SIR Epidemics in Contact nNetworks', *Journal of Theoretical Biology* **283**(1), 136–144.
- Zhang, Z., H. Wang, C. Wang and H. Fang (2015), 'Modeling Epidemics Spreading on Social Contact Networks', *IEEE Transactions on Emerging Topics in Computing* **3**(3), 410–419.

# The impact of supply chain networks on interactions between the anti-COVID-19 lockdowns in different regions

Hiroyasu Inoue,<sup>1</sup> Yohsuke Murase<sup>2</sup> and Yasuyuki Todo<sup>3</sup>

Date submitted: 31 October 2020; Date accepted: 3 November 2020

*To prevent the spread of COVID-19, many cities, states, and countries have 'locked down', restricting economic activities in non-essential sectors. Such lockdowns have substantially shrunk production in most countries. This study examines how the economic effects of lockdowns in different regions interact through supply chains, a network of firms for production, simulating an agent-based model of production on supply-chain data for 1.6 million firms in Japan. We further investigate how the complex network structure affects the interactions of lockdowns, emphasising the role of upstreamness and loops by decomposing supply-chain flows into potential and circular flow components. We find that a region's upstreamness, intensity of loops, and supplier substitutability in supply chains with other regions largely determine the economic effect of the lockdown in the region. In particular, when a region lifts its lockdown, its economic recovery substantially varies depending on whether it lifts lockdown alone or together with another region closely linked through supply chains. These results propose the need for inter-region policy coordination to reduce the economic loss from lockdowns.*

<sup>1</sup> Associate Professor, Graduate School of Simulation Studies, University of Hyogo.

<sup>2</sup> Research Scientist, Advanced Institute for Computational Science, RIKEN.

<sup>3</sup> Professor, Graduate School of Economics, Waseda University.

Copyright: Hiroyasu Inoue, Yohsuke Murase and Yasuyuki Todo

# 1 Introduction

COVID-19, a novel coronavirus (SARS-CoV-2) disease, has been spreading worldwide. To prevent its spread, many cities, regions, and countries were or have been ‘locked down’, suppressing economic activities. On 18 April 2020, 158 countries out of 181 required closing temporarily or working from home for some sectors in some or all cities. Although some countries later lifted their lockdowns, the number of countries in a lockdown remained 95 on 30 July 2020 [1].

Closing workplaces shrinks the economic output of locked down regions. The negative economic effect of a lockdown in one region may diffuse through supply chains, i.e., supplier-client relationships of firms, to other regions that are not necessarily locked down. When a firm is closed by a lockdown strategy, its client firms located anywhere should suffer decreased production because of the lack of supply of intermediate goods and services. Suppliers of the closed firm should also see reduced production because of a shortage of demand.

Many studies have empirically confirmed the propagation of economic shocks through supply chains, particularly shocks originating from natural disasters [2, 3, 4, 5, 6, 7]. Some examine the diffusion of the effect of lockdowns because of COVID-19 on production across regions and countries and estimate the total effect using input–output (IO) linkages at the country-sector level [8, 9, 10, 11] and supply chains at the firm level [12].

Several works focusing on natural disasters [5, 6] pay attention to how the network structure of supply chains affects the propagation of shocks, finding that the scale-free property, non-substitutability of suppliers, and loops are major drivers of such propagation. However, the role of the network structure has not been fully examined in the context of the propagation of the lockdown effect. However, this issue should be of great interest from the perspective of network science for the following two reasons.

First, the literature on network interventions has investigated what types of individuals or groups in a network, such as those with high centrality, should be targeted to promote (prevent) the diffusion of positive (negative) behaviours and outcomes [13, 14]. Similarly, we are interested in how the economic effect of imposing and lifting a lockdown in one region, an example of a network intervention, diffuses to other regions. Compared with existing works, this study is novel in many respects. For example, we consider interventions in a network of firms and their economic outcomes, while previous studies focus on the health behaviours and outcomes in human networks [15], with a few exceptions that examine economic outcomes in human networks [16]. In addition, because a lockdown is usually imposed in a city, state, or country, the scale of interventions is large. Those firms targeted by such interventions are exogenously determined by geography, and thus we should assess the network characteristics of exogenously grouped nodes rather than the endogenously connected ones identified by network centrality [13, 17] or community detection algorithms [18].

Second, at any point amid the spread of COVID-19, some regions have imposed a lockdown, while others have remained open. Therefore, when we evaluate the lockdown strategy of a region, the interactions between the strategies of different regions need to be taken into account. In other words, the economic effect of a lockdown in a region depends on whether other regions connected through supply chains are similarly locked down. For example, Sweden did not impose a strict lockdown, unlike other European countries. However, it still expects a 4.5% reduction in gross domestic product (GDP) in 2020, a decline comparable to those in neighbouring countries that did lock down, possibly because of its close economic ties with its neighbours [19]. Motivated by the Swedish experience, this study examines the network structure between regions that is usually ignored in the literature on network interventions and discusses the need for policy coordination among regions depending on their network characteristics. Some studies call for inter-regional and international policy coordination in the presence of spillover effects in the context of health, environment, and macroeconomics [20, 21], but they do not explicitly incorporate the network structure.

We conduct a simulation analysis applying actual supply-chain data of 1.6 million firms and experiences of lockdowns in Japan to an agent-based model of production. Specifically, we analyse the network characteristics of a prefecture in Japan that led to greater economic recovery by lifting its lockdown when all other prefectures remained locked down. In addition, to further highlight the interactions between regions, our simulation investigates how the characteristics of the supply-chain links between two prefectures affect their economic recovery when they simultaneously lift their lockdowns. One novelty of our study is to decompose supply-chain flows into potential and loop flow components and test the role of upstreamness (potential) in supply chains and intra- and inter-prefectural loops in diffusion.

## 2 Data

The data used in this study are taken from the Company Information Database and Company Linkage Database collected by Tokyo Shoko Research (TSR), one of the largest credit research companies in Japan. The former includes information about the attributes of each firm, including the location, industry, sales, and number of employees, whereas the latter includes the major customers and suppliers of each firm. Because of data availability, we use the data on firm attributes and supply chains in 2016. The number of firms in the data is 1,668,567 and the number of supply-chain links is 5,943,073. Hence, our data identify the major supply chains of most firms in Japan, although they lack information about supply-chain links with foreign entities. Because the transaction value of each supply-chain tie is not available in the data, we estimate sales from a supplier to each of its customers and consumers using the total sales of the supplier and its customers and IO tables for Japan for 2015. In this estimation process, we must drop firms without any sales information. Accordingly, the number of firms in our final analysis is 966,627 and the number of links is 3,544,343. Although firms in the TSR data are classified into 1,460 industries according to the Japanese Industrial Standard (JIS) classification, we simplify them into the 187 industries classified in the IO tables. Supplementary Information A provides the details of the data construction process.

In the supply-chain data described above, the degree, or the number of links, of firms follows a power-law distribution [5], as often found in the literature [22]. The average path length between firms, or the number of steps between them through supply chains, is 4.8, indicating a small-world network. Using the same dataset, previous studies [5, 23] find that 46–48% of firms are included in the giant strongly connected component (GSCC), in which all firms are indirectly connected to each other through supply chains. The large size of the GSCC clearly shows that the network has a significant number of cycles unlike the common image of a layered or tree-like supply-chain structure.

## 3 Methods

### 3.1 Model

Agent-based models that incorporate the interactions of agents through networks have been widely used in social science recently [24, 25, 26]. Following the literature, we employ the dynamic agent-based model of Inoue and Todo [5, 6], an extension of the model of Hallegatte [27] that assumes supply chains at the firm level. In the model, each firm utilises the inputs purchased from other firms to produce an output and sells it to other firms and consumers. Firms in the same industry are assumed to produce the same output. Supply chains are predetermined and do not change over time in the following two respects. First, each firm utilises a firm-specific set of input varieties and does not change the input set over time. Second, each firm is linked with fixed suppliers and customers and cannot be linked with any new firm over time. Furthermore, we assume that each firm keeps inventories of each input at a level randomly determined from the Poisson distribution. Following Inoue and Todo [5], in which parameter values are calibrated from the case of the Great East Japan earthquake, we assume that firms aim to keep inventories for 10 days of production on average (see Supplementary Information B.1 for the details).

When a restriction is imposed on the production of a firm, both the upstream and the downstream of the firm is affected. On the one hand, the demand of the firm for the parts and components of its suppliers immediately declines, and thus suppliers have to shrink their production. Because demand for the products of suppliers' suppliers also declines, the negative effect of the restriction propagates upstream. On the other hand, the supply of products from the directly restricted firm to its customer firms declines. Then, one way for customer firms to maintain the current level of production is to use their inventories of inputs. Alternatively, customers can procure inputs from other suppliers in the same industry already connected before the restriction if these suppliers have additional production capacity. If the inventories and inputs from substitute suppliers are insufficient, customers have to shrink their production because of a shortage of inputs. Accordingly, the effect of the restriction propagates downstream through supply chains. Such downstream propagation is likely to be slower than upstream propagation because of the inventory buffer and input substitution.

### 3.2 Lockdowns in Japan

In Japan, lockdown strategies were implemented at the prefecture level under the state of emergency [28] first declared on 7 April 2020 in seven prefectures with a large number of confirmed COVID-19 cases. Because populated regions tended to be affected more and earlier, these seven prefectures were industrial clusters in Japan, including Tokyo, Osaka, Fukuoka and their neighbouring prefectures. The target of the state of emergency was expanded to all 47 prefectures on 16 April. The state of emergency was lifted for 39 prefectures on 14 May and for an additional three on 21 May; it was lifted for the remaining five prefectures on 25 May. Supplementary Information Figure A.3 summarises the timeline of the lockdowns in different prefectures.

Although the national government declared a state of emergency, the extent to which the restrictions were imposed was determined by each prefecture government. Therefore, the level of the lockdown in each prefecture may have varied. Although all prefectures were in the state of emergency from April 16 to May 14, prefectures with a large number of confirmed COVID-19 cases, such as the seven prefectures in which the state of emergency was first declared, requested more stringent restrictions than others. The national or prefecture government can only request closing workplaces, staying at home, and social distancing rather than require these actions through legal enforcement or punishment; however, strong social pressure in Japan led people and businesses to voluntarily restrict their activities to a large extent. As a result, production activities including those in sectors not officially restricted shrunk substantially (Mainichi Newspaper, 27 May 2020).

### 3.3 Simulation procedure

**Replication of the actual effect** In our simulation analysis, we first confirm whether our model and data can replicate the actual reduction in production caused by the lockdown of Japan during the state of emergency. Because we cannot observe the extent to which each firm reduces its production capacity by obeying governmental requests, the rate of reduction in production capacity for each sector assumed in our simulation analysis depends on its characteristics. Specifically, the rate of reduction in a sector is the product of the level of reduction determined by the degree of exposure to the virus given by [9] and the share of workers who cannot work at home given by [8]. For example, in lifeline/essential sectors such as the utilities, health, and transport sectors, the rate of reduction is assumed to be zero; in other words, the production capacity in these sectors does not change on lockdown. In sectors in which it is assumed that exposure to the virus is low (10%) and 47.5% of workers can work at home, such as the wholesale and retail sectors, the rate of reduction is 5.25% ( $= 0.1 \times (1 - 0.475)$ ). Sectors with medium exposure (50%) and a lower share of workers working at home (26.8%), such as the iron and other metal product sectors, reduce production capacity by 35.2% ( $= 0.5 \times (1 - 0.268)$ ). See Supplementary Information Table B.1 for the rate of reduction of each sector.

After the lockdown in a prefecture is lifted, all the firms in that prefecture immediately return to their pre-lockdown production capacity. Moreover, we assume that inventories do not decay over time: inventories stocked before the lockdown can be fully utilised after the lockdown is lifted. The following results are averaged over 30 Monte Carlo runs.

**Interactions among regions** After checking the accuracy of our simulation model, we examine how changing the restriction level of the lockdown in a region affects production in another region. For this purpose, we experiment with different sets of sector-specific rates of reduction in production capacity by multiplying the benchmark rates of reduction defined above by a multiplier such as 0.4 or 0.8. For example, when the benchmark rate of reduction in a sector is 35.2%, as in the case of the iron and other metal product sectors, and the multiplier is 0.4, we alternatively assume a rate of reduction of 14.1%.

Moreover, we assume that the rates of reduction can vary among prefectures because each prefecture can determine its own level of restrictions under the state of emergency (Section 3.2). In practice, the restrictions requested by the prefecture government were tougher and people were more obedient to the requests in the seven prefectures in which the state of emergency was first declared because of their large number of confirmed COVID-19 cases (Figure A.3(b)) than in other prefectures. Accordingly, we run the same simulation assuming different rates of reduction for the two types of prefectures, defined as more and less restricted groups, to investigate how different rates of reduction in one group affect production in the other.

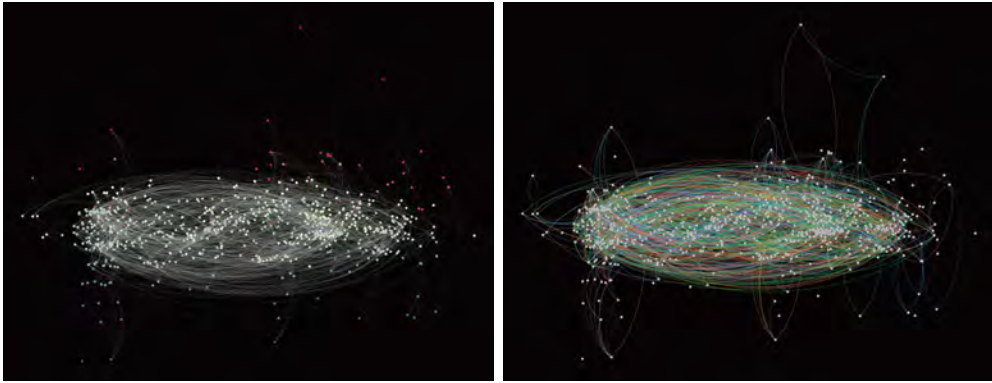


Figure 1: Visualisation of supply chains for top 1,000 firms in terms of sales. Each dot indicates a firm. Firms with a higher HH potential are located more upward in both panels. In the left panel, the grey lines illustrate the potential flows computed from the HHD. The red and blue node colours respectively represent higher and lower HH potentials. The right panel shows loop flows computed from HHD, while the different colours represent different cycles.

**Lifting lockdown in only one region** In practice, some prefectures lifted their lockdowns earlier than others (Section 3.2). Although this may have led to the recovery of value added production, or gross regional product (GRP), the extent of such a recovery should have been affected by the links between firms in the prefecture and others still locked down. To highlight this network effect, we simulate what would happen to the GRP of a prefecture if it lifted its lockdown while all others were still imposing lockdowns. Then, we investigate what network characteristics of each prefecture determine the recovery from lockdown, measured by the ratio of the increase in the GRP of the prefecture by lifting its lockdown to the reduction in its GRP because of the lockdown of all prefectures.

In particular, we focus on four types of network characteristics. First, when a prefecture is more isolated from others in the supply-chain network, the effect of others' lockdowns should be smaller. We measure the level of isolation using the number of links within the prefecture relative to the total degree of firms (total number of links from and to firms) in the prefecture.

Second, an alternative and more interesting measure of isolation is the intensity of loops in supply chains. Although supply chains usually flow from suppliers of materials to those of parts and components and to assemblers, some suppliers use final products such as machinery and computers as inputs. This results in many complex loops in supply chains [29], in which negative shocks circulate and can become aggravated [5]. Such loops in a network are found to generate instability in the system dynamics literature [30] and more recently in the context of supply chains [31]. In the case of lifting the lockdown in only one prefecture, the loops within that prefecture may magnify its recovery because of the circulation of positive effects in the loops. To measure the intensity of the loops in the supply chains within a prefecture, we apply the Helmholtz–Hodge decomposition (HHD) to all the flows in the network and decompose each directed link from firm  $i$  to firm  $j$ ,  $F_{ij}$ , into a potential (or gradient) flow component,  $F_{ij}^{(p)}$ , and a loop (or circular) flow component,  $F_{ij}^{(c)}$  [32]. Supplementary Information B.3 explains the details of the HHD. Figure 1 illustrates potential and loop flows of top 1,000 firms in terms of sales. In particular, the right panel identifies a number of loops in supply chains. Then, our measure of the intensity of the loops for prefecture  $a$  is the ratio of the total loop flows within the prefecture  $\sum_{i,j \in a} F_{ij}^{(c)}$  to the total degree of all the firms in the prefecture denoted by  $F_a$ .

Third, we pay attention to the upstreamness of firms in supply chains. Theoretically, upstream firms are affected by supply-chain disruptions through a lack of demand, whereas downstream firms are affected through a lack of supply. However, the effect of upstream and downstream links can differ in size. A recent sectoral analysis [33] finds that the profits of more upstream sectors in global value chains are substantially lower than those of more downstream sectors, implying that negative economic shocks propagate upstream more than downstream. To clarify the possible effect of upstreamness, we define the upstream position of each firm  $i$  in supply chains using its Helmholtz–Hodge potential,  $\phi_i$ , computed from the potential flows obtained from the HHD for the whole network. The HH potential is

higher when the firm is located in a more upstream position. In practice, it is higher for the mining, manufacturing, and information and communication sectors, while lower for the wholesale, retail, finance, healthcare, and accommodation and food service sectors [29]. We average the HH potential over the firms in each prefecture to measure the upstreamness of the prefecture in supply chains (see Supplementary Information Figure B.2 for this measure for each prefecture).

Finally, even when the supplies of parts and components from other prefectures are shut down because of their lockdowns, the negative effect can be mitigated if suppliers can be replaced by those in the prefecture lifting its lockdown. Existing studies [2, 5] have found that input substitutability can largely mitigate the propagation of negative economic shocks through supply chains. By assumption, suppliers of firms in prefecture  $a$  that are in other prefectures on lockdown can be replaced by suppliers in prefecture  $a$  that are in the same industry and already connected. To measure the degree of supplier substitutability for prefecture  $a$ , we divide the number of the latter suppliers by the number of the former.

**Lifting lockdowns in two regions simultaneously** In practice, each prefecture government determined its restriction level of lockdown after observing the spread of COVID-19 in its prefecture and typically ignored the economic interactions with other prefectures through supply chains. This may have led to the misvaluation of the economic effect of lockdown. To emphasise the role of the interactions between prefectures in the economic effect of lockdown, our simulations analyse the economic effect of lifting the lockdown in a prefecture on its GRP when another prefecture lifts its lockdown simultaneously. We define a relative measure of recovery using the ratio of the increase in the GRP of prefecture  $a$  when it lifts its lockdown together with prefecture  $b$  ( $\Delta GRP_a^{ab}$ ) to its increase when it lifts its lockdown alone ( $\Delta GRP_a^a$ ).

Presumably, the characteristics of the links between the two prefectures largely affect their recovery. Expanding the case of lifting the lockdown in only one prefecture described just above, we are particularly interested in the following variables. First, we define the intensity of the directional links from prefectures  $a$  to  $b$  and from  $b$  to  $a$  by

$$Link_{ab} \equiv \sum_{i \in a, j \in b} F_{ij} / F_a \quad (1)$$

and

$$Link_{ba} \equiv \sum_{i \in a, j \in b} F_{ji} / F_a, \quad (2)$$

respectively, where  $F_a$  is the total degree of firms in prefecture  $a$ , as defined before. Second, we focus on potential flows using the HHD as above and define the intensity of potential flows from prefectures  $a$  to  $b$  and from  $b$  to  $a$  by

$$Pot_{ab} \equiv \sum_{i \in a, j \in b} F_{ij}^{(p)} / F_a \quad (3)$$

and

$$Pot_{ba} \equiv \sum_{i \in a, j \in b} F_{ji}^{(p)} / F_a, \quad (4)$$

respectively. Third, the intensity of the loops between prefectures  $a$  and  $b$  is given by

$$Loop_{ab} \equiv \sum_{i \in a, j \in b} F_{ij}^{(c)} / F_a. \quad (5)$$

Supplementary Information B.3 describes how to calculate  $Pot_{ab}$ ,  $Pot_{ba}$ , and  $Loop_{ab}$  using a simple example.

Finally, when suppliers of firms in prefecture  $a$  are located outside prefectures  $a$  and  $b$  and thus are locked down, they can be replaced by suppliers in the same industry in prefecture  $b$  that are already connected with firms in prefecture  $a$ . To measure the degree of this supplier substitutability, we divide the total number of the latter suppliers by the total number of the former. See Supplementary Information B.4 for the details.

### 4 Results

#### 4.1 Simulation of the effect of the actual lockdown

In Figure 2, the blue lines show the results of the 30 Monte Carlo runs conducted to estimate the effect of the actual lockdown in Japan given the sector-specific rates of reduction in production capacity assumed in the literature [33, 9] and shown in Supplementary Information B.1. The horizontal axis indicates the number of days since the declaration of the state of emergency (April 7) and the vertical axis represents the total value added production, or GDP, of Japan on each day. See Section 3.2 for the sequence of the state of emergency across the country. Averaged over the 30 runs, the estimated loss in GDP is 13.1 trillion yen (124 billion U.S. dollars), or 2.5% of yearly GDP.

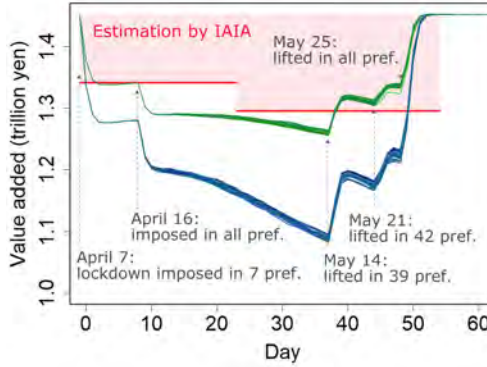


Figure 2: Simulations of value added (GDP) during the actual lockdown. The blue and green lines show the simulation results given the sector-specific rates of reduction in production capacity assumed in the literature [33, 9] and shown in Supplementary Information B.1 and 65% of those rates to calibrate the actual production dynamics, respectively. Each line represents the daily GDP from one Monte Carlo run. The red segments indicate the daily GDP estimated from pre-lockdown GDP and the post-lockdown monthly Indices of All Industry Activity (IAIA) for April and May.

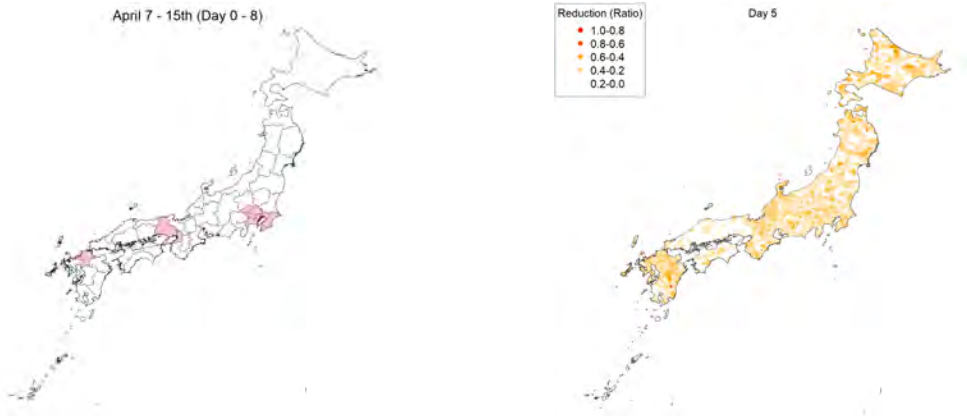


Figure 3: Geographical visualisation of the effect of lockdowns. In the left panel, locked-down prefectures in the first stage of the state of emergency (day 0-8) are shown in red, while the right panel presents the rate of reduction in production averaged over firms in each municipality on day 5, using different colours for different rates of reduction.

Covid Economics 56, 9 November 2020: 157-194



Without relying on our model and simulation, we also estimate the changes in daily GDP from pre-lockdown GDP and the post-lockdown monthly Indices of All Industry Activity (IAIA) [34]. The average daily GDP in April and May estimated from the IAIA is illustrated by the red lines in Figure 2 (see Supplementary Information C.1 for the detailed procedures). The total loss of GDP estimated by the IAIA, or the pink area in Figure 2, is 7.52 trillion yen (1.44% of GDP), 57.4% of the estimate from our simulations. Our simulation thus overestimates the loss of GDP from the lockdown, possibly because the assumed rates of reduction in production capacity due to the lockdown taken from the literature [8, 9] are larger than the actual rates in Japan. Therefore, we experiment with different rates of reduction in production capacity by multiplying the benchmark rates by a weight to calibrate changes in production. We find that a weight of 65% results in a close fit between our estimates and those from the IAIA and show the results using green lines in Figure 2.

In either case (blue or green lines), the production loss rises during the lockdown. For example, value added declined monotonically from days 9 to 37 when all prefectures were in the state of emergency, assuming a fixed rate of reduction in production capacity throughout the period. This is because the economic contraction in different regions interacted with each other through supply chains and thus worsened over time. This worsening trend in GDP is consistent with GDP estimated using the IAIA.

Another notable finding from the simulation is that prefectures that were not locked down were heavily affected by those in lockdowns. To highlight this, the left panel of Figure 3 shows locked-down prefectures in the first stage of the state of emergency (day 0-8) in red, while the lower-right panel presents the rate of reduction in production averaged over firms in each municipality on day 5. From these figures, it is clear that the economic effect of lockdowns in some prefectures diffuse to others that are not locked down. A video is available for the temporal and geographical visualisation. See Appendix C.1.

In addition, because of the network effect, the earlier lifting of the lockdown in some prefectures does not result in a full recovery of production in these prefectures. Notably, when the lockdown was lifted in 39 prefectures on day 37 (14 May), the simulated GDP showed a sharp recovery but dropped again substantially a few days after the recovery. This drop occurred because the lockdown remained active in eight prefectures including the top two industrial clusters in Japan, namely, greater Tokyo and greater Osaka. Although economic activities returned to normal in these 39 prefectures, their production did not recover monotonically but rather declined again because the major industrial clusters linked with them were still locked down. This finding points to the interactions of the economic effect of lockdown between regions through firm-level supply chains.

## 4.2 Interactions between lockdowns in different regions

Next, we experiment with simulations assuming different restriction levels of lockdown, or different sets of multipliers for the sector-specific benchmark rates of reduction in production capacity, between the more and less restricted groups (Section 3.3). The more restricted group comprises the seven prefectures with a large number of COVID-19 cases (pink ones in panel (b) of Figure A.3), whereas the less restricted group includes the other 40 prefectures. The left, middle, and right panels of Figure 4 indicate the loss in GDP for different multipliers for the more restricted group when fixing the multiplier for the less restricted group at 0%, 50%, and 100%, respectively. Here, 100% corresponds to the rates of reduction shown in Supplementary Information Table B.1 and used in the previous subsection and 0% means no restriction. In each bar, the blue and red parts show the loss of value added in the more and less restricted groups, respectively.

As shown, the total loss of GDP increases in the restriction level of lockdown in both groups. For example, the total production loss is 1.57% of GDP when the multiplier is 50% for both groups (the left bar in the middle panel), while it is larger, or 3.89%, when the multiplier is 100% for both (the right panel). More interestingly, the left panel shows that while the less restricted group imposes no restrictions, its value added decreases more (i.e. the red part in Figure 4 increases) as the more restricted group imposes more restrictions. When the level of restrictions in the more restricted group is the highest (i.e. the multiplier is 100%), the loss in value added in the less restricted group without any lockdown is large: 3.93 trillion yen, or 2.12% of its pre-lockdown value added. These results clearly indicate that even when prefectures are not locked down, their economies can be damaged because of the propagation of the effect of the lockdowns in other prefectures through supply chains.

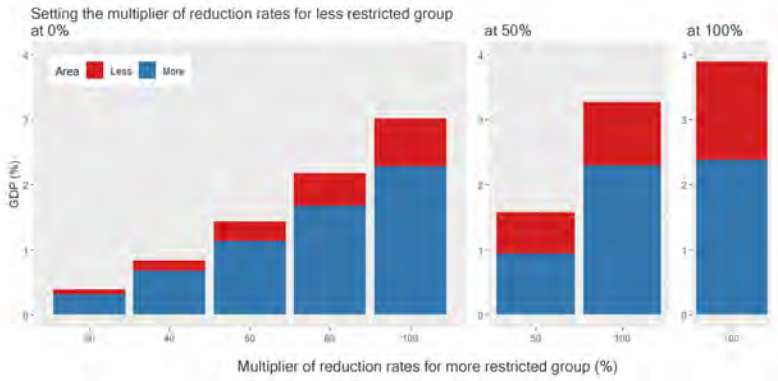


Figure 4: Loss in value added as a percentage of total value added (GDP) assuming different restriction levels of lockdown for 60 days between the more and less restricted groups. A restriction level is defined by a multiplier for the sector-specific benchmark rates of reduction in production capacity. For example, the left bar presents the result assuming a multiplier of 0% (i.e., no restriction) for the less restricted group and 20% for the more restricted group. The red and blue parts of each bar show the loss of value added in the less and more restricted groups, respectively, as a percentage of GDP.

### 4.3 Effect of lifting the lockdown in one region

We further examine, when only one prefecture lifts its lockdown, while all the other prefectures remain locked down, how the recovery of that prefecture from lifting its lockdown is determined by its network characteristics. Figure 5 illustrates the recovery rate of each prefecture defined as the ratio of the total gain of its value added, or gross regional production (GRP), from lifting the lockdown to its total loss from the lockdown of all the prefectures for two weeks. Red prefectures recover the most, yellow ones recover moderately, and white ones recover slightly. See Supplementary Information Figure C.4 for the recovery rate of each prefecture.

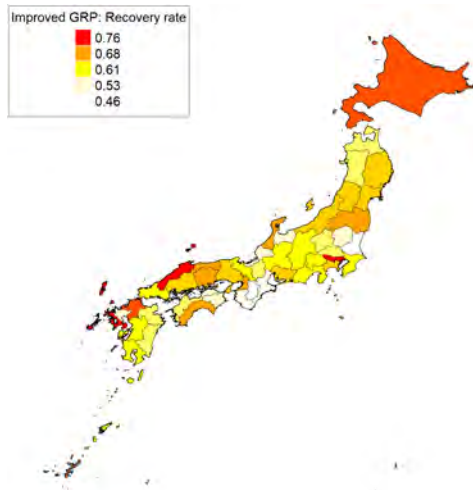


Figure 5: Choropleth map of the recovery rate for each prefecture. The recovery rate is defined as the ratio of the total gain of a prefecture's GRP from lifting its own lockdown to its total loss from the lockdown of all the prefectures for two weeks.

One notable finding from this figure is that the prefectures that recover the most, or the red prefectures

in Figure 5, include Hokkaido, Shimane, and Okinawa, which are remote from industrial hubs in terms of both geography and supply chains, suggesting the effect of network characteristics on economic recovery by lifting a lockdown (see Supplementary Information Figure A.1 for inter-prefecture supply chains and Supplementary Information Figure A.2 for the name and location of each prefecture).

We further examine the correlation between the recovery rate and network measures explained in Section 3.3 (i.e. those for isolation, loops, upstreamness, and supplier substitution) and test the significance of the correlation using ordinary least squares (OLS) estimations. Figure 6 illustrates the correlation between the recovery rate and network measures. To control for the effect of the prefecture's economic size on its recovery (Figure 6(f)), we include GRP in logs in all the OLS estimations and exclude the effect of GRP from the recovery rate in Figure 6. The number of links of each prefecture could also be controlled for; however, because its correlation coefficient with GRP is 0.965 (Supplementary Information Table C.1), we do not use the total links in our regressions to avoid multicollinearity. Supplementary Information Table C.2 presents the OLS results.

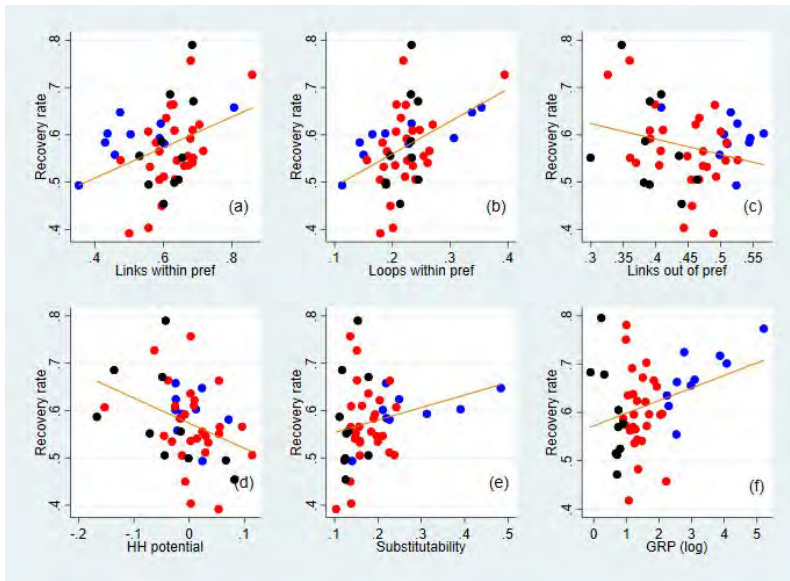


Figure 6: Correlation between the recovery rate and selected network measures. The vertical axis indicates the recovery rate defined as the ratio of the increase in the GRP of a prefecture by lifting its own lockdown to its decrease because of the lockdown of all the prefectures. Except for panel (f), the effect of GRP is excluded from the recovery rate. The horizontal axis indicates the share of the links within the prefecture to its all links in (a), the share of the loop flows within the prefecture to its total flows in (b), the share of the links to other prefectures to all links in (c), the standardised potential flows in (d), the share of substitutable suppliers to all suppliers outside the prefecture in (e), and GRP in logs in panel (f). The orange line in each panel specifies the fitted value from a linear regression that controls for the effect of GRP. The blue, black, and red dots show prefectures whose GRP is among the top 10, bottom 10, and others, respectively.

In panels (a) and (b) of Figure 6, the supply-chain links and loops within the prefecture are found to be positively correlated with the recovery rate. These results suggest that when a prefecture is more isolated in the network and has more loops within it, the positive effect of lifting a lockdown circulates in the loops, which can mitigate the propagation of the negative effects of other prefectures' lockdowns. By contrast, the outward links to other prefectures and the HH potential of the prefecture are negatively and significantly correlated with the recovery rate (panels (d) and (e)). These findings imply that prefectures with more upstream firms in supply chains tend to recover less from lifting their own lockdowns. Panel (f) indicates that the recovery rate is higher when more suppliers in other prefectures under lockdown can be replaced by those in the prefecture lifting its lockdown.

#### 4.4 Effect of lifting the lockdowns in two regions simultaneously

Finally, we simulate the effect on the production of prefecture  $a$  if it lifted its lockdown together with prefecture  $b$ . We compare the recovery in prefecture  $a$ 's GRP by lifting its lockdown together with prefecture  $b$  and that by lifting its lockdown alone and compute the relative recovery measure, as shown in Supplementary Information Figure C.5. Using a regression framework as above, we investigate how the relative recovery measure of prefecture  $a$  is affected by the network relationships between prefectures  $a$  and  $b$ . Figure 7 illustrates the correlation between selected key variables and the relative recovery. In the regression analysis, we always control for the GRP of prefecture  $b$ , its squares, and the number of links between and prefectures  $a$  and  $b$  that may affect the relative recovery (Figure 7 (e) and (f)). Then, we exclude these effects from the relative recovery in panels (a)–(d) in the figure. Supplementary Information Table C.4 presents the results of the OLS estimations.

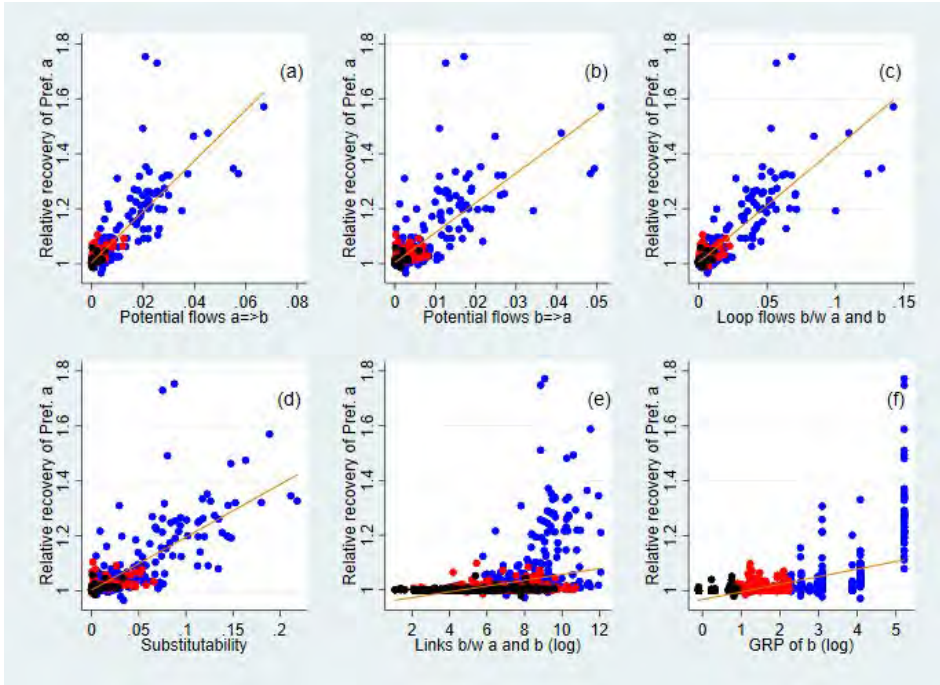


Figure 7: Correlation between the relative recovery and selected network measures. The vertical axis indicates the relative recovery of prefecture  $a$ , defined as the ratio of the increase in the GRP of prefecture  $a$  by lifting its lockdown together with prefecture  $b$  to its increase by lifting its lockdown alone. The effect of the GRP of  $b$  and total links between the two are excluded from the relative recovery measure. The variable in the horizontal axis is given by Equations 3 and 4 in panels (a) and (b), respectively, Equation 5 in (c), the share of substitutable suppliers in  $b$  for those in  $a$  among  $a$ 's locked-down suppliers in (d), the number of links between prefectures  $a$  and  $b$  in (e) and the GRP of  $b$  in logs in (f). The orange line in each panel signifies the fitted value from a linear regression that controls for the effect of the GRP of  $b$  and total number of links between  $a$  and  $b$  in (a)–(d). The blue, black, and red dots show the pairs of prefectures  $a$  and  $b$  for which the GRP of  $b$  is among the top 10, bottom 10, and others, respectively.

Panels (a) and (b) of Figure 7 show that even after controlling for the effect of economic size and number of links between the two prefectures, the ratio of potential flows from prefecture  $a$  to  $b$  and from  $b$  to  $a$  to the total flows of  $a$  is positively correlated with the relative recovery. Supplementary Information Figure C.6 shows similarly positive correlation between for the number of links between the two, rather than potential flows, and the recovery. These results suggest that the recovery from lifting a lockdown is greater when two prefectures closely linked through their supply chains, regardless of the

direction, lift their lockdowns together. Further, we find that prefecture  $a$  recovers more when prefectures  $a$  and  $b$  are linked through more circular flows (panel (c)), confirming that the positive impacts of lifting a lockdown can circulate and be strengthened in inter-regional supply-chain loops. Panel (d) indicates that if prefecture  $a$ 's suppliers in other prefectures are locked down but can be replaced by suppliers in prefecture  $b$  easily, prefecture  $a$ 's recovery is higher when the two prefectures lift their lockdowns together. Although the correlation between the relative recovery measure and network variables seems to be largely driven by the observations for which the GRP of prefecture  $b$  is large (depicted by the blue dots in Figure 7), we find that the positive correlation still exists without these observations (Supplementary Information Figure C.7).

## 5 Discussion and Conclusion

Our simulation analysis reveals that the economic effects of lockdowns in different regions interact with each other through supply chains. Our results and their implications can be summarised as follows.

First, when a firm is locked down, its suppliers and customer firms are affected because of a lack of demand and supply, respectively. Therefore, the production of regions can recover more by lifting their lockdowns together when they are closely linked through supply chains in either direction (Figure 7(a)–(b)). Besides the total number of links between the two regions, the intensity of such links compared with those with others is also important.

Second, when the firms in a region are in more upstream positions in the whole network or they are mostly suppliers of simple parts, the production of the region does not recover substantially by lifting its lockdown alone (Figure 6(d)). Although the negative economic effect of lockdown can propagate downstream and upstream, firms can mitigate downstream propagation easily using inventory or replacing locked-down suppliers. The difference between the downstream and upstream effects of lockdown is aggravated as the effect propagates further through supply chains. This finding is in line with the literature [33, 35] that also finds the upstream accumulation of negative effects on profits and assets. In practice, our result implies that a region with many small- and medium-sized suppliers of simple materials and parts should be cautious about whether it lifts its lockdown, which may not result in a large economic benefit but still promote the spread of COVID-19.

Third, the production of a region can recover more by lifting its lockdown when it is more isolated in the network or embodies more supply-chain loops within the region (Figures 6(a) and (b)). Similarly, the production of the two regions can recover more by lifting their lockdowns together when their inter-regional links have more loops (Figure 7(c)). These results imply that the positive economic effect of lifting a lockdown circulates and is intensified in loops, consistent with those in [5]. Supply-chain loops exist between two regions when the final goods produced are used as inputs by suppliers, while suppliers provide parts and components to final-good producers and the loop stretches across two regions. The importance of loops in the diffusion of the economic effects in networks is not fully recognised either in the academic literature or in policymaking.

Finally, the recovery of a region from its lockdown is greater when suppliers still locked down can be replaced by those within the region or in other regions without a lockdown in place (Figures 6(e) and 7(f)). The role of the substitutability of suppliers in mitigating the propagation effect through supply chains has been empirically found in the literature [2, 7, 5, 6]. In practice, this finding suggests two management strategies for regional governments and firms. To minimise the economic loss from lockdown, a region should develop a full set of industries to allow the substitution of any industry to be possible. Alternatively, the firms in the region should be linked with geographically diverse suppliers so that suppliers in a locked-down region can be replaced by those in other regions without a lockdown.

All these results point to the need for policy coordination among regions when regional governments impose or lift a lockdown. Although this study uses the inter-firm supply chains within a country and considers the economic effect of prefecture-level lockdowns, our results can be applied to the effect of country-level lockdowns propagating through international supply chains. For example, many suppliers of German firms are located in Eastern Europe and many suppliers of US firms are in Mexico. Our results thus suggest that the economic gains of Eastern Europe and Mexico from lifting their lockdowns is minimal if Germany and the United States, respectively, remain locked down. In addition, our framework can be applied to the case of other infectious diseases, and it is likely to suggest a need for the inter-regional and international coordination of lockdown strategies to prevent the spread of infection.

## Acknowledgement

This research used the computational resources of the supercomputer Fugaku (the evaluation environment in the trial phase) provided by the RIKEN Center for Computational Science. OACIS [36] and CARAVAN [37] were used for the simulations in this study. This research was conducted as part of a project entitled ‘Research on relationships between economic and social networks and globalization’ undertaken at the Research Institute of Economy, Trade, and Industry (RIETI). The authors are grateful for the financial support of JSPS Kakenhi Grant Nos. JP18K04615 and JP18H03642. We thank Yoshi Fujiwara for advising how to calculate the HHD.

## 6 Data Availability

The data that support the findings of this study are available from Tokyo Shoko Research (TSR), but restrictions apply to the availability of these data, which were used under license for the current study, and so are not publicly available. Data are however available with permission of Tokyo Shoko Research (TSR).

## References

- [1] Thomas Hale, Sam Webster, Anna Petherick, Toby Phillips, and Beatriz Kira. Oxford COVID-19 government response tracker. <https://www.bsg.ox.ac.uk/research/research-projects/coronavirus-government-response-tracker>, 2020.
- [2] Jean-Noël Barrot and Julien Sauvagnat. Input specificity and the propagation of idiosyncratic shocks in production networks. *The Quarterly Journal of Economics*, 131(3):1543–1592, 2016.
- [3] Christoph E Boehm, Aaron Flaaen, and Nitya Pandalai-Nayar. Input linkages and the transmission of shocks: Firm-level evidence from the 2011 Tōhoku earthquake. *Review of Economics and Statistics*, 101(1):60–75, 2019.
- [4] Vasco M Carvalho, Makoto Nirei, Yukiko U Saito, and Alireza Tahbaz-Salehi. Supply chain disruptions: Evidence from the Great East Japan earthquake. Technical Report No. 17-5, Columbia Business School Research Paper, 2016.
- [5] Hiroyasu Inoue and Yasuyuki Todo. Firm-level propagation of shocks through supply-chain networks. *Nature Sustainability*, 2:841–847, 2019.
- [6] H. Inoue and Y. Todo. Propagation of negative shocks through firm networks: Evidence from simulation on comprehensive supply-chain data. *PLoS ONE*, 14(3), 2019.
- [7] Yuzuka Kashiwagi, Yasuyuki Todo, and Petr Matous. International propagation of economic shocks through global supply chains. Technical Report E1810, WINPEC Working Paper, 2018.
- [8] Barthélémy Bonadio, Zhen Huo, Andrei A Levchenko, and Nitya Pandalai-Nayar. Global supply chains in the pandemic. NBER Working Paper Series No. 27224, National Bureau of Economic Research, 2020.
- [9] Dabo Guan, Daoping Wang, Stephane Hallegatte, Jingwen Huo, Shuping Li, Yangchun Bai, Tianyang Lei, Qianyu Xue, Steven J Davis, D’Maris Coffman, et al. Global economic footprint of the covid-19 pandemic. *Nature Human Behavior*, 4:577–587, 2020.
- [10] Fergal McCann and Samantha Myers. Covid-19 and the transmission of shocks through domestic supply chains. Financial Stability Notes No. 2020-3, Central Bank of Ireland, 2020.
- [11] Warwick J McKibbin and Roshen Fernando. The global macroeconomic impacts of COVID-19: Seven scenarios. *Covid Economics, Vetted and Real-Time Papers*, 10:1–23, 2020.

- [12] Hiroyasu Inoue and Yasuyuki Todo. The propagation of the economic impact through supply chains: The case of a mega-city lockdown against the spread of covid-19. *Covid Economics, Vetted and Real-Time Papers*, 2:43–59, 2020.
- [13] Thomas W Valente. Network interventions. *Science*, 337(6090):49–53, 2012.
- [14] Thomas W Valente. Putting the network in network interventions. *Proceedings of the National Academy of Sciences*, 114(36):9500–9501, 2017.
- [15] Ruth F Hunter, Kayla de la Haye, Jennifer M Murray, Jennifer Badham, Thomas W Valente, Mike Clarke, and Frank Kee. Social network interventions for health behaviours and outcomes: A systematic review and meta-analysis. *PLoS medicine*, 16(9):e1002890, 2019.
- [16] Valerio Leone Sciabolazza, Raffaele Vacca, and Christopher McCarty. Connecting the dots: implementing and evaluating a network intervention to foster scientific collaboration and productivity. *Social Networks*, 61:181–195, 2020.
- [17] Garry Robins and Philippa Pattison. Interdependencies and social processes: Dependence graphs and generalized dependence structures. In Peter J Carrington, John Scott, and Stanley Wasserman, editors, *Models and methods in social network analysis*, volume 28, book section 10, pages 192–214. Cambridge University Press, Cambridge, 2005.
- [18] Mark EJ Newman and Michelle Girvan. Finding and evaluating community structure in networks. *Physical review E*, 69(2):026113, 2004.
- [19] Peter S. Goodman. Sweden has become the world’s cautionary tale, July 2020.
- [20] Michael Kremer and Edward Miguel. The illusion of sustainability. *Quarterly Journal of Economics*, 112(3):1007–1065, 2007.
- [21] John B Taylor. International monetary coordination and the great deviation. *Journal of Policy Modeling*, 35(3):463–472, 2013.
- [22] Albert-László Barabási. *Network science*. Cambridge University Press, 2016.
- [23] Yoshi Fujiwara and Hideaki Aoyama. Large-scale structure of a nation-wide production network. *The European Physical Journal B*, 77(4):565–580, 2010.
- [24] Robert Axtell, Bruce Blair, Samuel Bowles, Art DeVany, Malcolm DeBevoise, Steven Durlauf, Samuel David Epstein, Herbert Gintis, Alvin Goldman, and Scott Page. *Generative Social Science: Studies in Agent-based Computational Modeling*. Princeton University Press, Princeton, 2006.
- [25] Blake LeBaron and Leigh Tesfatsion. Modeling macroeconomics as open-ended dynamic systems of interacting agents. *American Economic Review*, 98(2):246–50, 2008.
- [26] Charles J Gomez and David MJ Lazer. Clustering knowledge and dispersing abilities enhances collective problem solving in a network. *Nature communications*, 10(1):1–11, 2019.
- [27] Stéphane Hallegatte. An adaptive regional input-output model and its application to the assessment of the economic cost of Katrina. *Risk analysis*, 28(3):779–799, 2008.
- [28] The Prime Minister of Japan and His Cabinet. Government responses on the coronavirus disease 2019. [http://japan.kantei.go.jp/ongoingtopics/\\_00013.html](http://japan.kantei.go.jp/ongoingtopics/_00013.html), 2020.
- [29] Yuichi Kichikawa, Hiroshi Iyetomi, Takashi Iino, and Hiroyasu Inoue. Community structure based on circular flow in a large-scale transaction network. *Applied Network Science*, 4(1):92, 2019.
- [30] Peter M Senge and Jay W Forrester. Tests for building confidence in system dynamics models. *System dynamics, TIMS studies in management sciences*, 14:209–228, 1980.
- [31] Güven Demirel, Bart L MacCarthy, Daniel Ritterskamp, Alan R Champneys, and Thilo Gross. Identifying dynamical instabilities in supply networks using generalized modeling. *Journal of Operations Management*, 65(2):136–159, 2019.

- [32] X. Jiang, L.-H. Lim, Y. Yao, and Y. Ye. Statistical ranking and combinatorial hodge theory. *Mathematical Programming*, 127(1):203–244, 2011.
- [33] Nicole Branger, René Marian Flacke, and Steffen Windmueller. Industry returns in global value chains: The role of upstreamness and downstreamness. SSRN 3476690, Social Science Research Network, 2019.
- [34] Ministry of Economy, Trade, and Industry. Indices of all industry production. <https://www.meti.go.jp/english/statistics/tyo/zenkatu/index.html>, 2020.
- [35] Jiangtao Fu, Petr Matous, and Yasuyuki Todo. Trade credit in global supply chains. RIETI Discussion Paper Series 18-E-049, Research Institute of Economy, Trade and Industry, 2018.
- [36] Yohsuke Murase, Takeshi Uchitane, and Nobuyasu Ito. An open-source job management framework for parameter-space exploration: Oacis. In *Journal of Physics: Conference Series*, volume 921, page 012001, 2017.
- [37] Yohsuke Murase, Hiroyasu Matsushima, Itsuki Noda, and Tomio Kamada. Caravan: a framework for comprehensive simulations on massive parallel machines. In *International Workshop on Massively Multiagent Systems*, pages 130–143. Springer, 2018.
- [38] Ministry of Economy, Trade and Industry, Japan. The 2015 updated Input-output table. [https://www.soumu.go.jp/english/dgpp\\_ss/data/io/index.htm](https://www.soumu.go.jp/english/dgpp_ss/data/io/index.htm), 2015.
- [39] C. Otto, S.N. Willner, L. Wenz, K. Frieler, and A. Levermann. Modeling loss-propagation in the global supply network: The dynamic agent-based model acclimate. *Journal of Economic Dynamics and Control*, 83:232–269, 2017.
- [40] Celian Colon, Stephane Hallegatte, and Julie Rozenberg. *Transportation and Supply Chain Resilience in the United Republic of Tanzania: Assessing the Supply-Chain Impacts of Disaster-Induced Transportation Disruptions*. World Bank, 2019.
- [41] Ministry of International Affairs and Communications. *Japan Standard Industrial Classification (Revision 13)*, 2013 (accessed June 1, 2020).
- [42] H. Iyetomi, H. Aoyama, Y. Fujiwara, W. Souma, I. Vodenska, and H. Yoshikawa. Relationship between macroeconomic indicators and economic cycles in u.s. *Sci. Rep.*, 10:8420, 2020. <https://doi.org/10.1038/s41598-020-65002-3>.
- [43] RS MacKay, S Johnson, and B Sansom. How directed is a directed network? *arXiv preprint arXiv:2001.05173*, 2020.
- [44] Y. Fujiwara, H. Inoue, T. Yamaguchi, H. Aoyama, and T. Tanaka. Money flow network among firms' accounts in a regional bank of japan. <https://ssrn.com/abstract=3662893>, July 2020.



# Supplementary Information

## A Data

### A.1 Supply chains

In the TSR data, the maximum number of suppliers and customers reported by each firm is 24. However, we can capture more than 24 by looking at supplier–customer relations from the opposite direction. Because the TSR data include the address of the headquarters of each firm, we can identify the longitude and latitude of each headquarters using the geocoding service provided by the Center for Spatial Information Science at the University of Tokyo.

Because the TSR data do not include the value of each transaction between two firms, we estimate it in two steps. First, we divide each supplier's sales into its customers in proportion to the sales of customers to obtain a tentative sales value. Second, we employ the IO table for Japan in 2015 [38] to transform these tentative values into more realistic ones. Specifically, we aggregate the tentative values at the firm-pair level to obtain the total sales for each pair of sectors. We then divide the total sales for each sector pair by the transaction values for the corresponding pair in the IO tables. The ratio is then used to estimate the transaction values between firms. The final consumption of each sector is allocated to all the firms in the sector using their sales as weights.

Although the supply chains used in our simulations are at the firm level, this study often uses features of the supply chains at the prefecture level because different prefectures imposed lockdowns to different degrees. Therefore, Figure A.1 illustrates the inter-prefecture supply chains. The red and blue lines show the inter-prefectural links between Tokyo and other prefectures and between other prefectures than Tokyo, respectively. We observe that Tokyo is the centre of supply chains in Japan, while several smaller hubs such as Aichi, Osaka, and Fukuoka also exist.

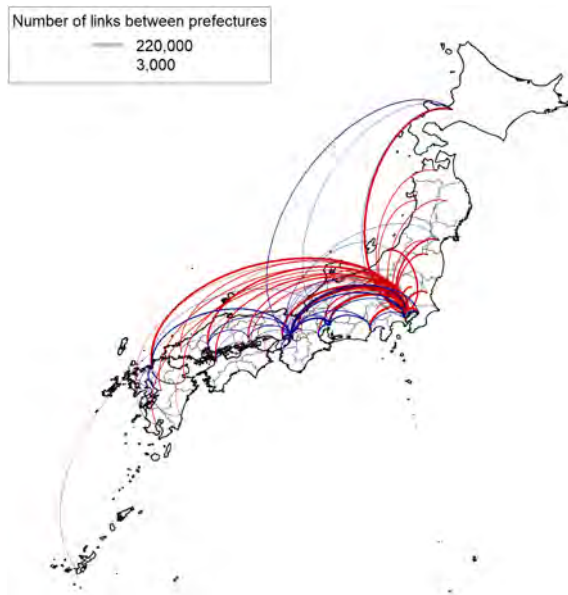


Figure A.1: Inter-prefectural links. Inter-firm links are aggregated into inter-prefectural links, ignoring the directions of the links. The inter-prefectural links between two prefectures are not shown here if the number of inter-firm links is less than 3,000. The links within each prefecture are also ignored. The red and blue lines show the inter-prefectural links between Tokyo and other prefectures and between two of other prefectures, respectively.

### A.2 Prefectures in Japan

Because this study uses prefectures as the unit of regions, it is important to provide information on the prefectures in Japan. Figure A.2 shows the locations, Japan Industrial Standard (JIS) codes, and names of the 47 prefectures. In Figures C.3 and the JIS codes are shown on the horizontal axis.

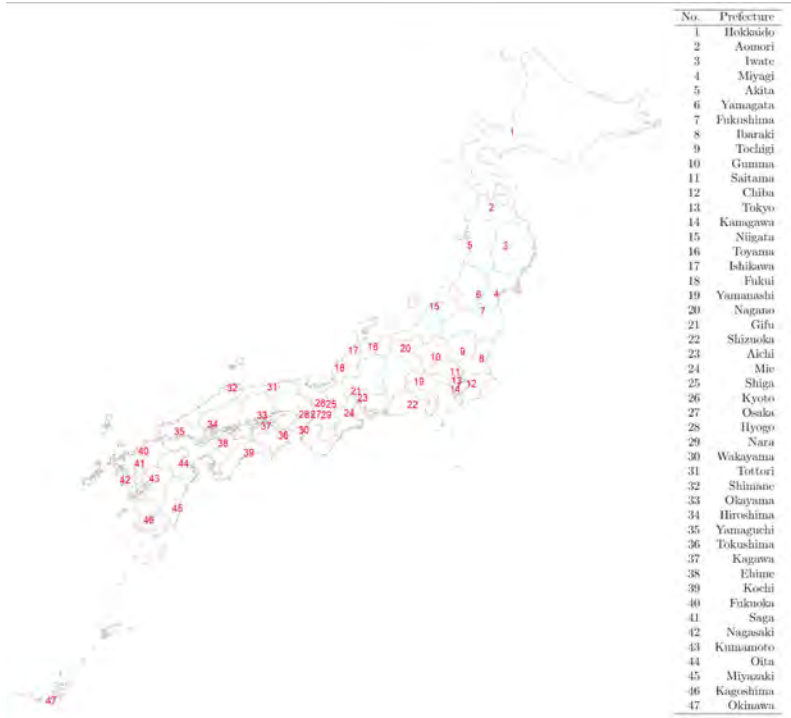


Figure A.2: Prefecture locations and their codes. The number on the map is the JIS code of each prefecture shown in the right table.

Covid Economics 56, 9 November 2020: 157-194

### A.3 Geographic presentation of the timeline of lockdowns

Supplementary Information Figure A.3 shows where and when the lockdowns were imposed to prefectures.

## B Methods

### B.1 Model

We rely on the model of Inoue and Todo [5, 6], an extension of the existing agent-based models used to examine the propagation of shocks by natural disasters through supply chains, including Hallegatte's model [27]. Each firm uses a variety of intermediates as inputs and delivers a sector-specific product to other firms and final consumers. Firms have an inventory of intermediates to address possible supply shortages.

In the initial stage before an economic shock, the daily trade volume from supplier  $j$  to customer  $i$  is denoted by  $A_{i,j}$ , whereas the daily trade volume from firm  $i$  to final consumers is denoted by  $C_i$ . Then, the initial production of firm  $i$  in a day is given by

$$P_{\text{ini}i} = \sum_j A_{j,i} + C_i. \quad (6)$$

On day  $t$  after the initial stage, the previous day's demand for firm  $i$ 's product is  $D_i^*(t-1)$ . The firm thus makes orders to each supplier  $j$  so that the amount of its product of supplier  $j$  can meet this demand,  $A_{i,j}D_i^*(t-1)/P_{\text{ini}i}$ . We assume that firm  $i$  has an inventory of the intermediate goods produced by firm  $j$  on day  $t$ ,  $S_{i,j}(t)$ , and aims to restore this inventory to a level equal to a given number of days  $n_i$  of the utilisation of the product of supplier  $j$ . The constant  $n_i$  is assumed to be Poisson distributed, where its mean is  $n$ , which is a parameter. In addition,  $n_i$  does not take a number smaller than 4, although the model in the previous literature sets this number to 2. Since the small minimum inventory size causes a bullwhip effect (fluctuation of production level), we set the number to 4 in this work and recalibrate the parameters. When the actual inventory is smaller than its target, firm  $i$  increases its inventory gradually by  $1/\tau$  of the gap, so that it reaches the target in  $\tau$  days, where  $\tau$  is assumed to be 6 to follow the original

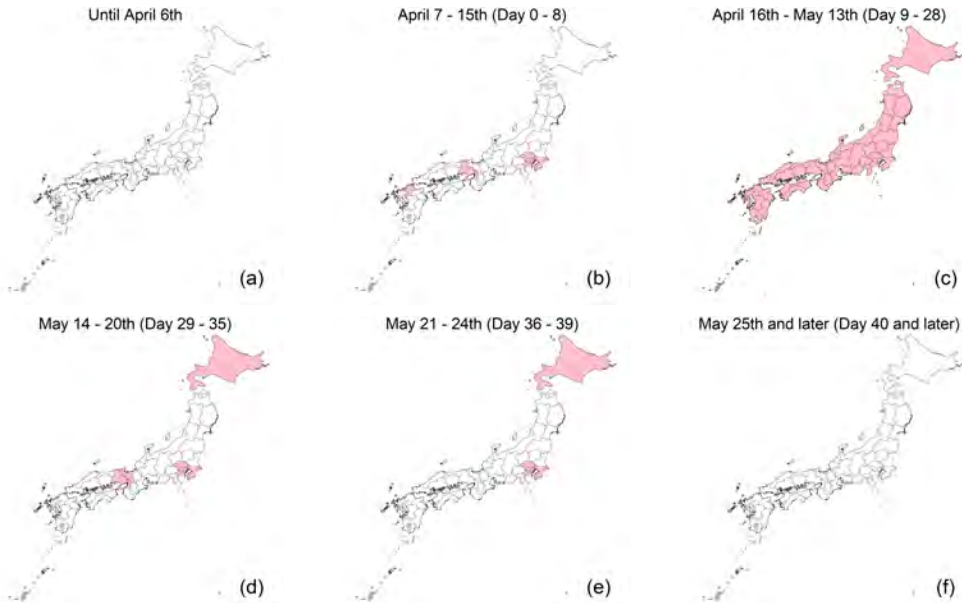


Figure A.3: Changes in locked down prefectures. The pink prefectures in each panel show those that were locked down during the period.

model [27]. Therefore, the order from firm  $i$  to its supplier  $j$  on day  $t$ , denoted by  $O_{i,j}(t)$ , is given by

$$O_{i,j}(t) = A_{i,j} \frac{D_i^*(t-1)}{P_{ini}} + \frac{1}{\tau} [n_i A_{i,j} - S_{i,j}(t)], \tag{7}$$

where the inventory gap is in brackets. Accordingly, total demand for the product of supplier  $i$  on day  $t$ ,  $D_i(t)$ , is given by the sum of final demand from final consumers and total orders from customers:

$$D_i(t) = \sum_j O_{j,i}(t) + C_i. \tag{8}$$

Now, suppose that an economic shock hits the economy on day 0 and that firm  $i$  is directly affected. Subsequently, the proportion  $\delta_i(t)$  of the production capital of firm  $i$  is malfunctioning. In this study,  $\delta_i$  is determined by the sector and prefecture to which firm  $i$  belongs, and a term for which a lockdown is imposed. Hence, the production capacity of firm  $i$ , defined as its maximum production assuming no supply shortages,  $P_{cap_i}(t)$ , is given by

$$P_{cap_i}(t) = P_{ini}(1 - \delta_i(t)). \tag{9}$$

The production of firm  $i$  might also be limited by the shortage of supplies. Because we assume that firms in the same sector produce the same product, the shortage of supplies suffered by firm  $j$  in sector  $s$  can be compensated for by supplies from firm  $k$  in the same sector  $s$ . Firms cannot substitute new suppliers for affected suppliers after the disaster, as we assume fixed supply chains. Thus, the total inventory of the products delivered by firms in sector  $s$  in firm  $i$  on day  $t$  is

$$S_{toti,s}(t) = \sum_{j \in s} S_{i,j}(t). \tag{10}$$

The initial consumption of products in sector  $s$  of firm  $i$  before the disaster is also defined for convenience:

$$A_{toti,s} = \sum_{j \in s} A_{i,j}. \tag{11}$$

The maximum possible production of firm  $i$  limited by the inventory of product of sector  $s$  on day  $t$ ,  $P_{proi,s}(t)$ , is given by

$$P_{proi,s}(t) = \frac{S_{toti,s}(t)}{A_{toti,s}} P_{ini}. \tag{12}$$

Then, we can determine the maximum production of firm  $i$  on day  $t$ , considering its production capacity,  $P_{cap_i}(t)$ , and its production constraints due to the shortage of supplies,  $P_{proi,s}(t)$ :

$$P_{max_i}(t) = \text{Min} (P_{cap_i}(t), \text{Min}_s(P_{proi,s}(t))). \tag{13}$$

Therefore, the actual production of firm  $i$  on day  $t$  is given by

$$P_{act_i}(t) = \text{Min} (P_{max_i}(t), D_i(t)). \tag{14}$$

When demand for a firm is greater than its production capacity, the firm cannot completely satisfy its demand, as denoted by Equation (9). In this case, firms should ration their production to their customers. We propose a rationing policy in which customers and final consumers are prioritised if they have small amount of order to their initial order, instead of being treated equally, as in the previous work [27].

Suppose that firm  $i$  has customers  $j$  and a final consumer. Then, the ratios of the order from customers  $j$  and the final consumer after the shock to the one before the shock denoted by  $O_{j,i}^{rel}$  and  $O_c^{rel}$ , respectively are determined by the following steps, where  $O_{j,i}^{sub}$  and  $O_c^{sub}$  are temporal variables used to calculate the realised order and are set to be zero initially.

1. Obtain the remaining production  $r$  of firm  $i$
2. Calculate  $O_{\min}^{rel} = \text{Min}(O_{j,i}^{rel}, O_c^{rel})$
3. If  $r \leq (\sum_j O_{j,i}^{rel} O_{j,i} + O_{\min}^{rel} C_i)$  then proceed to 8

4. Add  $O_{\min}^{rel}$  to  $O_{j,i}^{sub}$  and  $O_c^{sub}$
5. Subtract  $(\sum_j O_{\min}^{rel} O_{j,i} + O_{\min}^{rel} C_i)$  from  $r$
6. Remove the customer or the final consumer that indicated  $O_{\min}^{rel}$  from the calculation
7. Return to Step 2
8. Calculate  $O^{rea}$  that satisfies  $r = (\sum_j O^{rea} O_{j,i} + O^{rea} C_i)$
9. Obtain  $O_{j,i}^* = O^{rea} O_{j,i} + O_{j,i}^{sub}$  and  $C_i^* = O^{rea} C_i + O_c^{sub} C_i$ , where the realised order from firm  $j$  to supplier  $i$  is denoted by  $O_{j,i}^*(t)$ , and the realised order from a final consumer is  $C_i^*$
10. Finalise the calculation

Under this rationing policy, total realised demand for firm  $i$ ,  $D_i^*(t)$ , is given by

$$D_i^*(t) = \sum_j O_{i,j}^*(t) + C_i^*, \tag{15}$$

where the realised order from firm  $i$  to supplier  $j$  is denoted by  $O_{i,j}^*(t)$  and that from the final consumers is  $C_i^*$ . According to firms' production and procurement activities on day  $t$ , the inventory of firm  $j$ 's product in firm  $i$  on day  $t + 1$  is updated to

$$S_{i,j}(t + 1) = S_{i,j}(t) + O_{i,j}^*(t) - A_{i,j} \frac{P_{acti}(t - 1)}{P_{ini}}. \tag{16}$$

Several caveats of this model and data should be mentioned. First, we assume that firms cannot find any new supplier when facing a shortage of supplies from their current suppliers. Second, for simplicity, our model assumes that inputs from the service sector can be stored as inventory, just like inputs from manufacturing. Third, our model ignores changes in the prices of products and wages of labour incorporated in [39, 40] and focuses on the dynamics of production because of supply-chain disruptions. Fourth, the TSR data report only the location of the headquarters of each firm, not the location of its branches. Because the headquarters of firms are concentrated in Tokyo, production activities in Tokyo are most likely to be overvalued in our analysis. Fifth, because of data limitations, we ignore the international supply-chain links in our simulations. Finally, this study ignores the impacts of COVID-19 on human and firm behaviours in the post-COVID era. These behavioural changes may influence consumption and production that are assumed to remain the same in this era.

## B.2 Sectoral differences in production capacity after lockdowns

No data for production capacity (i.e.  $P_{cap}$  in the model) during the lockdown of Japan at the firm or sector level are available. Although the Indices of All Industry Activities (IAIA) provides data for *post-lockdown production* at the sector level (Section 3.3), or  $P_{act}$  in our model averaged within a sector, we need information about *production capacity*,  $P_{cap}$ . Therefore, we assume that the rate of reduction in production capacity for each sector is given by the degree of the reduction because of exposure to the virus [8] multiplied by the share of workers who cannot work at home [9] (Section 3.3). The rate of reduction because of exposure to the virus is determined by how the workers in the sector have to reduce their activities to avoid contact with others for infection prevention. Because [9] define the rate of reduction uniformly worldwide, we modify the rate for some sectors that clearly differ from the practice in Japan. Table B.1 shows the rates of reduction for each sector assumed in our simulations.

Table B.1: Sector-specific rates of reduction in production capacity. Sectors are classified by the JIS classification [41] at the two-digit level, except for industries 560, 561, and 569 for which we use three-digit codes to reflect the actual circumstances. The sector names are abbreviated. Table B.2 lists the sector descriptions and abbreviations.

Code	Sector (abbreviated)	Reduction rate	Work-at -home rate	Exposure level	Rationale
------	-------------------------	----------------	-----------------------	-------------------	-----------

1	AGR.	0.0866	0.134	0.1	Low exposure
2	FRS.	0.0866	0.134	0.1	Low exposure
3	FIS.	0.0866	0.134	0.1	Low exposure
4	AQA.	0.0866	0.134	0.1	Low exposure
5	MIN.	0.3185	0.363	0.5	Ordinary
6	CNS.GEN.	0.379	0.242	0.5	Ordinary
7	CNS.SPC.	0.379	0.242	0.5	Ordinary
8	EQP.	0.379	0.242	0.5	Ordinary
9	MAN.FOD.	0.38	0.240	0.5	Ordinary
10	MAN.BEV.	0.38	0.240	0.5	Ordinary
11	MAN.Text	0.334	0.332	0.5	Ordinary
12	MAN.LUM.	0.384	0.232	0.5	Ordinary
13	MAN.FUR.	0.384	0.232	0.5	Ordinary
14	MAN.PUL.	0.338	0.324	0.5	Ordinary
15	PRT.	0.338	0.324	0.5	Ordinary
16	MAN.CHM.	0.2645	0.471	0.5	Ordinary
17	MAN.PET.	0.3255	0.349	0.5	Ordinary
18	MAN.PLA.	0.352	0.296	0.5	Ordinary
19	MAN.RUB.	0.352	0.296	0.5	Ordinary
20	MAN.LET.	0.334	0.332	0.5	Ordinary
21	MAN.CER.	0.3545	0.291	0.5	Ordinary
22	MAN.IRN.	0.366	0.268	0.5	Ordinary
23	MAN.NFM.	0.366	0.268	0.5	Ordinary
24	MAN.FBM.	0.3475	0.305	0.5	Ordinary
25	MAN.GNM.	0.302	0.396	0.5	Ordinary
26	MAN.PRM.	0.302	0.396	0.5	Ordinary
27	MAN.BSM.	0.302	0.396	0.5	Ordinary
28	EPT.	0.1665	0.667	0.5	Ordinary
29	MAN.ELM.	0.29	0.420	0.5	Ordinary
30	MAN.INF.	0.1665	0.667	0.5	Ordinary
31	MAN.TRN.	0.252	0.496	0.5	Ordinary
32	MAN.MSC.	0.3525	0.295	0.5	Ordinary
33	ELE.	0	0.377	0	Lifeline
34	GAS.	0	0.377	0	Lifeline
35	HET.	0	0.377	0	Lifeline
36	WTR.	0	0.377	0	Lifeline
37	COM.	0	0.599	0	Lifeline
38	BRD.	0	0.808	0	Lifeline
39	INF.SVC.	0.0485	0.903	0.5	Ordinary
40	INT.	0	0.599	0	Lifeline
41	INF.DST.	0.096	0.808	0.5	Ordinary
42	RLW.TRP.	0	0.299	0	Lifeline
43	PAS.TRP.	0	0.299	0	Lifeline
44	FRE.TRP.	0	0.299	0	Lifeline
45	WTR.TRP.	0	0.299	0	Lifeline
46	AIR.TRP.	0	0.299	0	Lifeline
47	WRH.	0	0.299	0	Lifeline
48	SVC.TRP.	0	0.299	0	Lifeline
49	PST.SVC.	0	0.299	0	Lifeline
50	WHL.GEN.	0.0525	0.475	0.1	Low exposure
51	WHL.TEX.	0.0525	0.475	0.1	Low exposure
52	WHL.FOD.	0.0525	0.475	0.1	Low exposure
53	WHL.MAT.	0.0525	0.475	0.1	Low exposure
54	WHL.MCN.	0.0525	0.475	0.1	Low exposure
55	WHL.MSC.	0.0525	0.475	0.1	Low exposure
560	RTL.ADM.	0.0525	0.475	0.1	Low exposure
561	RTL.DPT.	0.525	0.475	1	Closed
569	RTL.MSC.	0	0.475	0	Lifeline

57	RTL.GEN.	0.0525	0.475	0.1	Low exposure
58	RTL.FOD.	0.0525	0.475	0.1	Low exposure
59	RTL.MCN.	0.0525	0.475	0.1	Low exposure
60	RTL.MSC.	0.0525	0.475	0.1	Low exposure
61	RTL.NST.	0.0525	0.475	0.1	Low exposure
62	FIN.BNK.	0.0214	0.786	0.1	Low exposure
63	FIN.ORG.	0.0214	0.786	0.1	Low exposure
64	FIN.LON.	0.0214	0.786	0.1	Low exposure
65	FIN.TRN.	0.0214	0.786	0.1	Low exposure
66	FIN.AUX.	0.0214	0.786	0.1	Low exposure
67	INS.	0.0214	0.786	0.1	Low exposure
68	RST.AGN.	0.0423	0.577	0.1	Low exposure
69	RTS.LES.	0.0423	0.577	0.1	Low exposure
70	RNT.	0.0362	0.638	0.1	Low exposure
71	SCI.	0.0172	0.828	0.1	Low exposure
72	SVC.PRF.	0.0362	0.638	0.1	Low exposure
73	ADV.	0.0362	0.638	0.1	Low exposure
74	SVC.TEC.	0.0362	0.638	0.1	Low exposure
75	ACM.	0.889	0.111	1	Closed
76	EAT.	0.4445	0.111	0.5	Ordinary
77	DEL.	0	0.479	0	Lifeline
78	LND.	0.2605	0.479	0.5	Ordinary
79	SVC.PSN.	0.2605	0.479	0.5	Ordinary
80	SVC.AMS.	0.521	0.479	1	Closed
81	SCH.	0.0172	0.828	0.1	Low exposure
82	EDC.	0.0172	0.828	0.1	Low exposure
83	MED.	0	0.247	0	Lifeline
84	HLT.	0	0.247	0	Lifeline
85	WEL.	0	0.247	0	Lifeline
86	PST.OFC.	0	0.638	0	Lifeline
87	CAS.	0.0362	0.638	0.1	Low exposure
88	WAS.	0.0362	0.638	0.1	Low exposure
89	SVC.AUT.	0.0362	0.638	0.1	Low exposure
90	SVC.MCN.	0.0362	0.638	0.1	Low exposure
91	SVC.EMP.	0.0362	0.638	0.1	Low exposure
92	SVC.BUS.	0.0362	0.638	0.1	Low exposure
93	PLT.	0.0362	0.638	0.1	Low exposure
94	REL.	0.0362	0.638	0.1	Low exposure
95	SVC.MSC.	0.0362	0.638	0.1	Low exposure
96	GOV.INT.	0	0.485	0	Lifeline
97	GOV.NAT	0	0.485	0	Lifeline
98	GOV.LOC.	0	0.485	0	Lifeline
99	NEC	0.181	0.638	0.5	Ordinary

Table B.2: Sector classifications and abbreviations.

Code	Description	Abbreviation
01	AGRICULTURE	AGR.
02	FORESTRY	FRS.
03	FISHERIES, EXCEPT AQUACULTURE	FIS.
04	AQUACULTURE	AQA.
05	MINING AND QUARRYING OF STONE AND GRAVEL	MIN.
06	CONSTRUCTION WORK, GENERAL INCLUDING PUBLIC AND PRIVATE CONSTRUCTION WORK	CNS.GEN.
07	CONSTRUCTION WORK BY SPECIALIST CONTRACTOR, EXCEPT EQUIPMENT INSTALLATION WORK	CNS.SPC.
08	EQUIPMENT INSTALLATION WORK	EQP.
09	MANUFACTURE OF FOOD	MAN.FOD.
10	MANUFACTURE OF BEVERAGES, TOBACCO AND FEED	MAN.BEV.
11	MANUFACTURE OF TEXTILE PRODUCTS	MAN.TEX
12	MANUFACTURE OF LUMBER AND WOOD PRODUCTS, EXCEPT FURNITURE	MAN.LUM.
13	MANUFACTURE OF FURNITURE AND FIXTURES	MAN.FUR.
14	MANUFACTURE OF PULP, PAPER AND PAPER PRODUCTS	MAN.PUL.
15	PRINTING AND ALLIED INDUSTRIES	PRT.
16	MANUFACTURE OF CHEMICAL AND ALLIED PRODUCTS	MAN.CHM.
17	MANUFACTURE OF PETROLEUM AND COAL PRODUCTS	MAN.PET.
18	MANUFACTURE OF PLASTIC PRODUCTS, EXCEPT OTHERWISE CLASSIFIED	MAN.PLA.
19	MANUFACTURE OF RUBBER PRODUCTS	MAN.RUB.
20	MANUFACTURE OF LEATHER TANNING, LEATHER PRODUCTS AND FUR SKINS	MAN.LET.
21	MANUFACTURE OF CERAMIC, STONE AND CLAY PRODUCTS	MAN.CER.
22	MANUFACTURE OF IRON AND STEEL	MAN.IRN.
23	MANUFACTURE OF NON-FERROUS METALS AND PRODUCTS	MAN.NFM.
24	MANUFACTURE OF FABRICATED METAL PRODUCTS	MAN.FBM.
25	MANUFACTURE OF GENERAL-PURPOSE MACHINERY	MAN.GNM.
26	MANUFACTURE OF PRODUCTION MACHINERY	MAN.PRM.
27	MANUFACTURE OF BUSINESS ORIENTED MACHINERY	MAN.BSM.
28	ELECTRONIC PARTS, DEVICES AND ELECTRONIC CIRCUITS	EPT.
29	MANUFACTURE OF ELECTRICAL MACHINERY, EQUIPMENT AND SUPPLIES	MAN.ELM.
30	MANUFACTURE OF INFORMATION AND COMMUNICATION ELECTRONICS EQUIPMENT	MAN.INF.
31	MANUFACTURE OF TRANSPORTATION EQUIPMENT	MAN.TRN.
32	MISCELLANEOUS MANUFACTURING INDUSTRIES	MAN.MSC.
33	PRODUCTION, TRANSMISSION AND DISTRIBUTION OF ELECTRICITY	ELE.
34	PRODUCTION AND DISTRIBUTION OF GAS	GAS.
35	HEAT SUPPLY	HET.



36	COLLECTION, PURIFICATION AND DISTRIBUTION OF WATER, AND SEWAGE COLLECTION, PROCESSING	WTR.
37	COMMUNICATIONS	COM.
38	BROADCASTING	BRD.
39	INFORMATION SERVICES	INF.SVC.
40	SERVICES INCIDENTAL TO INTERNET	INT.
41	VIDEO PICTURE INFORMATION, SOUND INFORMATION, CHARACTER INFORMATION PRODUCTION AND DISTRIBUTION	INF.DST.
42	RAILWAY TRANSPORT	RLW.TRP.
43	ROAD PASSENGER TRANSPORT	PAS.TRP.
44	ROAD FREIGHT TRANSPORT	FRE.TRP.
45	WATER TRANSPORT	WTR.TRP.
46	AIR TRANSPORT	AIR.TRP.
47	WAREHOUSING	WRH.
48	SERVICES INCIDENTAL TO TRANSPORT	SVC.TRP.
49	POSTAL SERVICES, INCLUDING MAIL DELIVERY	PST.SVC.
50	WHOLESALE TRADE, GENERAL MERCHANDISE	WHL.GEN.
51	WHOLESALE TRADE (TEXTILE AND APPAREL)	WHL.TEX.
52	WHOLESALE TRADE (FOOD AND BEVERAGES)	WHL.FOD.
53	WHOLESALE TRADE (BUILDING MATERIALS, MINERALS AND METALS, ETC)	WHL.MAT.
54	WHOLESALE TRADE (MACHINERY AND EQUIPMENT)	WHL.MCN.
55	MISCELLANEOUS WHOLESALE TRADE	WHL.MSC.
560	ESTABLISHMENTS ENGAGED IN ADMINISTRATIVE OR ANCILLARY ECONOMIC ACTIVITIES	RTL.ADM.
561	DEPARTMENT STORES AND GENERAL MERCHANDISE SUPERMARKET	RTL.DPT.
569	MISCELLANEOUS RETAIL TRADE, GENERAL MERCHANDISE	RTL.MSC.
57	RETAIL TRADE, GENERAL MERCHANDISE	RTL.GEN.
58	RETAIL TRADE (FOOD AND BEVERAGE)	RTL.FOD.
59	RETAIL TRADE (MACHINERY AND EQUIPMENT)	RTL.MCN.
60	MISCELLANEOUS RETAIL TRADE	RTL.MSC.
61	NONSTORE RETAILERS	RTL.NST.
62	BANKING	FIN.BNK.
63	FINANCIAL INSTITUTIONS FOR COOPERATIVE ORGANIZATIONS	FIN.ORG.
64	NON-DEPOSIT MONEY CORPORATIONS, INCLUDING LENDING AND CREDIT CARD BUSINESS	FIN.LON.
65	FINANCIAL PRODUCTS TRANSACTION DEALERS AND FUTURES COMMODITY TRANSACTION DEALERS	FIN.TRN.
66	FINANCIAL AUXILIARIES	FIN.AUX.
67	INSURANCE INSTITUTIONS, INCLUDING INSURANCE AGENTS, BROKERS AND SERVICES	INS.
68	REAL ESTATE AGENCIES	RST.AGN.
69	REAL ESTATE LESSORS AND MANAGERS	RTS.LES.
70	GOODS RENTAL AND LEASING	RNT.
71	SCIENTIFIC AND DEVELOPMENT RESEARCH INSTITUTES	SCI.

72	PROFESSIONAL SERVICES, N.E.C.	SVC.PRF.
73	ADVERTISING	ADV.
74	TECHNICAL SERVICES, N.E.C.	SVC.TEC.
75	ACCOMMODATION	ACM.
76	EATING AND DRINKING PLACES	EAT.
77	FOOD TAKE OUT AND DELIVERY SERVICES	DEL.
78	LAUNDRY, BEAUTY AND BATH SERVICES	LND.
79	MISCELLANEOUS LIVING-RELATED AND PERSONAL SERVICES	SVC.PSN.
80	SERVICES FOR AMUSEMENT AND RECREATION	SVC.AMS.
81	SCHOOL EDUCATION	SCH.
82	MISCELLANEOUS EDUCATION, LEARNING SUPPORT	EDC.
83	MEDICAL AND OTHER HEALTH SERVICE	MED.
84	PUBLIC HEALTH AND HYGIENE	HLT.
85	SOCIAL INSURANCE, SOCIAL WELFARE AND CARE SERVICES	WEL.
86	POSTAL OFFICE	PST.OFC.
87	COOPERATIVE ASSOCIATIONS, N.E.C.	CAS.
88	WASTE DISPOSAL BUSINESS	WAS.
89	AUTOMOBILE MAINTENANCE SERVICES	SVC.AUT.
90	MACHINE, ETC. REPAIR SERVICES, EXCEPT OTHERWISE CLASSIFIED	SVC.MCN.
91	EMPLOYMENT AND WORKER DISPATCHING SERVICES	SVC.EMP.
92	MISCELLANEOUS BUSINESS SERVICES	SVC.BUS.
93	POLITICAL, BUSINESS AND CULTURAL ORGANIZATIONS	PLT.
94	RELIGION	REL.
95	MISCELLANEOUS SERVICES	SVC.MSC.
96	FOREIGN GOVERNMENTS AND INTERNATIONAL AGENCIES IN JAPAN	GOV.INT.
97	NATIONAL GOVERNMENT SERVICES	GOV.NAT.
98	LOCAL GOVERNMENT SERVICES	GOV.LOC.
99	INDUSTRIES UNABLE TO CLASSIFY	NEC

### B.3 Helmholtz-Hodge decomposition

The Helmholtz-Hodge decomposition (HHD) decomposes a flow from a node to another in a network into a potential flow component and a loop flow component. A potential flow component is determined by the upstream/downstream location of the node in a network [32], whereas a loop flow component is given by a constraint such that the summation of the incoming and outgoing loop flows of all the nodes equals zero. This method has been used to find the structure of potential and loop flows in complex networks. See, for example, [29, 42, 43, 44].

Suppose we have a flow of a matrix denoted by  $B_{ij}$  such that a flow from node  $i$  to node  $j$  is represented by  $B_{ij}$ . For simplicity, we assume  $\forall i, j B_{ij} \geq 0$ .  $A_{ij}$  is a binary adjacency matrix generated from  $B_{ij}$ :

$$A_{ij} = \begin{cases} 1 & \text{if } B_{ij} > 0, \\ 0 & \text{otherwise.} \end{cases} \tag{17}$$

We define a ‘net flow’  $F_{ij}$  by

$$F_{ij} = B_{ij} - B_{ji}, \tag{18}$$

and a ‘net weight’  $w_{ij}$  by

$$w_{ij} = A_{ij} + A_{ji}. \tag{19}$$

Note that  $w_{ij}$  is symmetric,  $w_{ij} = w_{ji}$ , and non-negative,  $w_{ij} \geq 0$ , for any pair of  $i$  and  $j$ .

Then, the HHD is given by

$$F_{ij} = F_{ij}^{(c)} + F_{ij}^{(p)}, \tag{20}$$

where the loop flow  $F_{ij}^{(c)}$  satisfies

$$\sum_j F_{ij}^{(c)} = 0, \tag{21}$$

meaning that loop flows are divergence-free. The potential flow,  $F_{ij}^{(p)}$ , can be expressed as

$$F_{ij}^{(p)} = w_{ij}(\phi_i - \phi_j), \tag{22}$$

where  $\phi_i$  is the Helmholtz-Hodge potential of node  $i$  that identifies its upstream/downstream position in the network. More precisely,  $\phi_i$  is larger when node  $i$  is located in a more upstream position in the network and vice versa. Equation (22) indicates that the potential flow  $F_{ij}^{(p)}$  is the difference in the HH potential between two nodes when the two are linked and zero when they are not linked. We further assume

$$\sum_i \phi_i = 0 \tag{23}$$

for normalisation purposes. Then, equations (20)–(23) can be uniquely solved for  $F_{ij}^{(c)}$ ,  $F_{ij}^{(p)}$ , and  $\phi_i$  for all  $i$  and  $j$  in the whole network.

Figure B.1 shows a simple example to explain the intuition behind the potential and loop flows, potential obtained from the HHD, and potential and loop flow measures between two prefectures (i.e.  $Pot_{ab}$ ,  $Pot_{ba}$ , and  $Loop_{ab}$  defined in Section 4.4). The left panel shows a supply chain with six firms in prefectures  $a$  and  $b$ . The right top and bottom panels indicate the potential flows and loop flows, respectively decomposed by the HHD. The numbers in red in the right top panel represent the HH potential, or the upstreamness in supply chains, for each firm. Although there is no ‘loop’ in a standard sense among the firms in this example, the HHD identifies loop flows in the sense that the nodes in the loop are affected by each other. Hence, shocks circulate in the loop and work differently from those in the non-loop potential flows.

Specifically,  $Pot_{ab}$  is the sum of the total potential flows from the firms in prefecture  $a$  to those in prefecture  $b$  (there is only a potential flow from prefectures  $a$  to  $b$  in this example) divided by the total flows of firms in prefecture  $a$ . Therefore,  $Pot_{ab} = (2/3)/4 = 1/6$ .  $Pot_{ba}$  is the opposite direction and  $Pot_{ba} = 1/6$ . Because  $Loop_{ab}$  is the sum of the total loop flows between the firms in prefectures  $a$  and  $b$  (there are two loop flows between  $a$  and  $b$  in this example),  $Loop_{ab} = (2/3)/4 = 1/6$  and, similarly,  $Loop_{ba} = 1/6$ .

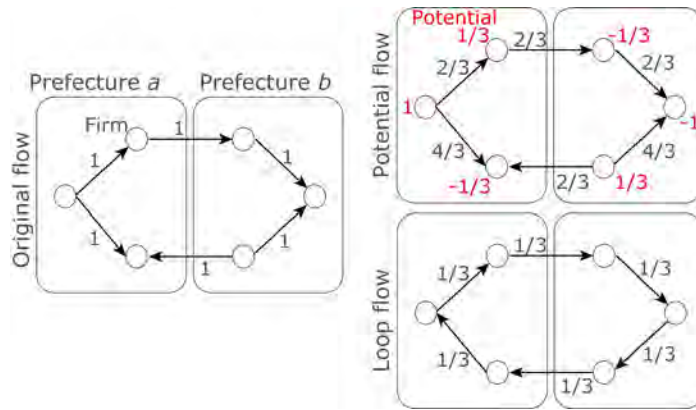


Figure B.1: An example of the HHD and loop and potential flow measures of prefectures. The left panel shows the supply chains of the six firms in the two prefectures. The right top and bottom panels present the potential flows and loop flows, respectively obtained from the HHD.

Figure B.2 shows the average of the HH potential  $\phi_i$  of the firms in the supply-chain network, which is normalised so that its overall average is zero, for each prefecture. This figure illustrates the large variation in the upstreamness of the firms at the prefecture level.

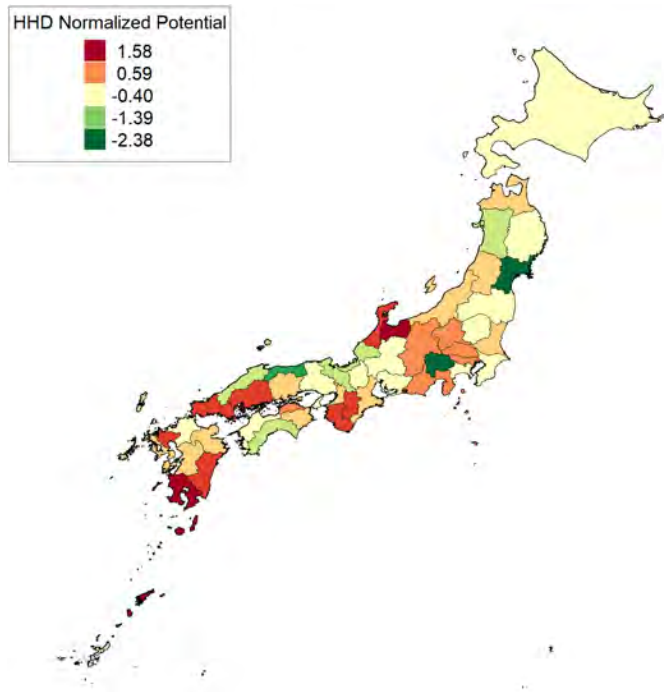


Figure B.2: Choropleth map of the potential calculated by the Helmholtz-Hodge decomposition. The average HH potential over all the firms in each prefecture is presented.

### B.4 Substitutability for two regions

Since the definition of the substitutability measure for two regions is not as simple as the definition for one region, we provide a further explanation. Figure B.3 is an example for the suppliers of a firm in prefecture *a*. The substitutability of prefecture *a* by prefecture *b* is a fraction. The denominator is the total number of suppliers that delivers goods to the firms in prefecture *a* except suppliers in prefecture *a* or *b*. (Here, we call this  $A_i$  in the figure.) Hereafter, a supplier means a supplier of a firm in prefecture *a*. The numerator is the total number of substitutable suppliers in  $A_i$ . A supplier in  $A_i$  is substitutable if a supplier in prefecture *b* belongs to the same industry as the focal supplier.

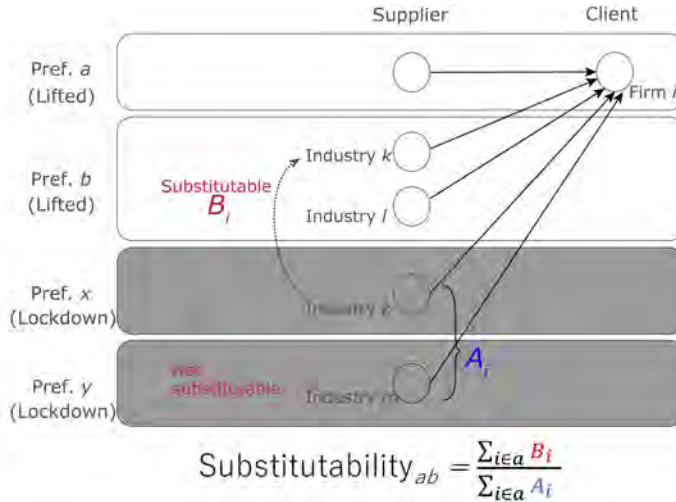


Figure B.3: An example of the substitutability measure for two regions. The bottom shows the equation.  $A_i$  is the total number of suppliers outside prefectures *a* and *b*. The bottom two suppliers are applicable. A supplier in prefecture *b* belongs to the same industry as the upper firm of the outside suppliers, whereas the lower firm of the outside suppliers is not substitutable. Hence,  $A_i = 2$  and  $B_i = 1$ .

## C Results

### C.1 Simulation of the effect of the actual lockdown

A video is available for the temporal and geographical visualisation of the lockdown simulation at [https://youtu.be/q029a\\_e1akU](https://youtu.be/q029a_e1akU). The map in the video indicates the rate of reduction in firm production averaged within each municipality. The red areas indicate that the production in the area is less than or equal to 20% of firms' capacity on average, whereas the light red and orange areas show firms with a more moderate decline in production. The inset in the video indicates Figure 2 and the number of days from the first lockdown. The visualisation clearly shows the areas that are not locked down are also affected by lockdowns of other areas. For example, from day 0 to day 8, only seven prefectures are locked down but most of the areas in Japan are affected (see Section 3.2 and Figure A.3). This reduction of the production happens because the demand reduction propagates to the suppliers without any buffer. On the other hand, the supply reduction can be mitigated because each client holds inventories for the intermediate goods.

### C.2 Estimation of daily GDP from IAIA

The IAIA indicates the changes in production in all industries in Japan compared with that in the previous month and in the same month in the previous year, based on firm surveys [34]. We assume that

daily production on 7 April (day 0) is the same as that in March and thus can be calculated from the IAIA in March. Then, we estimate the daily GDP in April (or May) by  $(\text{yearly GDP})/365 \times (\text{IAIA in April (May)})/(\text{IAIA in March})$  and illustrate it by the left (right) red line in Figure 2.

### C.3 Interconnected effect of the different strictness of regional lockdowns

In Section 4.2, we showed that the different lockdown strictness between the more and less restricted groups affects the economic losses of the two groups, particularly assuming that the lockdown continues for 60 days. We also experiment with different lockdown durations (i.e. 14 and 30 days) and show the results in Figures C.1 and C.2. The main result that the strictness of the lockdown in the more restricted group that includes the major industrial clusters substantially affects the economic loss of the other group by propagation through supply chains still holds.

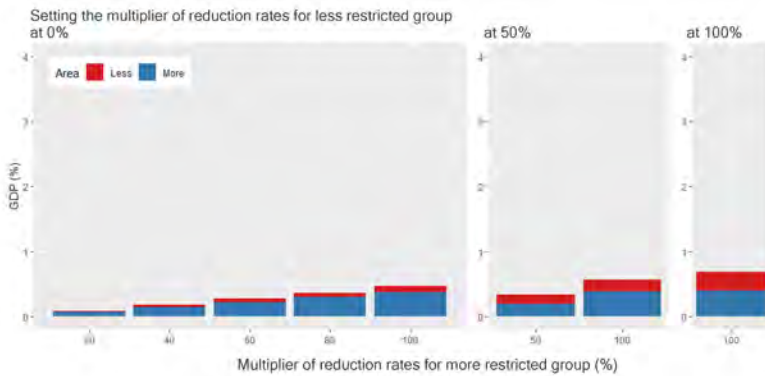


Figure C.1: Loss in value added as a percentage of total GDP assuming different restriction levels for a lockdown of 14 days between the more and less restricted groups. A restriction level is defined by a multiplier for the sector-specific benchmark rates of reduction in production capacity. The red and blue parts of each bar show the loss of value added in the less and more restricted groups, respectively as a percentage of GDP.

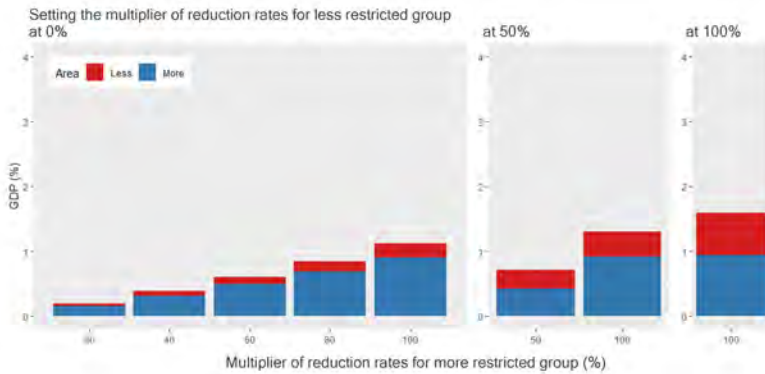


Figure C.2: Loss in value added as a percentage of total GDP assuming different restriction levels for a lockdown of 30 days between the more and less restricted groups. A restriction level is defined by a multiplier for the sector-specific benchmark rates of reduction in production capacity. The red and blue parts of each bar show the loss of value added in the less and more restricted groups, respectively as a percentage of GDP.

### C.4 Effect of lifting the lockdown in one region

Section 4.3 presents the effect of lifting the lockdown in a prefecture on its production, assuming that all the other prefectures are still locked down. Figure C.3 shows the ratio of the increase in national GDP from each prefecture lifting its lockdown to the decrease in GDP by all prefectures' lockdowns. The prefectures are horizontally aligned in order of JIS cods. The top three prefectures in terms of the recovery rate are Tokyo, Osaka, and Fukuoka.

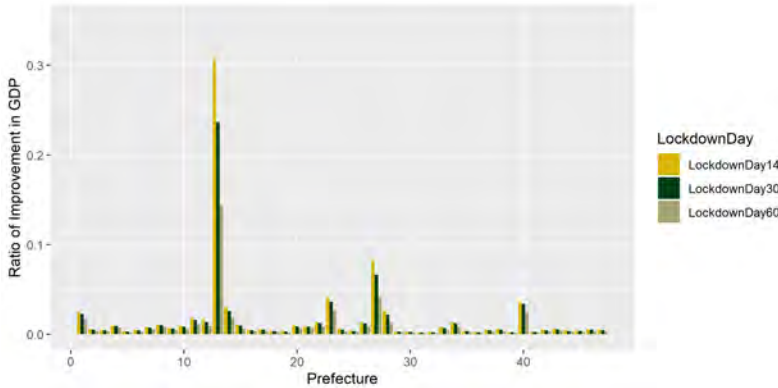


Figure C.3: Ratio of the improvement in GDP by lifting the lockdown in each prefecture. The improvement is defined as the ratio of the increase in national GDP by each prefecture lifting its lockdown to the decrease in GDP by all prefectures' lockdowns. The horizontal axis indicates the JIS codes of the prefectures. The yellow, dark green, and light green bars show the ratio of the improvement when lockdowns persist for 14, 30, and 60 days, respectively.

Figure C.4 illustrates the ratio of the increase in the value added production, or gross regional product (GRP), of each prefecture by lifting its lockdown to the decrease in its GRP by all prefectures' lockdowns, which is shown in Figure 5.

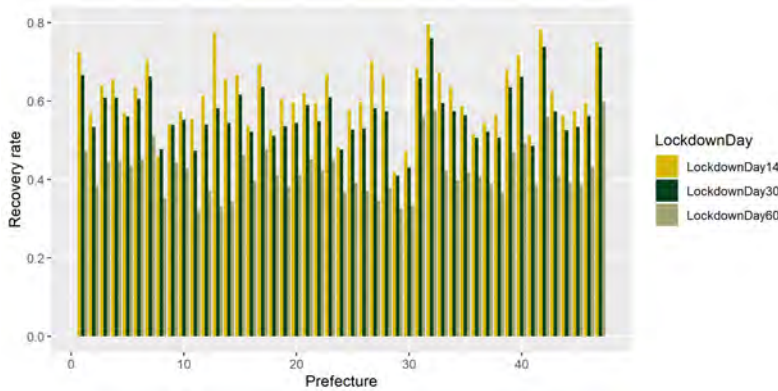


Figure C.4: Recovery rate in GRP by lifting the lockdown in each prefecture. The recovery rate is defined as the ratio of the increase in the GRP of each prefecture by lifting its lockdown to the decrease in its GRP by all prefectures' lockdowns. The horizontal axis indicates the JIS codes of the prefectures. The yellow, dark green, and light green bars show the recovery rate when lockdowns persist for 14, 30, and 60 days, respectively.

Covid Economics 56, 9 November 2020: 157-194

## C.5 Regression analyses

In Section 4.3, we conducted regression analyses to examine what attributes of prefectures cause a larger economic recovery by lifting the lockdown in only one prefecture, using Ordinary Least Squares (OLS) models. Table C.1 shows the correlation coefficients between all the variables used in the regression analysis and Table C.2 presents the detailed regression results.

Table C.1: Correlation matrix of the variables used in Section 4.3. The definitions of the variables are as follows. RecRatio: the recovery rate defined as the ratio of the increase in the GRP of each prefecture by lifting its lockdown to the decrease in its GRP by all prefectures' lockdowns. GRP: gross regional product (log). Links: the degree (log). InLink: the share of links within the prefecture to its all links. InLoop: the share of loop flows within the prefecture to its all flows. OutLink: the share of outward inter-prefectural links to all the links of the prefecture. Potential: the average HH potential of the firms in the prefecture. Sub: the share of substitutable suppliers to all suppliers of the prefecture located outside the prefecture.

Variable	RecRatio	GRP	Degree	InLink	InLoop	OutLink	Potential	Sub
RecRatio	1.000							
GRP	0.311	1.000						
Degree	0.370	0.965	1.000					
InLink	0.218	-0.467	-0.374	1.000				
InLoop	0.432	0.072	0.151	0.720	1.000			
OutLink	-0.046	0.676	0.661	-0.688	-0.351	1.000		
Potential	-0.321	0.104	0.090	-0.046	-0.076	0.193	1.000	
Sub	0.449	0.803	0.829	-0.246	0.307	0.573	0.096	1.000



Table C.2: Regression results for Section 4.3. The dependent variable is the recovery rate. See the caption of Table C.1 for the definitions of the independent variables. Standard errors are in parentheses. \*\*\* p<0.01, \*\* p<0.05, \* p<0.1.

	(1)	(2)	(3)	(4)	(5)	(6)	(7)
InLink		0.426*** (0.133)					0.401 (0.242)
InLoop			0.686*** (0.216)				-0.345 (0.425)
OutLink				-0.639** (0.245)			-0.375 (0.278)
Potential					-0.540** (0.202)		-0.527*** (0.179)
Sub						0.684** (0.275)	0.709** (0.283)
GRP	0.0261** (0.0119)	0.0443*** (0.0122)	0.0236** (0.0109)	0.0528*** (0.0152)	0.0292** (0.0112)	-0.0115 (0.0189)	0.0242 (0.0191)
Constant	0.572*** (0.0225)	0.285*** (0.0924)	0.424*** (0.0512)	0.816*** (0.0957)	0.565*** (0.0213)	0.507*** (0.0338)	0.445** (0.182)
Observations	47	47	47	47	47	47	47
R-squared	0.097	0.267	0.265	0.218	0.223	0.208	0.481

In Section 4.4, we conducted regression analyses to examine what attributes of prefectures cause a larger economic recovery by lifting the lockdown in two prefectures simultaneously, using OLS models. The relative recovery measure defined as the ratio of the increase in the GRP of prefecture *a* when it lifts its lockdown together with prefecture *b* to its increase when prefecture *a* lifts its lockdown alone. Table C.3 shows the correlation coefficients between all the variables used in the regression analysis and Table C.4 presents the detailed regression results.

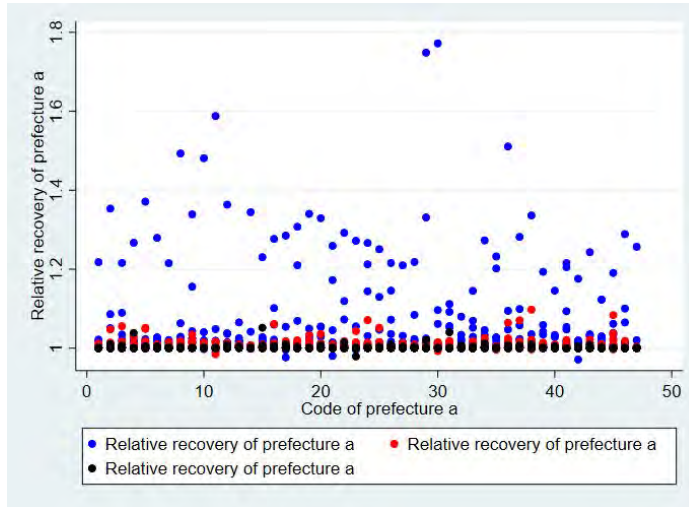


Figure C.5: Relative recovery from lifting the lockdown together to the recovery from lifting the lockdown alone. The relative recovery measure is defined as the ratio of the increase in the GRP of prefecture *a* when it lifts its lockdown together with prefecture *b* to its increase when prefecture *a* lifts its lockdown alone. The horizontal axis shows the JIS code of prefecture *a*. The colour of each dot indicates whether the GRP of prefecture *b* is among the top 10 (blue), the bottom 10 (black), or others (red).

Table C.3: Correlation matrix of the variables used in Section 4.4. The definitions of the variables are as follows. *Recov<sub>a</sub>*: the relative recovery of prefecture *a* defined as the ratio of the increase in the GRP of prefecture *a* by lifting its lockdown together with prefecture *b* to its increase by lifting its lockdown alone. *Link<sub>ab</sub>*: the share of links from *a* to *b* to all links from *a*. *Link<sub>ba</sub>*: the share of links from *b* to *a* to all links from *a*. *Pot<sub>ab</sub>*: the share of potential flows from *b* to *a* to the total links of *a*. *Pot<sub>ba</sub>*: the share of potential flows from *a* to *b* to the total links of *a*. *Sub<sub>ab</sub>*: the share of suppliers substitutable by those in *b* to *a*'s suppliers outside *a* and *b*. *Sub<sub>ba</sub>*: the share of suppliers substitutable by those in *a* to *b*'s suppliers outside *a* and *b*. *Loop<sub>ab</sub>*: the share of loop flows between *a* and *b* to the total flows between the two. *Bi<sub>ab</sub>*: the number of inter-prefecture links between *a* and *b* in logs. *GRP<sub>j</sub>*: GRP of *b* in logs.

Variable	<i>Recov<sub>a</sub></i>	<i>Link<sub>ab</sub></i>	<i>Link<sub>ba</sub></i>	<i>Pot<sub>ab</sub></i>	<i>Pot<sub>ba</sub></i>	<i>Sub<sub>ab</sub></i>	<i>Sub<sub>ba</sub></i>	<i>Loop<sub>ab</sub></i>	<i>Bi<sub>ab</sub></i>	<i>GRP<sub>b</sub></i>
<i>Recov<sub>a</sub></i>	1.000									
<i>Link<sub>ab</sub></i>	0.820	1.000								
<i>Link<sub>ba</sub></i>	0.818	0.966	1.000							
<i>Pot<sub>ab</sub></i>	0.870	0.927	0.961	1.000						
<i>Pot<sub>ba</sub></i>	0.808	0.915	0.955	0.968	1.000					
<i>Sub<sub>ab</sub></i>	0.071	0.185	0.238	0.182	0.243	1.000				
<i>Sub<sub>ba</sub></i>	0.813	0.961	0.966	0.946	0.948	0.237	1.000			
<i>Loop<sub>ab</sub></i>	0.879	0.911	0.952	0.986	0.979	0.206	0.940	1.000		
<i>Bi<sub>ab</sub></i>	0.392	0.543	0.564	0.499	0.528	0.572	0.572	0.504	1.000	
<i>GRP<sub>b</sub></i>	0.563	0.610	0.597	0.602	0.582	0.056	0.643	0.596	0.576	1.000

Table C.4: Regression results for Section 4.4. The dependent variable is the relative recovery measure. See the caption of Table C.3 for the definitions of the independent variables. Standard errors are in parentheses. \*\*\* p<0.01, \*\* p<0.05, \* p<0.1.

	(1)	(2)	(3)	(4)	(5)	(6)	(7)
<i>Link<sub>ab</sub></i>	0.519*** (0.0175)						0.440*** (0.0306)
<i>Link<sub>ba</sub></i>		0.619*** (0.0199)					-0.375*** (0.0460)
<i>Pot<sub>ab</sub></i>			8.333*** (0.198)				0.277 (0.624)
<i>Pot<sub>ba</sub></i>				8.076*** (0.271)			-17.82*** (0.644)
<i>Loop<sub>ab</sub></i>					3.841*** (0.0844)		10.06*** (0.309)
<i>Sub<sub>ba</sub></i>						1.564*** (0.0550)	-0.248** (0.0989)
<i>Bi<sub>ab</sub></i>	-0.00211*** (0.000413)	-0.00288*** (0.000415)	-0.00182*** (0.000352)	-0.00174*** (0.000407)	-0.00225*** (0.000341)	-0.00235*** (0.000423)	-0.000602** (0.000298)
<i>GRP<sub>b</sub></i>	-0.0186*** (0.00210)	-0.0186*** (0.00205)	-0.0135*** (0.00181)	-0.0232*** (0.00202)	-0.0120*** (0.00175)	-0.0220*** (0.00208)	-0.00540*** (0.00146)
<i>GRP<sub>b</sub><sup>2</sup></i>	0.00652*** (0.000490)	0.00676*** (0.000471)	0.00467*** (0.000422)	0.00795*** (0.000458)	0.00431*** (0.000405)	0.00712*** (0.000489)	0.00192*** (0.000350)
Constant	1.019*** (0.00236)	1.023*** (0.00233)	1.016*** (0.00208)	1.021*** (0.00236)	1.017*** (0.00200)	1.024*** (0.00239)	1.006*** (0.00168)
Observations	2,162	2,162	2,162	2,162	2,162	2,162	2,162
R-squared	0.713	0.721	0.778	0.714	0.794	0.706	0.865

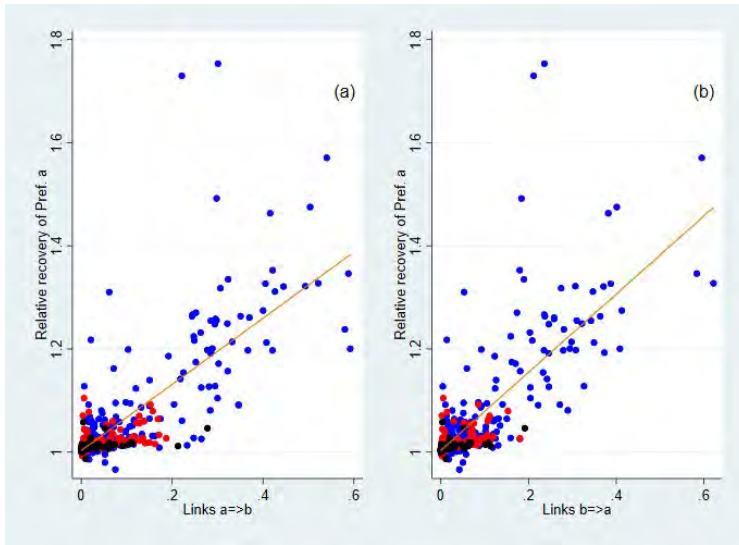


Figure C.6: Correlation between the relative recovery and selected network measures. The vertical axis indicates the relative recovery of prefecture  $a$ , defined as the ratio of the increase in the GRP of prefecture  $a$  by lifting its lockdown together with prefecture  $b$  to its increase by lifting its lockdown alone. The effect of the GRP of  $b$  and total links between the two are excluded from the relative recovery measure. The variable in the horizontal axis is given by Equations 1 and 2 in panels (a) and (b), respectively. The orange line in each panel signifies the fitted value from a linear regression that controls for the effect of the GRP of  $b$  and total number of links between  $a$  and  $b$ . The blue, black, and red dots show the pairs of prefectures  $a$  and  $b$  for which the GRP of  $b$  is among the top 10, bottom 10, and others, respectively.

To check the robustness of our main results, we experimented with different rates of reduction in production capacity, where we assume the share of working from home is zero for all the sectors in Supplementary Information Table C.3. In other words, in this alternative simulation analysis, we assume a stricter level of lockdown. Supplementary Information Figures C.8 and C.9 present the results, which are essentially the same as our benchmark results in Figures 6 and 7.

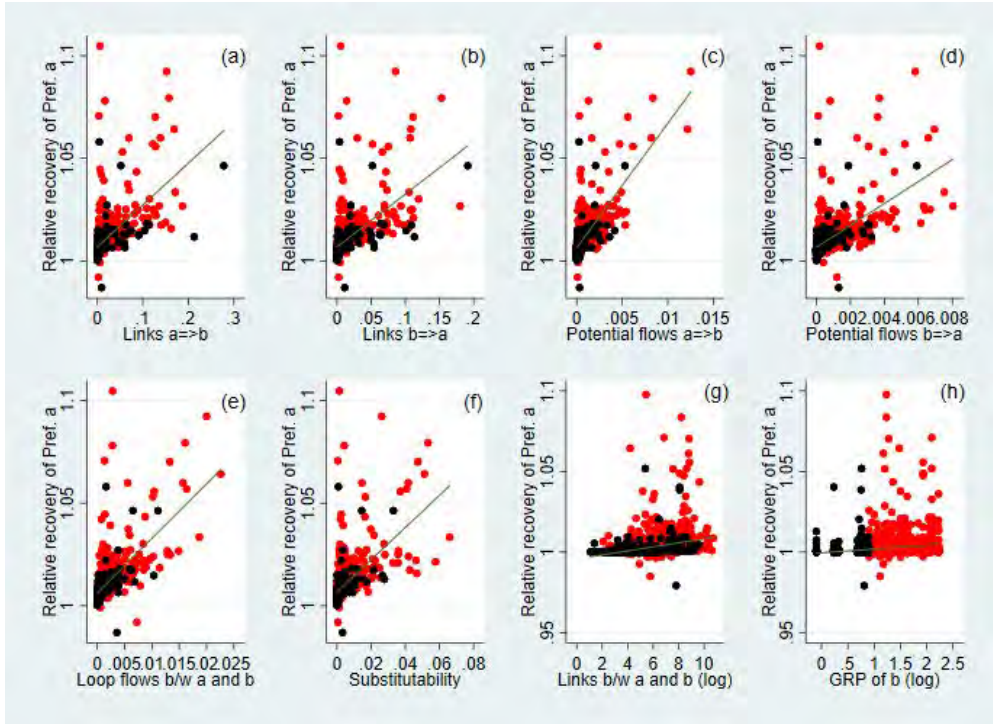


Figure C.7: Correlation between the relative recovery and selected network measures. See the caption of Figures 7 and C.6 for the definitions of the variables used here. The green line in each panel signifies the fitted value from a linear regression that controls for the effect of the GRP of  $b$  and total number of links between  $a$  and  $b$  in (a)–(g). The black and red dots show the pairs of prefectures  $a$  and  $b$  for which the GRP of  $b$  is among the bottom 10 and between 11 and 37, respectively.

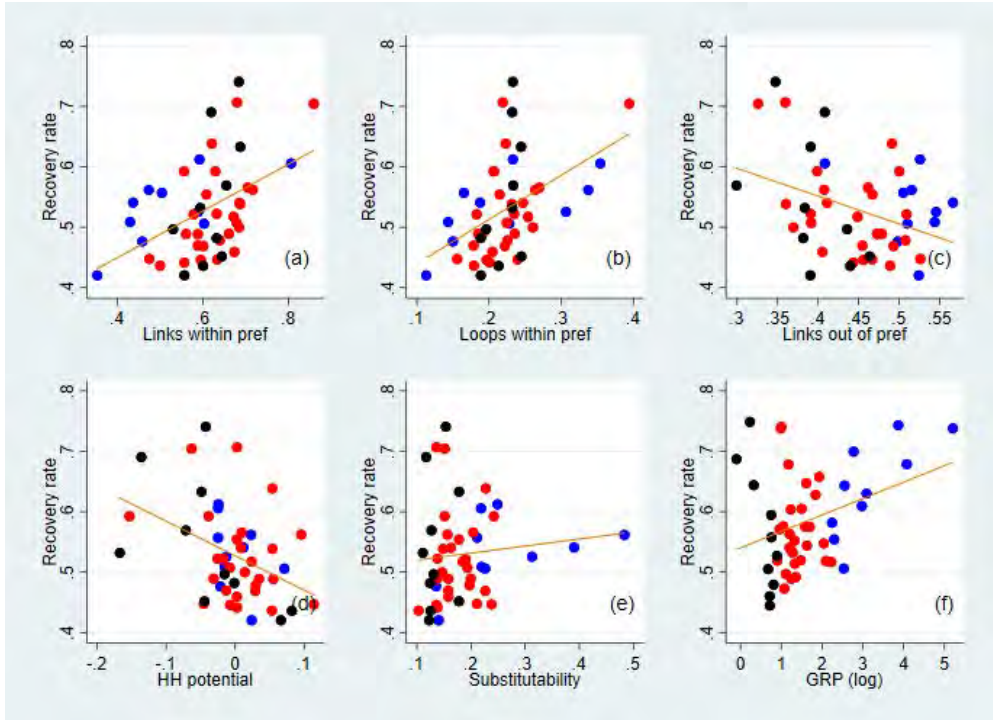


Figure C.8: Correlation between the recovery rate and selected network measures. See the caption of Figure 6 for the definitions of the variables used here. The orange line in each panel specifies the fitted value from a linear regression that controls for the effect of GRP in (b)–(f). The blue, black, and red dots show the prefectures whose GRP is among the top 10, the bottom 10, or others, respectively.

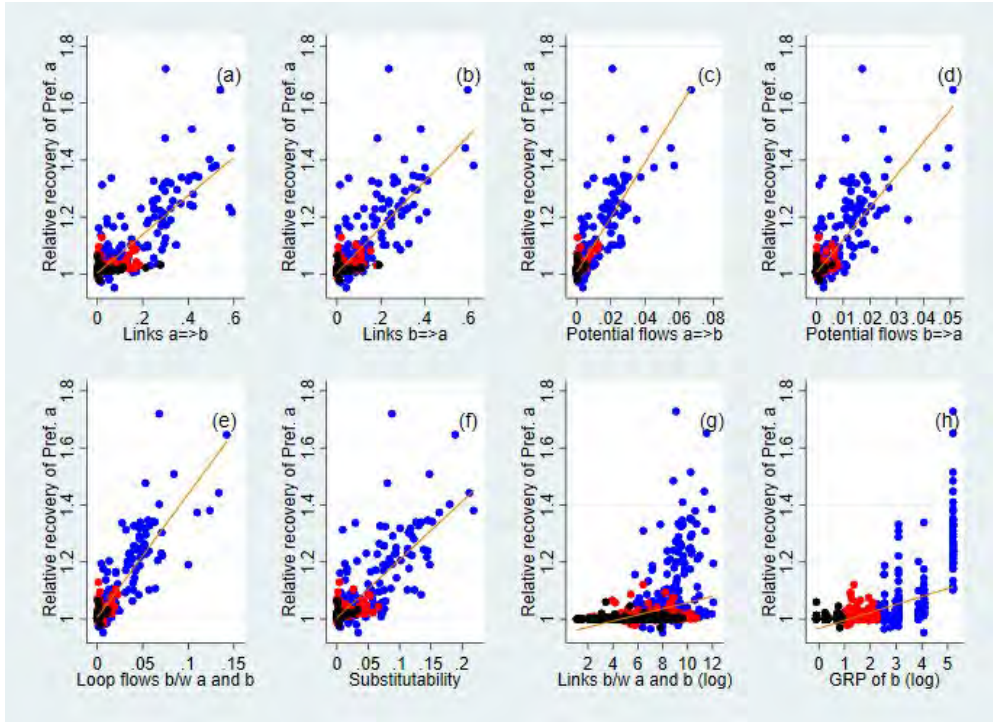


Figure C.9: Correlation between the relative recovery and selected network measures. See the caption of Figures 7 7 for the definitions of the variables used here. The red line in each panel signifies the fitted value from a linear regression that controls for the effect of the GRP of  $b$  and total number of links between  $a$  and  $b$  in (a)–(g). The blue, black, and red dots show the pairs of prefectures  $a$  and  $b$  for which the GRP of  $b$  is among the top 10, the bottom 10, or others, respectively.

# Reopening the economy and food security

Tuan Anh Luong<sup>1</sup>

Date submitted: 24 October 2020; Date accepted: 26 October 2020

*The COVID-19 pandemic has posed major challenges, of which food insecurity is one, to countries across the world. A number of policies have been put in place in response to the development of the outbreak. In this paper, I investigate the impacts of one of these policies, the reopening of the economy, on food security. Using a recent large-scale household survey in the United States, I find that food insecurity is a major problem that could adversely affect people's health. Using a report on containment policy across states in the United States to construct the level of this policy, I also find that this policy reduced the likelihood of food insecurity. While the overall impact of this policy is expected, how it influenced the causes of food security is more interesting. In particular, while it helped to increase the availability of food to the people in need, it decreased their ability to buy food. Not only reopening policy increased the expenses on food, which made food less affordable, it also had adverse effect on people's health which prevented them from going out to buy food. I also show how effective the multiple food programs were in the presence of reopening policy. These findings provide valuable evidence to policy makers in mitigating the impacts of the COVID-19 crisis.*

<sup>1</sup> Senior Lecturer, Department of Economics and Marketing, Faculty of Business and Law, De Montfort University.

Copyright: Tuan Anh Luong



# 1 Introduction

Food insecurity is a serious problem in the United States. Although there is some progress in alleviating the problem since 2008 when a surge of the number of food insecure households took place due to the financial crisis, there was still 14.3 million households, or 11.1 percent of the total households, that were classified as food insecure (Coleman-Jensen et al. 2019). This problem is not unique to the United States. Indeed, it was one of the main goals of the United Nations Millennium Development Goals and the Sustainable Development Goals initiative.

The consequences of food insecurity have been well established (see Gundersen, Kreider and Pepper 2011 for a review). The determinants of food insecurity, however, are less well understood. Sen (1981) claims that food insecurity is more of a demand concern, affecting the poor's access to food, than a supply concern, affecting the availability of food at the national level. Following this paradigm shift, most of the papers focus on looking at the economic resources of the household as predictors of food insecurity. Examples are average income (Gundersen and Gruber 2001), income volatility (Ribar and Hamrick 2003) and income shock (Leete and Bania 2010). However, income alone cannot explain the problem of food insecurity. According to Coleman-Jensen et al. (2019), 3.5 percent and 1.9 percent of households with an income exceeding 185 percent of the federal poverty line were food insecure and very low food secure, respectively.

The COVID-19 pandemic presents another challenge to reduce the number of people suffering from hunger and food insecurity, one of the United Nation Sustainable Development Goals. Indeed, it is one of the biggest threats together with Climate Change, Locust Crisis and Conflict. On April 21, the United Nations projected that “..(T)he number of people fac-

ing acute food insecurity (IPC/CH 3 or worse) stands to rise to 265 million in 2020, up by 130 million from the 135 million in 2019, as a result of the economic impact of COVID-19” (United Nation World Food Program). The same week, in the United States, the five-week total of job losses rose to a staggering 26 million, pushing millions more into food insecurity.

At the same time, this global crisis also provides a golden opportunity to evaluate the impacts of governmental policies in reducing food insufficiency. Indeed, governments at different levels (central and regional) responded to the development of the outbreak with the containment policy at various levels. This policy affected nearly all aspects of social life and, therefore, was likely to have an impact on food security. The variation of this policy across local governments in the United States and across time is the perfect framework for my analysis.

To the best of my knowledge, this paper brings the first evidence of the impacts of a policy that is not directly targeted at reducing food insufficiency. Indeed, most of the works in the literature looked at the impacts of the food stamp program or safety net program. In this paper, I evaluate the consequence of the containment policy (or rather the relaxation of this policy). To measure the degree of the containment policy, I rely on the reports by the Washington Post that track the development of the containment policy in each state of the United States. In particular, I characterize the changes in the containment policy across States by 4 levels: Major, Moderate, Minor and None, according to the types of business that were allowed to open. I also compare my measures with the ones provided by the New York Times to ensure the consistency of the measures.

To measure of the outcome of food security, I make use of a recent large-scale survey, the 2020 Household Pulse Survey (HPS). The survey was conducted by the United States Census Bureau in partnership with

five other agencies from the Federal Statistical System. The survey was conducted for a total of 8 weeks, starting from the week of April 23 (week 1) to that of June 18 (week 8). The survey was nationally representative and covered all 50 states and the District of Columbia. In my analysis, I make use of the answers to the question “In the last 7 days, which of the statements best describes the food eaten in your household?”. The four available answers are: (i) *Enough of the kinds of food (I/we) wanted to eat*; (ii) *Enough but not always the kinds of food (I/we) wanted*; (iii) *Sometimes not enough to eat* and (iv) *Often not enough to eat*. These answers are linked to the 4 levels of food security defined by the United States Department of Agriculture. With these ordered levels of food security, I apply the ordered logistic regression and the ordered probit regression to evaluate the impact of reopening policy on food security. I find that when the states relaxed their containment policy from Major restrictions to Moderate and No/Minor restrictions, the probability of experiencing food insecurity dropped, even when I control for an exhaustive set of household characteristics. For instance, the probability of having marginal food security is 32.3 percent under Major restriction policy (with a 95 percent confidence interval being from 31.5 percent to 33.1 percent), compared to 31.5 percent if under No/Minor restrictions (with a 95 percent confidence interval being from 30.9 percent to 32 percent) and 31.1 percent if under Moderate restrictions (with a 95 percent confidence interval being from 30.7 percent to 31.5 percent). Reopening policy, especially a move from Major restrictions to Moderate restrictions, also had similar impacts on expected food security. To further check my findings, I also apply the same analysis with a complementary survey, conducted by the National Opinion Research Center (NORC), University of Chicago. Consistent results are again found with this survey. In particular, reopening policy is documented to have a positive impact on food security. In addition, moving from Major restrictions to

Moderate restrictions was a favorable policy as far as expected food security is concerned.

The comprehensive HPS survey enables me to provide new evidence on the causes and the expectations of food security. In the HPS survey the respondents were asked to provide the causes of their food insecurity. There are 6 possible reasons from the ability to get food (monetary, logistically or mentally) to the availability of food (food not delivered, not available on stores or no free food). These answers recognize the fact that money is not always the cause of food insufficiency (Davis and You 2011). I find that reopening policy had positive impacts on the availability of food: more food were available in the stores and free food was accessible. However, this policy might backfire because it reduced the ability to get food. More precisely, more people reported the inability to afford or to get out to buy food with reopening policy. Indeed, I document that it increased the expenditures on prepared food and prepared meals, meaning food became less affordable. In addition, both people's health status and their mental health deteriorated with the policy. It suggests that people might not be able to go out to get food. Finally, the evidence of how reopening policy affected people's expectation regarding Food Security will be useful in building a theoretical framework that explains how governmental policies influence the causes of Food Security, especially the ones that relate to the people's behaviors.

All of these results will serve as useful evidence to policymakers in mitigating the effects of the COVID-19 crisis. Furthermore, my results suggest that reopening policy was effective in making free food accessible via home delivered meal service; religious organizations and family, friends or neighbors. However, there is no evidence that it was effective in food programs such as school free meals, food bank, soup kitchen or other community programs.

The remainder of the paper is organized as follows. In the next section I review the existing literature that relates to the determinants of food security, the impacts of the COVID-19 on food security and the effects of containment policy. In Section 3 I present the conceptual framework. In Section 4, I explain the identification strategy. The fifth section presents the data while the evidence is discussed in the fifth section. In particular, I show evidence of food security affecting mental health. I also characterize the people who experience food insecurity. The main focus is, however, how reopening policy affected food security which is also reported in Section 6. The final section provides the concluding remarks.

## 2 Related Literature

My paper bridges the gap between three interesting literatures. The first one looks for the determinants of food security. The second one investigates the impacts of the COVID-19 pandemic on food security. And the third one analyses the effects of containment policy.

Although food security is a prevalent problem, little is known about its determinants. The most salient candidate is the economic resources available to the households. [Gundersen and Gruber \(2001\)](#) suggested that average income over a period of time is a better determinant than current income. Other types of resources are also considered. According to [Ribar and Hamrick \(2003\)](#), assets can protect against food insecurity. Liquidity constraints ([Leete and Bania 2010](#)) and credit access ([Fitzpatrick and Coleman-Jensen 2014](#)) were also shown to affect the likelihood of experiencing food insufficiency. However, there is still a large variation of food insecurity unexplained by income ([Coleman-Jensen et al. \(2019\)](#)).

One of the unexplored venues that need to be addressed is the impacts

of macro and micro policy on food security. Most of the work focus on the policy intended directly to address the problem, such as food stamp and safety net program and the conclusion is pessimistic. [Bitler, Gundersen and Marquis \(2005\)](#) found that the impact from the Supplemental Nutrition Program for Women, Infants, and Children (WIC) was minimal. Their result was echoed by [Heflin, Arteaga and Gable \(2015\)](#) where they documented small effects of the Child and Adult Care Food Program on child food security. The contribution of my paper is the new evidence of the impacts of the containment policy on food security. Moreover, my paper advances the literature by addressing how this policy affected the causes of food security. In particular, reopening policy influenced not only the monetary cost of food, but also other types of costs such as health and the fear of going out. This result agrees with [Davis and You \(2011\)](#) that the safety-net program often ignored the non-monetary cost of food which explained the small effects of governmental policy.

The second related literature investigates the impact of COVID-19 on food security. A report by [Feeding America \(2020\)](#) predicted the level of food security based on different scenarios of unemployment and poverty. Under the optimistic scenario, food insufficiency would increase by 1 percent, or 3.3 million people. Under the pessimistic scenario, the increase would be 5.2 percent, or 17.1 million people. Using a survey that focused on mothers with young children, [Bauer \(2020\)](#) documented that more than 20 percent of households in America experienced food insecurity. The rate of food insecurity went up to 40 percent among households with children under 12. Perhaps closer to my study is the survey conducted by the National Opinion Research Center, University of Chicago. This COVID Impact Survey is complementary to the survey used in my analysis, albeit at a smaller scale. They reported that 28 percent of respondents being worried about their food running out before they had money to buy more in the first wave

of the survey (April 20th to April 26). This rate improved slightly in the second and third wave, at 27 and 20 percent respectively. Similar to my findings, they also found that demographic factors, such as race, education, income and the number of children, played an important role in explaining food insecurity. My paper differs from these papers by aiming to establish a causal relationship between the government response to the outbreak and food security.

This distinction brings me to the third emerging literature that investigates the impacts of the containment policy. Brodeur et al. (2020) used Google Trends data and found that containment policy led to mental health problems as more people searched for boredom, loneliness, worry and sadness. Glover et al. (2020) looked at the distributional effects of containment policy while Rampini (2020) proposed to lift containment policy sequentially, i.e. to allow a large fraction of economic activity by the less vulnerable population to resume. Baek et al. (2020) looked at the impact of stay-at-home order on unemployment. They found that the the direct effect of stay-at-home orders accounted for a significant but minority share of the overall rise in unemployment claims. So long as the underlying public health crisis persisted, undoing stay-at-home orders would only bring limited economic relief. My paper complements their studies by looking at the impact of the containment policy on food security.

### 3 Conceptual Framework

In this section I analyze the food insufficiency problem from both the demand and supply side.

### 3.1 Demand

I employ here a simplified model from Gundersen and Gruber (2001). There is a household maximizing its utility subject to the budget constraint. More precisely, the household solves the following problem:

$$\begin{aligned} & \max_{\{F, OG\}} U(F, OG) \\ & \text{subject to } p_F F + p_{OG} OG \leq Y \end{aligned}$$

In the above equation,  $F$  and  $OG$  are food and other good consumption,  $p_F$  and  $p_{OG}$  are the corresponding prices and  $Y$  is the total income. The first-order condition of this problem is:

$$\frac{\partial U / \partial F}{\partial U / \partial OG} = \frac{p_F}{p_{OG}}$$

Assuming the utility is monotone, the optimal solution will be on the budget line, i.e.:

$$p_F F + p_{OG} OG = Y$$

Let  $\underline{F}$  be the minimum food consumption and  $\underline{OG}$  be the minimum consumption on other good. The minimum expenditure is then:

$$p_F \underline{F} + p_{OG} \underline{OG} = \underline{E}$$

There are two possible explanations for food insufficiency from the demand side. First, the total income  $Y$  of the household drops below  $\underline{E}$ . In this case, the household cannot afford to buy both food and other goods to



satisfy its needs. Second, the price of food and other goods increase to the point that the minimum expenditure  $\underline{E}$  is higher than the total income  $Y$ .

I know from the HPS survey whether the respondents could afford to buy food. It could be because of the two reasons mentioned above. In particular, reported expenses on food and meals in the survey reveal whether food was affordable. In addition, the survey answers report that some people were unable or afraid to go out. As a result, the “transportation” cost rises which in turn increases the transaction price of food and other goods. This is consistent with [Davis and You \(2011\)](#) where they found that time was more the constraining factor than money in reaching the food security target.

### 3.2 Supply

At the macroeconomic level, the demand for food derived from the household optimization problem must be no higher than its supply. However, if the supply of goods, especially food, declined because of the pandemic, this condition might not have been satisfied which resulted in food insufficiency. Indeed, according to a report by [OECD \(2020\)](#), the biggest risk for food security could be consumers access to food. The stay-at-home orders might have prevented food from being produced and brought to the shelves. In theory, the drop in supply can be offset by a rise in price. However, price rigidity<sup>1</sup> implies that some households were unable to have sufficient food.

---

<sup>1</sup>The mean duration of price rigidity is at least 7 months ([Klenow and Kryvtsov 2008](#); [Nakamura and Steinsson 2008](#)).

## 4 Identification strategy

### 4.1 Reopening and food security

In order to find the causal effect of reopening on food insecurity, I need to establish an econometric model. In my survey, the respondents gave 4 answers to describe their situation: (i) enough food; (ii) enough food but not the food we wanted; (iii) sometimes not enough to eat and (iv) often not enough to eat. In the previous section I provide a number of reasons to explain food insufficiency. Admittedly, the severity of these problems determine the level of food security. Denote  $y^*$  one of the reasons of food insufficiency as described in the previous section. I then set up my model as follows:

$$\begin{aligned}
 y_{ist} &= 1(\text{Enough food}) \text{ if } y_{ist}^* \leq \tau_1 \\
 &= 2(\text{Enough but not always the kinds of food (I/we) wanted to eat}) \text{ if } \tau_1 < y_{ist}^* \leq \tau_2 \\
 &= 3(\text{Sometimes not enough to eat}) \text{ if } \tau_2 < y_{ist}^* \leq \tau_3 \\
 &= 4(\text{Often not enough to eat}) \text{ if } \tau_3 < y_{ist}^*
 \end{aligned} \tag{1}$$

The cut-offs  $\tau_i$  determine the severity of the food insufficiency. My hypothesis is that  $y^*$  depends on the household's characteristics and more importantly, on reopening policy:

$$y_{ist}^* = \alpha + \beta P_{st} + \gamma X_{ist} + \epsilon_{ist} \tag{2}$$

where  $P_{st}$  is the reopening policy in state  $s$  at time  $t$ .  $X_{ist}$  is the vector of household attributes, including age, marital status, gender, education and

income level, the number of adults and children in the household. From Equations (1) and (2) we have:

$$Prob(y_{ist} = y | U_{s,t-d}, X_{ist}) = Pr(\tau_{y-1} < y_y^* \leq \tau_y | X_{ci}, P_c) = F(\tau_y) - F(\tau_{y-1}) \quad (3)$$

where  $\tau_0 = 0$  and  $F(\cdot)$  is the cumulative distribution probability of the error term  $\epsilon_{ist}$ . If we assume  $\epsilon_{ist}$  follows a logistic distribution then we have an ordered logistic regression. Alternatively, if we assume  $\epsilon_{ist}$  follows a standard normal distribution then we have an ordered probit regression. These two regressions will be used in my analysis.

A major concern when I try to establish causality is the possibility of endogeneity. This come from two main sources: (i) *reverse causality* and (ii) *omitted variables*. If the number of people suffering from food insufficiency *directly* affected the reopening order then the coefficient  $\beta$  would be biased because of reverse causality. However, there is no evidence to suggest it was the case. Instead, the reopening order is likely to be the result of public health consideration, business pressure and political/public opinion. The U.S. government established five criteria for reopening: (i) a sustained two-week drop in coronavirus cases; (ii) a low number of daily new Covid-19 cases; (iii) a high coronavirus testing capacity; (iv) a low test positive rate and (v) a high availability of Intensive Care Unit (ICU) beds. However, not all the states met these criteria when they reopened. They had to balance public health concerns with the economic damage the containment policy inflicted. What tipped the balance was the political and public opinion. According to [Graham \(2020\)](#), the reason of reopening came from the “...power of the presidential bully pulpit and intense media coverage”. Therefore, the effect of food security on reopening was, at best,

indirect. In other words, the chance of a reverse causality is minimal.

This leaves me to the second possibility: omitted variables. I can think of two factors that are correlated with both food security and reopening policy: unemployment and the governor's partisan affiliation. Indeed, the unemployment rate increased to a record high 14.7 percent in April 2020 (Bureau of Labor Statistics 2020). The loss of income as a result of unemployment is one of the causes of food insufficiency as I discussed in the previous section. At the same time, the growing demand from the public to end enforced business closures meant that governors would find it harder to keep the business closed.

In addition to unemployment, the governor partisan identity is another potential factor that is correlated with both food security and reopening. It is documented that the Red states are poorer than the Blue states (Gelman et al. 2008). As a result, food security is more likely to be a problem in the former than in the latter. Moreover, Republican governors were more inclined to reopen their states than Democratic governors. Indeed, as of May 3rd 2020, of the 24 states reopening early, 17 are led by Republicans and 7 by Democrats.

I try to correct for the omitted variable problem that leads to endogeneity bias by controlling for a number of covariates and fixed effects. In particular, I control for the state-level unemployment rate that could affect both reopening policy and food security. Since the unemployment rate was only communicated one month later by the Bureau of Labor Statistics, I use the unemployment rate one month prior to the time the respondents were asked in the survey. I also use the state fixed effect to control for all state-level time-invariant factors, such as the governor's partisan affiliation, that could affect both reopening policy and food security.

## 4.2 Further investigations

In addition to the econometric techniques discussed above, to establish the causal relationship between reopening and food security, I look at the mechanism of how reopening affected food insecurity. The richness of my data enables me to carry such task. In particular, in my survey, respondents were asked why they did not have food in the past 7 days. More precisely, for the people who answered that they did not have enough food in the past 7 days, they were asked if the reason was one of the following: (1) cannot afford food; (2) cannot go out; (3) afraid to go out; (4) food not delivered or (5) food not available on stores. Moreover, they also reported whether they received free food which is also an important factor of food insecurity. Their answers allow me to investigate how reopening policy affected food security. More precisely, denote  $\pi_k$  the probability that food insufficiency resulted from one of the aforementioned reasons, I assume that this probability is a function of the vector of characteristics  $X$  and the reopening policy  $z$ :

$$\pi_k = \Pi(X, z) \quad (4)$$

Based on this assumption I then set up the following regression (I drop the subscript  $k$  to alleviate the notation):

$$\pi_{ist} = \alpha + \beta P_{st} + \gamma X_{ist} + u_{ist} \quad (5)$$

Again if we assume the error term  $u_{ist}$  follows the logistic distribution, we will have a logistic regression. Alternatively, we have a probit regression if  $u_{ist}$  follows the normal distribution.

To put more confidence in my findings, I carry further checks on the demand side. In particular, I make use of the reported expenses on food

and the health status of the respondents. In particular, I will have two additional regressions:

$$E_{ist} = \alpha + \beta P_{st} + \gamma X_{ist} + u_{ist} \quad (6)$$

$$H_{ist} = \alpha + \beta P_{st} + \gamma X_{ist} + u_{ist} \quad (7)$$

In Regression 6, the dependent variable  $E_{ist}$  is the reported expenses on food prepared and eaten at home and on prepared meals (e.g. eating out or delivered food) of a resident  $i$  in state  $s$  at time  $t$ . The estimated coefficient  $\beta$  in this regression will reveal how reopening policy affected the affordability of food which is one of the causes of food insecurity.

In Regression 7, the dependent variable  $H_{ist}$  is the reported health status of a resident  $i$  in state  $s$  at time  $t$ . The estimated coefficient  $\beta$  in this regression will reveal how reopening policy affected the ability of the resident to go out to buy food.

## 5 Data

### 5.1 Reopening

The U.S. started the stay-at-home order at the end of March 2020. Residents were asked not to go to non essential business to contain the COVID-19 outbreak. Later in May, a number of states began to lift this containment policy.

I use the Washington Post report to construct the phases of reopening across different States. In particular I divide the reopening policies into 4 categories: Major, Moderate, Minor and No restrictions. The first cat-

egory (Major restrictions) refers to the stay-at-home order. According to the categorization by the Washington Post, it indicates that "personal care businesses, such as salons and barbers, gyms and most non-essential businesses remain closed. Restaurants and bars may not seat patrons. Face coverings and six-foot distancing are required, and public gatherings larger than ten are not permitted". The second category (Moderate restrictions) starts when the state already reopens <sup>2</sup>. It means "many of the above businesses may reopen with limited capacity, while bars and gyms remain closed." The third category (Minor restrictions) implies further relaxation. Under this category, "bars, theaters, casinos or concert halls may reopen, with larger groups permitted."

In order to check the validity of my data construction, I compare to the reopening data provided by [Nguyen et al. \(2020\)](#). Based on the New York Times articles, they constructed the reopening dates for each state. In Table A1 in the Appendix I combine the reopening date in [Nguyen et al. \(2020\)](#) and the reopening categorization in the first four weeks in my data. In particular, week 1 refers to the week from April 23 to May 5; week 2 refers to the week from May 7 to May 12; week 3 refers to the week from May 14 to May 19 and week 4 refers to the week from May 21 to May 26.

We can see that in most states, my definition of reopening dates coincide with [Nguyen et al. \(2020\)](#). For instance, according to [Nguyen et al. \(2020\)](#) New York reopened on May 15. In my data, I categorize the policy in New York as Major restrictions until week 4 because May 15 fell into week 3. There are, however, a number of differences in Arizona, Delaware, Iowa, Louisiana, Michigan and New Hampshire. I explain the differences in the Appendix.

---

<sup>2</sup>Note that I switch the category after the state changes its policy. For instance, Alabama started reopening on April 30. As a result, while the category in the first week (from April 23 to May 5) is Major restrictions, the category in the second week (from May 7 to May 12) is Moderate restrictions.

Figure 1 provides the graphical illustration of reopening policy. At the end of the survey, South West, South East and Mid West reopened relatively further than other regions. Because there was a few instances (in Missouri in the final week and in Alaska from week 4) that we had No restrictions, I put No restrictions in the same category as Minor restrictions.

**Stylized Facts 1** *More relaxation are observed across states in the United States*

## 5.2 Food security

Data on food security outcomes and other household level control variables are from the 2020 Household Pulse Survey (HPS). The survey was conducted by the United States Census Bureau in partnership with five other agencies from the Federal Statistical System: The Bureau of Labor Statistics, the National Center for Health Statistics, the United States Department of Agriculture Economic Research Service, the National Center for Education Statistics, and the Department of Housing and Urban Development collaborated to develop the content for the HPS.

The survey was conducted for a total of 8 weeks, starting from the week of April 23 (week 1) to that of June 18. The survey is nationally representative and covers 50 states and the District of Columbia. In my analysis, I use answers to the question “In the last 7 days, which of the statements best describes the food eaten in your household?”. The four available answers are: (i) *Enough of the kinds of food (I/we) wanted to eat*; (ii) *Enough but not always the kinds of food (I/we) wanted*; (iii) *Sometimes not enough to eat* and (iv) *Often not enough to eat*. To be consistent with other studies, I link these answers to the levels of food security set by the United States Department of Agriculture. Accordingly, the food security status of each household lies somewhere along a continuum extending from



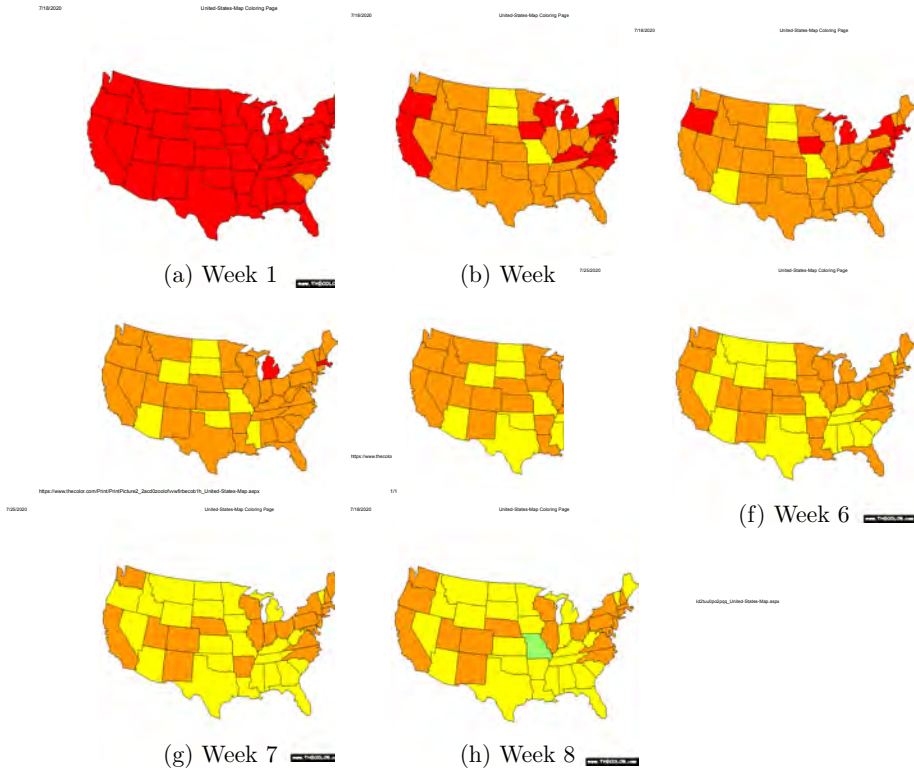


**Figure 1.** The reopening across States. The colors red, orange, yellow and green correspond to Major, Moderate, Minor and No restrictions.

high food security to very low food security. This continuum is divided into four ranges, characterized as follows:

- **High food security** - Households had no problems, or anxiety about, consistently accessing adequate food.

- **Marginal food security** - Households had problems at times, or anxiety about, accessing adequate food, but the quality, variety, and quantity of their food intake were not substantially reduced.

- **Low food security** Households reduced the quality, variety, and desirability of their diets, but the quantity of food intake and normal eating patterns were not substantially disrupted.

- **Very low food security** At times during the year, eating patterns of one or more household members were disrupted and food intake reduced because the household lacked money and other resources for food.

Following this characterization, I assign each answer to the question “In the last 7 days, which of the statements best describes the food eaten in your household?” to the four levels of food security. Alternatively, [Gundersen and Oliveira \(2001\)](#) defined food security as a binary variable. They then assigned the first two answers to food sufficiency and the last two answers to food insufficiency. There are two reasons for the characterization used in my analysis. First, it is consistent with the way the survey was designed. Indeed, the respondents who chose the last 3 answers were deemed food insecure. They were then asked why it was the case. Second, the 4-level characterization allows me to analyze in more details the food security situation of households as can be seen in the subsequent analysis.

In addition to the measures of food security, the survey also provides a number of household’s characteristics that I will use in my analysis. Table 1 provides the statistics of the food security outcomes as well as the key

characteristics. Compared to the situation prior March 13 2020, the current situation deteriorated. Indeed, while there were more than three quarters of the people reported food security prior March 13 2020, only two thirds of the people reported the same thing in the current situation. Moreover, people were pessimistic about the future. The percentage of people reporting expected food security drops to 58 percent. These numbers confirm the statement of the United Nations that the COVID-19 pandemic put more people at risk of food insecurity.

**Table 1.** Summary statistics

Variables	N	Mean	SD	Min	Max
<i>Outcomes</i>					
<i>Food security prior March 13, 2020</i>					
High	Marginal	Low	Very low		
77.80 %	17.14%	4.05%	1.01%		
<i>Food security in the past 7 days</i>					
High	Marginal	Low	Very low		
67.25%	26.68%	4.90%	1.17%		
<i>Expected Food security in the next 4 weeks</i>					
Very confident	Moderately confident	Somewhat confident	Not at all confident		
58.30%	19.45%	16.56%	5.69%		
Variables	N	Mean	SD	Min	Max
<i>Reasons for food insecurity</i>					
Cannot afford food (1=YES)	229,268	0.372	0.483	0	1
Cannot get out to buy food (1=YES)	229,268	0.111	0.314	0	1
Afraid to go (1=YES)	229,268	0.269	0.443	0	1
Food not delivered (1=YES)	229,268	0.0692	0.254	0	1
Food not available on stores (1=YES)	229,268	0.522	0.500	0	1
<i>Covariates</i>					
Age	720,487	51.59	15.74	18	88
Male (1=YES)	720,487	0.405	0.491	0	1
Hispanic (1=YES)	720,487	0.0851	0.279	0	1
Race	720,487	1.313	0.767	1	4
Recent job loss (1=YES)	716,527	0.391	0.488	0	1
Employed (1=YES)	716,337	0.572	0.495	0	1
Expect job loss (1=YES)	715,661	0.281	0.449	0	1
Kind of work	690,289	4.966746	3.337488	1	9
Number of persons in the household	720,487	2.844	1.620	1	10
Number of children	720,487	0.665	1.070	0	5
Education attainment	720,487	5.273	1.466	1	7
Marital status	715,076	2.208	1.598	1	5
Income	623,083	4.567	2.094	1	8
Unemployment pay	285,582	3.819	0.574	1	4

Note: the education attainment are (1) less than high school; (2) some high school; (3) high school graduate or equivalent; (4) some college; (5) associate's degree; (6) bachelor degree; (7) graduate degree.

The races are (1) White, (2) Black, (3) Asian; (4) Others

The marital status are (1) married; (2) widowed; (3) divorced; (4) separated; (5) never married.

The kind of work or unemployment benefits are (1) government; (2) private; (3) non profit; (4) self-employed; (5) family business; (6) paid leave; (7) full pay without leave; (8) partial pay; (9) no pay.

The income are (1) less than \$25,000; (2) \$25,000-\$34,999; (3) \$35,000-\$49,999; (4) \$50,000-\$74,999; (5) \$75,000-\$99,999; (6) \$100,000-\$149,999; (7) \$150,000-\$199,999; (8) above \$200,000

### 5.3 Unemployment

The final dataset used in my analysis is the unemployment data which is taken from the Bureau of Labor Statistics (BLS). Table A2 in the Appendix reports the state-level unemployment rate from February to May 2020. Note that the BLS only communicated the unemployment rates with a one-month lag. As a result, my assumption is that the governors, if they took into account unemployment when deciding to reopen their state, used the rate in the previous month. For instance, the rate in March would be used for reopening policy in April. One thing that I note from Table A2 is that unemployment started to pick up in February/March and rocketed in April and May. It coincides with the relaxation of the stay-at-home orders and suggests that unemployment could be a factor of consideration for reopening policy.

## 6 Evidence

### 6.1 The negative impacts of Food security on health

It is suggested that food security has a long-lasting effect on people's health (see Gundersen, Kreider and Pepper 2011). Food insufficiency not only affects adversely physical but also mental health (Stuff et al. 2004). My analysis provides additional evidence to support this view. Figures 2a, 2b, 2c and 2d show the percentage of people with various levels of health status based on their level of food security. In all figures, a consistent pattern emerges. Among the people who were food secure, more than half did not feel any mental problems. This percentage drops significantly to 30 percent among the people who had marginal food security and even further if they had low or very low food security. By contrast, less than one fifth of the people who did not experience food insecurity felt the problems frequently

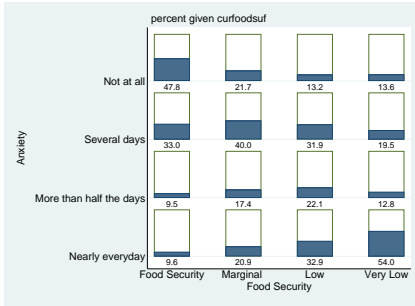
(more than half the days or nearly everyday). This percentage increases significantly to fifty percent for the people who had very low food security.

Figure 2e reports the relationship between Food Security and Health in general. Again Food Security and Health went in opposite direction. One quarter of the people who experienced food security felt excellent as far as their health was concerned. This percentage declined with the level of food security, down to 8 and 10 percent for the people who had low and very low food security. Similarly, nearly 40 percent of the food secure people felt very good with their health, but only 11.7 percent of the people who experienced very low food security felt so. By contrast, only 1.7 percent of the people who had food security felt poorly with their health. The number for the people who had very low food security rises up to 20.9 percent. These numbers confirm that food insecurity could lead to severe mental health problems. It is, therefore, important to eradicate Food Insecurity.

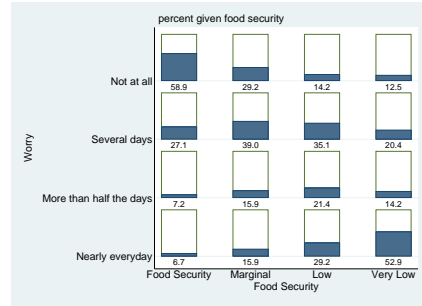
## 6.2 Characteristics of people who are food insecure

To check the consistency of the HPS survey, I look at the characteristics of the people who are food insecure. Table 2 characterizes these people. In the first two columns, I control for the characteristics such as the outcome of food security in the previous 7 days, together with demographic and socioeconomic factors such as age, race, gender, marital status, education attainment, household size and the number of children, and job-related variables. In Columns 3 and 4, I control further for the income level and the kinds of work or unemployment benefit. A number of interesting facts emerge from Table 2.

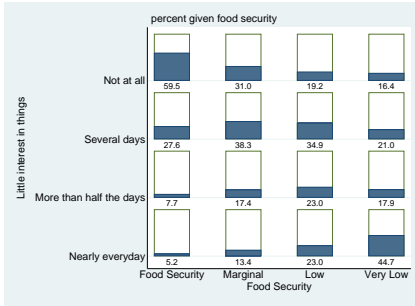
First, Food Security is a path dependent problem. People who had food insufficiency prior to March 13, 2020 were likely to continue this path. All the coefficients of prior food insecurity are significantly positive, suggesting



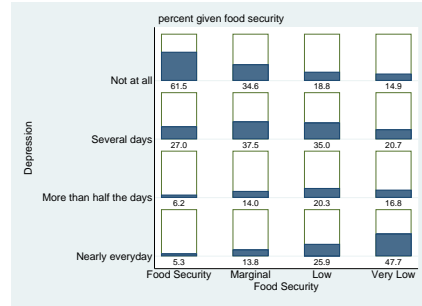
(a) Food security and Anxiety



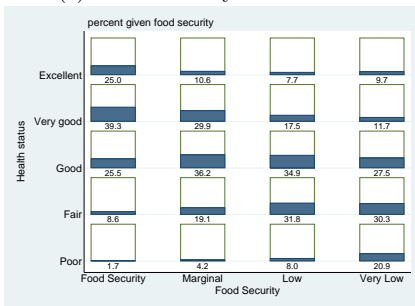
(b) Food security and Worries



(c) Food security and Interest



(d) Food security and Depression



(e) Food security and Health Status

Figure 2. Food Security and Health

that past food insecurity is a strong predictor of current food insecurity. Further evidence can be found in Figure 3a which shows the predictive probability of food security based on the situation prior March 13, 2020. According to this figure, 74 percent of people who had prior food security continued to do so. The percentage of people being food secure dropped to 27 percent and 5 percent for the people who had prior marginal food security and who had prior low food security, respectively. People who had prior very low food security had zero chance to be food secure. On the other hand, none of the people who had prior food security or marginal food security ended up in very low food security situation. By contrast, nearly half of the people in very low food security situation before March 13, 2020 continued to be in the same situation.

Second, food security is driven by the person's characteristics. Young and female were adversely affected. This is consistent with the situation in 2018 (Coleman-Jensen et al. 2019). White people fared better than Blacks, although the effect is gone once I controlled for the income level and the kind of work or unemployment benefit. There is weak evidence that Asians were in a better situation than Whites. Other races were in a worse situation than Whites.

In 2018, households with single woman or single man had a rate of food insecurity above the national average (Coleman-Jensen et al. 2019). This fact is replicated here as all the coefficients of marital status are significantly positive. It implies that relative to married people, people who were either widowed, divorced, separated or never married were more likely to have some food insecurity problem. Figure 3b predicts that while 59 percent of married people had food security, only 57, 56 and 54 percent of widowed, divorced and separated people were food secure, respectively.

Third, not only the personal information but also the household infor-

mation can predict the outcomes of food security. Household size, and especially the number of children, is a strong predictive factor. In particular, large household with numerous children is more likely to suffer food shortage, a fact that is consistent with the situation in 2018 (Coleman-Jensen et al. 2019). Household income is another strong predictor. All the coefficients of the income levels in Table 2 are significantly negative, implying that relative to the lowest income level (below \$25,000), households of higher income were less likely to have food security problem. Figure 3c shows that the predicted probability of having food security increases with the income level, while the predicted probability of having marginal food security decreases.

A contribution of my study is that I provide additional predictive factors of food security relative to Coleman-Jensen et al. (2019). In particular, I show here that education, job-related variables and all kinds of work/unemployment benefits have significant impacts. The coefficients of education are significantly negative, suggesting that people with high education level were less likely to experience food insecurity. Similarly, employed people were less likely to suffer food insufficiency. By contrast, people who lost jobs or expected to lose jobs were more likely to suffer from food insecurity. Columns 3 and 4 in Table 2 also show that relative to the people who worked for the government (public sector), the people who worked for non-profit/charitable organizations or those who were self-employed were less likely to have food insecurity. There are no strong evidence to suggest there is a difference between the public sector and the private sector or family business. Among the people who received unemployment benefit, those with paid leave or received full pay were equally well-off with the people in the public sector, while the people who received partial pay were more likely to suffer food insecurity.



**Table 2.** Demographics and Food Security

Variables	(1)	(2)	(3)	(4)
<i>Food security prior March 13, 2020</i>				
Marginal food security	2.721*** (0.026)	1.433*** (0.014)	2.623*** (0.029)	1.371*** (0.016)
Low food security	5.230*** (0.057)	2.576*** (0.031)	5.083*** (0.065)	2.485*** (0.034)
Very low food security	7.932*** (0.126)	3.869*** (0.066)	7.900*** (0.144)	3.853*** (0.075)
Age	-0.012*** (0.001)	-0.008*** (0.000)	-0.012*** (0.001)	-0.008*** (0.000)
Gender (male)	-0.087*** (0.018)	-0.046*** (0.011)	-0.049** (0.020)	-0.022* (0.012)
Hispanic	-0.005 (0.030)	-0.006 (0.017)	-0.064* (0.034)	-0.042** (0.019)
Black	0.075** (0.029)	0.057*** (0.018)	-0.015 (0.033)	0.003 (0.020)
Asian	-0.039 (0.043)	-0.034 (0.024)	-0.069 (0.048)	-0.051* (0.027)
Other race	0.161*** (0.040)	0.098*** (0.023)	0.154*** (0.044)	0.089*** (0.025)
Widowed	0.276*** (0.045)	0.173*** (0.026)	0.110** (0.050)	0.073** (0.029)
Divorced	0.301*** (0.026)	0.189*** (0.015)	0.154*** (0.029)	0.096*** (0.017)
Separated	0.410*** (0.065)	0.254*** (0.043)	0.261*** (0.072)	0.166*** (0.049)
Continued on next page				

Table 2 – continued from previous page

Variables	(1)	(2)	(3)	(4)
Never married	0.100*** (0.026)	0.066*** (0.015)	-0.026 (0.030)	-0.013 (0.018)
Education	-0.079*** (0.006)	-0.052*** (0.004)	-0.021*** (0.007)	-0.017*** (0.004)
Household size	0.009 (0.007)	0.004 (0.004)	0.020** (0.008)	0.011** (0.004)
Number of children	0.022* (0.012)	0.015** (0.007)	0.025* (0.013)	0.015** (0.008)
Employed	-0.190*** (0.019)	-0.125*** (0.011)	-0.136*** (0.039)	-0.095*** (0.022)
Job loss	0.349*** (0.022)	0.213*** (0.013)	0.328*** (0.025)	0.200*** (0.015)
Expect job loss	0.584*** (0.023)	0.351*** (0.014)	0.586*** (0.025)	0.350*** (0.015)
<i>Income level</i>				
\$25,000-\$34,999			-0.121*** (0.040)	-0.076*** (0.023)
\$35,000-\$49,999			-0.204*** (0.041)	-0.131*** (0.023)
\$50,000-\$74,999			-0.295*** (0.037)	-0.182*** (0.022)
\$75,000-\$99,999			-0.500*** (0.042)	-0.318*** (0.024)
\$100,000-\$149,999			-0.646*** (0.041)	-0.410*** (0.023)
\$150,000-\$199,999			-0.924***	-0.563***

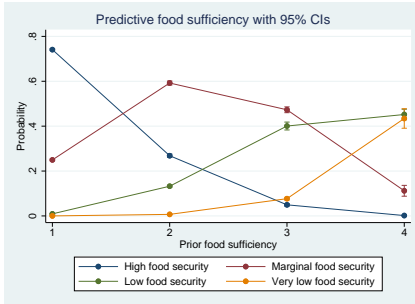
Continued on next page

Table 2 – continued from previous page

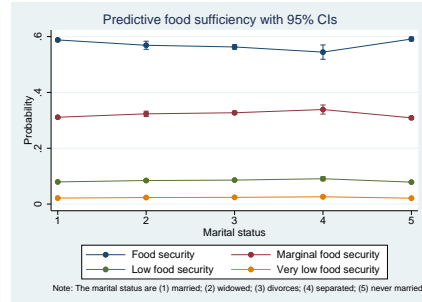
Variables	(1)	(2)	(3)	(4)
Above \$200,000			(0.046)	(0.026)
			-1.139***	-0.679***
			(0.050)	(0.030)
<i>Kind of work or unemployment benefit</i>				
Private sector			0.031	0.022
			(0.038)	(0.021)
Non profit			-0.057	-0.029
			(0.047)	(0.026)
Self-employed			-0.139***	-0.083***
			(0.053)	(0.030)
Family business			-0.190**	-0.101**
			(0.079)	(0.043)
Paid leave			-0.213**	-0.132**
			(0.097)	(0.057)
Full pay			-0.257***	-0.141***
			(0.059)	(0.038)
Partial pay			-0.117	-0.082*
N	627671	627671	534314	534314
Note: In addition the reported characteristics, I also controlled for the state fixed effects.				
Standard errors in parentheses. * p<0.1, ** p<0.05, *** p<0.01				

### 6.3 Reopening and Food insecurity

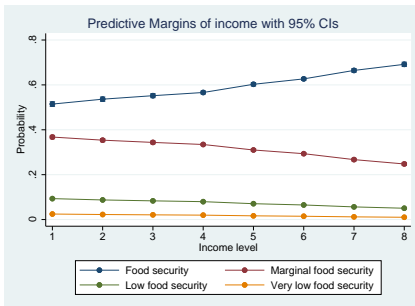
The main focus of my analysis is the impact of reopening policy on food security. Table 3 reports the results. In Columns 1 and 2, I apply the ordered logistic regression, while in Columns 3 and 4 I apply the ordered probit regression. Only reopening policy are controlled in Column 1 and



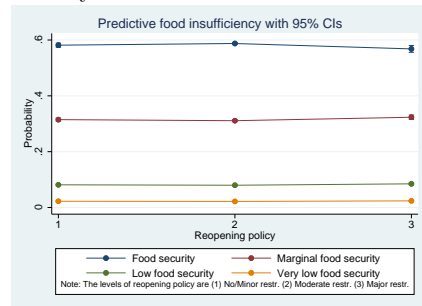
(a) Path dependent food security



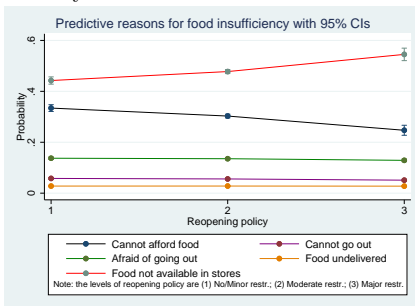
(b) Predicted probability of Food security based on marital status



(c) Predicted probability of Food security based on income level



(d) Predicted probability of Food security based on reopening policy



(e) Predicted probability of the causes of Food security based on reopening policy

Figure 3. Predicted Probability

3, while all other characteristics as in Table 2 are included in Columns 2 and 4. By controlling for the food insecurity status in the week prior to the survey as well as other characteristics, I pick up the effect of reopening policy within these groups. In other words, I ensure that the food insecurity results from the policy and not the historical status or the characteristics of the individuals.

Results in Table 3 report that all the coefficients of No/Minor restrictions and Moderate restrictions are significantly negative, implying that a move from Major restrictions (the omitted policy) to Moderate and No/Minor restrictions had a significant impact on food insecurity. Indeed, such a move decreased the probability of being food insecure. Figure 3d shows the predicted probability of having food security based on reopening policy. According to this figure, the probability of having food security under Major restriction policy is 56.8 percent (with a 95 percent confidence interval being from 55.5 percent to 58 percent), compared to 58.1 percent if under No/Minor restrictions (with a 95 percent confidence interval being from 57.4 percent to 58.9 percent) and 58.7 percent if under Moderate restrictions (with a 95 percent confidence interval being from 58.4 percent to 59.1 percent). By contrast, the probability of having marginal food security is 32.3 percent under Major restriction policy (with a 95 percent confidence interval being from 31.5 percent to 33.1 percent), compared to 31.5 percent if under No/Minor restrictions (with a 95 percent confidence interval being from 30.9 percent to 32 percent) and 31.1 percent if under Moderate restrictions (with a 95 percent confidence interval being from 30.7 percent to 31.5 percent).

Based on my model (Equation 2) I can calculate the probability of each of the level of food security in every state. Figure A1 in the Appendix illustrates these predicted probabilities. These probabilities show that the

**Table 3.** Impact of Reopening on Food security

	(1)	(2)	(3)	(4)
	Ordered logistic		Ordered probit	
No/Minor restrictions	-0.012 (0.033)	-0.106** (0.050)	-0.002 (0.020)	-0.051* (0.029)
Moderate restrictions	-0.098*** (0.030)	-0.144*** (0.043)	-0.054*** (0.019)	-0.074*** (0.025)
State FE	YES	YES	YES	YES
N	633161	534314	633161	534314

Note: In Column 1 and 3, I only control for reopening policy.

All the characteristics in Table 2 are included in Column 2 and 4.

Standard errors in parentheses. \*  $p < 0.1$ , \*\*  $p < 0.05$ , \*\*\*  $p < 0.01$

Southern States were the places where food insecurity was of great concern while the states in the Pacific Northwest found themselves in a better situation.

#### 6.4 How reopening affected food security

In the previous section, I provide evidence that reopening reduced the likelihood of food insecurity. However, to provide policy recommendations, I would need further investigations that help me understand the causes of food insufficiency. In the HPS survey, the respondents were asked to answer why they did not have enough food. They were to choose one of the following five answers: (i) cannot afford food; (ii) cannot get out to buy food; (iii) afraid to go out; (iv) food not delivered and (v) food not available on stores. In addition, the survey also asked if they received free food. All these answers are used to investigate the causes of food insecurity.

Table 4 reports how reopening affected the causes of food insufficiency. In Panel A, I use the logit model while in Panel B I use the probit model. Both models yield similar results. The coefficient of No/Minor and Moderate restrictions are significantly negative in Column 5, suggesting that

stores had more food after the states reopened (i.e. less people claimed that they experienced food insufficiency because of this cause). Perhaps the most intriguing result is that reopening policy affected the ability of the consumers to buy food. Results in Columns 1 and 2 suggest that more people did not have enough food because either they could not afford or they could not go out to buy food.

Figure 3e brings more evidence to illustrate how reopening affected the causes of food insecurity. According to this figure, under No/Minor restrictions, 33 percent of people who were food insecure could not afford food. This probability was only 30 percent under Moderate restrictions and reduced further to 25 percent under Major restrictions. On the other hand, my model predicts that under No/Minor restrictions, the probability of not having enough food because food was not available on the stores is 44 percent. This probability increases to 48 percent under Moderate restrictions and 55 percent under Major restrictions.

To explain how reopening policy affected the ability of consumers to get food, I look at its impacts on food expenses and people's health. In Table 5, the dependent variable in Column 1 is the expenses spent on food at supermarkets, grocery stores and other places. They are to be prepared and eaten at home. The dependent variable in Column 2 is the expenses on prepared meals such as eating out, fast food or delivered meals. Both the coefficients of No/Minor restrictions and Moderate restrictions are significantly positive in all categories of expenses, implying that reopening policy increased the monetary costs of food. Given the income of the respondents was unlikely to increase during the pandemic, it suggests that food became less affordable.

Table 6 shows how reopening affected people's health status and mental health. The level of health status is the dependent variable in Column 1.

**Table 4.** Causes of Food Insecurity

	(1)	(2)	(3)	(4)	(5)	(6)
<i>Panel A: Logit model</i>						
No/Minor restrictions	0.488*** (0.083)	0.268** (0.106)	0.068 (0.082)	0.045 (0.131)	-0.761*** (0.079)	0.338*** (0.095)
Moderate restrictions	0.216*** (0.072)	0.166* (0.089)	-0.069 (0.072)	-0.051 (0.106)	-0.422*** (0.069)	0.186** (0.086)
<i>Panel B: Probit model</i>						
No/Minor restrictions	0.295*** (0.049)	0.145*** (0.055)	0.038 (0.048)	0.024 (0.063)	-0.455*** (0.047)	0.170*** (0.046)
Moderate restrictions	0.131*** (0.042)	0.092** (0.046)	-0.041 (0.042)	-0.024 (0.051)	-0.251*** (0.042)	0.097** (0.041)
State FE	YES	YES	YES	YES	YES	YES
N	172633	172633	172633	172633	172633	534116

Note: Each column, except Column 6, corresponds to one particular reason for not having enough food. They are (1) cannot afford food (2) cannot get out (3) afraid to go out (4) food not delivered (5) food not available on stores.

Column 6 corresponds to the question whether the respondent received free food in the past 7 days.

All the person and household characteristics are included, as in Table 2

Standard errors in parentheses \* p<0.1, \*\* p<0.05, \*\*\* p<0.01



**Table 5.** Reopening and food expenditure

	(1) Prepared food	(2) Prepared meal
No/Minor restrictions	24.485*** (2.911)	15.265*** (1.891)
Moderate restrictions	11.698*** (2.404)	8.153*** (1.584)
State FE	YES	YES
N	526339	523631
R-squared	0.152	0.0974

Note: In the first column, the dependent variable is the expenditure on food to prepare and eat at home. In the second column, the dependent variable is the expenditure on prepared meals. All the household characteristics are controlled.

Standard errors in parentheses. \*  $p < 0.1$ , \*\*  $p < 0.05$ , \*\*\*  $p < 0.01$

Its value ranges from 1 (Excellent) to 5 (Poor). The frequency that people felt anxious, worried, had little interest and depressed are the dependent variables in Columns 2 to 5. The values of the frequency are from 1 (Not at all) to 5 (Nearly everyday).

Column 1 reports that reopening policy led to a deteriorating health status. As a result, people were not able to go out to buy food. Moreover, they felt more anxious, worried, depressed and had little interest (Columns 2 to 5), suggesting that they might have been afraid of going out. Indeed, if the belief was that reopening was imposed too soon, it would lead to more virus infection and more fear of going out.

Another cause of food insufficiency is the lack of free food. Column 6 in Table 4 suggests that state reopening increased the probability of people receiving free food. It prompts the question of how reopening affected the source of free food. Table 7 provides the evidence to answer this question. In this table, I employ the answers to the question of where people got free food. The available answers are (1) school or program aimed at children;

**Table 6.** Reopening and Health

	(1) Health Status	(2) Anxiety	(3) Worried	(4) Little interest	(5) Depression
Panel A: Ordered Logistic Regression					
No/Minor restrictions	0.142*** (0.039)	0.169*** (0.039)	0.221*** (0.040)	0.101** (0.040)	0.185*** (0.041)
Moderate restrictions	0.036 (0.032)	0.042 (0.033)	0.090*** (0.034)	0.010 (0.033)	0.066* (0.034)
Panel B: Ordered Probit Regression					
No/Minor restrictions	0.088*** (0.022)	0.101*** (0.023)	0.132*** (0.024)	0.067*** (0.024)	0.118*** (0.024)
Moderate restrictions	0.025 (0.018)	0.026 (0.020)	0.057*** (0.020)	0.014 (0.020)	0.046** (0.020)
State FE	YES	YES	YES	YES	YES
N	534864	534864	534864	534864	534864

Note: In Column 1, the dependent variable is the health status of the respondents, from 1 (Excellent) to 5 (Poor). From Column 2 to Column 5, the dependent variables are the frequency of the mental health problem, from 1 (Not at all) to 5 (Nearly everyday).

All the household characteristics are controlled.

Standard errors in parentheses. \* p<0.1, \*\* p<0.05, \*\*\* p<0.01

(2) food pantry or food bank; (3) home delivered meal service; (4) religious organizations; (5) shelter or soup kitchen; (6) other community program or (7) family; friends or neighbors. For each answer, I study how reopening affected the probability of having free food from these sources. Each column in Table 7 corresponds to one of the answers above. The coefficients of reopening policies are significantly positive in Columns 3, 4 and 7. It suggests that the relaxation of the stay-at-home order helped the meal delivery service and the religious organizations such as churches, temples or mosques to reach out more to people in need of food. At the same time, these people were more likely to receive assistance from their family, friends or neighbors.

## 6.5 Reopening and the expected food security

In the previous section, I show how reopening influenced the causes of Food Security. An interesting feature is that not only the monetary cause was affected but also other causes such as the ability to go out for food. It suggests that the government's policy could alter the people's behavior and mitigate the problem. Building such a theoretical framework will be an interesting venue for future research. It requires, however, evidence of how reopening policy affects the people's expectation, as far as Food Security is concerned.

As far as I know, there is a lack of evidence on the expected food security. Table 8 provides evidence to fill this gap. The respondents in the survey were asked how confident they were that they could afford enough food in the next 4 weeks. The answers were from "Not at all confident" to "Very confident". In other words, the answers ranged from very low food security to high food security.

In Columns 1 and 2, I apply the ordered logistic regression while in

**Table 7.** The sources of free food

	(1)	(2)	(3)	(4)	(5)	(6)	(7)
<i>Panel A: Logit model</i>							
No/Minor restrictions	-0.008 (0.182)	0.216 (0.227)	0.637 (0.393)	0.816*** (0.252)	-0.213 (0.478)	-0.006 (0.213)	0.541** (0.220)
Moderate restrictions	0.223 (0.152)	0.006 (0.208)	0.715** (0.318)	0.207 (0.234)	-0.244 (0.370)	0.029 (0.184)	0.057 (0.204)
<i>Panel B: Probit model</i>							
No/Minor restrictions	0.001 (0.106)	0.134 (0.131)	0.297* (0.174)	0.454*** (0.132)	-0.091 (0.195)	0.007 (0.119)	0.311** (0.127)
Moderate restrictions	0.112 (0.089)	0.004 (0.120)	0.319** (0.145)	0.113 (0.121)	-0.080 (0.158)	0.021 (0.104)	0.032 (0.117)
State FE	YES	YES	YES	YES	YES	YES	YES
N	32599	32599	32599	32599	32599	32599	32599

Note: each column corresponds to the question where they got free groceries and free food.

The answers are (1) school or program aimed at children; (2) food pantry or food bank

(3) home delivered meal service; (4) religious organizations; (5) shelter or soup kitchen

(6) other community program or (7) family; friends or neighbors

Standard errors in parentheses \* p<0.1, \*\* p<0.05, \*\*\* p<0.01

Columns 3 and 4 I apply the ordered probit regression. In Columns 1 and 3, only the reopening policies are controlled while all the characteristics that are controlled previously (for example in Table 2) are controlled in Columns 2 and 4.

In all specifications, the coefficients of No/Minor restrictions are negative. Since the Major restriction policy is the omitted policy, these results imply that people who lived in the states where the containment policy moved from Major restrictions to None or Minor restrictions expected to experience food insufficiency. By contrast, the coefficients of Moderate restrictions are all positive, although not statistically significant. They suggest that people slightly expected an improving food security situation when the states moderately relaxed their stay-at-home orders. These two results suggest that people prefer a measured reopening to a more drastic move as far as expected food security is concerned.

**Table 8.** Impact of Reopening on expected Food security

	(1)	(2)	(3)	(4)
	Ordered logistic		Ordered probit	
No/Minor restrictions	-0.148*** (0.031)	-0.025 (0.045)	-0.090*** (0.019)	-0.014 (0.025)
Moderate restrictions	0.020 (0.029)	0.030 (0.038)	0.010 (0.018)	0.018 (0.021)
State FE	YES	YES	YES	YES
N	592186	534328	592186	534328

Note: In Column 1 and 3, I only control for reopening policy.

All the characteristics in Table 2 are included in Column 2 and 4

Standard errors in parentheses. \*  $p < 0.1$ , \*\*  $p < 0.05$ , \*\*\*  $p < 0.01$

## 6.6 Robustness checks

In this section, I provide further evidence to support the finding that reopening policy alleviated food insecurity. First, I include data on state-

level unemployment to address the potential omitted variables. Second, I employ an alternative dataset to check if the finding is driven by my survey.

As I discussed in the identification strategy section, unemployment is a variable that is potentially correlated with both the dependent variable, food security, and the independent variable, reopening policy. Since unemployment rates were only communicated one month later by the Bureau of Labor Statistics, I add the unemployment rate of the previous month in Columns 1 and 2 in Table 9. The results in both columns confirm that my finding remains unchanged: reopening policy reduced the likelihood of food insecurity.

In the second robustness check, I employ another survey, conducted by the National Opinion Research Center (NORC), University of Chicago. This survey is at a smaller scale than the HPS: it only covered 17 states in the U.S., compared to 51 states in the HPS. The NORC has 3 waves, compared to 8 waves in the HPS. And finally, in each wave there were 8-9000 responses while the HPS has ten times the responses.

Although smaller in size, the NORC survey can provide complementary evidence. In this survey, the respondents were asked if they did not have the money to buy the food needed. I will use their answers as an indicator of food security. In particular, the answers ranged from "Often true" to "Sometimes true" and "Never true". They are then assigned to "Very Low Food Security" to "Low Food Security" and "Food Security".

In addition to answering whether they had money to buy food, respondents were also asked if they worried that food would run out before they had money to buy more. I use their answers as an indicator of the expected food security. This survey, however, does not have information on the reasons of food insecurity.

Table 9 provides the results. In Columns 3 and 4, the dependent variable is the current Food security. We can see that in all specifications, the coefficients of No/Minor restrictions and Moderate restrictions are positive. Note that a high answer means more food security. Therefore, the results suggest that moving from Major restrictions to Moderate and No/Minor restrictions improved the food security. In Columns 5 and 6, the dependent variable is the expected Food security. The coefficients of both types of reopening policy are positive, although only those of Moderate restrictions are significant. Again it is consistent with the finding with the HPS survey that people were in favor of a move from Major restrictions to Moderate restrictions.

## 7 Concluding remarks

The COVID-19 pandemic has posed major challenges to governments across the world. Food insecurity is one of the threats that this pandemic is projected to bring. Policy makers have responded to the development of the outbreak with a number of policies, including the containment (and the relaxation) policy. My analysis shows that reopening policy reduced the likelihood of experiencing food insufficiency. While the overall impact of this policy is expected, how it influenced the causes of food security is more interesting. In particular, while reopening policy increased the food supply (more food available on stores and more people receiving free food), it reduced the people's ability to get food (either they could not afford to buy food or they could not go out to get food). In addition, there is evidence that reopening policy helped a number of venues to get free food, such as meal service, religious organizations and from friends/relatives/neighbors.

While my findings must be taken with some cautions due to the identification assumptions, they yield valuable evidence to policy makers to

**Table 9.** Robustness checks

	(1)	(2)	(3)	(4)	(5)	(6)
	HPS survey		NORC survey			
	Food Security			Expected Food Security		
No/Minor restrictions	-0.015 (0.038)	-0.004 (0.022)	0.065 (0.167)	0.044 (0.093)	0.188 (0.147)	0.088 (0.083)
Moderate restrictions	-0.082*** (0.025)	-0.041*** (0.015)	0.154 (0.111)	0.096 (0.059)	0.282*** (0.092)	0.162*** (0.050)
State FE	YES	YES	YES	YES	YES	YES
N	597883	597883	14207	14207	14296	14296

Note: In Columns 1 and 2 I use the HPS survey while in Columns 3 to 6 I use the NORC survey. The dependent variables in Columns 1 and 2 are the food security outcomes, as in previous tables. In Columns 3 and 4, respondents were asked if they did not have money to buy food. The answers were ordered so that low level corresponded to low food security and high level corresponded to high food security. Similarly, in Columns 5 and 6, respondents were asked if they worried their food would run out before they got money to buy more. In Columns 3 and 5 the ordered logistic regression was applied while in Columns 4 and 6 the ordered probit regression was applied. Standard errors in parentheses \* p<0.1, \*\* p<0.05, \*\*\* p<0.01



mitigate the effects of the pandemic on food security. In particular, while reopening policy in general alleviated the problem of food insufficiency, it might have some unintended effects such as making it more difficult to the people to get the food they needed. My findings prompt future research to a number of interesting venues. For instance, at the time this paper was written there was lack of understanding of how reopening policy was decided. It made the task to find the appropriate instrument to address the potential endogeneity bias a challenging one. Additionally, a theoretical framework is also an interesting venue. For example, while the literature focuses on the economic and financial constraints as determinants of food insecurity, my findings show that there are more factors such as transportation and the fear of going out, especially during the time of crisis, that might have significant impacts on the ability to get sufficient food.

## 8 Appendix

### 8.1 The reopening dates

Nguyen et al. (2020) provides the reopening dates based on the articles in the New York Times, while I use the categorization in the Washington Post. While in most states, my data provide the same dates, there are still a number of differences. I explain the differences as below.

In Arizona, my reopening date is May 1 because "On April 22, the governor issued an order that elective surgeries could resume May 1." The reopening date in Nguyen et al. (2020) is May 8.

In Delaware, my reopening date is May 8 because "On May 5, the governor announced interim steps for small businesses to begin reopening May 8." The reopening date in Nguyen et al. (2020) is June 1.

In Iowa, the reopening day is May 15 because while "On May 1, 77 of Iowas 99 counties that hadnt had coronavirus cases or had seen a downward trend in infections over the previous two weeks began operating again with limited capacity", only "On May 15, the remaining 22 counties were allowed to reopen gyms and restaurant dine-in services, and personal services such as hair salons and barbershops could reopen by appointment. Social gatherings of more than 10 people are still prohibited." The reopening date in Nguyen et al. (2020) is May 1.

In Louisiana, the reopening day is May 1 because "restaurant patrons were now being allowed to eat their takeout food in outdoor seating areas as long as no employees serve them beginning May 1." The reopening date in Nguyen et al. (2020) is May 15.

In Michigan, the reopening date in my data is May 22 because " On May 22, businesses and restaurants in northern Michigan reopened at reduced

capacity under a new executive order the governor issued May 18.” The reopening date in [Nguyen et al. \(2020\)](#) is May 7.

In New Hampshire, the reopening date is May 11 because ”On May 1, the governor announced a modified stay-at-home order in effect until May 31. Under the new order, certain businesses such as golf courses, retail stores and salons began reopening May 11, with certain occupancy and physical distancing restrictions.” The reopening date in [Nguyen et al. \(2020\)](#) is May 4.

## 8.2 Supplementary table and figure

Table A1. Reopening policy across states

State	Reopening date	Week 1	Week 2	Week 3	Week 4
Alabama	30/04/2020	Major	Moderate	Moderate	Moderate
Alaska	24/04/2020	Major	Moderate	Moderate	None
Arizona	08/05/2020	Major	Moderate	Minor	Minor
Arkansas	04/05/2020	Major	Moderate	Moderate	Moderate
California	08/05/2020	Major	Major	Moderate	Moderate
Colorado	01/05/2020	Major	Moderate	Moderate	Moderate
Connecticut	20/05/2020	Major	Major	Major	Moderate
Delaware	01/06/2020	Major	Major	Moderate	Moderate
District of Columbia	29/05/2020	Major	Major	Major	Major
Florida	04/05/2020	Major	Moderate	Moderate	Moderate
Georgia	24/04/2020	Major	Moderate	Moderate	Moderate
Hawaii	07/05/2020	Major	Moderate	Moderate	Moderate
Idaho	01/05/2020	Major	Moderate	Moderate	Moderate
Illinois	01/05/2020	Major	Moderate	Moderate	Moderate
Indiana	04/05/2020	Major	Moderate	Moderate	Moderate
Iowa	01/05/2020	Major	Major	Major	Moderate
Kansas	04/05/2020	Major	Moderate	Moderate	Moderate
Kentucky	11/05/2020	Major	Major	Moderate	Moderate
Louisiana	15/05/2020	Major	Moderate	Moderate	Moderate
Maine	01/05/2020	Major	Moderate	Moderate	Moderate
Maryland	15/05/2020	Major	Major	Major	Moderate
Massachusetts	18/05/2020	Major	Major	Major	Major
Michigan	07/05/2020	Major	Major	Major	Major
Minnesota	27/04/2020	Major	Moderate	Moderate	Moderate
Mississippi	27/04/2020	Major	Moderate	Moderate	Minor
Missouri	04/05/2020	Major	Minor	Minor	Minor
Montana	26/04/2020	Major	Moderate	Moderate	Moderate
Nebraska	04/05/2020	Major	Moderate	Moderate	Moderate
Nevada	09/05/2020	Major	Major	Moderate	Moderate
New Hampshire	04/05/2020	Major	Major	Moderate	Moderate
New Jersey	02/05/2020	Major	Moderate	Moderate	Moderate
New Mexico	01/05/2020	Major	Moderate	Moderate	Moderate
New York	15/05/2020	Major	Major	Major	Moderate
North Carolina	08/05/2020	Major	Major	Moderate	Moderate
North Dakota	01/05/2020	Major	Minor	Minor	Minor
Ohio	01/05/2020	Major	Moderate	Moderate	Moderate
Oklahoma	24/04/2020	Major	Moderate	Moderate	Minor
Oregon	15/05/2020	Major	Major	Major	Moderate
Pennsylvania	08/05/2020	Major	Major	Moderate	Moderate
Rhode Island	09/05/2020	Major	Major	Moderate	Moderate
South Carolina	20/04/2020	Moderate	Moderate	Moderate	Moderate
South Dakota	01/05/2020	Major	Minor	Minor	Minor
Tennessee	27/04/2020	Major	Moderate	Moderate	Moderate
Texas	01/05/2020	Major	Moderate	Moderate	Moderate
Utah	01/05/2020	Major	Moderate	Moderate	Moderate
Vermont	27/04/2020	Major	Moderate	Moderate	Moderate
Virginia	15/05/2020	Major	Major	Major	Moderate
Washington	05/05/2020	Major	Moderate	Moderate	Moderate
West Virginia	04/05/2020	Major	Moderate	Moderate	Moderate
Wisconsin	20/04/2020	Major	Major	Moderate	Moderate
Wyoming	01/05/2020	Major	Moderate	Moderate	Minor

Table A2. Monthly unemployment rates by State

	Feb	March	April	May (projected)
Alabama	2.7	3.0	13.8	9.9
Alaska	5.8	5.2	13.5	12.6
Arizona	4.5	6.1	13.4	8.9
Arkansas	3.5	5	10.8	9.5
California	3.9	5.5	16.4	16.3
Colorado	2.5	5.2	12.2	10.2
Connecticut	3.8	3.4	8.3	9.4
Delaware	3.9	5.0	14.9	15.8
District of Columbia	5.1	6.0	11.7	8.9
Florida	2.8	4.4	13.8	14.5
Georgia	3.1	4.6	12.6	9.7
Hawaii	2.7	2.4	23.8	22.6
Idaho	2.7	2.5	11.8	8.9
Illinois	3.4	4.2	17.2	15.2
Indiana	3.1	3.0	17.5	12.3
Iowa	2.8	3.3	11.0	10.0
Kansas	3.1	2.8	11.9	10.0
Kentucky	4.2	5.2	16.6	11.0
Louisiana	5.2	6.7	15.1	13.3
Maine	3.2	3.0	10.4	9.3
Maryland	3.3	3.3	10.1	9.9
Massachusetts	2.8	2.8	16.2	16.3
Michigan	3.6	4.3	24.0	21.2
Minnesota	3.1	2.9	8.7	9.9
Mississippi	5.4	5.1	16.3	10.6
Missouri	3.5	3.9	10.2	10.1
Montana	3.5	3.6	11.9	9.0
Nebraska	2.9	4.0	8.7	5.2
Nevada	3.6	6.9	30.1	25.3
New Hampshire	2.6	2.4	17.1	14.5
New Jersey	3.8	3.7	16.3	15.2
New Mexico	4.8	6.3	11.9	9.2
New York	3.7	4.1	15.3	14.5
North Carolina	3.6	4.3	12.9	12.9
North Dakota	2.2	2.0	9.1	9.1
Ohio	4.1	5.8	17.6	13.7
Oklahoma	3.2	2.9	14.7	12.6
Oregon	3.3	3.5	14.9	14.2
Pennsylvania	4.7	5.8	16.1	13.1
Puerto Rico	8.8			
Rhode Island	3.4	4.7	18.1	16.3
South Carolina	2.5	3.2	12.8	12.5
South Dakota	3.3	3.1	10.9	9.4
Tennessee	3.4	3.3	15.5	11.3
Texas	3.5	5.1	13.5	13.0
Utah	2.5	3.8	10.4	8.5
Vermont	2.4	3.1	16.5	12.7
Virginia	2.6	3.3	11.2	9.4
Washington	3.8	5.1	16.3	15.1
West Virginia	4.9	6.0	15.9	12.9
Wisconsin	3.5	3.1	13.6	12.0
Wyoming	3.7	3.8	9.6	8.8

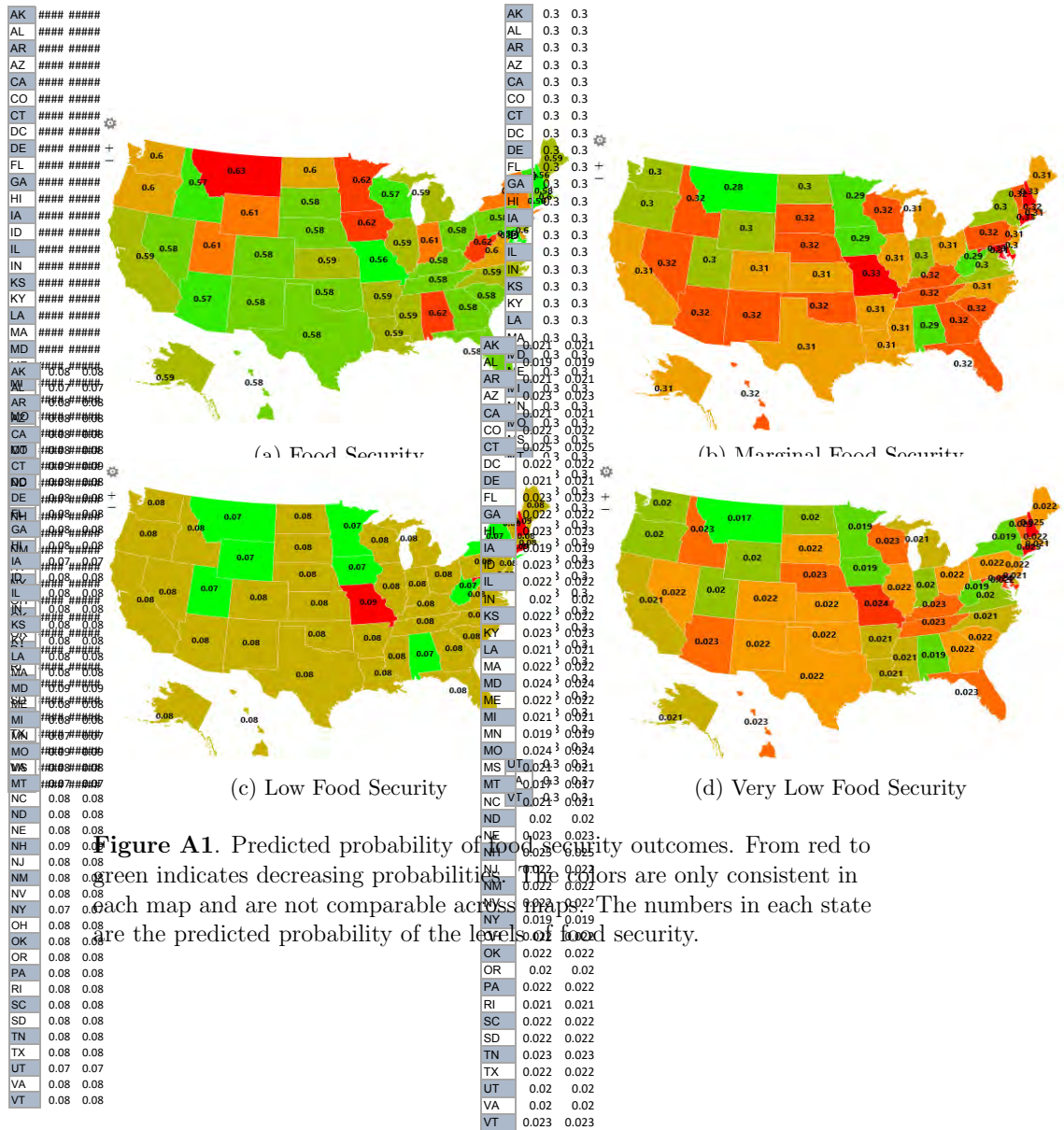


Figure A1. Predicted probability of food security outcomes. From red to green indicates decreasing probability. The colors are only consistent in each map and are not comparable across maps. The numbers in each state are the predicted probability of the levels of food security.

## References

- Baek, C., P. McCrory, T. Messer, and P. Mui. 2020. "Unemployment effects of stay-at-home orders: Evidence from high-frequency claims data." IRLLE Working Paper No. 101-20.
- Bauer, L. 2020. "The COVID-19 crisis has already left too many children hungry in America." Brookings Institute, The Hamilton Project.
- Bitler, M., C. Gundersen, and G.S. Marquis. 2005. "Are WIC Nonrecipients at Less Nutritional Risk Than Recipients? An application of the Food Security Measure." *Review of Agricultural Economics*, 27: 433–438.
- Brodeur, A., A. Clark, S. Fleche, and N. Powdthavee. 2020. "COVID-19, Lockdowns and Well-Being: Evidence from Google Trends." IZA DP No. 13204.
- Bureau of Labor Statistics, U.S. Department of Labor. 2020. "Unemployment rate rises to record high 14.7 percent in April 2020." *The Economics Daily*.
- Coleman-Jensen, A., M. Rabbitt, C. Gregory, and A. Singh. 2019. "Household Food Security in the United States in 2018." U.S. Department of Agriculture, Economic Research Service, Economic Research Report No. 270.
- Davis, G., and W. You. 2011. "Not enough money or not enough time to satisfy the Thrifty Food Plan? A cost difference approach for estimating a moneytime threshold." *Food Policy*, 36: 101–107.
- Feeding America. 2020. "The Impact of the Coronavirus on Food Insecurity."
- Fitzpatrick, K., and A. Coleman-Jensen. 2014. "Food on the Fringe: Food Insecurity and the Use of Payday Loans." *Social Service Review*, 88(4): 553–593.
- Gelman, A., D. Park, B. Shor, J. Bafumi, and J. Cortina. 2008. *Red State, Blue State, Rich State, Poor State Why Americans Vote the Way They Do*. Princeton University Press.
- Glover, A., J. Heathcote, D. Krueger, and J. Rios-Rull. 2020. "Health versus Wealth: On the Distributional Effects of Controlling a Pandemic." *Covid Economics*, 6: 22–64.
- Graham, D. 2020. "Why Are the States Reopening?" *The Atlantic*.
- Gundersen, C., and J. Gruber. 2001. "The Dynamic Determinants of Food Insufficiency." In *Second Food Security Measurement and Research Conference. Food Assistance and Nutrition Research Report*. Vol. 2.
- Gundersen, C., and V. Oliveira. 2001. "The Food Stamp Program and Food Insufficiency." *American Journal of Agricultural Economics*, 83(4): 875–887.
- Gundersen, C., B. Kreider, and J. Pepper. 2011. "The Economics of Food Insecurity in the United States." *Applied Economic Perspectives and Policy*, 33(3): 281–303.

- Heflin, C., I. Arteaga, and S. Gable.** 2015. "The Child and Adult Care Food Program and Food Insecurity." *Social Service Review*, 89: 77–98.
- Klenow, P., and O. Kryvtsov.** 2008. "State-Dependent or Time-Dependent Pricing: Does It Matter for Recent U.S. Inflation." *Quarterly Journal of Economics*, 123(3): 863–904.
- Leete, L., and N. Bania.** 2010. "The Effect of Income Shocks on Food Insufficiency." *Review of the Economics of the Household*, 8: 505–526.
- Nakamura, E., and J. Steinsson.** 2008. "Five Facts About Prices: A Reevaluation of Menu Cost Models." *Quarterly Journal of Economics*, 123(4): 1415–1464.
- Nguyen, T., S. Gupta, M. Andersen, A. Bento, K. Simon, and C. Wing.** 2020. "Impacts of State reopening policy on human mobility." NBER Working Paper 27235.
- OECD.** 2020. "Food Supply Chains and COVID-19: Impacts and Policy Lessons."
- Rampini, A.** 2020. "Sequential Lifting of COVID-19 Interventions with Population Heterogeneity." mimeo.
- Ribar, D., and K. Hamrick.** 2003. "Dynamics of Poverty and Food Sufficiency." United States Department of Agriculture report.
- Sen, A.** 1981. *Poverty and Famines: An Essay on Entitlement and Deprivation*. Clarendon Press.
- Stuff, J., P. Casey, K. Szeto, J. Gossett, J. Robbins, P. Simpson, C. Connell, and M. Bogle.** 2004. "Household Food Insecurity Is Associated with Adult Health Status." *The Journal of Nutrition*, 134(9): 2330–2335.